



PLATTE RIVER RECOVERY IMPLEMENTATION PROGRAM

Draft Final

Shoemaker Island Flow-Sediment-Mechanical “Proof of Concept” Experiment

2015 Annual Summary Report and 3-Year Summary

August 2017

Submitted to:

Platte River Recovery Implementation Program
4111 4th Avenue, Suite 6
Kearney, NE 68845

Submitted by:

EA Engineering, Science, and Technology, Inc.,
PBC
221 Sun Valley Blvd, Suite D
Lincoln, NE 68528

GMA Hydrology, Inc.
PO Box 1516
Weaverville, CA 96093

Northern Hydrology and Engineering
PO Box 2515
McKinleyville, CA 95519

Western Ecosystems Technology, Inc.
415 West 17th Street, Suite 200
Cheyenne, WY 82001



Table of Contents

EXECUTIVE SUMMARY	ES-1
I. INTRODUCTION	I-1
II. PURPOSE	II-1
II.A. Program Management Objectives and Management Strategies	II-1
II.B. Hypotheses	II-1
II.C. Experiment Purpose	II-3
III. EXPERIMENT DESIGN CONSIDERATIONS	III-1
III.A. Overview of Data Collection	III-1
III.B. Area of Interest	III-2
III.C. Data Collection	III-2
IV. MONITORING AND ANALYSIS METHODS	IV-1
IV.A. Topography and Bathymetry	IV-2
IV.A.1. Primary River Cross Sections	IV-2
IV.A.2. Bar Topography	IV-4
IV.A.3. Longitudinal Profile	IV-5
IV.B. Documentation of Bank and Channel Features Using Ground Photography	IV-6
IV.C. Bed and Bar Material Sampling.....	IV-6
IV.D. Vegetation Type, Density, and Green Line	IV-7
IV.D.1. Vegetation Survey.....	IV-7
IV.D.2. Vegetation Roughness	IV-7
IV.D.3. Vegetation Green Line.....	IV-8
IV.E. Stage Recorders	IV-8
IV.F. Discharge	IV-8
IV.G. Sediment Transport Measurements.....	IV-9
IV.G.1. Turbidity	IV-9
IV.G.2. Suspended-Sediment-Depth Integrated Sampling	IV-10
IV.G.3. Experimental ‘Box’ Sampling	IV-10
IV.G.4. Bedload Monitoring.....	IV-11
IV.G.5. Scour and Fill Monitoring.....	IV-11
IV.H. Modeling.....	IV-11
V. RESULTS: JUNE 2015 HIGH FLOW EVENT	V-1
V.A. Hydrologic Setting	V-1
V.A.1. Discharge: June 2015 High Flow.....	V-1
V.B. Field Observations	V-2
V.B.1. Field Classification of Nested Alluvial Features	V-2
V.B.2. Pools and Thalweg Maintenance	V-3
V.B.3. Documentation of Bank and Channel Features	V-3
V.C. Channel Geometry	V-4
V.C.1. Bar Topography	V-4



V.C.2.	Primary and Supplemental River Cross Sections	V-5
V.C.3.	Longitudinal Profile	V-8
V.C.4.	Vegetation	V-9
V.C.5.	Treated and Natural River Areas	V-12
V.C.6.	Unvegetated Channel Widths	V-13
V.C.7.	Vegetation Roughness	V-13
V.D.	Sediment	V-13
V.D.1.	Turbidity	V-13
V.D.2.	Suspended Sediment	V-14
V.D.3.	Total Load and Bedload	V-14
V.D.4.	Scour Monitoring	V-15
V.D.5.	Bed and Bar Sampling	V-15
VI.	CONCLUSIONS FOR 2015 HIGH FLOW EVENT	VI-1
VI.A.	Learning Objectives	VI-1
VI.A.1.	Evaluate the relationship between peak flows (magnitude and duration) and bar height and area.	VI-1
VI.A.2.	Evaluate the relationship between peak flows (magnitude and duration) and riparian plant mortality	VI-2
VI.A.3.	Evaluate ability of FSM management strategy to create and/or maintain habitat for whooping cranes, least terns and piping plovers	VI-2
VII.	MODELING OF THE SHORT DURATION HIGH FLOW	VII-1
VII.A.	Effect of a SDHF	VII-2
VII.B.	Effect of Sediment Supply	VII-3
VII.C.	Effect of Grain Size	VII-3
VII.D.	Effect of Hydrograph Shape and Duration	VII-5
VII.E.	SDHF Conclusions	VII-6
VIII.	THREE YEAR SUMMARY	VIII-1
VIII.A.	Timeline of Events	VIII-1
VIII.B.	Inter Year Summary	VIII-3
VIII.B.1.	Evaluate the relationship between peak flows (magnitude and duration) and bar height and area.	VIII-3
VIII.B.2.	Evaluate the relationship between sediment supply and bar height and area	VIII-4
VIII.B.3.	Evaluate the relationship between grain size and bar height and area	VIII-4
VIII.B.4.	Evaluate the relationship between peak flows (magnitude and duration) and riparian plant mortality	VIII-5
VIII.B.5.	Evaluate ability of FSM management strategy to create and/or maintain habitat for whooping cranes, least terns and piping plovers	VIII-7
IX.	REFERENCES	IX-1



Tables

- 4-1 Coordinates and Elevation for Cross Section Pins and Benchmarks
- 4-2 Survey Codes
- 5-1 Geomorphic Monitoring and Modeling Support Summary – June 2015 High Flow and August 2015 Effort
- 5-2 FSM Management Strategy Flow Benchmarks and June 2015 High Flow Event Magnitude and Durations
- 5-3 June 2015 High Flow Discharge Summary – Collected Between Cross Sections 2 and 3
- 5-4 Bar Data Summary – July 2014 and August 2015
- 5-5 Sand Bar Data Summary – July 2014 and August 2015
- 5-6 Primary Cross Section Area and Volume Change by Average End Area Method – July 2014 to August 2015
- 5-7 Supplemental and Primary Cross Section Area and Volume Change by Average End Area Method – July 2014 to August 2015
- 5-8 Shoemaker Study Reach Vegetated Bars, Sand Bars, and Water/River Bed Area – July 2014 and August 2015
- 5-9 June 2015 High Flow Suspended Sediment Sample Data
- 5-10 June 2015 High Flow Suspended Sediment Transport Equations by Size Class
- 5-11 June 2015 High Flow Sediment Load Totals by Size Class
- 5-12 June 2015 High Flow Sediment Sample Summary
- 5-13 2015 Bed and Bar Sample Summary
- 8-1 Shoemaker Island FSM Experiment Monitored Flow Events, Field Efforts, Total River Flow at the Grand Island Gaging Station

- 8-2 Shoemaker Study Reach – 3 Year Breakdown



Figures

- 3-1 Site Map
- 3-2 Monitoring Cross Section Locations
- 4-1 February 2015 Ice Floe Through the Shoemaker Study Reach
- 4-2 Schematic Figure Showing Scour Chain
- 5-1 Hydrograph Grand Island Gage (USGS 06770500) Total River Flow (TRF) with July 2014 and August 2015 Field Efforts
- 5-2 Stage Discharge Relation for Shoemaker Study Reach – June 2015 High Flow
- 5-3 Shoemaker Reach Split Flow Discharge and Sampling Events During June 2015 High Flow
- 5-4 Shoemaker Reach Split Flow Discharge and USGS Total River Flow Discharge at Grand Island – June 2015 High Flow
- 5-5 Bar Attributes – July 2014 and August 2015
- 5-6 Area of All Bars Surveyed – July 2014 and August 2015
- 5-7 Sand Bars Surveyed – July 2014 and August 2015
- 5-8 Mean Sand Bar Height Above 1,200 cfs TRF Stage - August 2015
- 5-9 Typical Primary Cross Section – Bottom Profile – July 2014 and August 2015
- 5-10 Cumulative and Net Volume Change at the 37 Primary and Supplemental Cross Sections – August 2015
- 5-11 Platte River Water Surface Slope Profile Through the Shoemaker Study Reach
- 5-12 Vegetation Plots
- 5-13 Bar 46 in July 2014 (November 2014 Aerial)
- 5-14 Bar 46 in July 2014 – Ground Photo
- 5-15 Bar 46 in August 2015 (July 2015 Aerial)
- 5-16 Maximum Un-Vegetated Channel Widths at the 18 Primary Cross Sections – August 2015
- 5-17 Vegetation Roughness Polygons
- 5-18 Platte River Bedload Discharge – June 2015 High Flow
- 6-1 Cumulative Distributions of Sand Bar and Vegetated Bar Area Relative to the June 2015 High Flow 3-Day Mean Peak Discharge Stage
- 8-1 Mean Sand Bar Height Above 1,200 cfs TRF Stage – July 2014
- 8-2 Bar Attributes April 2013, July 2014, and August 2015
- 8-3 D50 Ranges for 2013 Pre and Post, 2014 Pre and Post, and 2015 Post
- 8-4 Area of All Bars Surveyed – April 2013, July 2014, and August 2015

Appendices

Appendix A – Geomorphology



Appendix B – Photos
Appendix C – Vegetation Survey

Attachments

Attachment I – Fixed Bed Modeling
Attachment II – Mobile Bed Modeling
Attachment III – One-Dimensional Bank Erosion Analysis



EXECUTIVE SUMMARY

The Platte River Recovery Implementation Program (Program) was initiated on January 1, 2007 between Nebraska, Wyoming, Colorado, and the Department of the Interior to address endangered species issues in the central and lower Platte River Basin. In an effort to improve the survival of whooping cranes during migration, improve least tern and piping plover production, and avoid adverse impacts to pallid sturgeon in the Lower Platte River, the Program is evaluating the ability of a Flow-Sediment-Mechanical (FSM) management strategy to achieve these goals. The management actions include:

- 1) Flow— Augment Q1.5 through flow releases to create short duration high flows (SDHF) of 5,000 to 8,000 cubic feet per second (cfs) for 3 days in 2 out of 3 years.
- 2) Sediment— Augmentation of approximately 150,000 tons of medium sand annually to offset sediment deficit upstream of Kearney.
- 3) Mechanical— Channel widening, clearing, and leveling of in-channel bars and flow consolidation (85-90 percent of 8,000 cfs in a single channel).

The Shoemaker Island Complex, which is assumed to be in sediment balance, was chosen as the location to implement the FSM “Proof of Concept”. The Shoemaker Island Complex is located approximately 1.6 miles downstream of Highway 11, and extends 2.6 miles downstream to a point approximately 1.1 miles upstream of South Alda Road, which is in the downstream portion of the Associated Habitat reach. Over a three-year period, the experiment evaluated the performance of the FSM management actions, in creating and/or maintaining channel characteristics that are consistent with the Program’s management objectives. Learning objectives for the Shoemaker Island Complex management experiment include:

- 1) Evaluate the relationship between peak flows (magnitude and duration) and sandbar height and area.
- 2) Evaluate the relationship between peak flows (magnitude and duration) and riparian plant mortality.
- 3) Evaluate the ability of the FSM management strategy to create and/or maintain habitat for whooping cranes, least terns, and piping plovers.

Data were collected to monitor changes within the Shoemaker reach relative to high flow events and to other management actions such as disking vegetated bars and constructing nesting bars. Field data are used to parameterize and calibrate the two-dimensional fixed-bed hydrodynamic model and the two-dimensional mobile-bed model. The key data collected during the three year effort (2013, 2014, and 2015) included:

- High resolution aerial photographs
- LiDAR
- Flow rate, depth, velocity, and water-surface elevation
- Sediment transport (suspended load and grain size distribution)
- Scour and fill monitoring via scour chains



- 45 • Bed material characteristics (grain size distribution, bulk density, porosity)
- 46 • Channel cross-section and longitudinal topography
- 47 • Vegetation type, density, stem diameter, height, and green line elevation on bars
- 48 (established vegetation and where new growth vegetation was apparent) and channel
- 49 banks
- 50 • Channel width
- 51 • Bar topography and morphometry
- 52 • Land-based photography
- 53 • Channel unobstructed view width.

54

55 The three-year study examined four distinct high flow events:

- 56 • 2013 Short Duration Medium Flow (6 days over 2,000 cfs with a 3-day mean peak of
- 57 3,552 cfs)
- 58 • Fall 2013 High Flow (28 days over 2,000 cfs with a 3-day mean peak of 9,700 cfs)
- 59 • June 2014 High Flow (30 days over 2,000 cfs with a 3-day mean peak of 7,320 cfs)
- 60 • June 2015 High Flow (72 days over 2,000 cfs with a 3-day mean peak of 15,700 cfs).

61

62 The 2013 SDMF did not meet the target for a SDHF and the 2013 fall flood was not directly
63 monitored, so the conclusions discussed below pertain primarily to the 2014 and 2015 high flow
64 events and are framed in the context of the three Learning Objectives:

65

66 **1. Evaluate the relationship between peak flows (magnitude and duration) and**
67 **sandbar height and area.**

68

69 The 2013 SDMF was monitored pre and post the high flow event and the magnitude and duration
70 of the event did not demonstrably affect the height and area of sand and vegetated bars in the
71 Shoemaker study reach.

72

73 The Fall 2013 High Flow was not monitored for its effects on the height and area of sand and
74 vegetated bars in the Shoemaker study reach.

75

76 The June 2014 High Flow was monitored pre and post the high flow event and the magnitude
77 and duration was sufficient enough to affect height and area of sand and vegetated bars in the
78 Shoemaker study reach.

79

80 **Sand Bar Height and Area:** Sand bar topography data was analyzed to describe the
81 height and area of new sand bars that evolved during the June 2014 high flow event.
82 Fourteen new sand bars greater than 0.25 acres were formed during the June 2014 high
83 flow event with a mean height of 0.36 feet above the 1,200 cfs TRF stage or a mean
84 depth of 1.55 feet below the formative event 3-day mean peak discharge stage of 7,320
85 cfs. The maximum height of the 3-day mean peak stage above the 1,200 cfs TRF stage
86 was 2.46 feet and the minimum height was 1.49 feet. None of the new sand bars formed
87 to a height to greater than or equal to least tern and piping plover minimum sandbar
88 height criterion of 1.5 feet above the 1,200 cfs TRF stage. Sand bar area decreased from



89 104 acres pre to 48 acres post high flow event for bars greater 0.25 acres in size. Of the
90 48 acres of sand bars greater than 0.25 acres surveyed post high flow, 7 acres were new
91 bars that evolved during the high flow event. Overall there was a net reduction in the
92 number of sand bars greater than 0.25 acres, the minimum sandbar area criterion for terns
93 and plovers.
94

95 **Vegetated Bar Area:** Vegetated bar area in the Shoemaker study reach increased from
96 49 acres pre high flow to 117 acres post the June 2014 high flow event. New vegetation
97 that germinated and grew post high flow was primarily warm season annual plants;
98 barnyard grass, cockle burr, Malabar sprangle top, and common ragweed as opposed to
99 perennials (e.g. eastern cottonwood, willow trees, common reed, curly dock, bulrush sp.,
100 purple loosestrife).
101

102 The June 2015 High Flow was monitored post high flow event and the magnitude and duration
103 that was sufficient to affect the height and area of sand bars and area of vegetated bars in the
104 Shoemaker study reach.
105

106 **Sand Bar Height and Area:** Sand bar topography data collected post 2014 high flow
107 and post 2015 high flow were analyzed to describe the height and area of sand bars that
108 were transformed/created by the June 2015 high flow event. All of the surveyed sand
109 bars (59.6 acres) and 97.8 percent of the vegetated bars (62.1 acres out of 63.5 acres) in
110 the study reach were subjected to river flows during the June 2015 high flow. The June
111 2015 high flow event did not result in the growth of sand bars equal to or greater than 1.5
112 feet above the 1,200 cfs TRF. Twenty-three sand bars greater than 0.25 acres were
113 surveyed post the June 2014 high flow event with a mean height of 0.52 feet above the
114 1,200 cfs TRF stage or a mean depth of 2.14 feet below the formative event 3-day mean
115 peak discharge stage of 15,700 cfs. The mean height of the 3-day mean peak stage above
116 the 1,200 cfs TRF stage was 2.59 feet with a maximum and minimum height of 4.05 and
117 1.38 feet, respectively. The mean height of sand bars above the 1,200 cfs TRF stage
118 surveyed in July 2014 (M=0.36 ft) were found to be significantly higher ($p<0.05$) than
119 sand bars surveyed August 2015 (M=0.52). The number of sand bars in the Shoemaker
120 study reach >0.25 acres decreased from 40 bars surveyed July 2014 to 23 bars surveyed
121 August 2015 and sand bar area increased from 48.5 acres to 59.6 acres, respectively. The
122 formative flow event did increase mean bar height by 0.16 feet, however none of the sand
123 bars met or increased in height to the minimum height of 1.5 feet or higher than the 1,200
124 cfs TRF stage for tern and plover habitat.
125

126 **Vegetated Bar Area:** Vegetated bar area had a net decrease of 53 acres in the
127 Shoemaker study reach from the post 2014 to the post 2015 bar surveys. Sand bars had a
128 net increase of 8 acres and water/river bed area (elevations less than 1,200 cfs TRF stage)
129 increased by 45 acres. The June 2015 high flow was effective at removing vegetated bars
130 in the study reach with the majority being replaced by open water/river bed.
131



132 **2. Evaluate the relationship between peak flows (magnitude and duration) and**
133 **riparian plant mortality.**
134

135 The 2013 SDMF was monitored pre and post the high flow event and the magnitude and duration
136 of the event did not demonstrably affect vegetated bars or the vegetation assessment plots in the
137 Shoemaker study reach.
138

139 **Vegetation Plot Assessment:** Perennial vegetation was present in 24 vegetation plots,
140 nine of which were inundated during the 2013 SDMF. Disturbance of the vegetation did
141 not occur because inundation was shallow and velocity and shear stress were low.
142

143 The Fall 2013 High Flow was not specifically monitored for its effects on vegetated bars or on
144 the vegetation assessment plots in the Shoemaker study reach. However, vegetation surveys
145 prior to the high flow (post 2013 SDMF) and following the high flow (pre-2014 high flow)
146 bracket this flow.
147

148 **Vegetation Plot Assessment:** Nineteen of the 24 plots with perennial vegetation were
149 inundated by the Fall 2013 high flow. Nine of these plots were disked prior to the high
150 flow. All perennial vegetation that was present post 2013 SDMF was removed from
151 inundated plots, with the exception of one plot where disturbance was uncertain.
152

153 The June 2014 High Flow was monitored pre and post the high flow event and the magnitude
154 and duration was sufficient enough to affect vegetated bars and the vegetation assessment plots
155 in the Shoemaker study reach.
156

157 **Vegetated Bar Mortality:** Vegetated bar area increased post the June 2014 high flow
158 event in the Shoemaker study reach by 68 acres. The increase in vegetation was
159 attributable to low Platte River flows (<500 cfs) that exposed sand bars and permitted the
160 germination and growth of annual plants on bars. Any net plant mortality on bars that
161 may have occurred during the June 2014 high flow was negated by the post event low
162 flows that were conducive to the growth of annual plants.
163

164 **Vegetation Plot Assessment:** Sixteen plots with perennial vegetation were inundated in
165 June 2014. Six plots of these plots were disturbed, six plots were undisturbed, and
166 disturbance was uncertain in four plots. This response of perennial vegetation lands
167 between the end members of 2013 SDMF (no perennial vegetation was disturbed within
168 the plots) and Fall 2013 High Flow (all perennial vegetation was disturbed in the plots).
169

170 The June 2015 High Flow was monitored post high flow event and the magnitude and duration
171 was sufficient enough to affect vegetated bars and the vegetation assessment plots in the
172 Shoemaker study reach.
173

174 **Vegetated Bar Mortality:** The June 19, 2015 daily mean flow was 16,000 cfs at Grand
175 Island, NE which is a 15-year recurrence interval peak flow. The magnitude of the June



176 2015 high flow inundated all of the surveyed sand bars (59.6 acres) and 97.8 percent of
177 the vegetated bars (62.1 acres out of 63.5 acres) in the study reach. Vegetated bar area
178 decreased post the June 2015 high flow event in the shoemaker study reach by 53 acres.
179 Sand bar area in the study reach increased by 7.7 acres and water/riverbed area increased
180 by 45.2 acres. The extended period (72 days) of flow greater than 2,000 cfs eroded
181 vegetated bars and inundated sand bars that would typically support the growth of annual
182 plants.

183
184 **Vegetation Plot Assessment:** Disturbance of perennial vegetation during the 2015 High
185 Flow was similar to the disturbance following the Fall 2013 High Flow. Twenty-two
186 vegetation plots with perennial vegetation were inundated. Eight of these plots were
187 disked in the fall of 2014. All perennial vegetation was removed from the inundated
188 plots.

189
190 Hydraulic data was pooled for all vegetation plots with perennial vegetation present for the four
191 high flow events that occurred between 2013 and 2015. The Mann-Whitney-Wilcoxon test was
192 used to compare populations of disturbed and undisturbed plots for depth, velocity, and shear
193 stress. The results of the analysis indicate that there is statistically significant difference
194 ($P < 0.05$) between the disturbed and undisturbed populations for all three hydraulic parameters
195 (depth, velocity, and shear stress). Undisturbed plots have a mean depth, velocity, and shear
196 stress of 0.5 ft, 0.7 ft/s, and 0.9 Pa while disturbed plots have values of 1.8 ft, 2.5 ft/s, and 7.3 Pa.

197
198 These results of the pooled data for all perennial vegetation indicates velocities that disturb the
199 vegetation are relatively low with a mean velocity of 2.5 ft/s. This velocity falls into the
200 “uprooting initiating” velocity class for 1-year old cottonwood, suggesting that there should be
201 some disturbance, but not uprooting of all plants, as observed, which requires a much higher
202 velocity of >10.8 ft/s. There were no plots with 1 or 2-year old cottonwood during the 3-year
203 period to compare results. Pollen-Bankhead et al. (2012) estimated the initiation of uprooting of
204 reed canarygrass to begin when velocities of reed canarygrass is 4.4 ft/s and all plants uprooted
205 requires >28.8 ft/s. Six of the eight plots with reed canarygrass were disturbed (all vegetation
206 removed), one was disked and one was undisturbed. Disturbed plots of reed canarygrass also has
207 lower velocities than required for initiation of uprooting. Velocities at disturbed reed
208 canarygrass plots ranged from 2-4 ft/s, while initiation of uprooting is estimated at 4.4 ft/s and
209 uprooting of all reed canarygrass requires velocities >28.8 ft/s. There were 4 plots with
210 *Phragmites sp.* Two of the plots with *Phragmites sp.* were disturbed by high flows (complete
211 removal of all vegetation in the plot), one plot was disked, and one was undisturbed. Both
212 disturbed plots had velocities < 1.7 ft/s which substantially lower than that required to initiate
213 uprooting (34.8 ft/s), or complete removal >69 ft/s to uproot all plants. There are insufficient
214 data to create new statistical relations for these species; however, the results suggest that the that
215 other forces (such as scour) are likely destabilizing vegetation well below the thresholds required
216 to uproot vegetation by drag forces alone.

217
218 One-dimensional bank erosion modeling using the USDA-ARS BSTEM model was applied to
219 evaluate the relationship between lateral erosion and vegetation mortality. Vegetation root



220 structure can reduce lateral erosion by increasing the resistive forces of the bank. Vegetation
221 mortality can occur when bank failure occurs. The results below are based on a small number of
222 bank sites where detailed information collected (e.g. topography, grain size, root structure,
223 rooting depth) and general observations at the vegetation plots. Banks tended to be stable when
224 roots extended to the toe of the channel and eroded when banks were unvegetated or vegetated
225 with shallow root systems. Bank erosion occurred both during high flows and moderate flows.
226 Bank erosion that was observed during short duration flows (2013 SDMF) and predicted for
227 SDHF was insufficient to produce substantial vegetation mortality as observed in the vegetation
228 plots and bank sites. The 2014 High Flow was a similar magnitude to a SDHF and produced
229 substantially more vegetation mortality due to longer flow duration. Further increasing flow
230 magnitude (as occurred in the Fall 2013 High Flow and 2015 High Flow) results in additional
231 vegetation mortality across bars through a combination of vertical and lateral erosion and high
232 drag forces; however, three of the four modeled bank sites that were stable in 2014 remained
233 stable through the 2015 high flow. These results from the bank sites indicate that deeply rooted
234 plants are highly resistant to hydraulic forces. The role of rooting depth at the vegetation plots is
235 unknown because this parameter was not estimated or measured at these sites.

236
237 **3. Evaluate the ability of the FSM management strategy to create and/or maintain**
238 **habitat for whooping cranes, least terns, and piping plovers.**

239
240 The FSM management strategy includes:

241
242 **Flow:** Augment Q1.5 through flow releases to create short duration high flows (SDHF) of 5,000
243 to 8,000 cubic feet per second (cfs) for 3 days in 2 out of 3 years.

- 244
245
 - 2013 SDMF – The 3-day mean peak discharge was 3,840 cfs with a flow duration of 6-
246 days with flows greater than 2,000 cfs.
 - June 2014 High Flow - The 3-day mean peak discharge was 7,320 cfs and duration of 30-
247 days with flows greater than 2,000 cfs.
 - June 2015 High Flow - The 3-day mean peak discharge was 15,700 cfs and duration of
248 72-days with flows greater than 2,000 cfs.

249
250
251
252 **Sediment:** Augmentation of approximately 150,000 tons of medium sand annually to offset
253 sediment deficit upstream of Kearney.

- 254
255
 - To our knowledge, no sediment was added above Shoemaker during the 3-year study.
256 Measured sediment loads and volume changes within Shoemaker relate to this learning
257 objective by informing the mechanics of habitat (bar) formation.

258
259 **Mechanical:** Channel widening, clearing, and leveling of in-channel bars and flow consolidation
260 (85-90 percent of 8,000 cfs in a single channel).

- 261
262
 - River bed/bars in the Shoemaker study reach were mechanically treated before the first
263 geomorphology survey was completed in March, 2013. Additionally, mechanical



264 treatment of bars/riverbed occurred annually in October and herbicide treatment was
265 early spring.

266
267 The 2013 SDMF did not have a measurable effect on least tern, piping plover and whooping crane
268 habitat. Post the June 2014 and June 2015 high flow 14 and 23 sand bars, respectively were
269 surveyed in the study reach greater than 0.25 acres in size the minimum areal extent for least tern
270 and piping plover habitat. The height of all the surveyed sand bars post 2014 and 2015 high
271 flows were less than least tern and piping plover nesting suitability criterion for sand bar height
272 greater than 1.5 feet above 1,200 cfs TRF stage. The areal extent of sand bars >0.25 acres in size
273 that met minimum nesting suitability criterion of less than 20 percent vegetation coverage (or
274 >80% sand) decreased by 55 acres post the June 2014 high flow and increased by 11 acres post
275 June 2015 high flow.

276
277 The sediment data was not evaluated relative to the creation and maintenance of least tern, piping
278 plover and whooping crane habitat. Changes in sediment storage and the measured (or
279 estimated) sediment loads were as follows:

- 280
- 281 • The 2013 SDMF total sediment load was 27,700 and volume change was a net deficit of
282 16,000 cubic yards (cy).
 - 283 • The Fall 2013 High Flow was not directly monitored and the estimated total sediment
284 load was 170,000 and estimated volume change was a net deposition of 82,920 cy.
 - 285 • The June 2014 High Flow total sediment load was 99,300 tons and volume change was a
286 net deficit of 10,300 cy.
 - 287 • The June 2015 High Flow total sediment load was 966,000 tons and volume change was
288 a net deposition of 48,000 cy.
- 289

290 Sand bar area greater than 0.25 acres in size the minimum areal extent for least tern and piping
291 plover habitat in the mechanically treated portion of the study reach decreased by 50 acres post
292 the June 2014 high flow and increased by 5 acres post the June 2015 high flow. Unobstructed
293 channel width that met whooping crane roosting criterion is 750 ft with a target of 1,150 ft. Of
294 the eighteen monitored river cross sections six mechanically treated segments exceeded the
295 minimum criterion post the 2013 SMF. Eight and 9 mechanically treated segments exceeded the
296 minimum criterion post the June 2014 and June 2015 high flow, respectively.

297 298 **Model Findings**

299
300 Mobile-bed models are sediment transport models that predict changes in the channel form
301 through erosion and deposition. Two models were applied with a focus on Learning Objective 1:
302

- 303 i). The relationship between sediment transport (surplus/deficit) and the frequency of
304 sandbar occurrence.
- 305 ii). The relationship between sediment grain size distribution and sandbar height
306 potential.
- 307 iii). The role of hydrograph duration and shape in sandbar height.



308
309 These analyses were conducted to determine the role of these parameters within the context of
310 the target volume of water available for a SDHF.
311
312 The models were developed and calibrated using measurements collected during the 2013 and
313 2014 high flows. The mobile bed model was not applied to 2015 High Flow because the data
314 collected in 2014 was sufficient to calibrate the model within the flows of interest (SDHF), and
315 the high flow was clearly outside the range of flows (both in magnitude and duration) that the
316 mobile-bed models were developed to analyze.
317
318 The results of the mobile-bed modeling analysis are consistent with field observations in the
319 Shoemaker reach that SDHF events are not likely to create bars with sufficient height or areas to
320 achieve biological objectives. While there were differences in sediment transport (cut/fill) and
321 total number of bars formed, the relative changes in bar area and height during a SDHF were
322 minor. Differences in peak magnitude (5,000 cfs - 8,000 cfs) and duration of peak flow (3 - 6.5
323 days), grain size (0.5, 1 mm, 2 mm) and sediment supply changes (0.5 – 2x sediment supply) did
324 not produce statistically significant changes in the bar forms created during the SDHF. These
325 results are limited to the effect of one SDHF event. The conclusion from the modeling analysis
326 is consistent with field measurements of barform changes following a short duration medium
327 flow and three distinct high flow events (Fall 2013, June 2014 and June 2015) that met or
328 exceeded the target SDHF.
329



330

I. INTRODUCTION

331 In 2013, the Platte River Recovery Implementation Program (Program) contracted EA
332 Engineering, Science, and Technology, Inc., PBC (EA) to implement a Flow-Sediment-
333 Mechanical (FSM) Proof of Concept Experiment. Team members for the implementation of the
334 Experiment include: GMA Hydrology (GMA) fluvial geomorphology and sediment transport
335 monitoring, Northern Hydrology and Engineering (NHE) hydraulic and sediment transport
336 modeling, and Western Ecosystems Technology, Inc. (WEST) vegetation monitoring, mapping
337 and classification. This report presents results of the third year of “Proof of Concept” monitoring,
338 modeling, data analysis, and a summary of the three-year experiment findings.

339

340 Year 3 monitoring and data analysis efforts focus on a natural high flow event. The monitored
341 runoff period during which discharge was greater than 2,000 cubic feet per second (cfs) lasted
342 from May 11, 2015 to July 21, 2015 and produced a peak discharge of 16,100 cfs at the Grand
343 Island gaging station. Year 3 modeling included hydrodynamic predictions for the natural high
344 flow event and the effect of a hypothetical SDHF event with a range of sediment supplies and
345 grain sizes.

346

347 Section II and III provide the purpose and experiment design, respectively for the FSM “Proof of
348 Concept” Experiment. Section IV presents the methods used to collect relevant data pre and post
349 a high flow event during Year 3, and Section V presents the results of the Year 3 field data.
350 Section VI provides a summary of the Year 3 model objectives and results; further detail can be
351 found in Attachments I and II. Section VII presents the findings of the FSM action on the
352 geomorphology of the Platte River relative to the “Learning Objectives” for the Shoemaker
353 Island Complex Management Experiment during Year 3. Section VIII presents a discussion of
354 the inter year observations (2013, 2014, and 2015) of the geomorphologic changes of the Platte
355 River relative to the high flow events in the Shoemaker Study Reach.

356



357

II. PURPOSE

358 II.A. Program Management Objectives and Management Strategies

359 The Program's management objectives are to 1) improve survival of whooping cranes during
360 migration, 2) improve least tern and piping plover production, and 3) avoid adverse impacts to
361 pallid sturgeon in the Lower Platte River. The Program is tasked with evaluating the ability of
362 the FSM management strategy to achieve these management objectives. The FSM strategy
363 includes the following management actions:

364

365 1) Flow— Augment Q1.5 through flow releases to create short duration high flows (SDHF)
366 of 5,000 to 8,000 cfs for 3 days in 2 out of 3 years.

367

368 2) Sediment— Augmentation of approximately 150,000 tons of medium sand annually to
369 offset sediment deficit upstream of Kearney.

370

371 3) Mechanical— Channel widening, clearing, and leveling of in-channel bars and flow
372 consolidation (85-90 percent of 8,000 cfs in a single channel).

373 II.B. Hypotheses

374 The Program uses a process of rigorous adaptive management to reduce uncertainty associated
375 with the ability of management actions to create and/or maintain suitable habitat for the
376 Program's target species. This is achieved by explicitly acknowledging uncertainty in the form
377 of alternative hypotheses of management action performance and testing the hypotheses through
378 implementation of management experiments. Uncertainty associated with implementation of the
379 FSM management strategy is formalized in the Program's Adaptive Management Plan (AMP) in
380 the form of physical process broad and priority hypotheses. Broad hypotheses that pertain to the
381 FSM management strategy include:

382

383 **PP-1:** Flows of varying magnitude, duration, frequency, and rate of change affect the
384 morphology and habitat quality of the river, including:

385

386 • Flows of 5,000 to 8,000 cfs magnitude in the habitat reach for a duration of 3 days at
387 Overton on an annual or near-annual basis will build bars to an elevation suitable for least
388 tern and piping plover habitat.

389

390 • Flows of 5,000 to 8,000 cfs magnitude in the habitat reach for a duration of 3 days at
391 Overton on an annual or near-annual basis will increase the average width of the
392 vegetation-free channel.

393

394 • Variations in flows of lesser magnitude will positively or negatively affect the sandbar
395 habitat benefits for least terns and piping plovers.

396



397 **PP-2:** Between Lexington and Chapman, eliminating the sediment imbalance of approximately
398 400,000 tons annually in eroding reaches will:

- 399
- 400 • Reduce net erosion of the river bed.
- 401
- 402 • Increase the sustainability of a braided river.
- 403
- 404 • Contribute to channel widening.
- 405
- 406 • Shift the river over time to a relatively stable condition, in contrast to present conditions
407 where reaches vary longitudinally between degrading, aggrading, and stable conditions.
- 408
- 409 • Reduce the potential for degradation in the north channel of Jeffrey Island resulting from
410 headcuts.
- 411

412 **PP-3:** Designed mechanical alterations of the channel at select locations can accelerate changes
413 towards braided channel conditions and desired river habitat using techniques including:

- 414
- 415 • Mechanically cutting the banks and bars to widen the channel to a width sustainable by
416 Program flows at that site, and distributing the material in the channel.
- 417
- 418 • At specific locations, narrowing the river corridor and increasing stream power by
419 consolidating more than 85 percent of river flow into one channel will accelerate the plan
420 form change from anastomosed to braided, promoting wider channels and more sandbars.
- 421
- 422 • Clearing vegetation from banks and bars will help to increase the width-to-depth ratio of
423 the river.
- 424

425 These hypotheses provide a broad view of the possible changes in river morphology/channel
426 characteristics that may be produced through implementation of FSM management actions.

427
428 The following more detailed hypotheses address uncertainty in underlying physical process
429 relationships and are formalized in the AMP as flow, sediment, and mechanical priority
430 hypotheses. Tier I physical process priority hypotheses include:

431
432 **Flow #1:** Increase the variation between river stage at peak (indexed by Q1.5 flow at Overton)
433 and average flows (1,200 cfs index flow), by increasing the stage of the peak (1.5-year) flow
434 through Program flows, will increase the height of sandbars between Overton and Chapman by
435 30 percent to 50 percent from existing conditions.

436
437 **Flow #3:** Increase 1.5-year Q with Program flows will increase local boundary shear stress and
438 frequency of inundation at existing green line. These changes will increase riparian plant
439 mortality along margins of channel, raising elevation of green line. Raised green line equals
440 more exposed sandbar area and wider unvegetated main channel.



441
442 **Flow #5:** Increase magnitude and duration of a 1.5-year flow will increase riparian plant
443 mortality along the margins of the river. There will be different relations (graphs) for different
444 species.

445
446 **Sediment #1:** Average sediment augmentation near Overton of 185,000 tons/year under existing
447 flow regime and 225,000 tons/year under Governance Committee (GC) proposed flow regime
448 achieves a sediment balance to Kearney.

449
450 **Mechanical #2:** Increase the Q1.5 in the main channel by consolidating 85 percent of the flow,
451 and aided by Program flow and a sediment balance, flows will exceed stream power thresholds
452 that will convert main channel from meander morphology in anastomosed reaches to braided
453 morphology with an average braiding index greater than 3.

454 **II.C. Experiment Purpose**

455 The Shoemaker Island Complex is located in the downstream portion of the Associated Habitat
456 reach where the channel is assumed to be in sediment balance, which is one of the reasons why
457 this area was chosen for implementation of a replicate “Proof of Concept” management
458 experiment. The experiment will evaluate the performance of the FSM management actions, as
459 discussed above, in creating and/or maintaining channel characteristics that are consistent with
460 the Program’s management objectives. Learning objectives provided in the Request for Proposal
461 for the Shoemaker Island Complex management experiment include:

462
463 **1) Evaluate the relationship between peak flows (magnitude and duration) and**
464 **sandbar height and area.** Understanding the relationship between river stage at peak
465 discharge and sandbar height in relation to maximum water surface elevation are
466 fundamental to testing the Program’s FSM management strategy. The Environmental
467 Impact Statement (EIS) analysis assumed that sandbars form to the water surface
468 elevation during high flow events but that under the current flow regime, the difference
469 between the 1.5-year return frequency flow elevation and the normal water surface
470 elevation during the summer nesting months is not sufficient to create sandbars that are
471 high enough for nesting. As such, doubling the 1.5-year return frequency flow from
472 approximately 4,000 cfs to approximately 8,000 cfs would increase bar heights by 30
473 percent to 50 percent as presented in Priority Hypothesis Flow 1. Sandbar formation
474 during the natural flow events of 2010 and 2011, which exceeded SDHF magnitude and
475 duration, indicates that sandbars are not forming to the water surface elevation during
476 high flow events; however, this has raised additional questions about:

- 477
478 i). The relationship between sediment transport (surplus/deficit) and the frequency of
479 sandbar occurrence.
480 ii). The relationship between sediment grain size distribution and sandbar height
481 potential.
482 iii). The role of hydrograph duration and shape in sandbar height.

483



- 484 **2) Evaluate the relationship between peak flows (magnitude and duration) and**
485 **riparian plant mortality.** Understanding the relationship between flow and riparian
486 plant mortality is fundamental to testing the Program’s FSM management strategy.
487 Modeling conducted during the EIS development indicated that increasing the 1.5- year
488 return frequency flow from approximately 4,000 cfs to approximately 8,000 cfs through
489 the use of SDHF in 2 years out of 3 years (under sediment balance) would increase
490 riparian plant mortality sufficiently to maintain wide, braided, unvegetated main channels
491 with exposed sandbars. This relationship is presented in Program Priority Hypotheses
492 Flow 3. Analysis of existing system and project-scale vegetation monitoring is ongoing.
493 Preliminary results indicate a need to continue to evaluate the interaction between scour
494 and inundation mortality as well as the role of lateral erosion in vegetation removal from
495 sandbars.
496
- 497 **3) Evaluate ability of FSM management strategy to create and/or maintain habitat for**
498 **whooping cranes, least terns and piping plovers.** Linking physical process
499 relationships to target species habitat requirements is fundamental to the development of
500 management experiment performance criteria and action adjustments. The overarching
501 Program objectives relate to target species survival and productivity. As such, Program
502 management strategies must be capable of creating and/or maintaining river conditions
503 that are suitable for achieving those objectives. Specifically, the FSM management
504 strategy must be able to scour enough vegetation to maintain unobstructed view widths
505 suitable for whooping crane roosting, and build/maintain bars of sufficient height and
506 lack of vegetation to function as least tern and piping plover nesting habitat.



507

III. EXPERIMENT DESIGN CONSIDERATIONS

508 This document describes the field activities that were completed during the 2015 Shoemaker
509 Island FSM “Proof of Concept” Experiment. Many factors and lessons learned from the 2013
510 and 2014 experiment monitoring and data analysis (PRRIP 2014 and PRRIP 2015a) were
511 considered for the 2015 Shoemaker Island FSM “Proof of Concept” project, including the
512 location, duration, data needs for model input, and refinement of methods and procedures used
513 during the 2013 and 2014 field data collection activities. The Shoemaker Island Flow-Sediment-
514 Mechanical “Proof of Concept” Experiment Monitoring and Analysis Plan (PRRIP 2015b)
515 presented the plans for the experiment monitoring and analysis.

516

517 The 2015 Shoemaker Island FSM “Proof of Concept” experiment monitoring is the third and
518 final year of monitoring for the three-year experiment. This document describes the field
519 activities and subsequent analyses that were completed during 2015.

520 III.A. Overview of Data Collection

521 The Shoemaker Island Complex was selected for this FSM “Proof of Concept” due to its location
522 and its suitability to investigate a number of the Program’s hypotheses. The primary focus of
523 fieldwork efforts was to monitor changes within the Shoemaker reach relative to high flow
524 events and relate those changes to other management actions such as diking vegetated bars and
525 construction of nesting bars. Monitoring in 2015 describes geomorphic change related to a
526 significant high flow event: the June 2015 high flow at 16,100 cfs Total River Flow (TRF)
527 instantaneous peak discharge at the Grand Island gage on June 19, 2015 (a nearly identical peak
528 occurred on June 5, 2015 at 16,200 cfs, but the June 5 peak was slightly higher at Shoemaker,
529 thus we refer to the June 19, 2015 event as the annual peak). Data collected fell into three
530 primary categories, though many data types fall into multiple categories:

531

532 1. Geomorphic monitoring

533

534 2. Model development, calibration and verification

535

536 3. Vegetation monitoring

537

538 The geomorphic and vegetation monitoring of the Shoemaker reach included numerous elements
539 which also supported modeling efforts, notably:

540

- 541 • Sediment loads were computed using 2015 sample data, continuous discharge and
542 checked against estimates based on 2013-2014 datasets.

- 543 • Volume change and topographic changes were developed from cross section and
544 longitudinal profile surveys.

- 545 • Scour rates, bed and bar grain size distributions, water surface slope and stage at cross
546 sections were measured.



- 547 • Continuous discharge monitoring and limited bedload sampling were conducted during
548 the 2015 monitoring effort.

549
550 The primary predictive components of the experiment design are the two-dimensional fixed-bed
551 and mobile-bed hydrodynamic models. Field data are used to parameterize and calibrate the
552 models. Many tasks, such as stage observations at cross sections, provide calibration and
553 thereby increase model accuracy. Virtually all monitoring tasks provide intrinsic value to the
554 Program as stand-alone metrics; were the mobile-bed model effort to be inconclusive, most of
555 the other monitoring tasks provide direct evaluation of management actions and channel
556 response.

557 **III.B. Area of Interest**

558 The Shoemaker Island Complex was selected for this FSM “Proof of Concept” due to its location
559 on the river where it is assumed that sediment is in balance (i.e. the sediment loads entering and
560 exiting the reach are approximately equal and the reach is neither aggrading nor degrading) and
561 is not directly impacted by irrigation or transportation infrastructure. The FSM “Proof of
562 Concept” Experiment documented degradation in the study reach of 16,000 cubic yards (cy) in
563 2013 and 10,300 cy of degradation in 2014 (PRRIP 2014 and PRRIP 2015a). The fall 2013 high
564 flow event which was not monitored produced a net deposition of 82,900 cy in the study reach
565 (PRRIP 2015a).

566
567 The Shoemaker Island Complex is located approximately 12 miles southwest of Grand Island,
568 Nebraska (Figure 3-1). Access to Program lands was provided via two gates along Shoemaker
569 Island Road. The study site begins approximately 1.6 miles downstream of Highway 11 (Wood
570 River Road), and extends 2.6 miles downstream to a point approximately 1.1 miles upstream of
571 South Alda Road (Figure 3-1).

572 **III.C. Data Collection**

573 Aerial photographs, taken July 2015, were obtained from the Program to facilitate development
574 of a site study plan in which cross section locations, profile alignments, and sampling sections
575 were determined. The resulting data collection locations within and surrounding the study site
576 are summarized and illustrated on monitoring network site maps provided in Appendix A;
577 Figures A-1 through A-3.

578
579 The 2015 spring runoff began unusually early and was of significant magnitude that no “Pre”
580 data were collected. The following summarizes the key data collected during and after the spring
581 runoff period:

- 582
583 • Flow rate, depth, velocity, and water-surface elevation
584 • Sediment transport (suspended load, and grain size distribution)
585 • Bed material characteristics (grain size distribution, bulk density, porosity)
586 • Channel cross-section and longitudinal topography



- 587 • Vegetation type, density, stem diameter, height, and green line elevation on bars
- 588 (established vegetation and were new growth vegetation was apparent) and channel banks
- 589 • Channel width
- 590 • Bar topography and morphometry
- 591 • Land-based photography
- 592 • Channel unobstructed view width



593

IV. MONITORING AND ANALYSIS METHODS

594 The monitoring and analysis methods conformed to the established Project-Scale
595 Geomorphology and Vegetation Monitoring protocol (PRRIP 2011), the detailed methods are
596 presented in the Experiment and Monitoring and Analysis Plan (PRRIP 2015b). The field
597 activities completed for the 2015 Shoemaker Island FSM “Proof of Concept” experiment did not
598 address all of the tasks specified in the monitoring and analysis protocol and plan. The desired
599 experiment called for the completion of a pre high flow, high flow, and post high flow
600 monitoring. Pre high flow monitoring was not performed in the spring of 2015 due to
601 persistently high flows in the Platte River that prevented safe wading access to the river. Data
602 analysis for the 2015 FSM experiment focuses on geomorphic change between the June 2014
603 and the August 2015 monitoring efforts relative to the June 2015 natural high flow event.
604

605 The June 2015 high flow, peaking at 16,100 cfs, in the Grand Island gaging station hydrograph,
606 occurred from May 11, 2015 to July 20, 2015. Post high flow monitoring data were collected
607 from August 24, 2015 to August 28, 2015 and September 1, 2015 to September 2, 2015. The
608 following summarizes the data that were collected during and following the June 2015 high flow.
609

610 Sampling activities during the June 2015 high flow:

- 611
- 612 • Maintained and downloaded automated stage and turbidity recorders
- 613 • Conducted stage monitoring at 18 cross sections
- 614 • Conducted depth and velocity (discharge) measurements between cross sections 2 and 3
- 615 • Conducted suspended sediment depth integrated sampling between cross sections 2 and 3
- 616 • Conducted box suspended sediment depth integrated sampling between cross sections 2
- 617 and 3
- 618 • Collected bedload samples to compare with Modified Einstein predictions of total
- 619 sediment load
- 620

621 Sampling activities following the June 2015 high flow:

- 622
- 623 • Surveyed 18 monumented cross sections
- 624 • Surveyed 19 supplemental cross sections
- 625 • Surveyed exposed bars
- 626 • Maintained and downloaded automated stage recorders
- 627 • Conducted suspended sediment depth integrated sampling between cross sections 2 and 3
- 628 • Completed ground photography
- 629 • Collected bed and bar material samples
- 630 • Conducted vegetation sampling at assessment plots
- 631 • Field verified vegetation cover polygons for models
- 632 • Conducted depth and velocity (discharge) measurements between cross sections 2 and 3
- 633 • Monitored scour chains (none were found)



634 **IV.A. Topography and Bathymetry**

635 Topography and bathymetry data were obtained using several approaches, including LiDAR
636 survey, ground surveys at primary and supplemental river cross sections, and bar topography.
637

638 Topographic, bathymetric, and ground surveys were completed using survey-grade Real Time
639 Kinematic (RTK) / Global Positioning System (GPS) survey equipment. Primary Survey control
640 points established on March 22, 2013 by a licensed Nebraska Surveyor were used to facilitate the
641 2015 base station deployments. The horizontal reference datum for all surveys was in North
642 American Datum of 1983 (NAD 1983) and the vertical reference datum was the North American
643 Vertical Datum of 1988 (NAVD 1988). The Nebraska State Plane Coordinate System in US
644 survey feet was utilized.

645 **IV.A.1. Primary River Cross Sections**

646 The primary river cross sections were oriented perpendicular to the river center-line, and cross-
647 sections were spaced approximately 800 feet apart. Eighteen cross sections were established
648 throughout the 2.6 mile long reach of the Platte River as shown in Figure 3-2 and in Appendix
649 A-1 to A-3. Nineteen supplemental cross sections were established between the primary cross
650 sections to provide improved spatial resolution for volume change calculations. The primary and
651 supplemental river cross sections were surveyed September 1 and 2, 2015.
652

653 Existing monuments established by the Program for the Channel Geomorphology and In-channel
654 Vegetation Monitoring (PRRIP 2011) were utilized as control points by the licensed surveyor.
655 Temporary benchmarks were established for local base station deployment for the post high flow
656 survey. Capped rebar monuments were established on the north and south banks of the Platte
657 River at the 18 cross sections (Figure 3-2), with a few exceptions. Top-of-bank access was not
658 granted to the south bank of the Platte River from cross section 1 to cross section 9. Pins
659 successfully placed at the top of bank are designated with “Set.” Pins that could not be placed
660 due to restricted access are designated with an “R” for the south bank of the river. The
661 coordinates and elevations for the cross section pins, and benchmarks are included in Table 4-1.
662

663 For each cross section easting, northing, and elevation data points were taken for defined features
664 across the cross section. Features were identified and logged in the data recorder when a point
665 was taken. At a minimum, the following features were noted:

- 666 • Left and right bank pins
- 667 • Top and toe of bank
- 668 • Left and right edge of water at main banks
- 669 • All edges of water across the cross section
- 670 • Top and toe of bank for each bar
- 671 • Bed or ground elevation along the cross section green line (where vegetation cover
672 exceeds 25 percent)
- 673 • Edge of canopy of permanent woody vegetation greater than 1.5 meters tall



- 674
- 675
- 676
- 677
- Any other significant geomorphic feature in the cross section, including whether the flow is consolidated at the cross section or if flow is split between multiple channels
 - Other points of interest identified by the investigators

678 A standard set of survey codes was developed to describe significant features that were surveyed
679 (Table 4-2). To adequately define the channel bed, GPS readings were taken at significant
680 breaks in slope. The Stakeout Line function on the survey data logger was used to ensure
681 repeatable straight line surveys defined by paired cross section monument pins. All cross section
682 data collected during the survey were downloaded and compiled electronically into spreadsheets
683 for analysis, and used in identifying volumetric changes of the channel over time.

684

685 The survey of a bar's perimeter and transects was completed as part of the bar topography—
686 described in later sections. The edge of mature vegetation and new annual vegetative growth on
687 bars was noted during the survey. The study area was limited to the main Platte River channel
688 on the south side of Shoemaker Island, and did not include survey of the smaller channel
689 approximately 2 miles north of the study area.

690

691 Cross section data were edited during post processing to minimize implied topographic change
692 resulting from variation in point density, point location or survey alignment as follows:

- 693
- Alignments for anomalous points were checked in ArcGIS
 - Cross sections were checked against bar surveys
 - Cross sections were checked against the approximate peak water surface elevation to determine locations which were not inundated

694

695

696

697

698

699 For volume change computation, the average end area method was used to compute change
700 between the 2014 post monitoring event and September 2015 post monitoring event. The
701 primary drivers of geomorphic change during this period are the February 2015 ice floe (Figure
702 4-1) and the June 2015 high flow. Volume change was calculated using the 18 monumented
703 cross sections and the 19 supplemental cross sections (n=37). The cross section data were
704 examined in ArcGIS. Areas showing anomalous results (e.g. deposition or erosion in areas that
705 were not inundated or areas in which nesting bars had been constructed near the western project
706 boundary) were omitted from area change calculations. Areas of lateral erosion were identified
707 and summed as a separate category. Changes above the peak flow elevation were included if
708 they were associated with vertical bank failure resulting from lateral erosion. Vertical incision at
709 the toes of banks was included in “lateral erosion” when it occurred inland of the former toe. The
710 distance between cross-sections was measured along the channel centerline. The changes in cross
711 section area were averaged from one section to the next, and then multiplied by the distance
712 between sections. The resulting volume of cut and fill between each section was summed over
713 the reach.

714

715 Supplemental ground cross sections were surveyed to provide additional
716 topographic/bathymetric data (and primarily, to add resolution/accuracy for volume change
717 calculations) above, below, and within the study area. Within the study area 17 supplemental



718 cross sections located equidistant between the 18 primary cross sections were surveyed and a
719 cross section was completed approximately 400-feet upstream and downstream of primary cross
720 section 1 and 18 (Figure 3-2). This effort resulted in a total of 19 additional cross sections within
721 and adjacent to the study reach. Supplemental cross sections were surveyed using RTK/GPS
722 post June 2015 high flow. The supplemental cross sections were also used to facilitate surface
723 development for the fixed-bed and mobile-bed hydrodynamic models (Attachments I and II).

724
725 Supplemental ground survey cross sections were surveyed across the channel using similar
726 methods to the primary river cross sections. The Stakeout Line function on the survey data
727 logger utilized established coordinates to delineate cross sections and ensured repeatable straight
728 line surveys (Table 4-1). Each cross section extended across all active channels and bars of the
729 Platte River and extended from the confining bank to confining bank, but did not include the
730 upland portions of the cross section beyond the potential bank erosion/deposition zone, or areas
731 where access was not permitted.

732 **IV.A.2. Bar Topography**

733 Survey data were collected to define the shape and topography of all natural and constructed
734 bars. A bar is defined as the portion of the ground surface that is dry at 1,200 cfs TRF. The
735 water surface elevation at 1,200 cfs TRF was estimated throughout the study reach with a 2D
736 model (see Attachment 1). The model result (a .TIN file) was imported into the Carlson SurvCE
737 data logger software. The predicted water surface elevation was used as a guide by the survey
738 crew to ensure that “toe” survey points extended to the edges of the bars at 1,200 cfs TRF. This
739 approach was particularly helpful when flows were higher than 1,200 cfs TRF and the edge of
740 the bar was submerged.

741
742 Data collected included: cross-stream and longitudinal (i.e., parallel to flow) transects, the top-
743 of-bank and toe-of-bank perimeter of each bar, and any supplementary survey points deemed
744 necessary by the survey crews to adequately define the topography of the bar surface. The
745 surveys included a minimum of three cross-stream transects, with maximum spacing of 200 feet.
746 For bars less than 1 acre in size, a single longitudinal transect was surveyed from the midpoint of
747 the upstream end of the bar to the midpoint of the downstream end of the bar, with doglegs as
748 needed to run through the highest “crest” of the bar. For bars larger than 1 acre in size, at least
749 two additional transects were surveyed approximately midway between the primary longitudinal
750 transect and the water’s edge on either side of the bar. Ground photography was also completed
751 for each bar above the water-surface elevation at the time of the survey.

752
753 One-hundred and forty-one bars were individually surveyed post high flow from August 24,
754 2015 to August 28, 2015 in the Shoemaker study reach by the survey crew. Five bars were
755 located on property that was not accessible because permission was not granted by the
756 landowner. Generally, the bars were numbered from upstream to downstream with a few
757 exceptions.

758
759 To assess the ability of a high flow event to create and/or modify bars in the Shoemaker study
760 reach area the vegetation coverage of surveyed bars was assessed pre (July 2014) and post



761 (August 2015) the monitored high flow (June 2015). Bars were grouped to evaluate the effect of
762 Program activities on the bars, suitability of bars for tern and plover habitat and the ability of a
763 high flow event to create new bars.

764

765 • Natural bars and treated bars. A natural bar is a bar or area of the river bed that has not
766 been treated by Program activities. A treated bar is a bar or area of the river bed that was
767 mechanically treated by Program diking in September 2014. The treated area surveyed
768 in the Shoemaker study reach is presented in Figure 5-5.

769 • Sand bars and vegetated bars. A sand bar is a bar whose area above 1,200 cfs TRF stage
770 is 80 percent or greater sand. A vegetated bar is a bar whose area above 1,200 cfs TRF
771 stage is 20 percent or greater vegetated.

772 • Bars less than 0.25 acres and bars greater than 0.25 acre. A bar area in acres is
773 determined at the 1,200 cfs TRF stage.

774

775 Bar survey data were loaded into ArcGIS with Spatial Analyst extension for analysis. A
776 topographic surface (raster) of the study reach after the June 2015 high flow was developed
777 using survey data and supplemental LiDAR data. LiDAR was used to develop the topography of
778 bars, or portion of bars, that were not surveyed and for the floodplains.

779

780 Bars were delineated by computing the difference between the bed elevation and the predicted
781 water surface elevation at 1,200 cfs TRF (see Attachment 1). Negative values are areas where
782 the bed is below water (no bar) and positive values are bars. This calculation resulted in all
783 surveyed bars set to a zero elevation at the edge of the bar and height is the bar height above the
784 1,200 cfs TRF water surface elevation. Bar features were entered into a GIS attribute table for
785 each bar surveyed for data analysis. Bar attributes included: July 2014 and August 2015 survey,
786 treated or natural, sand or vegetated, and bar area at the
787 1,200 cfs TRF elevation.

788

789 Mean bar height is computed by averaging the height of all
790 cells in each polygon. Mean bar height can change by
791 changes to the bar such as: (1) direct erosion of an existing
792 bar (e.g. vertical erosion), (2) deposition on top of an
793 existing bar, and/or (3) deposition adjacent to the existing
794 bar. Mean bar height may increase without deposition on the
795 bar if lower areas of the bar are eroded. Mean bar height
796 may decrease without erosion of the bar if deposition occurs
797 that has a lower elevation than the rest of the bar.

798 **IV.A.3. Longitudinal Profile**

799 Longitudinal profiles were surveyed through the reach to
800 provide a post June 2015 high flow ground surface. Surveys
801 were conducted by wading and using the same GPS/RTK
802 system described earlier (see adjacent photo). Longitudinal



**GPS/RTK longitudinal profile
surveying.**



803 profiles typically followed the dominant flow paths of deepest water and where possible,
804 followed the 2014 alignment.

805 **IV.B. Documentation of Bank and Channel Features Using Ground Photography**

806 Ground photography was captured at each primary river cross section to document and describe
807 bank condition, vegetation type, structure, and bar features. Four photographs were taken on
808 each bank of the main channel from the monument point, with the photographs oriented across
809 the channel, looking up and downstream, through the cross section, and back towards the bank.
810 The up and downstream oriented photo points were located at least 25 feet from the cross section
811 line and a survey flag was placed on the cross-section line for visual identification.

812
813 Three photographs were also taken on the perimeter of each bar; one at the upstream midpoint of
814 the bar looking downstream across the bar, and one at the downstream midpoint of the bar
815 looking upstream. When the entire bar was not visible in the photographs, additional photos
816 were taken with similar up and downstream oriented views from appropriate location(s) in the
817 middle of the bar so that the collection of photos covers essentially the entire bar.

818
819 Additional photographs and survey points document scour chain locations, stage monitors, and
820 bulk sample and bulk density sample locations. The location of the photo points were
821 documented with a GPS camera and cross section/bar identification, point identification
822 included; date, time, lens, azimuth, and waypoint number for each photograph.

823 **IV.C. Bed and Bar Material Sampling**

824 Bed and bar material samples were collected post June 2015 high flow, concurrent with
825 topography survey of the river bars. Due to natural variation in grain size in river channels,
826 multiple samples were collected in the channel and on the bars to provide a well-distributed
827 sample set and reduce uncertainty in bed and bar material data. When possible, 2014 sample
828 locations were reoccupied.

- 829
- 830 • Main Channel Bed Samples— A minimum of two bed material samples were collected in
831 the main channel at every other surveyed cross section, at or near the cross section
832 primary flow line.
 - 833
 - 834 • Bar Samples— Collected from emergent natural and constructed bars larger than 0.4
835 acres at some cross sections. If a surface armor layer or coarse surface layer was present,
836 it was noted and the surface was sampled separately prior to sampling the subsurface
837 material.
 - 838

839 Bed samples were collected with a rigid ABS tube that contained slightly less volume than the
840 sample bags. The tube had a beveled end to allow for easy dredging; the other end was open and
841 covered with a very fine mesh screen that trapped the sediment, while allowing water to pass
842 through. Using a sampler that has slightly less volume than the sample bags allowed the entire



843 sample to be placed directly into the bag without the potential for sorting or loss of fines. This
844 also allowed for a similar volume of material to be sampled each time at each sample point.

845
846 Bulk density samples were collected on bars by driving a 3-inch diameter by 6-inch-long
847 cylinder into a bar surface to its full depth, then excavating down to the aperture and carefully
848 incising a flat blade across the aperture to trap the sample in the cylinder.

849
850 All bed/bar samples were transferred to individual sample bags, labeled with the cross section
851 ID, sample number, and date the sample was taken. The location of the sample was recorded
852 with the RTK rover. Samples were shipped to the GMA Coarse Sediment Laboratory in
853 Placerville, California. Samples were sieve-analyzed for grain size distribution and—in the case
854 of bulk density samples—for total mass and density. The samples were processed in accordance
855 with ASTM Standard D422. The results reported for each sample were compiled in Microsoft
856 Excel and include the sample description, total sample weight, and the weight and percent
857 passing for each of the sieve sizes. The D5, D16, D50, D84, D95 grain size of each sample was
858 also reported.

859 **IV.D. Vegetation Type, Density, and Green Line**

860 Vegetation monitoring methods for Shoemaker Island are described in the following sections.

861 **IV.D.1. Vegetation Survey**

862 The vegetation plots assessed for the 2015 experiment were established during the 2013 “Proof
863 of Concept” Experiment. A hand held sub-foot GPS unit was used to relocate the center of the
864 2013 plot and the vegetation was surveyed for the 2015 experiment. A total of seven vegetative
865 assessment plots were located along each of the 18 primary river cross sections for a total of 126
866 plots within the study reach. These plots were measured post the June 2015 high flow, to
867 provide an assessment of the vegetation present. Each vegetation assessment plot was a 3.3 feet
868 x 3.3 feet (1 meter x 1 meter) quadrat and were evenly spaced along the cross section starting
869 randomly from the north side. The plots were offset upstream from the cross section by 5 feet or
870 more to avoid disturbing vegetation underneath the cross section line during other work.
871 Oblique and vertical photos of all plots were taken using a GPS camera. The following data
872 were collected at each plot:

- 873
- 874 • Density of live and dead stems of eastern cottonwood, willows, and common reed
875 (*Phragmites sp.*).
 - 876 • Presence of other species (presence/absence).
 - 877 • Photos showing total percent vegetation and percent sand.
- 878

879 **IV.D.2. Vegetation Roughness**

880 Polygons delineating aerial extent of uniform vegetation on the bars were mapped using ArcGIS
881 to identify areas of uniform hydraulic roughness for modeling. When warranted, bars were



882 subdivided to account for variation in bar vegetation and sand areas with no vegetation. Stem
883 counts (all stems), stem diameter, and stem heights were determined by vegetation types for
884 several 3.3 feet x 3.3 feet (1-meter x 1-meter) sub-plots across the polygon of a bar. Vegetative
885 counts for several plots were averaged and extrapolated to obtain stem density, average stem
886 diameter and height for the uniform vegetative polygons. The number of plots taken per polygon
887 was determined in the field by the plant biologist to adequately describe the vegetation based on
888 density, type of vegetation, and areal extent of the polygon.

889 **IV.D.3. Vegetation Green Line**

890 A vegetation green line is the edge of vegetation on a bar or wetted channel, defined by at least
891 25-percent vegetative cover. Green line edges were surveyed during the primary and
892 supplemental cross section surveys and the bar topography surveys. Surveyed green line edge
893 data was used to define vegetative bar area and elevation.

894 **IV.E. Stage Recorders**

895 In-Situ Inc. Level TROLL® 500 pressure transducers were installed between cross sections 2
896 and 3 and at cross section 18 to record river stage during the 2015 “Proof of Concept”
897 Experiment. Transducer elevations were surveyed during the primary cross section topography
898 surveys. The vented transducers were installed April 18, 2015 at cross section 18 and May 24,
899 2015 between cross section 2 and 3, set to record river stage in feet at 15-minute intervals and
900 monthly maintenance and downloading of data collected by the pressure transducers was
901 scheduled for the duration of the study.

902
903 Water surface elevation is a model input and is the primary calibration parameter for the two-
904 dimensional hydrodynamic model. Stage references (t-posts) were established along the north
905 bank of some cross sections. Posts were surveyed using 3 minute occupations to a vertical
906 accuracy of approximately 0.03 feet. Water surface elevations (stage) were manually measured
907 from the posts down to the water surface during the peak of runoff, providing field verification
908 of stage and a water surface slope through the reach.

909 **IV.F. Discharge**

910 Continuous discharge data were required for modeling and sediment load computation for the
911 period of interest: the June 2015 high flow. Direct discharge measurements were collected
912 during and after the June 2015 high flow. Computed continuous discharge data were compared
913 with from one or more the following sources:

- 914
- 915 • USGS 15-minute gage data for Kearney (USGS 06770200),
 - 916 • Nebraska Department of Natural Resources (NDNR) 30-minute gage at Shelton; and
 - 917 • USGS 15-minute gage data at Grand Island (USGS 06770375).
- 918

918
919 The project site is located:



- 920
- 921
- 922
- 923
- 924
- 32 miles downstream of the United States Geological Survey (USGS) gage near Kearney;
 - 10.3 miles downstream of the NDNR Shelton Road gage; and
 - 13.5 miles upstream of the Highway 34 USGS gage east of Grand Island.

925 The gages listed above measure total river discharge. Fifteen-minute discharge records were
926 obtained for (1) the basis of any scaled discharge relations for Shoemaker (using the TRF ratio
927 developed from the Shoemaker HEC-RAS model, generally 82 percent), and (2) for
928 hydrographic comparison with hydrographs developed for Shoemaker.

929 Some low flow discharge measurements were collected within the project area after the June
930 2015 high flow. Low flow measurements were collected using conventional wading techniques
931 and a Price AA current meter, a 4 foot topset rod, a JBS Systems Aquacalc pro data collector,
932 and a rangefinder. High flow measurements were collected at the upstream end of the project
933 site using a Price AA meter, 50 lb sounding weight and a B-reel deployed from a boat. Bank
934 observers directed the boat operator to remain on the cross section.

935 Discharge data were used to compute sediment loads and provide the hydrograph for fixed-bed
936 and mobile-bed hydrodynamic models. Techniques, data sources and assumptions are detailed in
937 Section V.A.
938

939 **IV.G. Sediment Transport Measurements**

940 Suspended sediment monitoring was completed to facilitate sediment load computations. The
941 Modified Einstein Procedure (MEP) was employed as in 2013 (EA 2013) and some bedload
942 samples were collected for comparison.

943 **IV.G.1. Turbidity**

944 The purpose of recording continuous turbidity is to provide a surrogate for suspended sediment
945 concentration, namely to detect temporal changes in concentration that are not necessarily
946 correlated with changes in discharge (as when banks collapse on the falling limb of a
947 hydrograph). Suspended sediment samples are collected along with turbidity to develop
948 turbidity versus suspended sediment concentration (SSC) relation.
949

950 A Eureka Manta 2 water quality data sonde was installed between cross sections 2 and 3 on May
951 24, 2015. The data sonde was positioned on the left bank where a relatively deeper river channel
952 had been observed during field efforts to ensure adequate depth for the duration of the sonde
953 deployment. The data sonde was set to record turbidity and temperature at 15 minute intervals
954 and scheduled for maintenance and the downloading of data at 1 week intervals for the duration
955 of the study. The turbidity probe on the Eureka Manta 2 was equipped with a wiper to minimize
956 the effects of bio-fouling.
957

958 The turbidity data sonde was lost in early May due to the erosion of the river bottom around the
959 stakes used to anchor the sonde. The sonde was subsequently retrieved in late August after the



960 river stage had dropped and was located by a redundant safety cable attached to the sonde.
961 Usable turbidity data were retrieved from the data sonde from May 24, 2015 to May 30, 2015.

962 **IV.G.2. Suspended-Sediment-Depth Integrated Sampling**

963 Suspended sediment transport sampling was performed by depth integrated sampling at the
964 turbidity sonde located between cross sections 2 and 3. Suspended sediment monitoring was
965 performed using a DH-59 suspended sediment sampler with a 3/16-inch nozzle from a 16 foot
966 cataraft and, during lower flows, by wading between cross sections 2 and 3 using a DH-48
967 suspended sediment sampler with 1/4 inch nozzle.

968 Samples were collected using techniques according to USGS protocols as described by Edwards
969 and Glysson (1998), using the Single Equal-Width Increment method. Depth integrated samples
970 were composed of two passes (of approximately 8 equally spaced verticals) using the same
971 stationing and the same transit rate. The transit rate was manually determined at the thalweg as
972 the rate which fills the bottle 70-90 percent full. Suspended sediment samples were analyzed for
973 concentration and grain size distribution at the GMA fine Sediment Laboratory in Placerville,
974 California. The samples were processed in accordance with ASTM Standard D422. The results
975 reported for each sample were compiled in Microsoft Excel and include the sample description,
976 total sample weight, and the weight and percent passing 0.063, 0.125, 0.25, 0.5, 1, and 2 mm
977 sized sieves.

978 **IV.G.3. Experimental 'Box' Sampling**

979 If very large sample sets are desirable to reduce uncertainty in suspended sediment load
980 computations, correlation samples (single vertical samples paired with full cross section samples)
981 can provide high resolution at a low cost. Correlation sampling (also known as box sampling) is
982 a well-established protocol employed by the USGS and others where a strong relation exists
983 between single vertical concentrations and cross sectional concentrations. This technique was
984 evaluated for the Platte River during the 2013 Short Duration Medium Flow (SDMF) and the
985 2014 "Proof of Concept" experiment showed a high correlation between box and full-cross-
986 section concentrations. The relationship of the "at-a-point" single vertical samples to cross
987 sectional values is of interest between Cross Sections 2 and 3, when personnel could not always
988 wade across the channel. Such a correlation, or "box coefficient," can be used to transform
989 single vertical samples to the cross sectional value. This method is highly practical in areas with
990 strong point-to-cross section relations: a single operator can collect many times more samples
991 over a broader range of conditions than technicians employing the full cross section method.
992 "Box" suspended sediment samples were collected using the depth integrated technique (at a
993 single vertical generally adjacent to a "thalweg") as previously described.

994
995 Box samples were collected in 2015 but since no samples were collected outside periods when
996 full DIS sampling was occurring, development of a box-DIS sample relation was un-necessary
997 and these data were not used.



998 **IV.G.4. Bedload Monitoring**

999 Bedload monitoring was not included in the 2015 scope of work. However, two bedload samples
1000 were collected during suspended sediment monitoring for the purpose of comparison with
1001 Modified Einstein-predictions of total sediment load.

1002 **IV.G.5. Scour and Fill Monitoring**

1003 Scour chains are a new monitoring approach for the Program and data from the first year (2013)
1004 implementation was considered a pilot study. Aerial photo analysis and two-dimensional fixed
1005 bed modeling (PRRIP, 2014, Attachment 2?) guided development of strata (e.g. active bars,
1006 vegetated bars) in which to sample. In order to maximize the utility of monitoring observations,
1007 sampling areas were located along cross sections to the degree possible. Monitoring areas
1008 focused on mechanically treated bars, untreated vegetated surfaces, untreated unvegetated active
1009 bars, vegetated high flow channel, and unvegetated active channel.

1010
1011 In 2014, scour chains were driven vertically into
1012 selected features to provide estimates of scour and fill
1013 values (Pittman 2002) relative to the peak flow
1014 magnitude. The chains were attached to steel anchors
1015 buried as deep as possible (~ 2 feet) into the feature of
1016 interest (Figure 4-2). A wire tie was used to mark the
1017 ground surface. Subsequent deflection (measured
1018 from the tie upstream to the 90-degree bend)
1019 following scour events indicates the magnitude of
1020 scour. The distance from the 90-degree bend to the
1021 new bar surface indicates fill.



Scour chain deployed pre runoff event, 2014.

1022
1023 Each chain location was surveyed with GPS/RTK during the post June 2014 high flow
1024 monitoring. Since there was no pre monitoring event in 2015, scour chain monitoring relates to
1025 the 2014 post monitoring thus bracketing the February 2015 ice floe and the June 2015 high flow
1026 event. No scour chains were recovered in 2015.

1028 **IV.H. Modeling**

1029 Fixed-bed and mobile-bed hydrodynamic models and one-dimensional bank erosion models
1030 were used to estimate responses of channel morphology and vegetation to the implementation of
1031 FSM Program Management Action in the Platte River during the 3-year study period. Models
1032 were developed in Year 1 of the study (2013) with a focus on informing the learning objectives
1033 and included a lateral erosion model (BSTEM), a 2-D fixed bed models (FaSTMECH and
1034 EFDC) and 2-D mobile bed models (FaSTMECH and EFDC). In Year 1 (2013), the models
1035 were calibrated using data collected during the 2013 SDMF and run for higher flows and
1036 durations that would be typical of target SDHF using input parameters extrapolated from data
1037 collected in 2013. The primary limitation of the Year 1 (2013) 2-D modeling analysis was a lack



1038 of high flow calibration data to confirm model results for the high flow simulations. Calibration
1039 and verification of the lateral erosion model was limited by little to no observed erosion of
1040 vegetated bars.

1041
1042 Two high flows occurred following the 2013 SDMF. One high flow occurred in the fall of 2013
1043 (fall 2013 high flow) and a second in June 2014 (June 2014 high flow). Water surface elevation
1044 data were collected by Program staff for model calibration during the fall 2013 high flow and by
1045 the EA project team during the June 2014 high flow. High flow simulations in Year 2 (2014)
1046 confirmed that model parameters selected in Year 1 were suitable for high flow fixed-bed
1047 simulations. Additional data was collected to calibrate the lateral erosion model on vegetated
1048 bars.

1049
1050 The highest peak flow with the longest duration of the study period occurred in 2015 (Year 3).
1051 However, this high flow was clearly outside the range of flows (both in magnitude and duration)
1052 that the 2-D mobile-bed models were developed to analyze. Similarly, the lateral erosion
1053 analysis and monitoring data in Year 2 clearly demonstrated that substantial lateral erosion of
1054 bars would occur across both vegetated and non-vegetated bars if the rooting depth did not
1055 extend to the toe of the channel. Although the rooting depth is clearly an important parameter
1056 for predicting lateral erosion, this parameter was not part of the data collection effort, except for
1057 cross-sections specifically targeted for BSTEM analysis during the 2014 high flow. No data was
1058 collected prior to the 2015 high flow to support additional analyses of lateral erosion during the
1059 2015 high flow.

1060
1061 The specific objectives of the two-dimensional fixed-bed model for Year 3 (2015 high flow)
1062 include:

- 1063
- 1064 1. Predict water surface elevations at 1,200 cfs TRF with updated topography (collected
1065 following the June 2015 High Flow event) and 3-day average peak flow for the June
1066 2015 High Flow for bar area and height computations (see PRRIP 2016) (Learning
1067 Objective 1). The results of this analysis are provided in Attachment 1, Figure 3.
1068
 - 1069 2. Predict the velocity during the peak and 3-day average peak flow for the June 2015 High
1070 Flow event to compare the measured and predicted vegetation patch response resulting
1071 from drag forces alone (Learning Objective 2). These model predictions do not account
1072 for riparian plant mortality from lateral erosion or vertical scour and is limited to
1073 responses of the target species (*Phragmites sp.*, reed canarygrass, and 1-2-year-old
1074 cottonwood).

1075
1076 A technical memorandum with detailed information on the methods, model development and
1077 results can be found in Attachment I Fixed Bed Model.



1078

V. RESULTS: JUNE 2015 HIGH FLOW EVENT

1079 A natural high flow peaked through the Shoemaker study reach on June 19, 2015. Persistently
1080 high river flows prevented safe river access for the collection of pre high flow data. Post high
1081 flow data were collected from August 24, 2015 to August 28, 2015 and September 1, 2015 to
1082 September 2, 2015. High flow data were collected from May 26, 2015 to July 17, 2015. The
1083 results from the 2015 field activities are presented in the following sections and a summary of
1084 field data and analysis is provided in Table 5-1.

1085 V.A. Hydrologic Setting

1086 V.A.1. Discharge: June 2015 High Flow

1087 The Shoemaker Island Study reach was monitored during and after the June 2015 high flow
1088 resulting from snowpack melt and heavy rainfalls in the South Platte River basin. Snowpack in
1089 the headwaters of the South Platte River in Colorado was near normal at 93 percent of the
1090 median snowpack on May 2, 2015 (Denver Post 2015). Heavy rainfall of up to 9.0 inches in
1091 northeast Colorado from May 1, 2015 to May 10, 2015 (NWS 2016) produced a peak discharge
1092 of 14,900 cfs at the Roscoe, Nebraska USGS gage on May 26, 2015 (USGS 2015). The June
1093 2015 high flow hydrograph (May 11, 2015 at 02:45 to July 20, 2015 at 18:30) recorded at the
1094 Grand Island Platte River gage (USGS 06770500), located 13.5 miles downstream of the study
1095 reach is presented in Figure 5-1. The total river flow (TRF) instantaneous peak reported for the
1096 Grand Island gage was 16,100 cfs, on June 19, 2015 with a 3-day mean peak discharge of 15,700
1097 cfs TRF and a volume of 1.231 million acre feet (for flows over 2,000 cfs). The June 2015 three-
1098 day mean peak discharge exceeded the Program-defined SDHF event of 5,000 to 8,000 cfs by
1099 196 percent and exceeded the SDHF defined volume (50,000 to 75,000 acre-feet) by 1,641
1100 percent. Table 5-2 present the Program's FSM management strategy flow "Benchmark"
1101 magnitude and duration compared to the June 2105 high flow. However, the June 2015 high
1102 flow event does not meet the Program's definition for a SDHF event. As defined above, the June
1103 2015 high flow was not augmented (through flow releases) with Environmental Account water to
1104 produce a SDHF event. The Platte River high flow that was monitored for this report will be
1105 referenced as the June 2015 high flow.

1106

1107 The Platte River stream gage at Grand Island provided the historical streamflow data to calculate
1108 descriptive statistics and streamflow exceedance probabilities. The Grand Island gage record
1109 spans from April 1, 1934 to June 6, 2016. The record contains 30,018 observations, of which
1110 29,993 are mean daily discharges and 25 days of no record (ice). The Grand Island June 19, 2015
1111 daily mean discharge was 16,000 cfs, which is exceeded by only 0.15 percent of the mean daily
1112 streamflows at that location (1 in 667 year event). Of the 29,993 records, only 45 days recorded
1113 mean daily values greater than 16,000 cfs (USGS 2016). The magnitude of the June 2015 high
1114 flow inundated all of the surveyed sand bars (59.6 acres) and 97.8 percent of the vegetated bars
1115 (62.1 acres out of 63.5 acres) in the study reach.

1116



1117 The Kearney, Shelton and Grand Island gages estimate TRF in the Platte River. Shoemaker
1118 Island splits the Platte River flow upstream of the project site into a north channel and a south
1119 channel. Approximately 18 percent (USGS 2014, EA 2013) of Platte River discharge passes
1120 through the river channel north of Shoemaker Island and approximately 82 percent flows through
1121 the south channel (through the Shoemaker study reach). This ratio is predicted by averaging
1122 relations between total river and Shoemaker discharge (from 100 to 15,000 cfs TRF), generated
1123 from the HEC-RAS model provided by the Program (PRRIP 2013). The ratio ranges from 77 to
1124 95 percent.

1125
1126 The target discharge rates for flow releases and biological objectives are referenced to the TRF,
1127 not the portion of the flow that passes through the study reach. Therefore, references in our
1128 study may be made to the TRF or the flow in the Shoemaker study reach, referred to as split flow
1129 (SF). The target ecological flow (1,200 cfs TRF) provided by the Program, equates to a split flow
1130 of approximately 954 cfs through the Shoemaker study reach.

1131
1132 In order to develop the 2015 hydrograph for Shoemaker SF, we collected 12 discharge
1133 measurements ranging from 1,020 to 10,800 cfs (Table 5-3) and used these to develop the stage
1134 discharge relation described in Figure 5-2. The pressure transducers installed between cross
1135 sections 2 and 3 provided poor records so we used the data from cross section 18 (lagged by one
1136 hour) to develop the rating and compute the 15-minute discharge record (Rantz 1982) for the
1137 upstream end of Shoemaker from April 14, 2015 at 11:15 to September 16 at 11:15 (Figure 5-3)
1138 The peaks occurring on June 4 and June 18 are nearly identical in magnitude (11,400 and 11,600
1139 cfs SF). Comparing Shoemaker split flow discharge to the USGS discharge at Grand Island
1140 shows that the hydrograph shapes agree fairly well while the discharge magnitudes expectedly
1141 differ (11,600 cfs SF vs 16,100 cfs TRF for the peak on June 4) (Figure 5-4). These gaging
1142 records suggest 28 percent of the total flow bypasses Shoemaker during this high flow, while the
1143 HEC-RAS model described earlier predicts 23 percent flows through the north channel (at
1144 16,000 cfs TRF). These differences may be attributed to: assumptions built into the HEC-RAS
1145 model, changing bed conditions which may alter the proportion of water that each channel
1146 carries from year to year, potential stream gaging error and to the fact that a small amount of
1147 Shoemaker discharge bypasses the upstream end of the project (3 percent of the SF at 11,000
1148 cfs).

1149 **V.B. Field Observations**

1150 **V.B.1. Field Classification of Nested Alluvial Features**

1151 Within and adjacent to the main channel in the at Shoemaker study reach different scales of
1152 nested alluvial features were identified:

- 1153
1154 1. High, densely vegetated bars which appear relatively stable, confine and direct primary
1155 high flow paths.

1156



- 1157 2. Large macroforms, often colonized by herbaceous species, direct the primary low flow
1158 pathways into a characteristic braided pattern. *Phragmites sp* occurred in a few areas in
1159 the project site.
1160
- 1161 3. Meso-scale bars and dunes remain unvegetated and highly active, even at low flows.
1162 Dunes on the order of 1–2 feet tall were observed migrating through the primary low
1163 flow channels during all phases of fieldwork.
1164
- 1165 4. Microforms of highly mobile and sometimes much coarser material appear as ripples in
1166 the low gradient cross-over riffles which form between the meso-scale sandbars. Flow
1167 and sediment transport rates associated with the microforms is highly variable, often
1168 building, winnowing, or scouring in response to a beached canoe and then disappearing
1169 when the obstruction is removed.
1170
- 1171 5. During the high flows, it was observed that sand bars were forming to high elevations,
1172 and in some cases, up to the water surface; however, the sand bars did not appear to
1173 persist at that elevation, deflating on the falling limb of the hydrograph. The two-
1174 dimensional mobile-bed model did not predict this phenomenon.

1175 **V.B.2. Pools and Thalweg Maintenance**

1176 While a contiguous thalweg was seldom observed through any given channel, lateral scour pools
1177 associated with vertical banks along the outsides of bends, as well as multiple deep thread
1178 channels with pools present at channel confluences, seemed to persist throughout the 2015
1179 monitoring season. The combined effect of the February ice floe and the June 2015 high flow
1180 event was more effective at modifying flow patterns than the previous monitored events; the
1181 primary flow paths generally remained the same within monitoring seasons (2013, 2014), but
1182 varied greatly between 2014 and 2015 (Appendix A, Figures A-4 through A-6).

1183 **V.B.3. Documentation of Bank and Channel Features**

1184 Post June 2015 high flow photographs were taken to document bank condition, vegetation type,
1185 structure, and bar features. The left and right bank condition were photographed at the 18
1186 primary cross sections, 129 bars post high flow were photographed. Photos were taken with
1187 GPS enabled Nikon CoolPix AW100 camera with a 5-25 millimeter (mm) zoom lens. All
1188 photographs were cataloged and saved with photo specific GPS data using Nikon ViewNX 2
1189 geo-referencing program. The geo-referenced photos were provided to the Program for
1190 archiving.

1191 A photographic log is included in Appendix B which provides representative photos from the
1192 field monitoring activities and bank and channel features.
1193



1194 **V.C. Channel Geometry**

1195 **V.C.1. Bar Topography**

1196 **Bar Numbers and Area**

1197 A topographic survey of accessible bars in the study reach was completed following the June
1198 2015 high flow from August 24, 2015 to August 28, 2015. One-hundred and forty-one bars were
1199 surveyed and five bars were located on property where access was denied by the landowner.

1200
1201 Figure 5-6 presents the bars surveyed in the Shoemaker study reach July 2014 and August 2015.
1202 The number of bars surveyed decreased from 187 bars in July 2014 to 141 bars in August 2015,
1203 a 24 percent decrease and bar area decreased from 174.7 acres to 127.4 acres, a 26 percent
1204 decrease (Table 5-4). The net decrease in the number of vegetated bars surveyed was 13 and bar
1205 area decreased from 117.4 acres to 64.4 acres. The percent decrease in bar area for natural and
1206 treated vegetated bar area was similar at 46 percent and 45 percent, respectively.

1207
1208 The overall number of sand bars decreased from 143 bars surveyed in July 2014 to 110 sand bars
1209 August 2015, a 23 percent decrease. Conversely, total area of sand bars in the study reach
1210 increased from 57.3 acres to 65.0 acres, a 12 percent increase. Sand bar numbers in treated
1211 portions of the study reach decreased from 113 to 79 and sand bar area increased from 57.3 acres
1212 to 65.03 acres. Natural areas of the study reach saw an increase in sand bar numbers from 30 to
1213 31 and in area from 6.1 acres to 11.5 acres (Table 5-4).

1214
1215 The number of natural sand bars increased from 30 to 31 and sand bar area increased from 6.1
1216 acres to 11.5 acres. The number of sand bars in the treated areas less than 0.25 acres in size
1217 decreased from 81 to 59 bars and bar area decreased from 7.2 acres to 3.4 acres from the July
1218 2014 to August 2015. The number of sand bars in the treated area greater than 0.25 acres
1219 decreased from 32 to 20 bars, however, area increased from 44.1 acres to 50.1 acres (Table 5-5).

1220
1221 **Bar Habitat Suitability**

1222 The August 2015 survey documented 110 unique sand bars covering 65.0 acres (Figure 5-6).
1223 Additional minimum suitability criteria for tern and plover nesting habitat is for bare sand bars
1224 greater than 0.25 acres in size and a height of 1.5 feet above the 1,200 cfs TRF stage. The mean
1225 height of the 20 treated sand bars that were surveyed post formative event >0.25 acres in area
1226 was 0.52 feet above the 1,200 cfs TRF stage (Figure 5-8). The mean height for the three natural
1227 sand bars >0.25 acres was 0.44 feet above the 1,200 TRF stage. None of the post formative flow
1228 natural or treated sand bars met the minimum bar height criterion for tern and plover nesting
1229 habitat. Sand bars >0.25 acres formed to a mean height at an average depth of 2.27 feet below
1230 the maximum formative event height. Sand bars <0.25 acres in size formed to a height that was
1231 at an average depth of 2.63 feet less than the maximum formative flow event height.

1232
1233 Figure 5-7 and Table 5-5 presents surveyed bars in the Shoemaker study reach that meet
1234 minimum suitability criteria for tern and plover habitat. A bar that presents suitable habitat is 80
1235 percent or greater bare sand (sand bar), vegetation is less than 20 percent, woody or perennial
1236 vegetation is not established and mature annual plants are absent. Additional suitable habitat for



1237 a sand bar includes a surface area >0.25 acres at the 1,200 cfs TRF stage. Sand bars are further
1238 grouped as natural or treated to assess the impacts of Program activities on bars in the study
1239 reach. The overall number of sand bars >0.25 acres decreased from 40 bars surveyed July 2014
1240 to 23 bars surveyed August 2015. Sand bar area for bars >0.25 acres in size increased by 19
1241 percent from 48.5 acres to 59.6 acres.

1242 **V.C.2. Primary and Supplemental River Cross Sections**

1243 The 18 primary river cross sections were closely examined for topographic change (Appendix A
1244 Figure A-7 through A-24). All 37 sections (primary + supplemental) were used in volume
1245 change calculations for the June 2015 high flow and this was compared to a volume change
1246 calculation performed using only the 18 primary sections (in order to assess the effect of
1247 increasing spatial resolution).

1248
1249 A typical cross section is presented in Figure 5-9 showing the bottom profile and areas of
1250 aggradation and degradation. The 18 primary cross sections figures are presented in Appendix
1251 A, Figures A-7 through A-24. The 19 supplemental cross sections figures are presented in
1252 Appendix A, Figures A-25 through A-43. The volume change calculations are provided in
1253 Tables 5-6 and 5-7, and a cumulative graph of sediment volume changes for each cross section is
1254 provided in Figure 5-10.

1255
1256 Most of the stage observation posts were scoured during the June 2015 high flow. In order to
1257 estimate water surface at each cross section we used the water surface slope equation developed
1258 in previous years and adjusted it with 2015 peak stage observations from between cross sections
1259 2 and a 3 and at cross section 10 (Figure 5-11). The water surface plotted on the cross sections
1260 corresponds to approximately 11,600 cfs, the 2015 SF peak discharge.

1261
1262 With the exaggerated y axis, small amounts of lateral erosion do not show up in the Excel cross
1263 section plots in Appendix A, Figures A-7 through A-24. The 1:1 scale was used in ArcGIS to
1264 assess change. In discussing cross section change, we attempt to ignore the “noise” of the small
1265 scale bedforms commonly observed migrating through the reach—though these are included in
1266 the area-change calculations—and focus instead on detecting the processes which influence
1267 management objectives:

- 1268
- 1269 • Lateral erosion of any scale
 - 1270 • Scour or deposition to a depth greater than the amplitude of commonly occurring
1271 bedforms in active channels (typically >1.5 feet); and
 - 1272 • Any change believed to be attributed to ice or other disturbance rather than the June high
1273 flow.
- 1274

1275 Lateral erosion is a subset of “total cut” and is presented separately in Tables 5-6 and 5-7 for
1276 comparative purposes. Cut and fill are discussed in the two-dimensional field, hence units are in
1277 square feet. 2014-2015 change is attributed to: August 2014 bar building at the downstream end,
1278 the February 2015 ice floe and the June 2015 high flow event. Notable changes in area for each
1279 of the primary river cross sections for the July 2014 to September 2015 period are as follows:



Cross Section	Notable Changes
1	This section was one of the few to show net cut, primarily as a result for bar erosion in the north channel. The vegetated bar exhibited over 3 feet of lateral erosion along the northern aspect. The aggradation above the high water line may have been due to the ice floe, which clearly impacted this area (Figure 4-1). Overall change = 234 ft ² cut.
2	The northern bank retreated approximately 5 feet in this area (also observed during high flow monitoring: the stage recorder was scoured and relocated five times). While the south channel scoured two feet, most of the change is in the form of aggradation in the main channel. Overall change = 270 ft ² fill.
3	Scour and fill are fairly balanced here, with a bar and a channel of very similar dimensions forming along the north half of the channel. Overall change = 43.7 ft ² fill.
4	This section exhibits the noise common along wider sections (>900 ft) observed in previous years' monitoring. Again, scour and fill are fairly balanced. Overall change = 52.5 ft ² cut.
5	Significant bank retreat (80 ft) and thalweg scour (2 feet) along the south bank is offset by bar building in mid channel for a net positive change Overall change = 145 ft ² fill.
6	This section is the first to intersect the nesting bars (Bar 18 in 2014) constructed in fall 2013 (after the high flows). Most of this constructed bar is now eroded. Overall change = 126 ft ² fill.
7	This section shows the largest cut of any of the 18 monumented sections. The constructed nesting bar scoured 1-2 feet and was essentially removed. Overall change = 242 ft ² cut.
8	The complete removal of the 2014 remaining nesting bar was offset by the development of a new bar which developed at approximately 1.5 feet lower in elevation. Overall change = 314 ft ² fill. <i>The next section downstream (supplemental I) shows the same response.</i>
9	This very wide section (>1,400 ft) shows nearly channel-wide aggradation and the filling of at least 7 flow threads. Overall change = 371 ft ² fill.
10	This section reveals significant expansion of a previously existing bar along the north side of the channel resulting in an overall volume change very similar to that observed at the previous section. Overall change = 340 ft ² fill.
11	While the difference between 2014 and 2015 appears quite noisy (redistribution of bars and channels), the overall cross sectional area change is essentially zero. Overall change = 4.3 ft ² fill.
12	The north bank retreated nearly 40 feet, but this erosion was offset by filling in the north channel and the development of two taller bars along the south side. Overall change = 273 ft ² fill.
13	The primary northern flow threads both show fill (up to 3 feet) and although the mid channel bar and one south side bar scoured, the net change remained positive. Overall change = 198 ft ² fill.
14	A new 3 foot deep primary flow thread developed along the north half of the channel and the tall bar in the south channel eroded; however, bar building in the middle of the channel resulted in net positive change. Overall change = 357 ft ² fill.
15	Channel filling and bar building offset the scour of the south side bar for the largest positive change in the study reach. Overall change = 390 ft ² fill.



Cross Section	Notable Changes
16	Similar to the last section, channel filling and bar building offset bar erosion for a net positive change. The constructed nesting island areas were excluded from the calculation (Appendix A, Figures A-1 through A-3). Overall change = 267 ft ² fill.
17	The thalweg along the north bank scoured considerably, deepening by over two feet. The constructed nesting island areas were excluded from the calculation (Appendix A, Figures A-1 through A-3). The large mid-channel bar development results in net positive change. Overall change = 101 ft ² fill.
18	The large constructed bar is omitted from the calculated area resulting on a net negative change. Overall change = 53.3 ft ² cut.

1281
1282 In order to assess the effect of increasing the number of cross sections, we first computed volume
1283 change using only the primary 18 sections. The changes in pre and post cross section area were
1284 averaged from one section to the next, and then multiplied by the distance between. Thus, the
1285 last row in Table 5-6 shows no values as the computation ends at the row for cross section 17;
1286 which is the change for the section between cross sections 17 and 18.

1287
1288 Only four computational sections (below cross sections 1, 4, 7 and 18) showed net cut (53.3 to
1289 242 cy). Of the total cut (202,400 cy), 16 percent was due to lateral erosion (32,600 cy). Every
1290 other section shows fill, generally in the form of bar building and channel filling. The net
1291 change for the reach, using only the primary 18 cross sections, was (rounded) 73,500 cy fill
1292 (Table 5-6).

1293
1294 In order to test the impact of increasing spatial resolution in volume change calculations, we
1295 repeated the calculations adding the 19 additional supplemental cross sections. This additional
1296 data collection step increased cross section survey time from 1 to 2 days. The volume change
1297 calculations are provided in Table 5-7, and a cumulative graph of sediment volume changes for
1298 each cross section is provided in Figure 5-10. By adding the 19 additional cross sections, the
1299 total volume change decreased by approximately 35 percent; from 73,500 cy to 48,000 cy fill
1300 (Table 5-7). We assume the most accurate volume change assessment to be using all 37 sections
1301 and hold 48,000 cy as our best estimate of change for the June 2015 high flow event. The volume
1302 attributed to lateral erosion was 32,600 cy using the 18 sections and as 24,600 cy using all 37
1303 sections, a 33 percent reduction.

1304
1305 The 2014 to 2015 braiding index was examined for the modeled 1,200 cfs TRF index flow. The
1306 number of channels was determined by breaking the discrete channels wherever the ground
1307 surface intersected the predicted water surface elevation at 1200 cfs TRF. The mean 2015
1308 braiding index for the 18 monumented cross sections increased from 3.5 in 2014 to 3.8 in 2015
1309 (Appendix A, Table A-1). The braiding indexes measured in the Shoemaker study reach have
1310 met the Program's goal for an average braiding index greater than 3.



1311 V.C.3. Longitudinal Profile

1312 The post 2014 and post 2015 longitudinal profiles are discussed here, with the reach broken into
1313 three areas: cross section 1-6 (Upper); cross section 7-12 (middle); cross section 13-18 (lower)
1314 (Appendix A: Figures A-44 to A-49). The meso and micro features described in Section V.B.1
1315 appear clearly in the profile plots: small ripples migrating over larger dunes and other bedforms.
1316 Data were collected along the two main flow paths identified through the project: the northern
1317 route, which includes the channel along the north side of the treated bars near cross section 6;
1318 and the southern route, which includes the portion of private property between cross sections 7
1319 and 10, for which field crews had no wading access. Only points that were collected in
1320 reasonable proximity between surveys (e.g. in the same flow thread) are considered comparable
1321 for detailed comparison and are indicated as such in Appendix A: Figure A-44 to Figure A-46.
1322 The combined effect of the February 2015 ice floe and the June 2015 high flow resulted in very
1323 different flow distribution (north and south thread alignments) and little of the profile is directly
1324 comparable. Planform alignments of the profile surveys are provided in Appendix A, Figure A-4
1325 to Figure A-6.

1326
1327 **North Alignment:** Although the profiles were hand surveyed and we followed the previous
1328 (post 2014) alignment as closely as possible, some flow threads were widely re-routed by the
1329 June 2015 high flow (Appendix A: Figure A-44 to A-46). The trendlines indicate relative fill,
1330 though since they depart in the downstream direction, and since the 2015 data plot increasingly
1331 higher than the 2014 data, they may indicate relatively more aggradation in the downstream
1332 direction (Figure 5-10). The trendline slopes indicate a very slight bed slope reduction, from
1333 0.001209 to 0.001184. The trendline analysis is only a very coarse indicator of the direction of
1334 change and because it includes sections that are not directly comparable, it should be regarded as
1335 only an indicator. The scour and fill between cross sections 1 and 3 appear fairly balanced. The
1336 upper half of the section between cross section 10 and 13 appears unchanged though the lower
1337 half shows fill of up to 3 feet. Below cross section 16, the thalweg along the north bank scoured
1338 up to 3 feet.

1339
1340 **South Alignment:** Only the uppermost section from cross section 1 to 3 was directly
1341 comparable on a feature-by-feature basis (Appendix A: Figure A-47 to A-49). The pools and bar
1342 riffle crests generally prograded downstream. While the first two pools scoured 1.5 to 2 feet, the
1343 last riffle crest aggraded by about a foot. Below here, channel change precludes detailed
1344 comparison, though below supplemental cross section N (station 9,560), the surveys do describe
1345 the same dominant geomorphic feature: the primary flow thread along the south side, paralleling
1346 the south bank. In this reach, the profiles illustrate a clear trend toward aggradation, with most of
1347 the pools filled and the bars growing in height. The trendline comparison (again, a very general
1348 indicator) suggests incision in the upstream reach and aggradation in the lowermost. As was the
1349 case with the north alignment, the departure results in a very small bed slope reduction, from
1350 0.001217 to 0.001116.



1351 **V.C.4. Vegetation**

1352 The response of vegetation to high flows was measured with vegetation assessment plots. The
1353 predicted response for 2015 high flow is limited to the effects of drag forces on uprooting
1354 vegetation and does not include the effects of lateral erosion, vertical scour, or duration of
1355 inundation.

1356 **V.C.4.1 Vegetative Assessment Plots**

1357 The July 2014 and August 2015 evaluation of the vegetation assessment plots showed a net
1358 decrease of vegetation in the assessed quadrants. The timing of the surveys July and August
1359 permitted the identification and percent cover estimation of perennial and annual plant growth in
1360 the assessed quadrants.

1361
1362 A total of seven vegetative assessment plots were located along each of the 18 primary river
1363 cross sections (Figure 5-12) for a total of 126 plots within the reach. However, one plot was
1364 located within the no access area on cross section 7 for a final assessed plot number of 125.
1365 Photo documentation of the 125 assessed plots is provided in Appendix C. The plots were
1366 measured July 2014 and August 2015 for:

- 1367
1368
- Density of live and dead stems of cottonwood trees, willows, and *Phragmites* sp.
 - Presence of other species (presence/absence).
 - Photos showing total percent vegetation and percent sand.
- 1369
1370

1371
1372 The July 2014 vegetation survey found 40 of the 125 plots contained vegetation for a 32 percent
1373 occurrence rate or 68 percent of the assessed plots contained no vegetation (Appendix C Figure
1374 C-1 to Figure C-3). The August 2015 vegetation survey found 36 of the 125 plots contained
1375 vegetation for a 29 percent occurrence rate or 71 percent of the assessed plots contained no
1376 vegetation being comprised of 100 percent sand and/or water. The number of plots documented
1377 to contain vegetation numerically decreased by 4 plots between the July 2014 and August 2015
1378 surveys a 10 percent decrease. The total aerial coverage of vegetation in the 125 assessed plots
1379 was 15.1 percent July 2014 and 6.3 percent August 2015. No vegetation was documented during
1380 the July 2014 survey in the seven plots assessed for primary cross sections 2 and 8, and August
1381 2015 vegetation survey documented no vegetation for primary cross section 3.

1382
1383 July 2014 coverage for vegetation in the 40 plots with vegetation ranged from 0.3 m² to 0.98 m²
1384 per quadrant (1 meter x 1 meter) or a total of 18.90 m² out of 125 m² assessed. August 2015
1385 coverage for vegetation in the 36 plots with vegetation ranged from 0.1 m² to 1.0 m² per
1386 quadrant (1 meter x 1 meter) or a total of 7.82 m² out of 125 m² assessed. Vegetation in
1387 quadrants documented July 2014 decreased from 18.90 m² to 7.82 m² in August 2015. Twenty
1388 quadrants that contained 7.92 m² of vegetation July 2014 were 100 percent sand/water for the
1389 August 2015 survey. Seventeen quadrants that were documented as 100 percent sand/water July
1390 2014 flow contained 1.63 m² of vegetation during the August 2015 assessment (Appendix C,
1391 Table C-1). No vegetation or all sand/water was documented in 85 of the July 2014 and 89 of
1392 the August 2015 quadrants.



1393 **V.C.4.2 Vegetation of Interest: Observed and Predicted Response**

1394 Pollen-Bankhead et al. (2012) developed relations between velocity and vegetation patch
1395 resistance were developed by for one-year old cottonwoods, two-year old cottonwoods, reed
1396 canarygrass and phragmites. These relations do not account for lateral erosion or vertical scour
1397 of vegetation. The classes include no uprooting, uprooting initiated, three classes of increasing
1398 velocity, and finally, a velocity class where all plants are expected to uproot.
1399 Spatial patterns of velocity consistent with these class are shown within the computational
1400 boundary for the June 2015 High Flow (Attachment I: Fixed Bed Modeling).

1401
1402 Results of the analysis indicate that there are no areas within the Shoemaker Reach where all
1403 plants in a patch are expected to be uprooted by drag forces alone, even during a very large
1404 magnitude high flow. Results for individual species of interest are provided below.

1405 **V.C.4.2.1 *Phragmites* sp.**

1406 Live or dead *Phragmites* sp. was not documented in any of the vegetative assessment plots in
1407 2014 or 2015 (Appendix C Figure C-4 to C-7 and Table C-1).

1408
1409 Vegetated Bar 46 (Figure 5-13) is an established bar with areas of bare sand, woody vegetation,
1410 annual and perennial plants including: Carolina lovegrass, common ragweed, purple loosestrife,
1411 Malabar sprangletop, river bulrush, barnyard grass, bur marigold, cocklebur, narrowleaf dock,
1412 false indigo, common reed, and lady's thumb. The ground photo from July 2014 (Figure 5-14)
1413 shows *Phragmites* sp. was limited to a strip of vegetation along the far edge of the bar, away
1414 from the initial area of active bank erosion. Substantial bank erosion occurred during the study
1415 period with 33 feet of erosion between November 2013 and May 2014 survey, and another 76
1416 feet of erosion during the 2014 high flow. Figure 5-15 shows the bar has completely eroded in
1417 August 2015 as a result of the June 2015 high flow, but at least some of the *Phragmites* sp.
1418 persisted along the channel margin. The rooting depth of vegetation on the bank in 2014 was
1419 documented to be 0.7 feet, and thus, did not limit the erosion of the bar. The rooting depth of the
1420 *Phragmites* sp. on this bar is unknown. Model results of the peak flood using topography
1421 following the high flow (bar is eroded) do not generate velocities high enough to remove
1422 *Phragmites* sp. by drag forces alone. These model predictions and field observations are not
1423 conclusive, but support evidence from other studies that this species persists even during flows
1424 that produce substantial channel change.

1425
1426 Sandbar Willow

1427 For the July 2014 survey eight live sandbar willow stems were documented in quadrant 13f and
1428 three dead stems were documented in quadrant 16g. Sandbar willows, live or dead were not
1429 noted in any of the August 2015 vegetation assessment plots. Model predictions were not made
1430 for sandbar willow.

1431 **V.C.4.2.2 Cottonwood Trees**

1432 No live or dead cottonwood stems were noted in the vegetation assessment quadrants surveyed in
1433 July 2014. No dead cottonwood stems were noted and 111 live cottonwood stems were



1434 documented in 14 of the vegetation assessment quadrants surveyed in August 2015. Live stems
1435 averaged 8 stems per quadrant ranging from a minimum of 1 to a maximum of 34 stems per
1436 quadrant. Average stem diameter for the 53 measured live cottonwoods was 0.96 mm and
1437 average height was 120 mm (~5 inches) maximum stem height was 385 mm (~15 inches). The
1438 14 quadrants with cottonwood stems were 35.7 percent vegetation, 57.2 percent sand and 7.1
1439 percent water in July 2014 and in August 2015 the same quadrants were 34.1 percent vegetation,
1440 65.9 percent sand, and zero percent water. The proportion of vegetation and sand in the
1441 quadrants was essentially unchanged from July 2014 to August 2015 in the 14 quadrants were
1442 new cottonwood growth was documented.

1443
1444 An independent-samples t-test was conducted to compare the mean height of vegetated quadrants
1445 with cottonwood trees to those without cottonwood trees above the 1,200 cfs TRF stage. At the
1446 95 percent confidence coefficient there was no significant difference in the mean height for
1447 quadrants with cottonwood trees ($M=1.00$, $SD=0.53$) and quadrants with no cottonwood trees
1448 ($M=0.86$, $SD=0.99$) above the 1,200 cfs TRF stage $t(33)=0.510$, $p=0.614$.

1449
1450 The velocities required for initiating uprooting of one-year old cottonwoods are generally
1451 predicted within the low flow channels and across all vegetated bars (Attachment I: Fixed Bed
1452 Modeling) during the June 2015 High Flow. Velocities across all bars are predicted to be within
1453 the two lowest uprooting classes (54 percent in the lowest class and 45 percent in the next higher
1454 class). Only 1 percent of the bar area did not meet the velocity criteria to initiate uprooting.

1455
1456 Two-year old cottonwoods require higher velocities to initiate uprooting. Similar to 1-year
1457 cottonwoods, only 1 percent of the bar area does not meet the criteria to initiate uprooting.
1458 However, 94 percent of the bar area is in the lowest velocity class for initiation of uprooting and
1459 5 percent is in the next higher velocity class during the June 2015 High Flow.

1460
1461 These results suggest that an event similar in magnitude to the 2015 high flow would uproot
1462 some of the established one-year old cottonwoods; however, uprooting of all plants is not
1463 predicted to occur by drag forces alone. Thus, some percentage of the cottonwoods that
1464 established in 2015 are likely to persist across these bars in the absence of removal through other
1465 means such as lateral erosion or disking.

1466 **V.C.4.2.3 Reed Canarygrass**

1467 Reed canarygrass occurred in four plots (3g, 10a, 12a, 12e) in July 2014. High flows removed
1468 vegetation from three of the plots (3g, 10a, 12e), and a combination of disking and/or high flows
1469 removed reed canarygrass from Plots 12a.

1470
1471 Velocities are predicted to be too low throughout the reach to initiate uprooting of reed canary
1472 grass by drag forces with the exception of a few small patches identified in higher velocity zones
1473 within the main channel during the June 2015 High Flow (Attachment I: Fixed Bed Modeling).

1474
1475 None of the observed plots provide a reasonable test of the Pollen-Bankhead (2012) estimates of
1476 when uprooting will occur by drag forces. The removal of reed canarygrass at plots 10a, 12a and



1477 3g appears to be due to substantial cut which likely occurred through lateral erosion. In these
1478 three cases, the plot started at the top of the vegetated bar and eroded to the wetted channel
1479 elevation. The adjacent bank remained vegetated and near vertical. Plot 12e was an exception.
1480 This plot remained on the top of the bar and aggraded 1.8 feet. This plot is adjacent to a very
1481 active channel and may have scoured before filling, contributing to the remove of the reed
1482 canarygrass. Assuming the Pollen-Bankhead (2012) results are reasonable for the role of drag
1483 forces alone, these results demonstrate the combined effects of lateral erosion, drag forces and
1484 vertical scour can remove this species. The integration of these three parameters is not possible
1485 with the existing set of models and requires a mobile-bed model that integrates lateral erosion.

1486 **V.C.5. Treated and Natural River Areas**

1487 The Shoemaker study reach from cross section 1 to cross section 18 of the active Platte River
1488 channel encompasses 380 acres of which 18 acres were inaccessible resulting in 362 surveyed
1489 acres. Of the 362 surveyed acres, 246 acres in July 2014 and 266 acres in August 2015 and have
1490 been subjected to mechanical disking by the Program to control vegetation, and 96 acres in
1491 August 2015 and 116 acres in July 2014 and have not been treated by the Program for vegetation
1492 control. Table 5-8 and Figure 5-5 present the surveyed areas for vegetated bars (>20 percent
1493 vegetated), sand bars (>80 percent sand), and water/river bed in the surveyed treated and natural
1494 areas of the Shoemaker study reach in July 2014 and August 2015.

1495
1496 In the treated portion of the study reach vegetative bar area decreased by 36 acres from 32
1497 percent to 17 percent of the treated area in the study reach from July 2014 to August 2015. Sand
1498 bar area in the treated portion remained proportionally the same at 21 percent to 20 percent but
1499 gained in area by 3 acres. Water/river bed area increased by 53 acres from 47 to 63 percent of the
1500 treated study reach. In the natural areas of the study reach not subjected to mechanical treatment
1501 the portion that was vegetated decreased by 18 acres from 33 percent to 20 percent. Sand bar
1502 area increased by 5 acres from 5 percent to 11 percent and the water/river bed area decreased by
1503 8 acres from 62 percent to 67 percent of the natural area in the study reach July 2014 to August
1504 2015 (Appendix C, Table C-1). The high flow limited the growth of new vegetation on sand
1505 bars or eroded vegetated bars in the study reach.

1506
1507 Vegetated areas in the natural and treated areas in the study reach decreased between the July
1508 2014 and August 2015 surveys by 15 percent and 12 percent, respectively. The response of the
1509 study reach to the loss of the vegetated areas was not the same for the treated and natural areas.
1510 The proportion of sand bars in the treated area remained the same at 21 percent in July 2014 and
1511 20 percent in 2015 and in the natural area from 5 percent to 12 percent. The proportion of
1512 water/riverbed in the treated areas increased from 47 percent in July 2014 to 63 percent in
1513 August 2015 and in the natural areas increased from 62 percent to 67 percent. Water/river bed
1514 areas of the study reach are characterized as having an elevation less than the 1,200 cfs TRF
1515 stage and a bar is at an elevation greater than the 1,200 cfs TRF stage.

1516
1517 Vegetated bar area had a proportionally similar 45 percent decrease in both the treated and
1518 natural areas of the study reach. This decrease in vegetated bar area will result in a net increase
1519 of sand bar or water/river bed area of the study reach. Increases to sand bar area and water/river



1520 bed area was not the same between the treated and natural areas in the study reach. For the
1521 treated areas sand bar area did not change (51.2 to 53.6 acres) and water/river bed area increased
1522 (115.1 to 168.4 acres). The natural areas in the study reach had an increase in sand bar area (6.1
1523 to 11.5 acres) and a decrease in water/river bed area (72.2 to 64.1 acres). The erosion of
1524 vegetative bars in the study reach by the high flow event did not result in a proportional increase
1525 in sand bar area.

1526 **V.C.6. Unvegetated Channel Widths**

1527 The occurrence of vegetation in the river channel at the 18 primary cross sections surveyed
1528 through the Shoemaker study reach is presented in Figure 5-16. The surveyed widths for water,
1529 mature vegetated bars, natural bars, and mechanically treated bars are presented from the south
1530 to the north bank of the river channel. In July 2104 and August 2015 Eleven of the 18 primary
1531 cross sections surveyed had unvegetated channel widths greater than 750. Average unvegetated
1532 cross section width in July 2104 was 1,286, ranging from 786 feet to 1,633 feet and in August
1533 2105 average unvegetated width was 1,069 feet, ranging from a minimum of 769 feet at transect
1534 4 to a maximum of 1,459 feet at transect 18.

1535 **V.C.7. Vegetation Roughness**

1536 Polygons of similar land cover were created for the bars and riparian areas in the study reach to
1537 estimate vegetation roughness. Polygons of uniform land cover were then used as a data input
1538 parameter for hydraulic modeling. One-hundred forty-six polygons were created for the 141 bars
1539 that were surveyed by plant biologists (Figure 5-17). A polygon was also created for each of the
1540 five bars located where access was denied by the landowner. Nine vegetation roughness
1541 polygons were created for riparian areas for hydraulic modeling of 8,000 cfs TRF Platte River
1542 flows. Vegetation roughness for the inaccessible bars and riparian areas was estimated from
1543 aerial photos, distant photos taken during field activities, and adjacent bar vegetation surveyed
1544 by the plant biologist

1545 **V.D. Sediment**

1546 **V.D.1. Turbidity**

1547 Turbidity data were collected from May 24, 2015 to May 30, 2015 between cross sections 2 and
1548 3 in the Shoemaker study reach. The turbidity data sonde was lost in early May due to the
1549 erosion of the river bottom around the stakes used to anchor the sonde. The sonde was retrieved
1550 in late August after the river staged had dropped. No turbidity data were usable for load
1551 computations. The continuous turbidity data were to be used as a surrogate for continuous
1552 suspended sediment concentration into the project area. The sensitivity of turbidity to short term
1553 variations in concentration (versus a discharge relation with concentration) facilitates more
1554 accurate load computation and an examination of temporal changes in the load, potentially
1555 related to geomorphic processes occurring in Shoemaker.



1556 **V.D.2. Suspended Sediment**

1557 Box samples were collected but were not analyzed; as all were collected during depth integrated
1558 sampling efforts and box samples were not required.

1559

1560 **Depth Integrated Sampling**

1561 For the June 2015 high flow event 18 DIS samples were collected between cross sections 2 and
1562 3. All but one sample were two-pass samples, for a total of 35 passes. Six passes were excluded
1563 from transport curve development due to the inclusion of coarse grains (assumed to be bedload
1564 collected by sampling error). Samples were collected between 994 and 11,000 cfs SF and
1565 concentrations ranged from 49 to 548 mg/l. Concentration and grain size data for all suspended
1566 sediment samples are provided in Table 5-9. Suspended sediment loads were computed directly
1567 from the concentration data as follows:

1568

- 1569 • All loads were computed as a function of discharge as no turbidity record was available.
1570 For the <0.063mm class, there was no relation with discharge and since no turbidity
1571 record was available, we proportionally fit hydrograph through sample values to produce
1572 sedigraph and load. One of the applied sediment transport models requires suspended
1573 sediment transport computed by size classes (see Attachment 2). The following size
1574 classes were developed from the grain size analyses performed on the sample data:
 - 1575 ○ <0.063mm (no relation with discharge)
 - 1576 ○ 0.063-0.25mm
 - 1577 ○ 0.25-0.5mm
 - 1578 ○ 0.5-1mm
 - 1579 ○ 1-2mm
 - 1580 ○ >2mm (zero transport)
- 1581 • The transport relations and their respective equations are provided in Appendix A: Figure
1582 53 to Figure 56. The transport equations are provided in Table 5-10
- 1583 • Equations were applied to the 15-minute discharge hydrograph over the June 2015 high
1584 flow computational period: April 14, 2015 at 11:15 to September 6, 2015 at 11:15.
- 1585 • The sedigraph method was applied to the continuous concentration curves by shifting to
1586 samples by fitting or proportional fitting between sample values.
- 1587 • Continuous (15 minute) concentration was transformed into continuous suspended
1588 sediment load (SSL) by the standard equation:
 - 1589 ○ $SSL \text{ (tons/day)} = 0.002697 * Q \text{ (cfs)} * SSC \text{ (mg/l)}$
- 1590 • Continuous SSL was summed over the computational period and divided by 96 (the
1591 number of 15 minute intervals in a day) to provide the load in tons (Table 5-11).
- 1592 • Total suspended load for the computational period was 505,000 tons, with the largest
1593 component being the 0.063-0.25mm size class (47 percent).

1594 **V.D.3. Total Load and Bedload**

1595 Total load was computed (from the suspended sediment data, hydraulic parameters measured
1596 during sampling efforts, and the 2015 bed material data) using the Modified Einstein (MEP)



1597 method as we did for 2013 monitoring (PRRIP 2014). The models required 15 minute
1598 continuous bedload (broken into the same six size classes as for suspended sediment) which we
1599 calculated by subtracting suspended load from total load (Table 5-12). These MEP-derived
1600 bedload values were plotted with previous years MEP-derived and 2013-2015 measured bedload
1601 values. A single regression fitted through the 2015 MEP-derived bedload data were used to
1602 compute continuous bedload as a function of discharge (Figure 5-18).

1603
1604 Using grain size distributions for bedload samples collected in 2015, we developed percentages
1605 for each size class and deconstructed the total load into the six size classes. Total load was then
1606 computed as the sum of suspended load and bedload: the June 2015 high flow event transported
1607 a total of 966,000 tons with 461,000 tons (48 percent) as bedload (Table 5-11). Seventy two
1608 percent of the bedload (332,600 tons) was >1mm and 25 percent of the total load was composed
1609 of the 0.063-0.25mm size class (Table 5-11).

1610 **V.D.4. Scour Monitoring**

1611 No scour chains were recovered in 2015 and we assume rates of scour or fill were simply too
1612 great to facilitate recovery of the post 2014 chains. The post 2014 chains were typically one to
1613 three feet deep. Staking to the 2014 locations revealed zero to 1.9 feet of fill at the downstream
1614 locations (with one exception where a 2 foot deep channel had developed). Above cross section
1615 7, channel change was significant enough to prevent staking to the 2014 locations; deep threads
1616 of flowing water had developed in former bar areas.

1617 **V.D.5. Bed and Bar Sampling**

1618 A total of 28 bed samples and 6 bar samples were collected following the June 2015 high flow
1619 and were analyzed by the GMA Coarse Sediment Laboratory in Placerville, California for grain
1620 size. Dry bulk density was computed for the 6 bar samples. Grain size analysis results for all
1621 bed and bar samples are provided in Appendix A: Table A-2 and Table A-3. Bed and bar sample
1622 data were utilized in model development. Due to extensive channel change, none of the
1623 individual 2014 samples were directly comparable (spatially) for examining the potential effect
1624 of the June 2015 high flow on grain size; areas which had been bars became flowing channels
1625 and vice versa.

1626
1627 The bulk density samples provide input data for mobile-bed models and facilitate volumetric
1628 conversions between sediment loads and volumes. The 28 bed and bar bulk samples are
1629 presented in Table 5-13. Sites labeled “bar” are very low lying bars generally at or less than the
1630 1,200 cfs TRF index flow. Comparing the overall bed and bar mean D50 between 2014 and
1631 2015 reveals virtually no change in the median grain size. The overall mean D50 decreased very
1632 slightly from 1.00mm to 0.97mm. The bar D50 remained virtually the same at 1.08mm in 2014
1633 and 1.07mm in 2015. Likewise, the mean bed D50 was 0.96mm in 2014 and 0.94mm in 2015.

1634
1635 The mean bulk density of post 2013 SDMF samples was 1.74 g/cm³ and this value was utilized
1636 to estimate volumes from computed sediment loads in 2013. The mean bulk density of the 2014
1637 samples was 1.67 g/cm³, representing a four percent difference from the 2013 accepted value.



1638 The difference is likely measurement error inherent in a small dataset (n=4 to 8). The mean bulk
1639 density measured in 2015 was again 1.74 g/cm^3 (Table 5-13).



1640 **VI. CONCLUSIONS FOR 2015 HIGH FLOW EVENT**

1641 Based on the results and evaluation of the data presented in this report, this section summarizes
1642 the conclusions that can be reached as directly related to the three Learning Objectives of the
1643 Shoemaker Island FSM Experiment. The FSM priority hypothesis provides a broad view of the
1644 possible changes in river morphology/channel characteristics that may be produced through
1645 implementation of FSM management action.

1646 **VI.A. Learning Objectives**

1647 The learning objectives for the “Shoemaker Island FSM “Proof of Concept” Experiment are:

- 1648
- 1649 1. Evaluate the relationship between peak flows (magnitude and duration) and sandbar
1650 height and area.
 - 1651 i). The relationship between sediment transport (surplus/deficit) and the frequency of
1652 sandbar occurrence.
 - 1653 ii). The relationship between sediment grain size distribution and sandbar height
1654 potential.
 - 1655 iii). The role of hydrograph duration and shape in sandbar height.
1656
 - 1657 2. Evaluate the relationship between peak flows (magnitude and duration) and riparian
1658 plant mortality.
1659
 - 1660 3. Evaluate the ability of FSM management strategy to create and/or maintain habitat for
1661 whooping cranes, least terns, and piping plovers.

1662 **VI.A.1. Evaluate the relationship between peak flows (magnitude and duration) and**
1663 **bar height and area.**

- 1664
- 1665 • The June 2015 high flow event at the Grand Island gage had a 3-day mean peak discharge
1666 of 15,700 cfs TRF that was 196 percent of the benchmark 3-day peak mean discharge of
1667 8,000 cfs TRF. An estimated volume of 1.231 million acre-feet (cumulative volume of
1668 flows greater than 2,000 cfs) that was 1,641 percent of the benchmark event volume of
1669 50,000 to 75,000 acre-feet passed the Grand Island gage from May 11 to July 20, 2015.
 - 1670 ○ Bar frequency decreased from 187 to 141 bars.
 - 1671 ○ Total bar area (sand and vegetated) decreased from 174 to 129 acres.
 - 1672 ■ Sand bar area increased by 7.7 acres
 - 1673 ■ Vegetated bars decreased by 53 acres.
 - 1674 ○ The mean height of the 3-day high flow stage above the 1,200 cfs TRF stage was
1675 2.59 feet with a maximum and minimum height of 4.05 and 1.38 feet,
1676 respectively.
 - 1677 ○ Mean depth below the formative event 3-day mean peak discharge stage for the
1678 23 sand bars >0.25 acres was 2.14 ft and mean bar height above the 1,200 cfs
1679 TRF stage was 0.52 feet.



1680 ○ Mean depth below the formative event 3-day mean peak discharge stage for the
1681 87 sand bars <0.25 acres 2.54 ft and mean bar height above the 1,200 cfs TRF
1682 stage was 0.16 feet.
1683

1684 None of the surveyed bars bars >0.25 acres in size meet the minimum tern and plover habitat
1685 for a bar height >1.5 feet or higher than 1,200 cfs TRF stage.

1686 **VI.A.2. Evaluate the relationship between peak flows (magnitude and duration) and**
1687 **riparian plant mortality.**

1688 • The July 2014 aerial coverage for the vegetation plots per 125 m² was 15.1 percent and
1689 decreased to 6.3 percent for the August 2015 survey. Bar vegetation decreased between
1690 the survey events from 18.90 m² in July 2014 to 7.82 m² in August 2015.
1691

1692 • Live or dead Phragmites sp. was not documented in any of the vegetation plots. Eight
1693 live and three dead sandbar willows (established growth) were documented in July 2014
1694 and none were present during the August 2015 survey. One-hundred and eleven live
1695 cottonwood stems were documented in the August 2015 vegetation plots. Cottonwood
1696 stems averaged 8 per quadrant with an average height of ~5 inches.
1697

1698 • Mean height of plots above the 1,200 cfs TRF stage with cottonwood tree growth was
1699 equal to plots with vegetation and no cottonwood trees. At the 95 percent confidence
1700 coefficient there was no significant difference in the mean height for quadrants with
1701 cottonwood.
1702

1703 • Removal of reed canarygrass was observed at four plots, primarily associated with large
1704 channel changes that had more than 1 foot of scour or fill. Comparison of the observed
1705 and model predictions based on Pollen-Bankhead (2012) demonstrates the combined
1706 effects of lateral erosion, drag forces and vertical scour can remove this species at
1707 substantially lower velocities than necessary to remove the plants by drag forces alone.
1708 The integration of the effect of drag forces, lateral and vertical erosion is not possible
1709 with the existing set of models and requires a mobile-bed model that integrates lateral
1710 erosion.

1711 **VI.A.3. Evaluate ability of FSM management strategy to create and/or maintain**
1712 **habitat for whooping cranes, least terns and piping plovers**

1713 Figure 5-5 provides a visual summary of bar attributes July 2015 and August 2015; before and
1714 after the June high flow event through the Shoemaker study reach. A decrease in the aerial
1715 extent of vegetated bars from July 2014 to August 2015 is evident in the figure. Vegetated bar
1716 area decreased for the mechanical treated and untreated (natural vegetation) bars in the study
1717 reach suggesting that the June 2015 high flow had a larger impact on vegetation than mechanical
1718 treatment by the Program. Additional conclusion relative to the FSM management actions are
1719 presented below.
1720



1721 • Flow

1722
1723 The June 2015 high flow event 3-day mean peak discharge of 15,700 cfs TRF increased the
1724 depth of water above the 1,200 cfs TRF stage by 2.59 feet to 4.05 feet. The post high flow
1725 survey documented 110 sand bars in the study reach. Of the 110 sand bars, the 23 that were
1726 greater than 0.25 acres in size had a mean height of 0.52 feet above the 1,200 cfs TRF stage or a
1727 mean depth of 2.14 feet below the formative event 3-day mean peak discharge stage. None of
1728 the surveyed sand bars >0.25 acres in size met the minimum tern and plover nesting suitability
1729 for sand bar height of >1.5 feet above 1,200 cfs TRF stage. No suitable sand bar habitat was
1730 documented post the June 2015 high flow event which exceeded a SDHF target flow duration
1731 and magnitude.

1732
1733 Bars that exceeded the minimum vegetation criteria (>20 percent vegetation) decreased from 44
1734 bars July 2014 to 31 vegetated August 2015 post the June 2015 high flow event. A 45 percent
1735 and 46 percent decrease in vegetated bar area was documented in the mechanically treated and
1736 natural areas in the study reach, respectively. Vegetated bars in the study reach decreased from
1737 117.4 acres in July 2014 to 64.4 acres in August 2015 a 45 percent study area decrease.
1738 Conversely, sand bar area in the study reach increased by 7.7 acres (13.4 percent), vegetated bar
1739 area decreased by 45.3 acres resulting in a 45.2-acre net increase in study reach area less than the
1740 1,200 cfs TRF stage (Table 5-4).

1741
1742 The cumulative area of bar depth relative to the 3-day mean peak discharge of 15,700 cfs TRF is
1743 presented on Figure 6-1. The graph shows that the mean depth below the 3-day mean peak
1744 discharge height for sand bars is greater than that for vegetated bars. All of the surveyed sand
1745 bars (59.6 acres) and 97.8 percent of the vegetated bars (62.1 acres out of 63.5 acres) in the study
1746 reach were inundated by the June 2015 high flow. An independent-samples t-test was conducted
1747 to compare the mean depth relative to the formative event 3-day peak mean discharge stage of
1748 sand bars and vegetated bars >0.25 acres in size. At a 95 percent confidence coefficient there
1749 was a significant difference in the mean depth for sand bars (M=2.14, SD=0.51) and vegetated
1750 bars (M=1.41, SD 0.43) below the formative discharge stage $t(40)=4.93$, $p=0.00$. The near
1751 complete inundation of sand and vegetated bars by the June 2015 high flow event did not result
1752 in the growth of sand bars equal to the height of vegetative bars in the study reach. The mean
1753 height of sand bars surveyed July 2014 (M=0.46, SD=0.29) were found to not be significantly
1754 different at the 95 percent confidence coefficient from the post formative high flow August 2015
1755 sand bar mean height (M=0.52, SD=0.28) $t(61)=-0.77$, $p=0.44$. The June 2015 formative high
1756 flow event which exceeded Program target flows did not increase the height of sand bars in the
1757 Shoemaker study reach.

1758
1759 • Sediment

1760
1761 Sediment supply into the Shoemaker Project was not augmented for the June 2015 high flow
1762 event, thus we cannot evaluate the effectiveness of geomorphic changes resulting from sediment
1763 augmentation for the June 2015 high flow. However, the results of the study indicate volume
1764 change from Fall 2014 to Fall 2015 was 48,000 cy fill. The total sediment load was 966,000 tons.



1765 Thus the implication is that given the 2015 hydrograph shape, with a total load of 966,000 tons,
1766 the reach is in sediment surplus.

- 1767
- 1768 • Mechanical
- 1769

1770 The erosion of vegetated bars in the mechanically treated and natural areas suggests that the high
1771 flow event had a greater impact on vegetated bars in the study reach than the mechanical
1772 treatment did. Vegetated bar area decreased by 45 percent and 46 percent in the mechanical
1773 treated and natural areas, respectively. Sand bar area in the mechanically treated areas increased
1774 by 5 percent (51.2 acres to 53.6 acres) and in the natural areas by 88 percent (6.1 acres to 11.5
1775 acres). Water/river bed area in the study reach less than the 1,200 cfs TRF stage increased in the
1776 mechanically treated area by 46 percent (115.1 acres to 168.4 acres) and in the natural areas
1777 decreased by 11 percent (72.2 acres to 64.1 acres). For the mechanically treated areas vegetated
1778 bar area decreased, sand bar area did not change and water/river bed area increased. For the
1779 natural areas in the study reach vegetated bar area decreased, sand bar area increased, water/river
1780 bed decreased. The erosion of vegetative bars in the study reach by the high flow event did not
1781 result in a proportional increase in sand bar area.

1782

1783 The occurrence of vegetation in the river channel at the 18 primary cross sections surveyed
1784 through the Shoemaker study reach is presented in Figure 5-16. The surveyed widths for water,
1785 mature vegetated bars, natural bars, and mechanically treated bars are presented from the south
1786 to the north bank of the river channel. Eleven of the 18 primary cross sections surveyed had
1787 unvegetated channel widths greater than 750 feet. Average unvegetated cross section width was
1788 1,069 feet, ranging from a minimum of 769 feet at transect 4 to a maximum of 1,459 feet at
1789 transect 18.

1790

1791 Two of the eighteen primary cross sections in the Shoemaker study reach had natural
1792 unvegetated cross sections lengths greater than 750 feet at 769 feet and 844 feet. Mechanical
1793 treatment increased unvegetated width to greater than 750 ft in nine additional primary cross
1794 sections. Average mechanically treated unvegetated cross section width was 1,127 feet, ranging
1795 from a minimum 827 feet at cross section 17 to a maximum of 1,459 feet at cross section 18.
1796 Seven of the 18 cross sections did not contain unvegetated lengths greater than 750 feet (Figure
1797 5-16).

1798

1799 The Shoemaker study reach covers 362 acres of Platte River main channel area. The study reach
1800 consists of 266 mechanically treated acres and 96 natural or untreated acres. If the untreated
1801 areas of the Study reach are considered typical then the treatment of the river bed and sand bars
1802 has altered the natural ratio of vegetated/sand bars and water/river bed in the study reach. For
1803 the August 2015 survey, untreated areas have a water/river bed to sand bar to vegetated bar ratio
1804 of 0.79:0.08:0.13 and mechanically treated areas are 0.63:0.20:17. Mechanical treatment has
1805 increased the aerial proportion of sand bars in the study reach, decreased the proportion
1806 water/river bed areas <1,200 cfs TRF stage in the study reach, and increased vegetation (pioneer
1807 taxa such as annual grasses on freshly disturbed soils) on bars compared to the untreated portion



1808 of the reach. Mechanical treatment appears to produce more sand bar area in the Shoemaker
1809 Reach.



1810

VII. MODELING OF THE SHORT DURATION HIGH FLOW

1811 Model runs in 2015 focused on Learning Objective 1: estimating the channel response to SDHF
1812 and sensitivity to changes in (a) sediment supply, (b) grain size, and (c) hydrograph shape
1813 (magnitude and duration). These runs were conducted to determine whether altering these
1814 parameters within the context of the target volume of water available for a SDHF could generate
1815 higher sand bars or more sand bar area. The model used in the analysis is FaSTMECH and
1816 EFDC. A detailed description of the models are provided in Attachment II.

1817

1818 Sediment supply within the Platte River can be managed by direct sediment augmentation;
1819 however, the field results suggest that the Shoemaker Reach is not deficient in sediment. The
1820 effect of sediment supply is estimated with the FaSTMECH model using twice the predicted
1821 equilibrium sediment supply (2x), equilibrium sediment supply (1x), and half the equilibrium
1822 sediment supply (0.5x). The effect of sediment supply is also estimated with EFDC using grain-
1823 size specific sediment rating curves derived from direct measurements at the project site using
1824 EFDC.

1825

1826 Bed material grain size in the Platte River varies longitudinally and may be affected by sediment
1827 augmentation of particular grain sizes. The effect of grain size is estimated using grain sizes of
1828 0.75 mm, 1 mm, and 2 mm using FaSTMECH.

1829

1830 SDHF are controlled releases that piggy back on natural river flows. The releases can
1831 theoretically be managed to produce a higher peak discharge of long flow duration. The effect of
1832 hydrograph shape is analyzed using hydrographs that have the same volume of water (60,000
1833 acre-feet), but have different peak magnitude and flow duration. A peak flow of 8,000 cfs, for 3-
1834 days is compared to a peak flow of 5,000 cfs for ~6.5 days using FaSTMECH.

1835

1836 A preliminary analysis of the effects of these parameters (sediment supply, grain size and
1837 hydrograph shape) were reported in PRRIP (2014). The mobile-bed model runs conducted in
1838 2015 are improved estimates of channel response. These runs utilize the model parameters
1839 calibrated to the 2014 high flow, post-processing methods requested by PRRIP, a modified
1840 duration of the peak flow to maintain a similar volume of water between the two hydrographs.
1841 Thus, these results supersede those reported in the PRRIP (2014). The results and conclusions of
1842 the fixed-bed analyses and bank erosion analyses reported in PRRIP (2014) remain unchanged.

1843

1844 Effects of these variables (sediment supply, grain size and hydrograph shape) are evaluated for:

1845

- 1846 • Populations of all bars (sand and vegetated) following the SDHF. This analysis is
1847 intended to demonstrate reach wide effects on all bars (Attachment II: Figure 10).
- 1848 • Populations of sand bars only following the SDHF. This analysis removes the influence
1849 of vegetated bars which may be less sensitive to the variables due to higher stability. The
1850 analysis is focused on the response of sand bars, which is the target bar type to meet
1851 biological objectives.



- 1852 • Populations of new sand bars only. This analysis focuses on new sand bars created
1853 during the high flow, which are expected to be most responsive to changes in variables.
1854

1855 A hydrograph with a 3-day peak of 8,000 cfs that contains ~60,000 acre-feet of water, a bed
1856 material grain size of 1 mm, and a sediment supply that is equivalent to an “equilibrium” supply
1857 is used as the basis for comparison (“base case”) of FaSTMECH runs. The same “base case” is
1858 applied in EFDC except for grain size and sediment supply. In EFDC, grain size is defined by
1859 multiple grain size classes, which more closely matches the measured bed material. Grain size
1860 specific sediment rating curves developed from paired measurements of sediment concentrations
1861 and flow is used to define the sediment supply, rather than an equilibrium supply. EFDC is only
1862 used to verify the effect of altering sediment supply.

1863 **VII.A. Effect of a SDHF**

1864 A hypothetical SDHF with a peak flow of 8,000 cfs for 3 days with a total volume of water of
1865 ~60,000 acre-feet, a bed material grain size of 1 mm and a sediment supply equivalent to an
1866 “equilibrium” sediment supply is used as a basis for comparison for effects of hydrograph shape,
1867 grain size and sediment supply. This run is referred to as the “base case”.
1868

1869 FaSTMECH predicted a total cut of 90,000 CY and fill of 94,000 CY with a net fill of 4,000 CY
1870 during the SDHF, indicating the reach is roughly at equilibrium (Attachment II: Table 6). The
1871 predicted net fill is likely an artifact of the initial conditions. The initial channel is plane bed and
1872 low relief bar formation develop over this plane bed over the course of the model run
1873 (Attachment II: Figure 8).
1874

1875 The overall acreage of bars declined slightly from 175 acres before the SDHF to 169 acres after
1876 the SDHF. The total number of bars decreased substantially from 303 bars before the SDHF to
1877 177 bars following the SDHF (Attachment II: Figure 11). Bar frequency declined primarily due
1878 to direct erosion of very small bars or translation of these small bars far enough downstream that
1879 they did not intersect with the original bar location (126 bars), accounting for a total of 2.5 acres
1880 of change. Many bars merge with adjacent bars which accounts for the decline of an additional
1881 35 bars. A statistically significant (p -value = 0.04) increase in individual bar areas occurred due
1882 to erosion of the smaller bars and merging of adjacent bars (Attachment II: Table 7). Total new
1883 bar area was 0.9 acres following the 8,000 cfs SDHF. New bars were generally small. Only one
1884 bar was close to reaching the biological target of 0.25 acres.
1885

1886 A very small (<0.1 feet), but statistically significant (p -value = 0.03), increase in mean bar height
1887 occurred following the SDHF. The maximum mean bar height of new bars was less than 0.6 feet
1888 (Attachment II: Figure 12 and Figure 13) which does not meet the biological objective of 1.5
1889 feet. A SDHF did not occur within the monitoring period. A smaller flow occurred (2013
1890 SDMF) as well as three larger flows (fall 2013 high flow, 2014 high flow and 2015 high flow).
1891 These high flows were higher in magnitude and longer in duration than the target SDHF. The
1892 field data at Shoemaker is consistent with the model results that a SDHF is insufficient for
1893 producing bar heights that meet the biological objective.
1894



1895 During high flow field efforts, bars were observed to grow in height on the rising limb of the
1896 hydrograph, reaching close to the water surface at the peak of the flow, then decline in elevation
1897 on the falling limb of the hydrograph. The model did not predict this phenomenon. Bars at the
1898 peak flow were not predicted to be higher than those at the end of the hydrograph. Capturing
1899 this phenomenon likely requires the application of a fully three-dimensional model.

1900 **VII.B. Effect of Sediment Supply**

1901 **Objective 1a:** Evaluate relationships between sediment supply and frequency of sand bar
1902 occurrence. The effect of sediment supply on bar frequency was evaluated with FaSTMECH
1903 and EFDC during a SDHF with a peak flow of 8,000 cfs TRF for 3 days. Sediment supply was
1904 doubled and reduced by half compared to the base case. Sediment supply was adjusted in
1905 FaSTMECH by modifying the equilibrium sediment supply and in EFDC by modifying the
1906 measured sediment concentrations.

1907
1908 Both models predicted negligible changes to bar frequency, height, and area in response to a
1909 change in the upstream sediment supply during one SDHF. FaSTMECH predicted a difference
1910 of 1 bar between the cases of half and double the equilibrium supply during a SDHF (Attachment
1911 II: Figure 16) and a difference of 4 bars across all cases for sand bars and new sand bars
1912 (Attachment II: Figure 17 and Figure 18). Some small differences occur in the total area of bars
1913 (lower sediment supply resulting in slightly more new bar area and higher bars (Attachment II:
1914 Figure 19), but these differences are not statistically significant (Attachment II: Table 9).

1915
1916 The most significant changes occurred at the project boundary in EFDC, which resulted in
1917 accumulations of sediment in the form of a delta as observed in previous years (PRRIP, 2014,
1918 2015). These sediment accumulations were localized and did not translate through the project
1919 reach during the SDHF. A significantly longer duration simulation is likely necessary to observe
1920 the long-term impacts of changes in sediment supply. It is also important to note that the channel
1921 response is inherently linked to the initial conditions of the channel bed. The channel geometry
1922 may be significantly different in reaches that have a chronic sediment deficit resulting in a
1923 different response to a change in sediment supply than the Shoemaker reach.

1924 **VII.C. Effect of Grain Size**

1925 **Objective 1b:** Evaluate the Relationship between grain size and sand bar height. The effect of
1926 bed material grain size on bar height and area was evaluated with FaSTMECH during a SDHF
1927 with a peak flow of 8,000 cfs TRF for 3 days. Bed material grain sizes of 0.75 mm, 1 mm (base
1928 case) and 2 mm were evaluated.

1929
1930 Bed material grain size affects the predicted amount of scour and fill, total number of bars,
1931 number of new bars and bar area. Reducing the bed material size from 1 mm to 0.75 mm
1932 increases cut by 22 percent and fill by 21 percent. Coarsening the bed material from 1 mm to 2
1933 mm decreases cut by 42 percent and fill by 40 percent (Attachment II: Table 6).

1934



1935 The total number of bars decreases substantially from the initial condition of 303 bars to 177 bars
1936 following an 8,000 cfs TRF SDHF for the base case (grain size = 1 mm). As discussed in the
1937 previous section, bar frequency declines due to merging of bars, erosion of smaller bars or
1938 downstream translation of bars. The decline in bar frequency for finer bed material (0.75 mm) is
1939 less pronounced (a reduction from 303 bars to 215 bars), but there is not a clear trend associated
1940 with increasing grain size (Attachment II: Figure 21). In the case of the finer grain size (0.75
1941 mm), the erosion of smaller bars appears to be somewhat offset by new bar development and a
1942 more active bed. As grain size is increased, the bed is less active and the higher bar frequency of
1943 bars in the coarser bed (188 versus 177) may be a result of a less active bed that resulted in less
1944 erosion of the smaller bars.

1945

1946 Total bar area decreases from 175 acres to 169 acres with a bed material grain size of 1 mm
1947 (base case). Decreasing the grain size to 0.75 mm results in a bar area of 173 acres, and
1948 increasing the grain size to 2 mm results in a decline in bar area to 166 acres. Thus, less total bar
1949 area is lost when grain sizes are smaller, with a total difference in bar area of about 4 percent.

1950

1951 The populations of average bar height and bar area for all bars (sand bars and vegetated bars),
1952 sand bars with grain sizes ranging between 0.75 and 2mm, are not statistically different
1953 (Attachment II: Figure 21, Figure 22, and Table 8)

1954

1955 The number of new bars formed during the SDHF is substantially larger with a finer grain size
1956 (74 new bars with a 0.75 mm grain size versus only 9 new bars with a 2 mm grain size)
1957 (Attachment II: Figure 23). Total new bar area also increases with finer grain size (1.7 acres for
1958 0.75 mm, 0.89 acres for 1 mm, 0.12 acres for 2 mm grain size) (Attachment II: Figure 25).
1959 However, these differences in total area are quite small relative to the total bar area in the project
1960 site, representing a change of less than 1 percent of the total bar area. There appears to be a trend
1961 of higher and larger bars with decreasing grain size (Attachment II: Figure 23, Figure 24, and
1962 Figure 25); however, the differences between the populations are not statistically significant
1963 (Attachment II: Table 8).

1964

1965 In all grain size cases, none of the bars met the biological target of 0.25 acres; however, one bar
1966 nearly met the target at 0.23 acres (0.75-mm grain size). Similarly, none of the bars met the
1967 height target of 1.5 feet above the 1,200 cfs water level for 1 mm and 2 mm grain size, and only
1968 one bar exceeded an average height of 1.5 feet when the bed material was 0.75 mm (Attachment
1969 II: Figure 24). Generally, average heights of bars were substantially lower than the target
1970 heights, with median heights of 0.1 feet or less.

1971

1972 While grain size appears to have an important effect on sediment transport, reflected in the total
1973 cut and fill that occurred throughout the project site, it does not appear to have a significant
1974 impact on bar height or area during one SDHF. Given the strong effect that grain size has on
1975 sediment transport cut and fill volumes, it is possible that over longer time scales, grain size
1976 could emerge as a statistically significant parameter.



1977 VII.D. Effect of Hydrograph Shape and Duration

1978 **Objective 1c:** Evaluate relationship between hydrograph (shape and duration) and sand bar
1979 height. The effect of hydrograph shape is evaluated using hydrographs that have the same
1980 volume of water (~60,000 acre-feet), but have different peak magnitude and flow duration. A
1981 peak flow of 8,000 cfs for 3 days (base case) is compared to a peak flow of 5,000 cfs for ~6.5
1982 days using FaSTMECH.

1983
1984 The SDHF hydrographs both produce a significant amount of cut and fill throughout the study
1985 reach (Attachment II: Table 6). The 8,000 cfs hydrograph produces roughly 17 percent more cut
1986 and 19 percent more fill than the 5,000 cfs hydrograph. Both hydrographs result in a small net
1987 fill, which was likely due to low relief bar formation on the otherwise plane bed channel present
1988 in the initial topography as stated earlier.

1989
1990 The total number of bars increased by 3 following a 5,000 cfs SDHF compared to the 8,000 cfs
1991 SDHF (Attachment II: Figure 11). Total bar area decreases from 175 acres, to 166 acres and 169
1992 acres, respectively, following a 5,000 cfs and 8,000 cfs TRF SDHF. The results of the statistical
1993 tests indicate there is not a statistically significant difference between populations of bar heights
1994 or bar areas due to the hydrograph shape of the SDHF (Attachment II: Table 7).

1995
1996 The difference in sand bar frequency following a 5,000 cfs and 8,000 cfs is small (140 bars
1997 following a 5,000 cfs peak flow versus 134 bars following an 8,000 cfs peak flow). While the
1998 median bar height appears slightly higher following an 8,000 cfs peak flow, the populations are
1999 not statistically different between the two flows (Attachment II: Figure 12 and Table 7)

2000
2001 The difference in number of new bars formed is minor, with 32 new bars formed following the
2002 5,000 cfs SDHF and 30 bars formed following the 8,000 cfs SDHF. Total new bar area is 0.5
2003 acres following the 5,000 cfs SDHF and 0.9 acres following the 8,000 cfs SDHF. New sand bars
2004 are less than 0.07 acres following the 5,000 cfs SDHF, and less than 0.23 acres following the
2005 8,000 cfs SDHF (Attachment II: Figure 13 and Figure 14). In both cases, no bars met the
2006 biological target of 0.25 acres. Mean new sand bar heights are less than 0.5 foot above the 1,200
2007 cfs water surface elevation for both hydrographs. These heights are substantially less than the
2008 biological target of 1.5 feet. Although there appears to be a tendency for higher bar heights and
2009 larger bar areas associated with a higher peak discharge, the populations following one SDHF
2010 are not statistically different (Attachment II: Table 7).

2011
2012 New bars are formed 0.4 to 1.7 feet below the peak stage with a median depth of 1.2 feet at 5,000
2013 cfs, while bars that formed during the 8,000 cfs SDHF formed 0.6 to 2.3 feet below the peak
2014 stage with a median value of 1.7 feet.

2015
2016 New bars formed during the 5,000 cfs and 8,000 cfs TRF SDHF were all lower and smaller than
2017 needed to achieve biological objectives of 0.25 acres and 1.5 feet above the 1,200 cfs TRF water
2018 level. Overall, bars on the reach scale did not change substantially with a single SDHF. It is
2019 possible that multiple events could produce a statistically significant difference in bar height and
2020 area, however; the results of the field study indicate the potential differences are relatively small.



2021 Hydrographs within the range of the target SDHF do not appear to be sufficient to achieve
2022 biological objectives.

2023 **VII.E. SDHF Conclusions**

2024 The results of the mobile-bed modeling analysis are consistent with field observations in the
2025 Shoemaker reach that SDHF events are not likely to create bars with sufficient height or areas to
2026 achieve biological objectives. While there were differences in sediment transport (cut/fill) and
2027 total number of bars formed, the relative changes in bar area and height during a SDHF were
2028 minor. Differences in peak magnitude (5,000 cfs -8,000 cfs) and duration of peak flow (3- 6.5
2029 days), grain size (0.5, 1 mm, 2 mm) and sediment supply changes (0.5 – 2x sediment supply) did
2030 not produce statistically significant changes in the bar forms created during the SDHF. These
2031 results are limited to the effect of one SDHF event. It is possible that some of these parameters
2032 may have a long-term effect that was not captured during this study. The conclusion from the
2033 modeling exercise is consistent with field measurements of barform changes following a short
2034 duration medium flow and three distinct high flow events (Fall 2013, June 2014 and June 2015)
2035 that met or exceeded the target SDHF.



2036

VIII. THREE YEAR SUMMARY

2037 The FSM “Proof of Concept” experiment was implemented by the Program to evaluate the
2038 ability of a Flow-Sediment-Mechanical (FSM) management strategy to achieve Program goals.
2039 The goals include: improve the survival of whooping cranes during migration, improve least tern
2040 and piping plover production, and avoid adverse impacts to pallid sturgeon in the Lower Platte
2041 River. General management actions include:

2042

- 2043 1. Flow— Augment Q1.5 through flow releases to create short duration high flows (SDHF)
2044 of 5,000 to 8,000 cubic feet per second (cfs) for 3 days in 2 out of 3 years.
- 2045 2. Sediment— Augmentation of approximately 150,000 tons of medium sand annually to
2046 offset sediment deficit upstream of Kearney.
- 2047 3. Mechanical— Channel widening, clearing, and leveling of in-channel bars and flow
2048 consolidation (85-90 percent of 8,000 cfs in a single channel).

2049

2050 The Shoemaker Island Complex, which is assumed to be in sediment balance, was chosen as the
2051 location to implement the FSM “Proof of Concept”. Over a three-year period, the experiment
2052 evaluated the performance of the FSM management actions, in creating and/or maintaining
2053 channel characteristics that are consistent with the Program’s management objectives. Learning
2054 objectives included:

2055

- 2056 1. Evaluate the relationship between peak flows (magnitude and duration) and sandbar
2057 height and area.
- 2058 2. Evaluate the relationship between peak flows (magnitude and duration) and riparian plant
2059 mortality.
- 2060 3. Evaluate the ability of the FSM management strategy to create and/or maintain habitat for
2061 whooping cranes, least terns, and piping plovers.

2062

VIII.A. Timeline of Events

2063 The findings from the 2013 and 2014 monitored high flow events were presented in their
2064 respective annual Shoemaker Island FSM “Proof of Concept” reports (PRRIP 2014a and PRRIP
2065 2015b). Findings from the 2015 monitoring effort were presented in this report. Following is a
2066 discussion of the inter year observations (2013, 2014, and 2015) of the geomorphologic changes
2067 of the Platte River to high flow events in the Shoemaker Study Reach.

2068

2069 Eight field efforts were expended to quantify the effects of four unique high flow events on the
2070 geomorphology of the Platte River in the Shoemaker study reach. “Proof of Concept”
2071 Experiment Milestones:

2072

2073 **March 25 to April 3 2013 - Field Effort**

2074 Geomorphology and vegetation surveys in the Shoemaker Study reach completed.

2075



2076 **April 13, 2013 to April 18, 2013 - Short Duration Medium Flow**

2077 The April SDMF (April 13, 2013 at 00:00 to April 18, 2013 at 23:45) recorded at the Grand
2078 Island Platte River gage (USGS 06770500), located 13.5 miles downstream of the study reach
2079 recorded a TRF instantaneous peak discharge of 3,840 cfs. The 3-day mean peak discharge was
2080 3,552 cfs TRF at a volume of 33,743 acre-feet. The April 2013 SDMF three-day mean peak
2081 discharge was 44 percent of the Program-defined SDHF event of 5,000 to 8,000 cfs and was 45
2082 percent of the SDHF defined volume of 50,000 to 75,000 acre-feet (Table 8-1). The April 2013
2083 high flow event was augmented (through flow releases) with Environmental Account water to
2084 produce a flow event. However, the 3-day mean peak discharge was 44 percent of the Program-
2085 defined SDHF and for this reason is referenced as a Short Duration Medium Flow (SDMF).
2086

2087 **April 13, 2013 to April 18, 2013 - Field Effort**

2088 River stage monitoring and sediment sampling completed during 2013 SDMF.
2089

2090 **April 26, 2013 to April 29, 2013 - Field Effort**

2091 Geomorphology and vegetation surveys in the Shoemaker Study reach completed post 2013
2092 SDMF.
2093

2094 **September 24, 2013 to November 1, 2013 – Fall 2013 High Flow**

2095 The fall 2013 high flow in the Platte River resulted from approximately 15 inches of rain that fell
2096 over the headwaters of the South Platte River Basin near Boulder, Colorado over a 7-day period
2097 starting on September 9, 2013 (Erdman 2013). The high flow hydrograph (September 24, 2013
2098 to November 1, 2013) at the Grand Island Platte River gage (USGS 06770500) recorded a TRF
2099 instantaneous peak discharge of 10,600, on October 3, 2013 with a 3-day mean peak discharge of
2100 9,700 cfs TRF and a TRF volume of 248,273 acre feet. The fall 2013 high flow three-day mean
2101 peak discharge was 121 percent of the Program-defined SDHF event of 5,000 to 8,000 cfs and
2102 was 331 percent of the SDHF defined volume of 50,000 to 75,000 acre-feet (Table 8-1). The fall
2103 2013 high flow event was not augmented (through flow releases) with Environmental Account
2104 water to produce a SDHF event.
2105

2106 **May 5, 2014 to May 9, 2014 – Field Effort**

2107 Geomorphology and vegetation surveys in the Shoemaker Study reach completed pre June 2014
2108 High Flow.
2109

2110 **June 6, 2014 to July 5, 2014 - June 2014 High Flow**

2111 The June 2014 high flow in the Platte River Resulted from snowpack melt in South Platte River
2112 basin. Snowpack in the headwaters of the South Platte River basin in Colorado was at 133
2113 percent of the median snowpack on May 1, 2014 (NRCS 2014). The June 2014 high flow
2114 hydrograph (June 6, 2014 at 00:00 to July 5, 2014 at 23:45) at the Grand Island Platte River gage
2115 (USGS 06770500) recorded a TRF instantaneous peak discharge of 8,800 cfs, on June 15, 2014
2116 with a 3-day mean peak discharge of 7,320 cfs TRF and a TRF volume of 181,270 acre feet. The
2117 June 2014 three-day mean peak discharge was 92 percent of the Program-defined SDHF event of
2118 5,000 to 8,000 cfs and exceeded the SDHF defined volume of 50,000 to 75,000 acre-feet by 241



2119 percent (Table 8-1). The June 2014 high flow event was not augmented (through flow releases)
2120 with Environmental Account water to produce a SDHF event.

2121

2122 **June 6, 2014 to June 26, 2014 - Field Effort**

2123 River stage monitoring and sediment sampling completed during June 2014 high flow.

2124

2125 **July 21, 2014 to July 26, 2014 - Field Effort**

2126 Geomorphology and vegetation surveys in the Shoemaker Study reach completed post June 2014
2127 high flow.

2128

2129 **May 11, 2015 to July 20, 2015 - June 2015 High Flow**

2130 The June 2015 high flow in the Platte River resulted from snow-pack melt and heavy rainfall in
2131 the South Platte River basin. Snowpack in the headwaters of the South Platte River in Colorado
2132 was near normal at 93 percent of the median snowpack on May 2, 2015 (Denver Post 2015).
2133 Heavy rainfall of up to 9.0 inches in northeast Colorado from May 1, 2015 to May 10, 2015
2134 (NWS 2016) produced a peak discharge of 14,900 cfs at the Roscoe, Nebraska USGS gage on
2135 May 26, 2015 (USGS 2015). The June 2015 high flow (May 11, 2015 at 02:45 to July 20, 2015
2136 at 18:30) at the Grand Island Platte River gage (USGS 06770500) recorded a total river flow
2137 (TRF) instantaneous peak discharge of 16,100 cfs, on June 19, 2015 with a 3-day mean peak
2138 discharge of 15,700 cfs TRF and a TRF volume of 1.231 million acre feet (for flows over 2,000
2139 cfs). The June 2015 three-day mean peak discharge exceeded the Program-defined SDHF event
2140 of 5,000 to 8,000 cfs by 196 percent and exceeded the SDHF defined volume (50,000 to 75,000
2141 acre-feet) by 1,641 percent (Table 8-1). The June 2015 high flow event was not augmented
2142 (through flow releases) with Environmental Account water to produce a SDHF event.

2143

2144 **May 26, 2015 to July 17, 2015 – Field Effort**

2145 River stage monitoring and sediment sampling completed during June 2015 high flow.

2146

2147 **August 24, 2015 to September 2, 2015 - Field Effort**

2148 Geomorphology and vegetation surveys in the Shoemaker Study reach completed post June 2015
2149 high flow.

2150 **VIII.B. Inter Year Summary**

2151 The conclusions and data that were presented for the four high flow events were re-examined to
2152 evaluate inter year changes. Inter year data were evaluated as they directly relate to the three
2153 Learning Objectives of the Shoemaker Island FSM Experiment. The FSM priority hypothesis
2154 provides a broad view of the possible changes in river morphology/channel characteristics that
2155 may be produced through implementation of FSM management action.

2156 **VIII.B.1. Evaluate the relationship between peak flows (magnitude and duration) and**
2157 **bar height and area.**

2158

2159



2160 The magnitude and duration of the monitored peak flows in the Shoemaker study reach did not
2161 increase bar height and area commensurate with flow.

- 2162
- 2163 • 2013 SDMF – The 3-day mean peak discharge was 3,840 cfs with a flow duration of 6-
2164 days with flows greater than 2,000 cfs.
- 2165 • June 2014 High Flow - The 3-day mean peak discharge was 7,320 cfs and duration of 30-
2166 days with flows greater than 2,000 cfs.
- 2167 • June 2015 High Flow - The 3-day mean peak discharge was 15,700 cfs and duration of
2168 72-days with flows greater than 2,000 cfs.

2169
2170 Bar height and area relative to the June 2014 high flow and the June 2015 high flow are
2171 presented in Figure 5-8 and Figure 8-1, respectively. None of the sand bars greater than 0.25
2172 acres in size surveyed post high flow events in 2014 and 2015 met the least tern and piping
2173 plover nesting suitability criterion for sand bar height greater than 1.5 feet above 1,200 cfs TRF
2174 stage.

2175

2176 **VIII.B.2. Evaluate the relationship between sediment supply and bar height and area.**

2177 Sediment supply within the Platte River can be managed by direct sediment augmentation;
2178 however, the field measurements of changes in sediment storage suggest that the Shoemaker
2179 Reach is not deficient in sediment.

2180

- 2181 • 2013 SDMF – Net sediment -16,000 cubic yards (cy)
- 2182 • Fall 2013 High Flow – Net sediment +82,920 cy
- 2183 • June 2014 High Flow – Net sediment -10,300 cy
- 2184 • June 2015 High Flow – Net sediment +73,500 cy

2185

2186 The effect of sediment supply is estimated with the FaSTMECH model using twice the predicted
2187 equilibrium sediment supply (2x), equilibrium sediment supply (1x), and half the equilibrium
2188 sediment supply (0.5x). The effect of sediment supply is also estimated with EFDC using grain-
2189 size specific sediment rating curves derived from direct measurements at the project site using
2190 EFDC.

2191 **VIII.B.3. Evaluate the relationship between grain size and bar height and area.**

2192 Bed material grain size of the Platte River varies longitudinally and may be affected by sediment
2193 augmentation of particular grain sizes. There was not a statistically significant change in the
2194 grain size within the Shoemaker Reach during the study period. The effect on bar height and area
2195 is estimated using grain sizes of 0.75 mm, 1 mm, and 2 mm using FaSTMECH. Grain size has
2196 an important effect on sediment transport, reflected in the total cut and fill that occurred
2197 throughout the project site, it does not appear to have a significant impact on bar height or area
2198 during one SDHF. Given the strong effect that grain size has on sediment transport cut and fill
2199 volumes, it is possible that over longer time scales, grain size could emerge as a statistically
2200 significant parameter.



2201 **VIII.B.4. Evaluate the relationship between peak flows (magnitude and duration) and**
2202 **riparian plant mortality.**

2203 The magnitude and duration of the monitored peak flows in the Shoemaker study reach impact
2204 on riparian plant mortality was inconclusive. The impacts of the monitored peak flows
2205 (magnitude and duration) could not be separated from the impacts of the Program’s mechanical
2206 disking activities, nesting island construction and herbicide treatment on riparian plants in the
2207 study reach.

- 2208
- 2209 • 2013 SDMF – Vegetated area in the study reach decreased from 125.9 acres pre to 124.1
2210 acres post the monitored SDMF flow event.
- 2211 • June 2014 High Flow – Vegetated area in the study reach increased from 49.2 acres pre
2212 to 117.4 acres post the monitored high flow event.
- 2213 • June 2015 High Flow – Vegetated area in the study reach decreased from 117.4 acres in
2214 July 2014 to 64.4 acres post the monitored high flow event.
- 2215

2216 Areal extend of sand bars, vegetated bars, and water/river bed area in mechanically treated areas
2217 and the untreated areas of the Shoemaker study reach for the three monitored flows are presented
2218 in Table 5-8.

2219

2220 **VIII.B.4.1 Summary of Lateral Erosion Predictions**

2221 Lateral/bank erosion contributes to riparian plant mortality by direct erosion of the banks, or
2222 undermining the banks below the root zone and producing geotechnical failures. Drag forces can
2223 pull vegetation from bars and vertical scour can expose root systems making them more
2224 susceptible to uprooting by drag forces. One-dimensional bank erosion modeling using the
2225 USDA-ARS BSTEM model was one component of the analysis conducted for the Shoemaker
2226 Reach of the Platte River over the past three years (WY 2013 – WY 2015). The analyses
2227 conducted with BSTEM supports previous research suggesting that lateral erosion is a primary
2228 fluvial process contributing to riparian plant mortality (Pollen-Bankhead et al., 2012).

2229

2230 The USDA Bank Stability and Toe Erosion Model (BSTEM) is a one-dimensional bank erosion
2231 model developed at the USDA Agricultural Research Services (Simon et al. 2011; USDA 2010).
2232 BSTEM estimates hydraulic erosion of the bank and bank toe based on hydraulic boundary shear
2233 stresses calculated from channel geometry and flow parameters. Hydraulic erosion occurs when
2234 the tractive force of the water column [shear stress] exceeds the resisting force of bank materials.
2235 Additional lateral erosion through geotechnical bank failure, (gravitational forces exceed
2236 cohesive forces), is based on equilibrium factor of safety calculations that include horizontal
2237 erosion, vertical tension cracks and cantilever failure (USDA 2010). Input requirements include
2238 bank geometry, soil type for bank material, vegetation coverage, channel slope, and water depth
2239 at the channel boundary for a given duration of time. Sediment transport is not incorporated into
2240 this model and the channel bed elevation is assumed to be fixed. This model does not
2241 incorporate incision of the channel bed and the bottom elevation of the bank toe can’t erode
2242 below the elevation of the channel bed.



2243
2244 The BSTEM model is a fixed-bed model, and thus, performed well when the bed and banks
2245 maintained a relatively stable configuration as occurred during the 2013 SDMF and in many
2246 areas during the 2014 high flow. The model performed poorly at locations where there were
2247 widespread channel changes that resulted in new bar growth or substantial bank erosion that
2248 substantially changed the flow hydraulics at the bank.

2249
2250 The 2013 SDMF did not change the overall configuration of the bars and channels, but lateral
2251 erosion was observed at 2 of the 5 bank sites analyzed with BSTEM. One site (BSTEM Site C:
2252 cross-section 6, Bar 7) has 10 feet of erosion and the second site (BSTEM Site E: cross-section
2253 10 bar 18) had 14 feet of lateral erosion. The model demonstrated that the erosion occurred both
2254 during the SDMF, and continued during moderate natural flows following the release. Roughly
2255 82% of the erosion occurred after the SDMF at BSTEM Site C and 45% occurred after the
2256 SDMF at BSTEM Site E.

2257
2258 BSTEM Site C was selected as a test case to determine how much erosion would occur during a
2259 hypothetical SDHF with a peak magnitude of 8,000 cfs. These results indicated that the amount
2260 of erosion over the SDHF was higher than over the same equivalent time as the SDMF, but that
2261 the total amount of erosion predicted during a SDHF was only 30% of the measured erosion that
2262 was observed over the 28-day period of more moderate flows.

2263
2264 These results indicate that after flows rise high enough to initiate erosion, sustained flows may be
2265 more effective at eroding banks than higher magnitude, shorter duration flows. Additional detail
2266 can be found in PRRIP (2014).

2267
2268 Vegetation on banks may reduce bank erosion by providing root strength to soil. Vegetated
2269 banks with roots that did not extend to the toe of the channel were modeled using the
2270 methodology as unvegetated banks with similar success (generally within 5% of the measured
2271 data, see PRRIP (2015)). The Manning's n value was adjusted such that the shear stress applied
2272 at the toe of the bank was equal to the shear stress predicted by the two-dimensional model. This
2273 methodology does not provide good predictive results when the rooting depth of the vegetation
2274 extends to the bottom, or toe, of the bank. Banks with deeply rooted vegetation (to or below the
2275 bottom of the bank) did not erode during both the 2013 SDMF or 2014 high flow. A review of
2276 the air photos indicates that three of the four sites that were stable in 2014 remained stable
2277 through the 2015 high flow.

2278
2279 BSTEM analyses were not conducted for the 2015 high flow due to a lack of pre-high flow data
2280 and substantial reorganization of the channel bed. BSTEM does not provide adequate results
2281 when large morphological changes occur in the channel that substantially alters the shear stress
2282 applied at the toe of the bank. Analysis of this type of high flow requires coupling of the mobile-
2283 bed and bank erosion model to adequately capture the changing hydraulic forces applied at the
2284 bank during the high flow.



2285 **VIII.B.5. Evaluate ability of FSM management strategy to create and/or maintain**
2286 **habitat for whooping cranes, least terns and piping plovers**

2287 Figure 8-2 provides a visual summary of bar attributes April 2013, July 2014, and August 2015.
2288 The images show that the aerial distribution of bar attributes have changed in the Shoemaker
2289 study reach through mechanical treatment and/or high flows. Tern and plover preferred bar
2290 attributes includes: ≥ 0.25 contiguous acre of bare sand (less than 20 percent vegetative cover)
2291 and ≥ 1.5 feet above the 1,200 cfs TRF stage. Unobstructed minimum channel widths for
2292 whooping crane roosting is 750 ft with a target of 1,150 ft to increase probability of roosting.
2293 Inter year conclusions relative to the FSM management actions are presented below.

2294 **VIII.B.5.1 Flow**

2295 The magnitude and duration of the monitored high flow events in the Shoemaker study reach
2296 were estimated using event specific stage/discharge data and data from USGS gaging station
2297 near Grand Island, NE. Three distinct flows were monitored for their effects on least tern, piping
2298 plover and whooping crane habitat in the Shoemaker study reach.
2299

2300 The 3-day mean peak discharge above the 1,200 cfs TRF stage at cross section 18 was 0.94-foot
2301 for the April 2013 SDMF, 1.60-foot for the 2014 high flow, and 2.69-foot for the 2015 high flow
2302 event. The April 2013 SDMF 3-day peak mean discharge stage increased the mean depth of
2303 water above the 1,200 cfs TRF stage by 1.04 feet. The June 2014 high flow 3-day mean peak
2304 discharge stage increased the depth of water above the 1,200 cfs TRF stage by 1.49 feet to 2.46
2305 feet. The June 2015 high flow event 3-day mean peak discharge stage increased the depth of
2306 water above the 1,200 cfs TRF stage by 2.59 feet to 4.05 feet. The duration of flows over 2,000
2307 cfs for the June 2014 high flow was 30 days and for the June 2015 high flow it was 71 days.
2308

2309 The 2013 SDMF was monitored pre and post the high flow event and the magnitude and duration
2310 of the event did not demonstrably affect the height and area of sand and vegetated bars in the
2311 Shoemaker study reach. The post June 2014 high flow survey documented 40 sand bars,
2312 encompassing 48.5 acres that were greater than 0.25 acres in size. The post June 2015 high flow
2313 survey documented 23 sand bars encompassing spanning 59.6 acres that were greater than 0.25
2314 acres in size.
2315

2316 None of the monitored flow events formed sand bars to a height that was equal to or greater than
2317 1.5 feet above the 1,200 cfs TRF stage. Sand bars >0.25 acres in size surveyed post June 2014
2318 high flow had a mean height of 0.39 feet above the 1,200 cfs TRF stage. Sand bars >0.25 acres
2319 in size surveyed post June 2015 high flow had a mean height of 0.52 feet above the 1,200 cfs
2320 TRF stage.
2321

2322 The monitored peak flows impact on unobstructed channel width could not be segregated from
2323 the impacts of the Program's mechanical disking activities, nesting island construction and
2324 herbicide treatment on riparian plants in the study reach.
2325
2326



2327 VIII.B.5.2 Sediment

2328 Sediment volume changes in the Shoemaker study reach was estimated for three monitored flow
2329 events and the fall 2013 high flow event. Volume change was estimated using the average end
2330 method and the 18 monumented cross sections for the 2013 SDMF and the fall 2013 high flow.
2331 The June 2014 and June 2015 high flow volume change estimate used the primary and
2332 supplemental cross sections (n=37). The 2013 SDMF had a net erosion of 16,000 cubic yards,
2333 fall 2013 high flow had a net deposition of 82,920 cy, June 2014 high flow had a net erosion of
2334 10,300 cy, and the June 2015 high flow had a net deposition of 48,000 cy. A summation of
2335 erosion/deposition in the Shoemaker study reach during the three-year study results in a net
2336 deposition of 104,620 cy of sediment. This result indicates that Shoemaker was not in a
2337 sediment deficit during the 3-year monitoring period. The net deposition of sediment in the
2338 Shoemaker study reach did not increase bar area or height during the three year “Proof of
2339 Concept” experiment.

2340
2341 Sediment supply into the Shoemaker Project was not augmented during the study, thus we
2342 cannot evaluate the effectiveness of geomorphic changes resulting from sediment augmentation.
2343 We can however examine channel response related to sediment load on an event-by-event basis
2344 and evaluate changes in grain size over the study period

2345
2346 The 2013 SDMF transported 15,200 tons of suspended load and 12,500 tons of bedload at the
2347 upstream boundary for a total load of 27,700 tons. Volume change calculations resulted in a
2348 deficit of 16,000 cy. The implication for this event is that given the hydrograph shape and
2349 sediment load, the reach was in sediment deficit.

2350 The fall 2013 high flow transported 93,300 tons of bedload, which summed with suspended load
2351 results in 170,000 tons transported into Shoemaker. Using the rounded mean of the 2013 and
2352 2014 bulk density calculated from bar samples (1.7 g/cm^3), we convert mass to volume which
2353 yields 119,000 cy for the total load. The calculated volume change was 83,000 cy of deposition.
2354 The implication is that with this (estimated) sediment supply, the reach is in a sediment-surplus
2355 condition, aggrading in response to the fall 2013 hydrograph and sediment load.

2356
2357 The June 2014 high flow transported 49,500 tons of bedload, which summed with suspended
2358 load results in 99,300 tons transported into Shoemaker. The calculated total sediment load
2359 volume is 69,000 cy. The percent difference in the total cut and total fill volumes is only 8
2360 percent. The calculated volume change resulted in a deficit of 10,300 overall cy. The
2361 implication is that with this (estimated) sediment supply, the reach is near sediment balance with
2362 the potential for a slight sediment-deficit condition, in response to the June 2014 hydrograph and
2363 sediment load. The 8 percent difference is quite small, given the uncertainty in our calculations
2364 (we saw a 10,000 cy difference just by adding the supplemental cross sections), therefore, the
2365 reach may likely be in sediment balance for this event.

2366
2367 The 2015 high flow event transported 505,000 tons of suspended sediment and 461,000 tons of
2368 bedload for a total load of 966,000 tons. The calculated volume change indicated a net
2369 deposition of 73,500 cy. The implication is that with the measured sediment supply, the reach is
2370 in a sediment-surplus condition, aggrading in response to the 2015 hydrograph and sediment



2371 load. As stated previously, over the three year study and over four distinct high flow periods, the
2372 Shoemaker Study reach is not in sediment deficit.

2373
2374 Grain size distributions from bed and bar samples showed little change in the D50 over the three
2375 year monitoring period. Of the 150 samples collected, we removed three that were collected in
2376 very unusual, very coarse riffles (Figure 8-3). The D50 ranged from 0.64 to 1.0mm and
2377 averaged 0.82mm. the final two sampling events (post 2014 and post 2015) show a very slight
2378 coarsening to approximately 1mm. However, there was no significant difference between the
2379 populations.

2380 **VIII.B.5.3 Mechanical**

2381 Concurrent with the three year “Proof of Concept” experiment to monitor the geomorphology of
2382 the Shoemaker study reach the Program annually performed mechanical disking of vegetation
2383 and constructed nesting bars. Nesting bars were constructed in early fall after the post high flow
2384 geomorphology surveys. Geomorphology data were not collected for the constructed bars and
2385 the mechanical impact of bar construction on vegetation was not evaluated. Mechanical disking
2386 of the river bed/bars in the Shoemaker study reach was performed prior to the first
2387 geomorphology survey in March 2013 and in early fall of 2013, 2014, 2015 during the
2388 experiment. No geomorphology surveys were completed in the Shoemaker study reach that
2389 predated mechanical disking of the river bed/bars for the “Proof of Concept” experiment.

2390
2391 The braiding index was examined for the five geomorphological surveys completed at the
2392 modeled 1,200 cfs TRF index flow. The mean braiding index for the five surveys at the 18
2393 monumented cross exceeded the Program’s goal for an average braiding index greater than 3.
2394 The five year mean braiding index was 4.1 ranging from a maximum of 5.1 in March, 2013 to a
2395 minimum of 3.5 in May and July, 2014.

2396
2397 The eighteen primary transects that were surveyed in the Shoemaker study reach were assessed
2398 to identify segments greater than 750 feet with no vegetation and evaluate the role of mechanical
2399 treatment in the “creation” of the segments. The Department of the Interior hypothesizes that an
2400 unobstructed minimum channel width of 750 feet and a target of 1,150 feet is needed to increase
2401 the probability of whooping crane roosting.

2402
2403 **2013** - Four of the 18 primary cross sections in the Shoemaker study reach had natural
2404 unvegetated transect widths greater than 750 feet ranging from 750 feet to 1,125 feet. With
2405 mechanical treatment, five additional primary cross sections were “created” that had widths
2406 greater than 750 feet— with two unvegetated widths greater than 1,150 feet. Average
2407 mechanical aided unvegetated cross section width 1,039 feet, ranging from a minimum 771 feet
2408 to a maximum of 1,604 feet. Nine of the 18 cross section did not contain unvegetated lengths
2409 greater than 750 feet.

2410
2411 **2014** - Three of the eighteen primary cross sections in the Shoemaker study reach had natural
2412 unvegetated cross sections lengths greater than 750 feet ranging from 803 feet to 933 feet. With
2413 mechanical treatment, eight additional primary cross sections were “created” that had widths



2414 greater than 750 feet— with eight unvegetated widths greater than 1,150 feet. Average
2415 mechanical aided unvegetated transect width was 1,286 feet, ranging from a minimum 786 feet
2416 to a maximum of 1,633 feet. Seven of the 18 cross sections did not contain unvegetated lengths
2417 greater than 750 feet.

2418
2419 **2015** - Two of the eighteen primary cross sections in the Shoemaker study reach had natural
2420 unvegetated cross sections lengths greater than 750 feet at 769 feet and 844 feet. With
2421 mechanical treatment, nine additional primary cross sections were “created” that had unvegetated
2422 widths greater than 750 feet— with three unvegetated widths greater than 1,150 feet. Average
2423 mechanically aided unvegetated cross section width was 1,127 feet, ranging from a minimum
2424 827 feet to a maximum of 1,459 feet. Seven of the 18 cross sections did not contain unvegetated
2425 lengths greater than 750 feet.

2426
2427 River bed/bars in the Shoemaker study reach were mechanically treated before the first
2428 geomorphology survey was completed the week of March 23, 2013. Data were not available for
2429 vegetation occurrence at the eighteen primary cross sections prior to mechanical treatment. The
2430 “Proof of Concept” experiment monitored unvegetated cross section widths resulting from an in
2431 place, mechanical treatment of vegetation. Based on our results and observations, mechanical
2432 treatment contributes to maintaining and/or decreasing vegetation in the study reach with: 9,353,
2433 feet of unvegetated width in April 2013, 14,155 feet in May, 2014, and 11,764 feet in September
2434 2015.

2435
2436 The Shoemaker study reach covers 362 acres of Platte River main channel area. At the time of
2437 the geomorphology surveys the study reach consisted of 252 mechanically treated acres in 2013,
2438 246 acres in 2014, and 266 acres in 2015. Natural area not subjected to mechanical treatment in
2439 the study reach was 110 acres in 2013, 116 acres in 2014, and 96 acres in 2015 (Table 8-2).

2440 River stage (depth) during mechanical treatment in the fall of the year limits/permits access to
2441 bars for treatment.

2442
2443 Figure 8-4 presents the acres and attributes for the bars in the study reach above the 1,200 cfs
2444 TRF stage. The increase of vegetated acres for the July 2014 survey resulted from the short high
2445 flow duration (flows greater than 2,000 cfs) of 30 days, which permitted the germination of
2446 annual plants on bars before the July 21 to July 31, 2014 survey. The amount of treated sand
2447 bars was consistent for the three annual surveys. Total area of natural sand bars in April 2013 is
2448 low because the river stage was greater than 1,200 cfs TRF and the sand bars were not surveyed.
2449 Total bar area increased during the late July 2014 survey as vegetated bars and river bed area
2450 decreased. The causative factor for the increase in vegetative bar area was not evident in the
2451 data. The August 2015 bar area proportions are comparable to what was documented in 2013, a
2452 stable condition for bar area in the study reach.



2453

IX. REFERENCES

- 2454 Abraham, D. and Pratt, T. June 2002. Quantification of Bedload Transport on the Upper
2455 Mississippi River Using Multibeam Survey Data and Traditional Methods. US Army Corps
2456 of Engineers – ERDC/CHL-VII-4.
- 2457 Abraham, D., Kuhnle, R., and Odgaard, A. 2011. Validation of Bed-Load Transport
2458 Measurements with Time-Sequenced Bathymetric Data. *Journal of Hydraulic Engineering*
2459 (137)7, 723-728.
- 2460 Denver Post. 2015. Colorado Experts to Update Snowpack, Flood Outlook.
2461 [http://www.denverpost.com/2015/03/16/colorado-experts-to-update-snowpack-flood-](http://www.denverpost.com/2015/03/16/colorado-experts-to-update-snowpack-flood-outlook/)
2462 [outlook/](http://www.denverpost.com/2015/03/16/colorado-experts-to-update-snowpack-flood-outlook/)
- 2463 Dinehart, R.L. 2002. Bedform Movement Recorded by Sequential Single-Beam Surveys in Tidal
2464 Rivers. *Journal of Hydrology* 258 (2002) 25-39.
- 2465 Edwards, T.K., and Glysson, G.D., 1998. Field Methods for Measurement of Fluvial Sediment:
2466 U.S. Geological Survey Techniques of Water-Resources Investigations, Book 3, Applications
2467 of Hydraulics, Chapter C2.
- 2468 Erdman, Jon. 2013. Colorado Flash Flooding: How It Happened, How Unusual. *The Weather*
2469 *Channel*. [http://www.weather.com/storms/severe/news/colorado-flash-flood-how-it-](http://www.weather.com/storms/severe/news/colorado-flash-flood-how-it-happened-unusual-20130912)
2470 [happened-unusual-20130912](http://www.weather.com/storms/severe/news/colorado-flash-flood-how-it-happened-unusual-20130912).
- 2471 Holmquist-Johnson, C.L., and Raff, D.A. Bureau of Reclamation Automated Modified Einstein
2472 Procedure (BORAMEP) Program for Computing Total Sediment Load. Federal Interagency
2473 Sedimentation Conference in Reno, NV., April 2-6, 2006. (PDF 145 KB)
- 2474 National Weather Service (NWS). 2015. Northeast Colorado may Rainfall 2015: Total Rainfall
2475 over Northeast Colorado from 5/1/15 to 5/10/15.
2476 <http://www.weather.gov/bou/2015mayrainfall>
- 2477 Pittman, S.A. 2002. A Geomorphic Investigation of Mainstem Spawning by Chinook Salmon
2478 (*Oncorhynchus tshawytscha*) in the Smith River, California. Masters thesis at California
2479 State University at Humboldt, Arcata, California.
- 2480 Platte River Recovery Implementation Program (PRRIP), 2011. DRAFT Project-scale
2481 Geomorphology and Vegetation Monitoring, April 22, 2011.
- 2482 PRRIP, 2013. HEC-RAS model of the Platte River, personal communication with Jason
2483 Farnsworth. August 2013.
- 2484 PRRIP, 2014. Shoemaker Island Flow-Sediment-Mechanical “Proof of Concept” Experiment
2485 2013Annual Summary Report. April 2014.



- 2486 PRRIP, 2015a. Shoemaker Island Flow-Sediment-Mechanical “Proof of Concept” Experiment
2487 2014 Annual Summary Report. December 2015.
- 2488 PRRIP, 2015b. Shoemaker Island Flow-Sediment-Mechanical “Proof of Concept” Experiment
2489 Monitoring and Analysis Plan. March 2015.
- 2490 Podolak, C. and Pittman, S., 2011. Marmot Dam Removal Geomorphic Monitoring and
2491 Modeling Project—Final Report June 2007 – October 2011. Report prepared for Sandy River
2492 Basin Watershed Council, 111 p. Available at
2493 <http://digital.library.ucr.edu/cdri/?record=1191>.
- 2494 Pollen-Bankhead, N, R. Thomas and A. Simon. 2012. Can Short Duration High Flows be Used
2495 to Remove Vegetation from Bars in the Central Platte River? Final report to the Platte River
2496 Recovery Implementation Program. Directed Vegetation Research Study.
- 2497 Rantz, S.E., and others, 1982, Measurement and computation of streamflow: U.S. Geological
2498 Survey Water-Supply Paper 2175, 2 v., 631 p.
- 2499 Simon, A., N. Pollen-Bankhead, and R. Thomas. 2011. Stream Restoration in Dynamic Fluvial
2500 Systems: Scientific Approaches, Analyses, and Tools, Geophysical Monograph Series 194,
2501 American Geophysical Union. 10.1029/2010GM001006.
- 2502 USDA. 2010. Bank Stability and Toe Erosion Model: Static Version 5.2,
2503 <http://ars.usda.gov/Research/docs.htm?docid=5045>, viewed on October 21, 2013.
- 2504 USGS. 2013. National Water Information System: Web Interface, Platte River near Grand
2505 Island.
- 2506 USGS 2014. pers. Comm. with J. Farnsworth, January 16, 2014.
2507 [http://waterdata.usgs.gov/ne/nwis/measurements?site_no=06770375&agency_cd=USGS&for
2508 mat=html_table_expanded](http://waterdata.usgs.gov/ne/nwis/measurements?site_no=06770375&agency_cd=USGS&format=html_table_expanded).
2509
- 2510 Water Year 2005 Technical Memo #1, TOUTLE RIVER-2 Bedload Sampler. Report for US
2511 Department of the Interior, Bureau of Reclamation, Trinity River Restoration Program,
2512 Shasta Lake, CA.



Table of Contents

Tables

Table 4-1	Coordinates and Elevation for Cross Section Pins and Benchmarks.....	1
Table 4-2	Survey Codes	4
Table 5-1	Geomorphic Monitoring and Modeling Support Summary – June 2015 High Flow and August 2015 Effort	5
Table 5-2	FSM Management Strategy Flow Benchmarks and June 2015 High Flow Event Magnitude and Durations	6
Table 5-3	June 2015 High Flow Discharge Summary – Collected Between Cross Sections 2 and 3	7
Table 5-4	Bar Data Summary – July 2014 and August 2015.....	8
Table 5-5	Sand Bar Data Summary – July 2014 and August 2015.....	9
Table 5-6	Primary Cross Section Area and Volume Change by Average End Area Method – July 2014 to August 2015.....	10
Table 5-7	Supplemental and Primary Cross Section Area and Volume Change by Average End Area Method – July 2014 to August 2015.....	11
Table 5-8	Shoemaker Study Reach Vegetated Bars, Sand Bars, and Water/River Bed Area – July 2014 and August 2015.....	13
Table 5-9	June 2015 High Flow Suspended Sediment Sample Data.....	14
Table 5-10	June 2015 High Flow Suspended Sediment Transport Equations by Size Class.....	15
Table 5-11	June 2015 High Flow Sediment Load Totals by Size Class	16
Table 5-12	June 2015 High Flow Sediment Sample Summary	17
Table 5-13	2015 Bed and Bar Sample Summary.....	18
Table 8-1	Shoemaker Island FSM Experiment Monitored Flow Events, Field Efforts, Total River Flow at the Grand Island Gaging Station	20
Table 8-2	Shoemaker Study Reach – 3 Year Breakdown	21



TABLES



Table 4-1 Coordinates and Elevation for Cross Section Pins and Benchmarks

Description	Northing	Easting	Elevation
Benchmarks			
12A-T1-L	2046980.74	340291.98	1,940.37
12A-T4-L	2047439.48	340490.18	1,941.30
12A-T7-L	2047882.54	340712.10	1,939.69
Primary Cross Sections			
1 R	2040775.00	337870.08	-
1LSET	2040753.55	338731.37	1,948.70
2 R	2041479.53	337940.10	-
2LSET	2041598.23	338659.28	1,947.13
3 R	2042288.34	337847.56	-
3LSET	2042382.74	338417.12	1,946.61
4 R	2043032.00	337442.10	-
4LSET	2043188.14	338373.92	1,946.69
5 R	2043827.94	337352.07	-
5LSET	2043971.93	338526.85	1,944.51
6 R	2044604.65	337126.32	-
6LSET	2044835.66	338545.96	1,942.62
7 R	2045513.15	337686.93	-
7LSET	2045366.49	338600.09	1,942.98
8 R	2046376.53	337852.15	-
8LSET	2045707.51	338834.39	1,942.14
9 R	2047145.68	338188.11	-
9LSET	2046230.78	339383.72	1,940.07
10RSET	2047892.86	338475.99	1,941.60
10LSET	2047142.72	339511.21	1,939.92
11RSET	2048555.07	338937.41	1,940.52
11LSET	2047788.14	339974.97	1,938.76
12RSET	2049184.35	339441.89	1,939.63
12LSET	2048509.37	340352.44	1,937.19
13RSET	2049914.29	339833.83	1,938.64
13LSET	2049113.66	340884.84	1,935.98
14RSET	2050447.30	340425.67	1,935.36
14LSET	2049629.27	341642.71	1,936.51



15RSET	2051139.03	340857.55	1,933.88
15LSET	2050216.65	342100.80	1,936.91
16RSET	2051874.58	341212.56	1,935.94
16LSET	2050921.97	342540.41	1,935.45
17RSET	2052463.62	341628.06	1,934.73
17LSET	2051614.11	342876.22	1,934.94
18RSET	2053214.06	342083.87	1,933.19
18LSET	2052327.76	343280.25	1,933.51
Supplemental Cross Sections			
A R	2040411.49	337854.83	-
A L	2040317.27	338643.21	-
B R	2041303.67	337915.49	-
B L	2041223.39	338758.56	-
C R	2041878.26	338011.93	-
C L	2041894.58	338536.54	-
D R	2042618.24	337706.52	-
D L	2042729.87	338377.12	-
E R	2043473.36	337380.12	-
E L	2043602.58	338399.60	-
F R	2044163.83	337370.07	-
F L	2044307.21	338439.95	-
G R	2045036.85	337616.91	-
G L	2045080.66	338537.36	-
H R	2045853.93	337737.36	-
H L	2045589.37	338655.16	-
I R	2046774.83	338024.18	-
I L	2045986.33	339127.69	-
J R	2047590.33	338341.02	-
J L	2046690.82	339536.37	-
K R	2048297.53	338772.69	-
K L	2047511.73	339841.80	-
L R	2048860.03	339168.52	-
L L	2048207.26	340052.33	-
M R	2049529.52	339648.65	-
M L	2048805.20	340625.76	-
N R	2050157.84	340178.59	-



N L	2049385.93	341185.33	-
O R	2050773.88	340745.25	-
O L	2049936.66	341868.66	-
P R	2051564.95	341007.90	-
P L	2050625.49	342317.34	-
Q R	2052186.29	341431.91	-
Q L	2051269.03	342750.29	-
R R	2052828.02	341867.30	-
R L	2051952.31	343047.54	-
S R	2053552.54	342302.75	-
S L	2052699.21	343448.73	-

The coordinate system for all of the anchor points:

Horizontal: NAD83 Nebraska State Plane, FIPS 2600. Units: US Survey Feet

Vertical: NAVD88, Geoid 03, Units: Feet



Table 4-2 Survey Codes

Cross Section Point Labels	Description
OB	Overbank topo
LTP	Left Top of Pin
RTP	Right Top of Pin
LTB	Left Top of Bank
RTB	Right Top of Bank
LEW	Left Edge of Water
REW	Right Edge of Water
LBB	Left Bottom of Bank
RBB	Right Bottom of Bank
TBR	Top of Bar
GTBR	Green Top of Bar
CB	Channel Bottom
CBG	Channel Bottom-Gravel
Bar Point Labels	Description
Top	Perimeter of the top of the Bar
Toe	Perimeter of the toe of the Bar
Tran	Cross Section
Bank	Top of the bank of the river
Supplemental Data Labels	Description
Wat ele	Water Elevation
Pst	Pressure Transducer Post
Wse	Water surface elevation at pressure transducer post
Bs	Bulk Sample
Bd	Bulk Density Sample
Sc	Scour Chain
Dck blnd	Duck Blind
Pnd water ele	Pond Water Elevation



Table 5-1 Geomorphic Monitoring and Modeling Support Summary – June 2015 High Flow and August 2015 Effort

Data Collection	During June 2015 High Flow	August 2015
Survey		
Control Survey		1
LiDAR Data QA/scaling		1
Monumented Cross Sections		18
Supplemental Cross Sections		19
Long Profile		2
Bar Surveys		141
Stage and Turbidity		
Stage Reference Observations	25	2
Continuous Stage Recorders	3	1
Continuous Turbidimeters	1	
Discharge		
Meter Measurements	11	1
Sediment Sampling		
Suspended Sediment	18	1
Bed & Bar Bulk Samples		35
Bedload	2	
Bedload Variability	7	
Scour Monitoring		
Scour Chains		11
Photography		
Aerial photo acquisition		1
Repeat ground photos		2,239
Lab Analyses		
Suspended Sediment Concentration, GSA	34	2
Bed and Bar GSA		29
Bulk Density Calculations		6
Bedload Grain Size Analyses		9
Data Analysis		
GeoSpatial		
Cross Section Data Reduction		18
Supplemental Cross Section Data Reduction		19
Long Profile Data Reduction		2
Bar Survey Spatial Analyses		141
Volume Change Calculations		1
Stage		
Water Surface Slope	1	
Continuous Stage Records	1	
Discharge		
Stage Discharge Ratings	1	
Continuous Discharge Record Computation	1	
Sediment Discharge		
Suspended Sediment Load Computation	7	
Bed & Bar Grain Size Comparisons	22	
Bedload or Total Load Calculations	7	



Table 5-2 FSM Management Strategy Flow Benchmarks and June 2015 High Flow Event Magnitude and Durations

	Program Flow Benchmarks (TRF)	June 2015 High Flow Event	
		Grand Island Gage (TRF)	Shoemaker Study Reach* (SF)
Peak Instantaneous Discharge, cfs	NA	16,100	11,270
3-day Peak Mean Discharge, cfs	5,000 – 8,000	15,700	11,200
Volume, acre-feet (unrounded, for flows above 2,000 cfs)	50,000 – 75,000	1.231 million	861,723
Duration, Days (for flows above 2,000 cfs)	3 - Days	72 – Days	72 - Days

*The 2015 hydrograph for the Shoemaker total river flow was developed using 15-minute pressure transducer stage data collected at cross section 18.



Table 5-3 June 2015 High Flow Discharge Summary – Collected Between Cross Sections 2 and 3

Measurement Number	WY Msmt #	Date	Made By	Width (feet)	Mean Depth (feet)	Area (ft2)	Mean Velocity (ft/sec)	Staff Height (feet)	Gage Height * (feet)	Discharge (cfs)	Rating 1.1			Method	Begin Time (hours)	End Time (hours)	Msmt Rating
											Comp. Shift (feet)	Used Shift (feet)	% Diff.				
1	2015-01	5/25/2015	GMA	480	4.74	2273	3.72	7.21	1932.17	8450	-0.08	0.00	-6	Boat	15:37	16:37	Poor
2	2015-02	5/28/2015	GMA	486	4.23	2055	4.31	7.09	1931.99	8860	0.16	0.00	10	Boat	13:10	13:50	Fair
3	2015-03	6/4/2015	GMA	516	4.59	2366	4.56	7.50	1932.48	10800	-0.01	0.00	-1	Boat	13:40	14:18	Poor
4	2015-04	6/5/2015	GMA	498	4.80	2392	4.43	7.47	1932.48	10600	-0.04	0.00	-2	Boat	13:03	13:35	Fair
5	2015-05	6/6/2015	GMA	483	4.80	2318	4.62	7.46	1932.48	10700	-0.02	0.00	-1	Boat	10:23	10:55	Fair
6	2015-06	6/15/2015	EA Engineering	491	4.12	2021	4.29	7.25	1932.21	8680	-0.08	0.00	-6	Boat	12:00	12:50	Poor
7	2015-07	7/2/2015	EA Engineering	477	3.82	1821	3.59	6.62	1931.69	6540	0.03	0.00	2	Boat	12:47	13:20	Poor
8	2015-08	7/3/2015	EA Engineering	486	3.53	1717	3.59	6.47	1931.57	6170	0.07	0.00	5	Boat	9:26	10:04	Fair
9	2015-09	7/6/2015	EA Engineering	486	2.93	1426	3.45	6.06	1931.25	4920	0.10	0.00	9	Boat	12:35	13:54	Fair
10	2015-10	7/9/2015	EA Engineering	483	2.33	1128	3.02	5.73	1931.03	3410	-0.09	0.00	-9	Boat	12:38	13:45	Fair
11	2015-11	7/14/2015	EA Engineering	444	2.08	921	2.50	5.09	1930.63	2300	-0.06	0.00	-8	Boat	12:25	13:08	Fair
12	2015-12	8/27/2015	GMA	488	1.01	491	2.08	4.28	1929.94	1020	0.02	0.00	2	Wading	12:15	13:06	Good



Table 5-4 Bar Data Summary – July 2014 and August 2015

	All Bars													
	Sand						Vegetated						All Bars	
	Natural		Treated		Total Sand		Natural		Treated		Total Vegetated			
	July 2014	August 2015	July 2014	August 2015	July 2014	August 2015	July 2014	August 2015	July 2014	August 2015	July 2014	August 2015	July 2014	August 2015
Number	30	31	113	79	143	110	18	15	26	16	44	31	187	141
Total Area (acres)	6.05	11.47	51.25	53.56	57.30	65.03	37.71	20.39	79.67	43.99	117.38	64.37	174.68	129.41
Minimum (acres)	<0.001	<0.001	0.001	<0.001	<0.001	<0.001	0.007	<0.001	0.002	0.007	0.002	<0.001	<0.001	<0.001
Maximum (acres)	1.53	8.81	18.31	8.95	18.31	8.95	19.67	6.53	19.95	18.21	19.95	18.21	19.95	18.21



Table 5-5 Sand Bar Data Summary – July 2014 and August 2015

	Sand Bars Only													
	<0.25 Acres						>0.25 Acres						All Sand Bars	
	Natural		Treated		Total <0.25		Natural		Treated		Total >0.25			
	July 2014	August 2015	July 2014	August 2015	July 2014	August 2015	July 2014	August 2015	July 2014	August 2015	July 2014	August 2015	July 2014	August 2015
Number	22	28	81	59	103	87	8	3	32	20	40	23	143	110
Total Area (acres)	1.62	2.02	7.19	3.43	8.81	5.46	4.44	9.45	44.05	50.13	48.49	59.58	57.30	65.03
Minimum (acres)	<0.001	<0.001	0.001	<0.001	<0.001	<0.001	0.283	0.312	0.260	0.273	0.251	0.273	<0.001	<0.001
Maximum (acres)	0.22	0.24	0.23	0.25	0.23	0.25	1.53	8.81	18.31	8.95	21.72	8.95	18.31	8.95



Table 5-6 Primary Cross Section Area and Volume Change by Average End Area Method – July 2014 to August 2015

Cross Section	Cut Area	Fill Area	Net Area Cut/Fill	Station	Distance to Next	Volume Cut	Volume Fill	Net Volume	Volume Cut	Volume Fill	Net Volume	Lateral Erosion Area	Lateral Erosion Volume	
	(ft ²)	(ft ²)	(ft ²)										(ft ³)	(ft ³)
1	346.4	112.8	-233.6	19,386	777	231,083	245,381	14,298	8,559	9,088	530	35.93	27,916	1,034
2	248.5	518.9	270.4	18,609	815	174,332	302,347	128,015	6,457	11,198	4,741	35	28,835	1,068
3	179.2	222.8	43.7	17,794	802	253,154	249,632	-3,522	9,376	9,246	-130	20.41	16,362	606
4	452.5	400.1	-52.5	16,992	777	377,952	414,031	36,080	13,998	15,334	1,336	146.35	113,696	4,211
5	520.5	665.8	145.3	16,215	824	390,065	501,865	111,799	14,447	18,588	4,141	307.25	253,160	9,376
6	426.3	552.4	126.0	15,391	801	399,297	352,885	-46,412	14,789	13,070	-1,719	113.54	90,997	3,370
7	570.1	328.2	-241.9	14,590	688	446,839	368,510	-78,329	16,550	13,649	-2,901	12.95	8,912	330
8	728.3	742.5	14.3	13,902	794	375,739	528,681	152,942	13,916	19,581	5,665		0	0
9	218.2	589.2	371.0	13,108	796	231,928	515,158	283,230	8,590	19,080	10,490		0	0
10	364.3	704.6	340.3	12,311	807	379,567	518,667	139,101	14,058	19,210	5,152	59.62	48,126	1,782
11	576.1	580.4	4.3	11,504	805	355,093	466,517	111,424	13,152	17,278	4,127		0	0
12	306.6	579.3	272.7	10,699	811	273,121	464,024	190,902	10,116	17,186	7,070	133.12	107,965	3,999
13	366.9	565.0	198.1	9,888	816	341,516	567,956	226,440	12,649	21,035	8,387	66.47	54,210	2,008
14	470.5	827.7	357.2	9,073	787	349,474	643,518	294,045	12,943	23,834	10,891	138.43	108,936	4,035
15	417.7	807.8	390.1	8,286	815	298,758	566,599	267,840	11,065	20,985	9,920	23.70	19,311	715
16	315.5	582.8	267.2	7,471	741	243,982	380,433	136,451	9,036	14,090	5,054	3	2,128	79
17	342.7	443.6	100.9	6,730	848	343,090	363,269	20,179	12,707	13,454	747	0.31	266	10
18	466.5	413.1	-53.3	5,882	0								0	0
*final row is rounded to nearest 100				13,500	13,500	5,465,000	7,449,500	1,984,500	202,400	275,900	73,500	1,100	880,800	32,600



Table 5-7 Supplemental and Primary Cross Section Area and Volume Change by Average End Area Method – July 2014 to August 2015

Cross Section	Cut Area	Fill Area	Net Area Cut/Fill	Station	Distance to Next	Volume Cut	Volume Fill	Net Volume	Volume Cut	Volume Fill	Net Volume	Lateral Erosion Area	Lateral Erosion Volume	
	(ft ²)	(ft ²)	(ft ²)										(ft)	(ft ³)
A	248.0	450.8	202.8	19,793	407	121,078	114,806	-6,272	4,484	4,252	-232	29.1	13,240	490
1	346.4	112.8	-233.6	19,386	505	150,956	83,931	-67,025	5,591	3,109	-2,482	35.9	26,279	973
B	252.0	219.9	-32.1	18,881	272	68,150	100,593	32,443	2,524	3,726	1,202	68.2	14,107	522
2	248.5	518.9	270.4	18,609	353	118,253	93,378	-24,875	4,380	3,458	-921	35.4	13,116	486
C	421.6	10.3	-411.3	18,256	462	138,876	53,882	-84,994	5,144	1,996	-3,148	39.0	13,725	508
3	179.2	222.8	43.7	17,794	348	114,872	82,142	-32,730	4,255	3,042	-1,212	20.4	6,365	236
D	481.8	249.8	-232.0	17,446	454	212,086	147,520	-64,566	7,855	5,464	-2,391	16.2	36,899	1,367
4	452.5	400.1	-52.5	16,992	425	194,692	209,317	14,625	7,211	7,752	542	146.3	38,122	1,412
E	464.3	585.7	121.3	16,567	352	173,417	220,372	46,956	6,423	8,162	1,739	33.2	59,945	2,220
5	520.5	665.8	145.3	16,215	336	171,604	191,236	19,633	6,356	7,083	727	307.2	54,251	2,009
F	501.9	473.5	-28.4	15,880	488	226,613	250,458	23,845	8,393	9,276	883	16.0	31,618	1,171
6	426.3	552.4	126.0	15,391	350	131,807	146,013	14,206	4,882	5,408	526	113.5	21,421	793
G	326.5	281.6	-44.9	15,041	451	202,299	137,593	-64,706	7,493	5,096	-2,397	8.8	4,908	182
7	570.1	328.2	-241.9	14,590	315	200,769	100,679	-100,090	7,436	3,729	-3,707	12.9	2,042	76
H	703.1	310.2	-392.9	14,274	373	266,894	196,299	-70,594	9,885	7,270	-2,615	0.0	0	0
8	728.3	742.5	14.3	13,902	414	284,201	267,457	-16,743	10,526	9,906	-620	0.0	0	0
I	643.6	548.5	-95.1	13,487	380	163,593	215,971	52,378	6,059	7,999	1,940	0.0	0	0
9	218.2	589.2	371.0	13,108	457	147,339	281,495	134,156	5,457	10,426	4,969	0.0	1,491	55
J	426.5	642.5	216.0	12,650	339	134,148	228,524	94,376	4,968	8,464	3,495	6.5	11,220	416
10	364.3	704.6	340.3	12,311	501	234,324	455,368	221,044	8,679	16,865	8,187	59.6	14,946	554
K	570.4	1111.8	541.4	11,810	306	175,335	258,788	83,452	6,494	9,585	3,091	0.0	0	0
11	576.1	580.4	4.3	11,504	383	225,886	224,378	-1,508	8,366	8,310	-56	0.0	11,156	413
L	604.4	592.3	-12.2	11,121	422	192,182	247,136	54,955	7,118	9,153	2,035	58.3	40,381	1,496
12	306.6	579.3	272.7	10,699	400	156,643	216,087	59,443	5,802	8,003	2,202	133.1	39,839	1,476



Cross Section	Cut Area	Fill Area	Net Area Cut/Fill	Station	Distance to Next	Volume Cut	Volume Fill	Net Volume	Volume Cut	Volume Fill	Net Volume	Lateral Erosion Area	Lateral Erosion Volume	
	(ft ²)	(ft ²)	(ft ²)										(ft)	(ft)
M	476.0	500.2	24.3	10,299	411	173,076	218,735	45,659	6,410	8,101	1,691	65.9	27,180	1,007
13	366.9	565.0	198.1	9,888	401	199,570	282,024	82,454	7,391	10,445	3,054	66.5	37,995	1,407
N	629.1	842.5	213.4	9,488	415	228,089	346,451	118,362	8,448	12,832	4,384	123.2	54,262	2,010
14	470.5	827.7	357.2	9,073	425	183,686	291,334	107,647	6,803	10,790	3,987	138.4	29,398	1,089
O	394.4	544.1	149.7	8,648	362	147,075	244,842	97,767	5,447	9,068	3,621	0.0	4,292	159
15	417.7	807.8	390.1	8,286	443	244,766	416,959	172,193	9,065	15,443	6,378	23.7	23,911	886
P	686.8	1073.7	386.9	7,843	372	186,305	307,877	121,573	6,900	11,403	4,503	84.2	16,183	599
16	315.5	582.8	267.2	7,471	394	155,986	231,749	75,762	5,777	8,583	2,806	2.9	648	24
Q	477.2	595.0	117.8	7,077	348	142,575	180,614	38,040	5,281	6,689	1,409	0.4	128	5
17	342.7	443.6	100.9	6,730	406	152,520	194,762	42,242	5,649	7,213	1,565	0.3	5,963	221
R	408.8	516.0	107.2	6,324	442	193,473	205,382	11,908	7,166	7,607	441	29.1	6,425	238
18	466.5	413.1	-53.3	5,882	404	129,398	194,764	65,366	4,793	7,213	2,421	0.0	2,080	77
S	174.3	551.4	377.0	5,478	0	0	0	0	0	0	0	10.3	0	0
*final values rounded to nearest hundred				468,200	14,300	6,342,500	7,638,900	1,296,400	234,900	282,900	48,000	1,700	663,500	24,600



Table 5-8 Shoemaker Study Reach Vegetated Bars, Sand Bars, and Water/River Bed Area – July 2014 and August 2015

	July 2014		August 2015	
	Acres	Percent	Acres	Percent
	Mechanically Treated Study Reach – 246 Acres		Mechanically Treated Study Reach – 266 Acres	
Vegetated Bars	79.7	32%	44.0	17%
Sand Bars	51.2	21%	53.6	20%
Water/River Bed	115.1	47%	168.4	63%
Total	246	100%	266	100%
	Natural Study Reach – 116 Acres		Natural Study Reach – 96 Acres	
Vegetated Bars	37.7	33%	20.4	21%
Sand Bars	6.1	5%	11.5	12%
Water/River Bed	72.2	62%	64.1	67%
Total	116	100%	96	100%



Table 5-9 June 2015 High Flow Suspended Sediment Sample Data

Site	Date/Time	Type	Discharge (cfs)	Measured Concentration (mg/l)	% Finer Than					
					0.062 mm	0.125 mm	0.25 mm	0.5 mm	1 mm	2 mm
XS 2-3	5/24/15 14:34	DIS	9070	488	9	17	65	94	99	100
	5/24/15 16:57	DIS	9150	548	11	19	67	93	99	100
	5/25/15 14:26	DIS	8980	436	8	15	63	94	99	100
	5/25/15 17:27	DIS	8930	498	8	15	61	91	98	100
	5/26/15 15:10	DIS	8590	526	10	16	56	85	93	100
	5/27/15 14:12	DIS	8360	536	8	14	45	73	93	100
	5/28/15 11:14	DIS	7930	332	13	21	61	93	99	100
	6/3/15 18:00	DIS	10700	394	13	22	62	94	99	100
	6/4/15 14:56	DIS	11000	343	9	20	66	96	99	100
	6/5/15 9:49	DIS	11100	445	6	15	54	84	97	100
	6/6/15 9:12	DIS	10800	512	5	12	45	89	99	100
	6/15/15 11:16	DIS	9230	371	15	25	72	96	99	99
	7/2/15 11:37	DIS	6400	211	41	52	77	95	99	100
	7/3/15 8:53	DIS	5870	194	35	46	74	95	99	100
	7/6/15 11:37	DIS	4490	160	35	48	71	90	98	100
	7/9/15 10:58	DIS	3750	103	29	42	73	93	99	100
7/14/15 11:17	DIS	2210	84	79	92	98	99	100	100	
8/27/15 13:21	DIS	994	49	50	61	79	95	100	100	

¹values are not rounded (Porterfield, 1972)



Table 5-10 June 2015 High Flow Suspended Sediment Transport Equations by Size Class

Size Class	Equation $y = SSC$	X-Variable
<0.063mm	No Relation	
0.063 - 0.25mm	$0.000313228 * Q^{1.46324}$	Water Discharge
0.25 - 0.5mm	$5.49746e-006 * Q^{1.840692}$	Water Discharge
0.5 - 1mm	$3.66218e-005 * Q^{1.47645}$	Water Discharge
0.5 - 1mm	$2.49043e-005 * Q^{1.34534}$	Water Discharge
1 - 2mm	Zero Transport	
>2mm	No Relation	



Table 5-11 June 2015 High Flow Sediment Load Totals by Size Class

	SS Loads (tons)	Bedload (tons)	Total (tons)
<0.063mm	99,923	92	100,016
0.063-0.25mm	236,316	4,795	241,110
0.25-0.5mm	135,106	32,502	167,607
0.5-1mm	28,587	91,050	119,637
1-2mm	5,593	168,224	173,817
>2mm	-	164,398	164,398
Total*	505,000	461,000	966,000

*only the Total is rounded as per Porterfield (1972)
Summing then rounding only the totals yields 967,000 tons



Table 5-12 June 2015 High Flow Sediment Sample Summary

Site	Date/Time	Discharge (cfs)	Measured Concentration (mg/l)	Measured SS Discharge (t/d)	Measured Bedload Discharge (t/d)	Bedload as Residual (t/d)	Measured Bedload + SS Discharge (t/d)	MEP Total Load (t/d)	MEP Total Sand Load >0.625mm (t/d)	Ratio of SS to Total
XS 2-3	5/24/15 14:34	9,070	488	11,940	NA	6,695	NA	18,635	17,586	64%
XS 2-3	5/24/15 16:57	9,150	548	13,539	NA	6,846	NA	20,385	18,898	66%
XS 2-3	5/25/15 14:26	8,980	436	10,578	NA	5,805	NA	16,383	15,576	65%
XS 2-3	5/25/15 17:27	8,930	498	12,012	NA	6,155	NA	18,167	17,217	66%
XS 2-3	5/26/15 15:10	8,590	526	12,193	NA	6,038	NA	18,231	17,020	67%
XS 2-3	5/27/15 14:12	8,360	536	12,090	NA	7,721	NA	19,811	18,801	61%
XS 2-3	5/28/15 11:14	7,930	332	7,102	NA	5,301	NA	12,403	11,470	57%
XS 2-3	6/3/15 18:00	10,700	394	11,383	NA	8,479	NA	19,862	18,346	57%
XS 2-3	6/4/15 14:56	11,000	343	10,196	NA	13,622	NA	23,818	22,893	43%
XS 2-3	6/5/15 9:49	11,100	445	13,322	NA	12,461	NA	25,784	24,947	52%
XS 2-3	6/6/15 9:12	10,800	512	14,937	NA	16,045	NA	30,982	30,295	48%
XS 2-3	6/15/15 11:16	9,230	371	9,255	NA	9,590	NA	18,845	17,440	49%
XS 2-3	7/2/15 11:37	6,400	211	3,653	NA	4,467	NA	8,120	6,589	45%
XS 2-3	7/3/15 8:53	5,870	194	3,077	NA	4,737	NA	7,814	6,723	39%
XS 2-3	7/6/15 11:37	4,490	160	1,937	NA	3,692	NA	5,629	4,922	34%
XS 2-3	7/9/15 10:58	3,750	103	1,041	NA	2,061	NA	3,102	2,797	34%
XS 2-3	7/14/15 11:17	2,210	84	502	NA	*	NA	NA	NA	NA
XS 2-3	8/27/15 13:21	994	49	131	NA	416	NA	546	474	24%

* MEP grain size error code



Table 5-13 2015 Bed and Bar Sample Summary

Field ID	Type	Date	Description	Feature	5-									Mass (g)	Dry Bulk Density (g/cm ³)
					D5	D16	D25	D35	D50	D65	D75	D84	D90		
1	Bulk	8/26/15	lateral bar lightly vegetated	Bar	0.1 mm	0.2 mm	0.3 mm	0.3 mm	0.4 mm	0.5 mm	0.5 mm	0.7 mm	0.8 mm	1,206	na
3	Bulk	8/26/15	unvegetated active bar coarse lens	Bar	0.2 mm	0.3 mm	0.4 mm	0.5 mm	1.0 mm	1.8 mm	2.6 mm	3.7 mm	4.7 mm	1,012	na
4	Bulk	8/26/15	unvegetated active bar fine lens	Bar	0.1 mm	0.2 mm	0.3 mm	0.3 mm	0.4 mm	0.6 mm	0.8 mm	1.2 mm	1.8 mm	995	na
7	Bulk	8/26/15	emergent bar - unvegetated	Bar	0.1 mm	0.2 mm	0.3 mm	0.4 mm	0.7 mm	1.2 mm	1.9 mm	3.0 mm	4.1 mm	1,872	na
8	Bulk	8/26/15	US end of large lightly vegetated bar	Bar	0.1 mm	0.2 mm	0.4 mm	0.6 mm	2.0 mm	3.8 mm	5.3 mm	7.2 mm	8.8 mm	1,328	na
12	Bulk	8/26/15	lateral bar lightly vegetated below XS13	Bar	0.1 mm	0.3 mm	0.4 mm	0.7 mm	1.6 mm	2.8 mm	3.8 mm	4.9 mm	5.9 mm	888	na
13	Bulk	8/26/15	Fine component of large 1.5' high lateral bar near XS16	Bar	0.1 mm	0.2 mm	0.3 mm	0.4 mm	0.7 mm	1.6 mm	2.7 mm	4.1 mm	5.8 mm	1,090	na
14	Bulk	8/26/15	Coarse component of large 1.5' high lateral bar near XS16	Bar	0.2 mm	0.3 mm	0.4 mm	0.6 mm	0.9 mm	1.6 mm	2.3 mm	3.3 mm	4.6 mm	1,434	na
19	Bulk	8/26/15	Fresh lateral bar above XS1	Bar	0.2 mm	0.3 mm	0.3 mm	0.4 mm	0.5 mm	0.8 mm	1.0 mm	1.4 mm	1.8 mm	1,168	na
21	Bulk	8/26/15	High new bar	Bar	0.1 mm	0.2 mm	0.3 mm	0.5 mm	0.9 mm	1.7 mm	2.4 mm	3.4 mm	4.5 mm	1,126	na
33	Bulk	8/27/15	Bar near XS6	Bar	0.2 mm	0.3 mm	0.3 mm	0.4 mm	0.6 mm	0.8 mm	1.0 mm	1.4 mm	1.8 mm	976	na
2	Bulk	8/26/15	active dune field in north channel	Bed	0.1 mm	0.2 mm	0.3 mm	0.3 mm	0.4 mm	0.6 mm	0.8 mm	1.0 mm	1.5 mm	2,438	na
5	Bulk	8/26/15	Active dune 2° flow channel	Bed	0.2 mm	0.3 mm	0.3 mm	0.4 mm	0.5 mm	0.6 mm	0.7 mm	0.8 mm	1.0 mm	1,690	na
6	Bulk	8/26/15	Dune 1° flow channel	Bed	0.2 mm	0.3 mm	0.4 mm	0.5 mm	0.7 mm	1.0 mm	1.4 mm	2.0 mm	2.7 mm	1,130	na
9	Bulk	8/26/15	Dune 2° flow channel	Bed	0.2 mm	0.4 mm	0.5 mm	0.6 mm	0.8 mm	1.1 mm	1.5 mm	1.9 mm	2.3 mm	992	na
11	Bulk	8/26/15	Same-all size classes seem mixed even with fine dune surfaces	Bed	0.2 mm	0.3 mm	0.4 mm	0.5 mm	0.7 mm	1.0 mm	1.5 mm	2.4 mm	3.9 mm	1,724	na
15	Bulk	8/26/15	Very fine flat dune	Bed	0.2 mm	0.3 mm	0.3 mm	0.4 mm	0.5 mm	0.8 mm	1.0 mm	1.4 mm	1.9 mm	1,330	na
16	Bulk	8/26/15	Coarser bedform 0.1' above water surface	Bed	0.2 mm	0.3 mm	0.3 mm	0.5 mm	0.8 mm	1.3 mm	1.9 mm	2.7 mm	3.7 mm	1,016	na
17	Bulk	8/26/15	Submerged bar @ XS17	Bed	0.2 mm	0.2 mm	0.3 mm	0.3 mm	0.4 mm	0.6 mm	0.8 mm	1.1 mm	1.7 mm	1,202	na
18	Bulk	8/26/15	XS1	Bed	0.2 mm	0.3 mm	0.4 mm	0.5 mm	0.7 mm	1.0 mm	1.5 mm	2.2 mm	3.0 mm	2,208	na
20	Bulk	8/26/15	Main thread (N) dune	Bed	0.3 mm	0.4 mm	0.6 mm	0.8 mm	1.2 mm	1.8 mm	2.5 mm	3.7 mm	5.1 mm	2,026	na
24	Bulk	8/27/15	tertiary channel near NB XS3	Bed	0.3 mm	0.6 mm	0.9 mm	1.2 mm	1.9 mm	2.6 mm	3.3 mm	4.2 mm	5.1 mm	2,322	na
27	Bulk	8/27/15	Main channel	Bed	0.2 mm	0.4 mm	0.6 mm	1.1 mm	2.6 mm	4.6 mm	6.8 mm	9.4 mm	11.7 mm	1,502	na
28	Bulk	8/27/15	N. channel around Tx Bar complex @XS5	Bed	0.3 mm	0.5 mm	0.7 mm	1.0 mm	1.6 mm	2.5 mm	3.3 mm	4.5 mm	5.5 mm	1,161	na
29	Bulk	8/27/15	Same channel S side	Bed	0.3 mm	0.3 mm	0.5 mm	0.6 mm	1.0 mm	1.5 mm	2.1 mm	3.0 mm	3.8 mm	2,142	na
31	Bulk	8/27/15	1° flow channel along south bank near BSTEM XS5	Bed	0.3 mm	0.4 mm	0.7 mm	1.2 mm	2.1 mm	3.1 mm	4.0 mm	5.0 mm	5.8 mm	2,126	na
32	Bulk	8/27/15	South channel below XS5 near property boundary	Bed	0.1 mm	0.2 mm	0.2 mm	0.3 mm	0.4 mm	0.6 mm	0.9 mm	1.4 mm	2.0 mm	1,784	na
35	Bulk	8/27/15		Bed	0.2 mm	0.3 mm	0.3 mm	0.4 mm	0.4 mm	0.6 mm	0.7 mm	1.0 mm	1.5 mm	1,806	na
22	BD	8/27/15	DS end of XS2 bar-unvegetated	Bar	0.2 mm	0.3 mm	0.4 mm	0.6 mm	0.8 mm	1.3 mm	1.7 mm	2.5 mm	3.3 mm	552	1.79



Field ID	Type	Date	Description	Feature	5-									Mass (g)	Dry Bulk Density (g/cm ³)
					D5	D16	D25	D35	D50	D65	D75	D84	D90		
23	BD	8/27/15	DS end of XS2 bar-lightly vegetated	Bar	0.2 mm	0.4 mm	0.5 mm	0.6 mm	0.8 mm	1.3 mm	1.7 mm	2.4 mm	3.3 mm	550	1.78
25	BD	8/27/15	fine lobe	Bar	0.2 mm	0.3 mm	0.4 mm	0.6 mm	1.0 mm	1.8 mm	2.6 mm	3.8 mm	5.0 mm	523	1.69
26	BD	8/27/15	coarser lobe	Bar	0.2 mm	0.4 mm	0.5 mm	0.8 mm	2.0 mm	3.4 mm	4.9 mm	6.7 mm	8.1 mm	470	1.52
30	BD	8/27/15	Mid channel new bar on XS5	Bar	0.2 mm	0.3 mm	0.4 mm	0.5 mm	0.9 mm	1.6 mm	2.3 mm	3.5 mm	4.8 mm	589	1.91
34	BD	8/27/15	Near XS8-highly braided 1.5' above WSE	Bar	0.2 mm	0.3 mm	0.4 mm	0.6 mm	0.9 mm	1.6 mm	2.3 mm	3.2 mm	4.0 mm	539	1.74
For the 6 bulk density samples:					mean	0.19	0.33	0.45	0.62	1.07	1.81	2.60	3.67	4.73	1.74
					min	0.16	0.28	0.39	0.55	0.81	1.25	1.74	2.43	3.26	1.52
					max	0.24	0.37	0.50	0.81	1.98	3.41	4.92	6.68	8.06	1.91



Table 8-1 Shoemaker Island FSM Experiment Monitored Flow Events, Field Efforts, Total River Flow at the Grand Island Gaging Station

	Program Benchmarks	Post SDMF Field Effort: 25 March 2013 to 3 April 2013	April 2013 SDMF (12 April 2013 to 18 April 2013)		Post SDMF Field Effort: 26 April 2013 to 29 April 2013	Fall 2013 High Flow (24 September 2013 to 1 November 2013)		Pre June 2014 High Flow Field Effort: 5 May 2014 to 9 May 2014	June 2014 High Flow (6 June 2014 to 5 July 2014)		Post June 2014 High Flow Field Effort: 21 July 2014 to 31 July 2014	June 2015 High Flow (11 May 2015 to 20 July 2015)		August 2015 Field Effort: 24 August 2015 to 2 September 2015
			Volume	% of Benchmark		Volume	% of Benchmark		Volume	% of Benchmark		Volume	% of Benchmark	
Peak Instantaneous Discharge, cfs	NA		3,840	NA		10,600	NA		8,800	NA		16,100	NA	
3-day Peak Mean Discharge, cfs	5,000 – 8,000		3,552	44%		9,700	121%		7,320	92%		15,700	196%	
Volume, acre-feet (unrounded, for flows above 2,000 cfs)	50,000 – 75,0000		33,743	45%		248,270	331%		181,270	242%		1.231 million	1641%	
Duration, Days (for flows above 2,000 cfs)	3		6			28			30			72		



Table 8-2 Shoemaker Study Reach – 3 Year Breakdown

	April 2013		July 2014		August 2015	
	Acres	Percent	Acres	Percent	Acres	Percent
	Mechanically Treated Study Reach - 252 Acres		Mechanically Treated Study Reach – 246 Acres		Mechanically Treated Study Reach – 266 Acres	
Vegetated Bars	46.1	18%	79.7	32%	44.0	17%
Sand Bars	54.3	22%	51.2	21%	53.6	20%
Water/River Bed	151.6	60%	115.1	47%	168.4	63%
Total	252.0	100%	246	100%	266.0	100%
	Natural Study Reach - 110 Acres		Natural Study Reach – 116 Acres		Natural Study Reach – 96 Acres	
Vegetated Bars	27.9	25%	37.7	33%	20.4	21%
Sand Bars	0.7	1%	6.1	5%	11.5	12%
Water/River Bed	81.4	74%	72.2	62%	64.1	67%
Total	110.0	100%	116	100%	96.0	100%



Table of Contents

Figures

Figure 3-1	Site Map.....	1
Figure 3-2	Monitoring Cross Section Locations	2
Figure 4-1	February 2015 Ice Floe Through the Shoemaker Study Reach.....	3
Figure 4-2	Schematic Figure Showing Scour Chain	4
Figure 5-1	Hydrograph Grand Island Gage (USGS 06770500) Total River Flow (TRF) with July 2014 and August 2015 Field Efforts.....	5
Figure 5-2	Stage Discharge Relation for Shoemaker Study Reach – June 2015 High Flow	6
Figure 5-3	Shoemaker Reach Split Flow Discharge and Sampling Events During June 2015 High Flow	7
Figure 5-4	Shoemaker Reach Split Flow Discharge and USGS Total River Flow Discharge at Grand Island – June 2015 High Flow	8
Figure 5-5	Bar Attributes – July 2014 and August 2015.....	9
Figure 5-6	Area of All Bars Surveyed – July 2014 and August 2015.....	10
Figure 5-7	Sand Bars Surveyed – July 2014 and August 2015	11
Figure 5-8	Mean Sand Bar Height Above 1,200 cfs TRF Stage - August 2015	12
Figure 5-9	Typical Primary Cross Section – Bottom Profile – July 2014 and August 2015	13
Figure 5-10	Cumulative and Net Volume Change at the 37 Primary and Supplemental Cross Sections – August 2015	14
Figure 5-11	Platte River Water Surface Slope Profile Through the Shoemaker Study Reach	15
Figure 5-12	Vegetation Plots.....	16
Figure 5-13	Bar 46 in July 2014 (November 2014 Aerial)	17
Figure 5-14	Bar 46 in July 2014 – Ground Photo	18
Figure 5-15	Bar 46 in August 2015 (July 2015 Aerial).....	19
Figure 5-16	Maximum Un-Vegetated Channel Widths at the 18 Primary Cross Sections – August 2015	20
Figure 5-17	Vegetation Roughness Polygons.....	21
Figure 5-18	Platte River Bedload Discharge – June 2015 High Flow	22
Figure 6-1	Cumulative Distributions of Sand Bar and Vegetated Bar Area Relative to the June 2015 High Flow 3-Day Mean Peak Discharge Stage.....	23

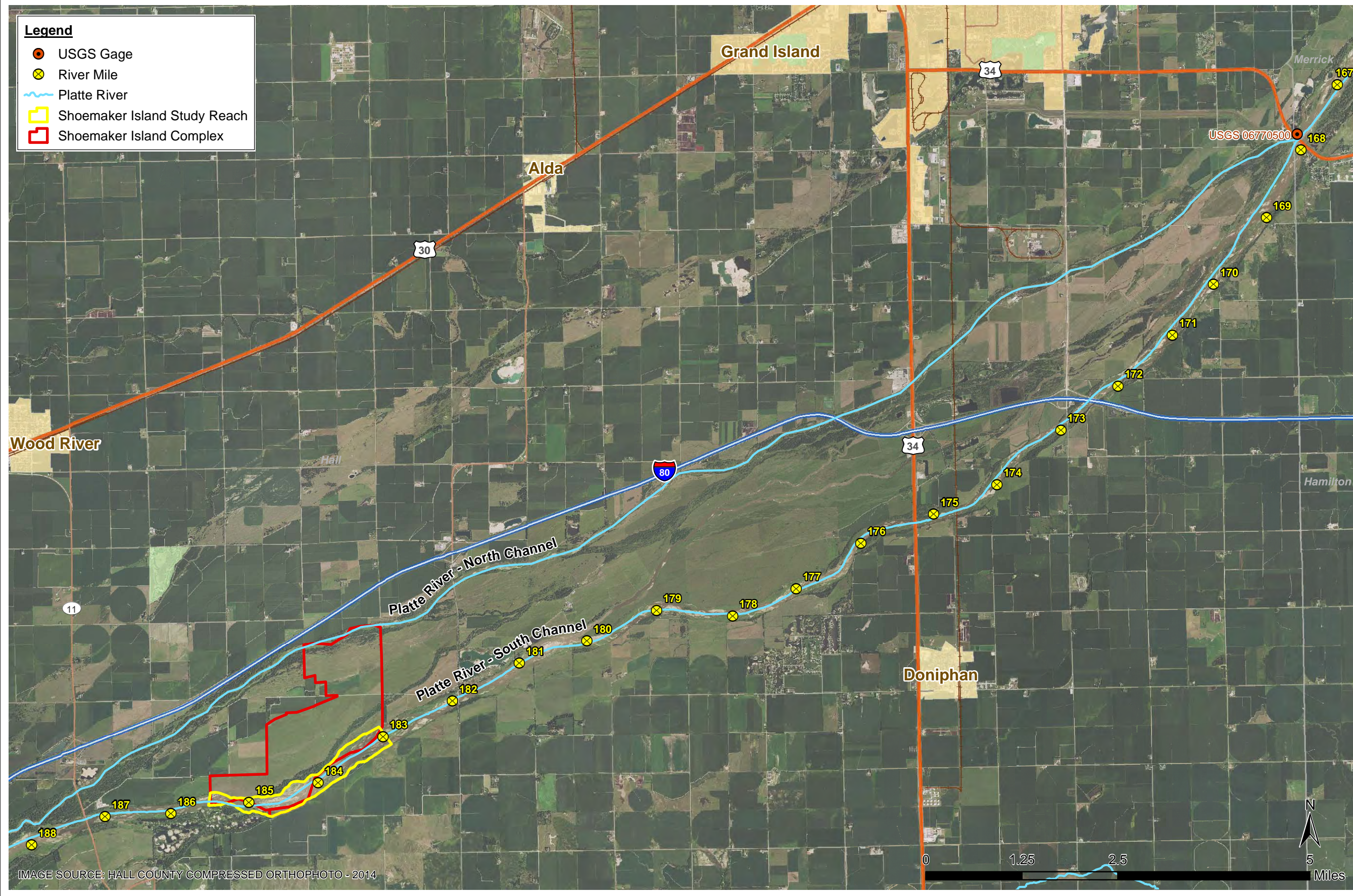


Figure 8-1	Mean Sand Bar Height Above 1,200 cfs TRF Stage – July 2014.....	24
Figure 8-2	Bar Attributes April 2013, July 2014, and August 2015	25
Figure 8-3	D50 Ranges for 2013 Pre and Post, 2014 Pre and Post, and 2015 Post.....	26
Figure 8-4	Area of All Bars Surveyed – April 2013, July 2014, and August 2015	27



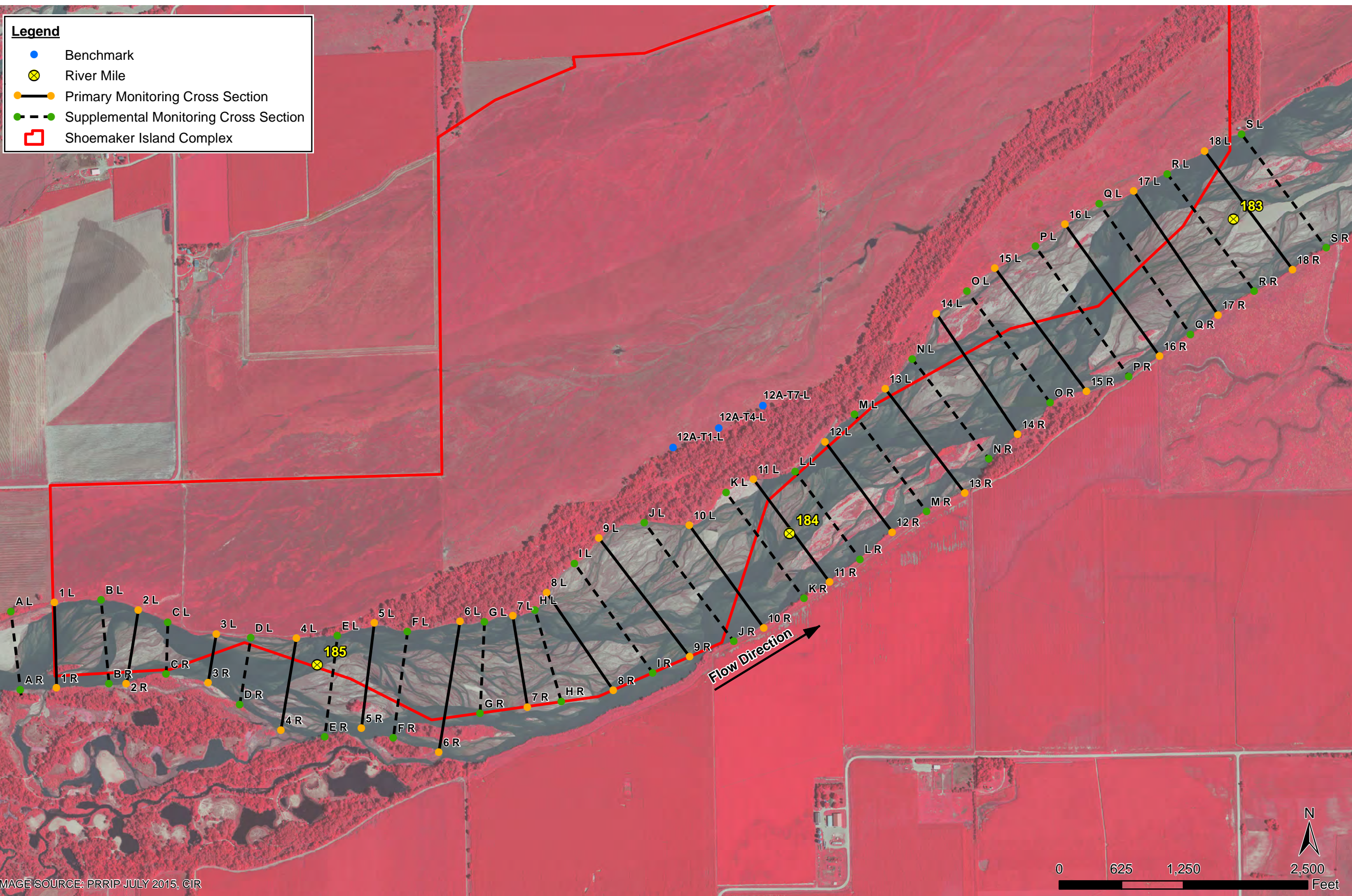
FIGURES

2016-05-26 F:\State & Local\Other\Platte River Recovery Program\Projects\1499201 - Shoemaker FSM Proof of Concept\Figures\MXD\015\MXD\3-1 - Site Location.mxd EA-Lincoln J.petersen



 PLATTE RIVER RECOVERY IMPLEMENTATION PROGRAM		DESIGNED BY	-	CHECKED BY	KMD	DATE	MAY 2016	SCALE	AS SHOWN	PROJECT NO.	1499201	FILE NAME	-	DRAWING NO.	-	FIGURE	3-1
		PROJECT MGR.	DLB	DRAWN BY	JKP												
SHOEMAKER ISLAND FSM PROOF OF CONCEPT <small>HALL COUNTY, NEBRASKA</small>						SITE MAP											

2017-03-27 F:\State & Local\Other\Platte River Recovery Program\Projects\1499201 - Shoemaker FSM Proof of Concept\Figures\WXD\2015\WXD\3-2 - Monitoring Cross Section Location.mxd EA-Lincoln_jpeterson



 PLATTE RIVER RECOVERY IMPLEMENTATION PROGRAM		DESIGNED BY	-	
		DRAWN BY	JKP	
CHECKED BY		KMD		
DATE		MAY 2016		
SCALE		AS SHOWN		
PROJECT NO.		1499201		
FILE NAME		-		
DRAWING NO.		-		
FIGURE		3-2		

MONITORING CROSS SECTION LOCATIONS

SHOEMAKER ISLAND FSM PROOF OF CONCEPT
HALL COUNTY, NEBRASKA



Figure 4-1 February 2015 Ice Floe Through the Shoemaker Study Reach





Figure 4-2 Schematic Figure Showing Scour Chain

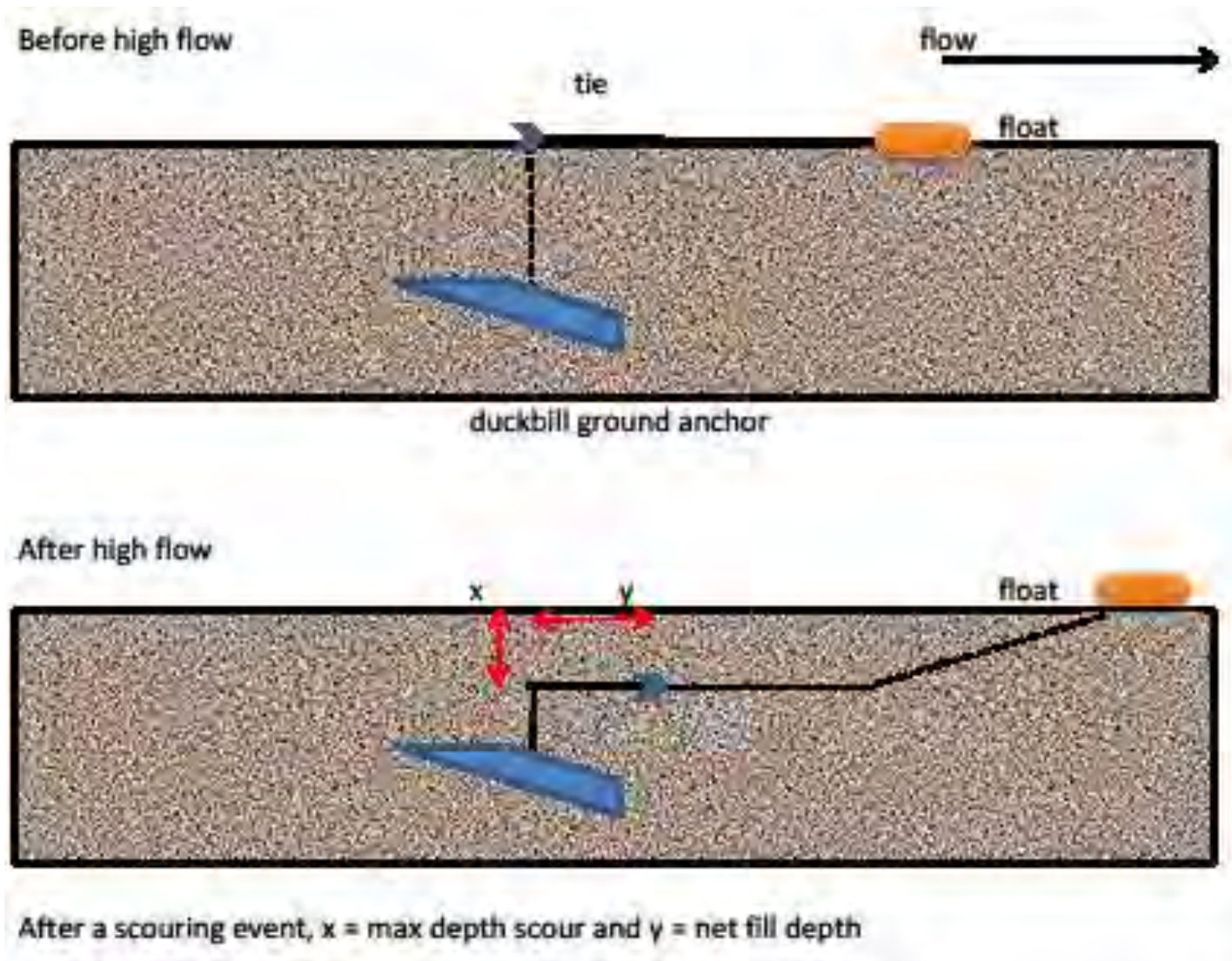




Figure 5-1 Hydrograph Grand Island Gage (USGS 06770500) Total River Flow (TRF) with July 2014 and August 2015 Field Efforts

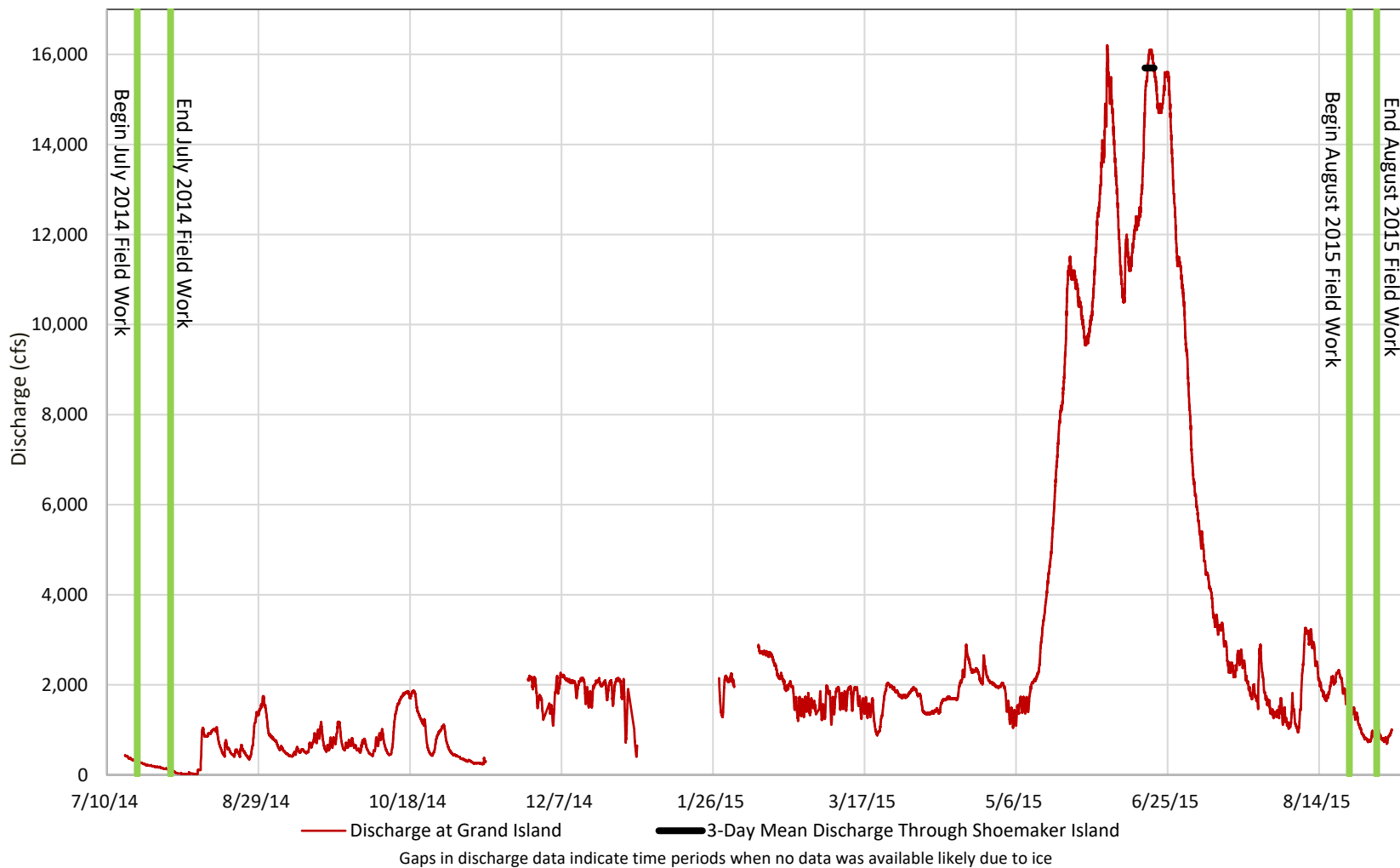




Figure 5-2 Stage Discharge Relation for Shoemaker Study Reach – June 2015 High Flow

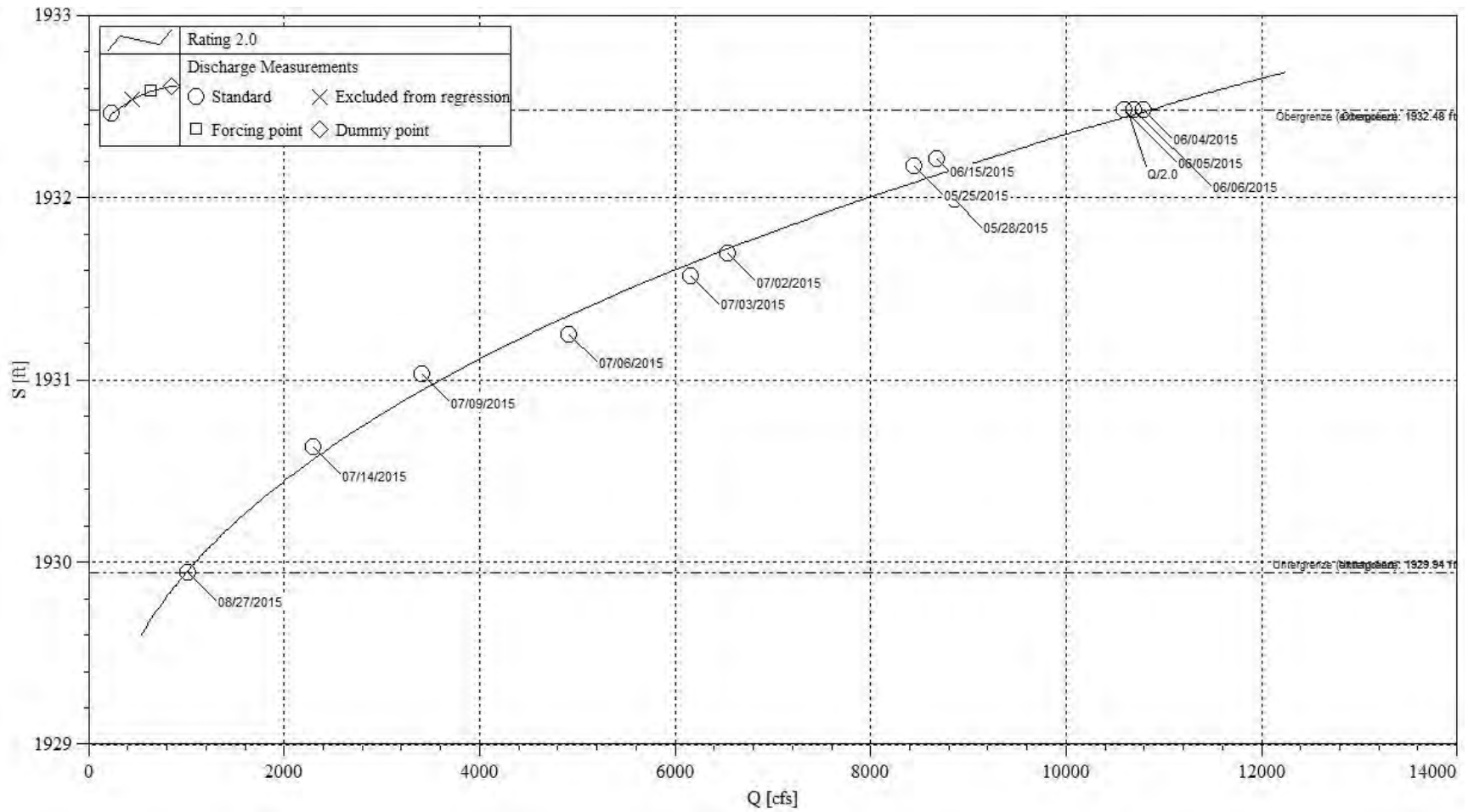
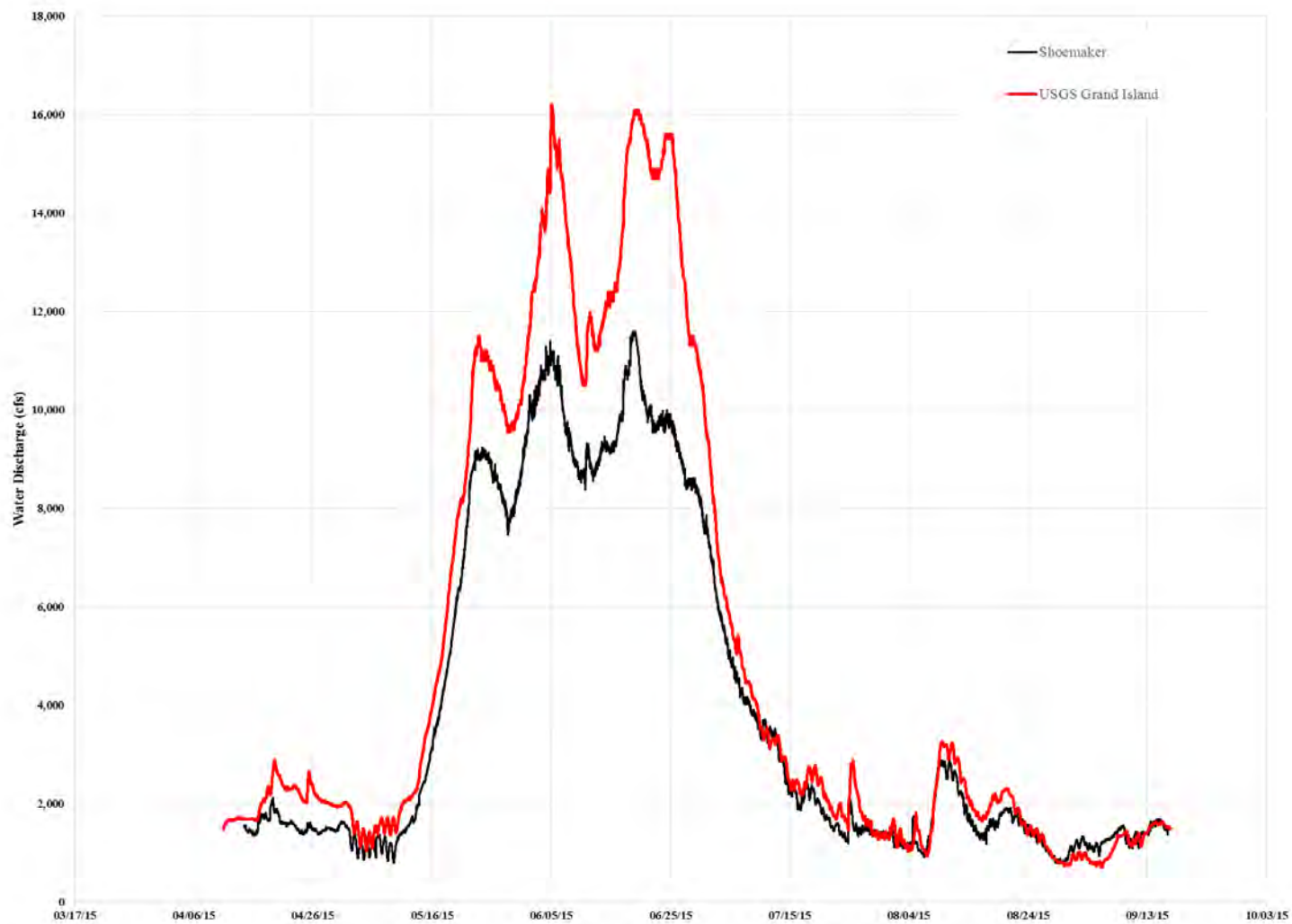




Figure 5-4 Shoemaker Reach Split Flow Discharge and USGS Total River Flow Discharge at Grand Island – June 2015 High Flow



2016-08-12 F:\State & Local\Other\Platte River Recovery Program\Projects\1499201 - Shoemaker FSM Proof of Concept\Figures\MXD\2015\MXD\5-5 - Pre Vs. Post.mxd EA-Lincoln_jpeterson

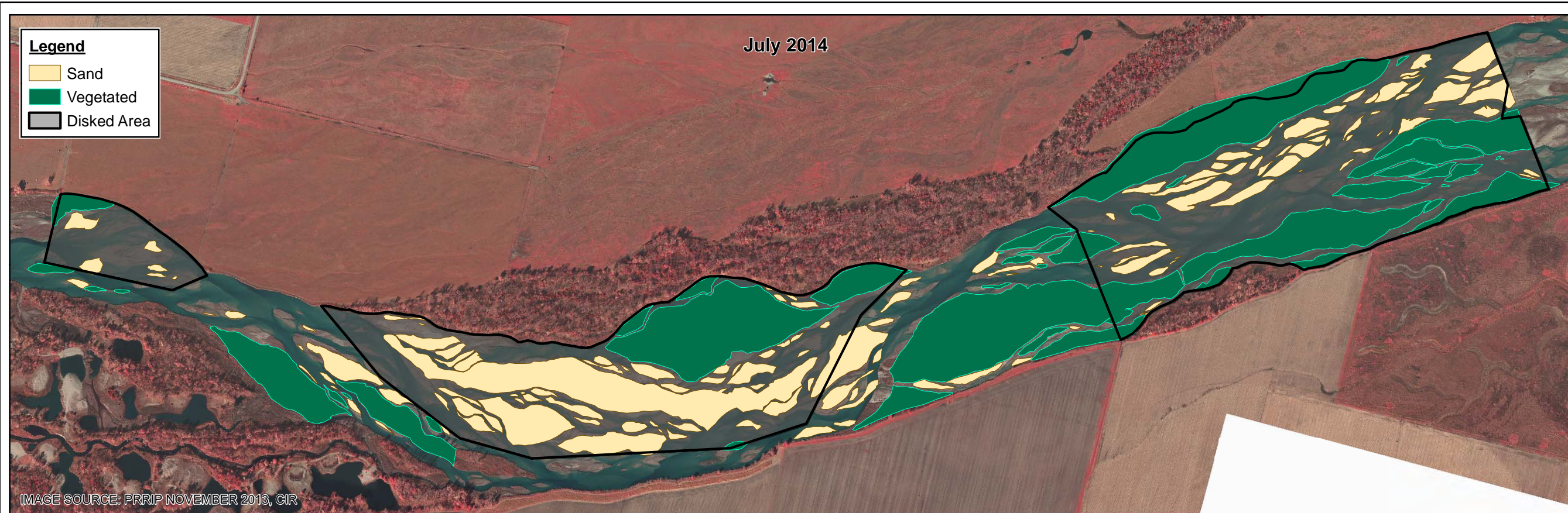


IMAGE SOURCE: PRRIP NOVEMBER 2013, CIR

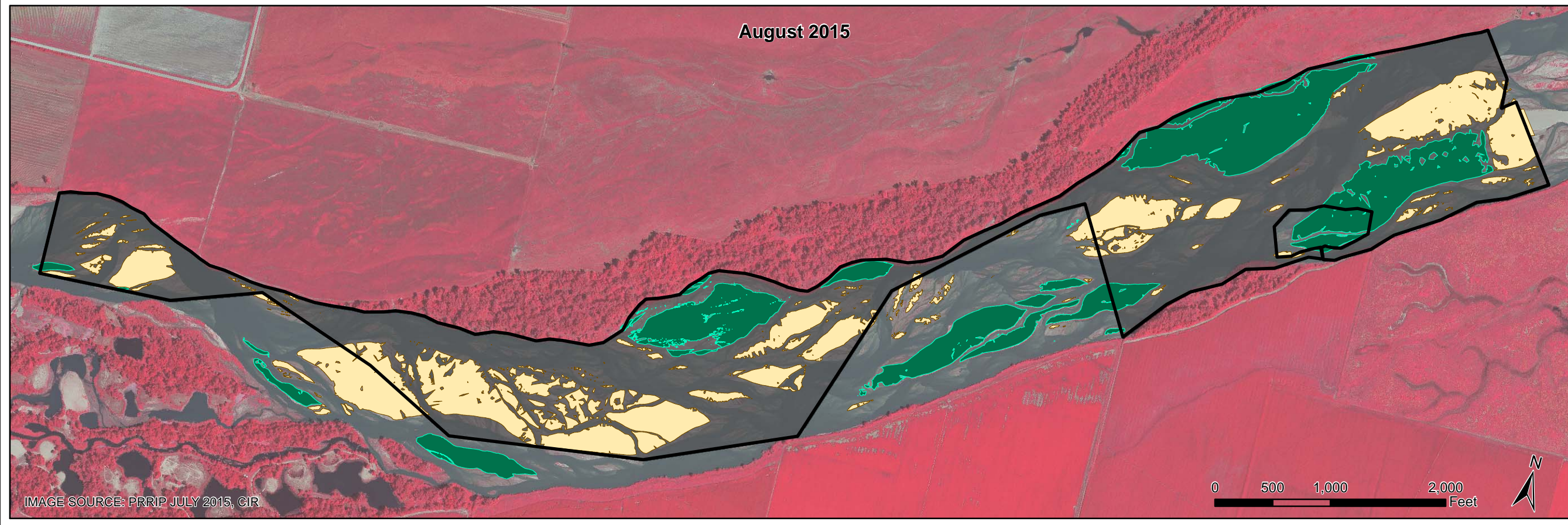


IMAGE SOURCE: PRRIP JULY 2015, CIR

 PLATTE RIVER RECOVERY IMPLEMENTATION PROGRAM		SHOEMAKER ISLAND FSM PROOF OF CONCEPT <small>HALL COUNTY, NEBRASKA</small>		BAR ATTRIBUTES JULY 2014 TO AUGUST 2015					
		PROJECT MGR. DLB	DESIGNED BY --	DRAWN BY JKP	CHECKED BY KMD	DATE AUG 2016	SCALE AS SHOWN	PROJECT NO. 1499201	FILE NAME -



Figure 5-6 Area of All Bars Surveyed – July 2014 and August 2015

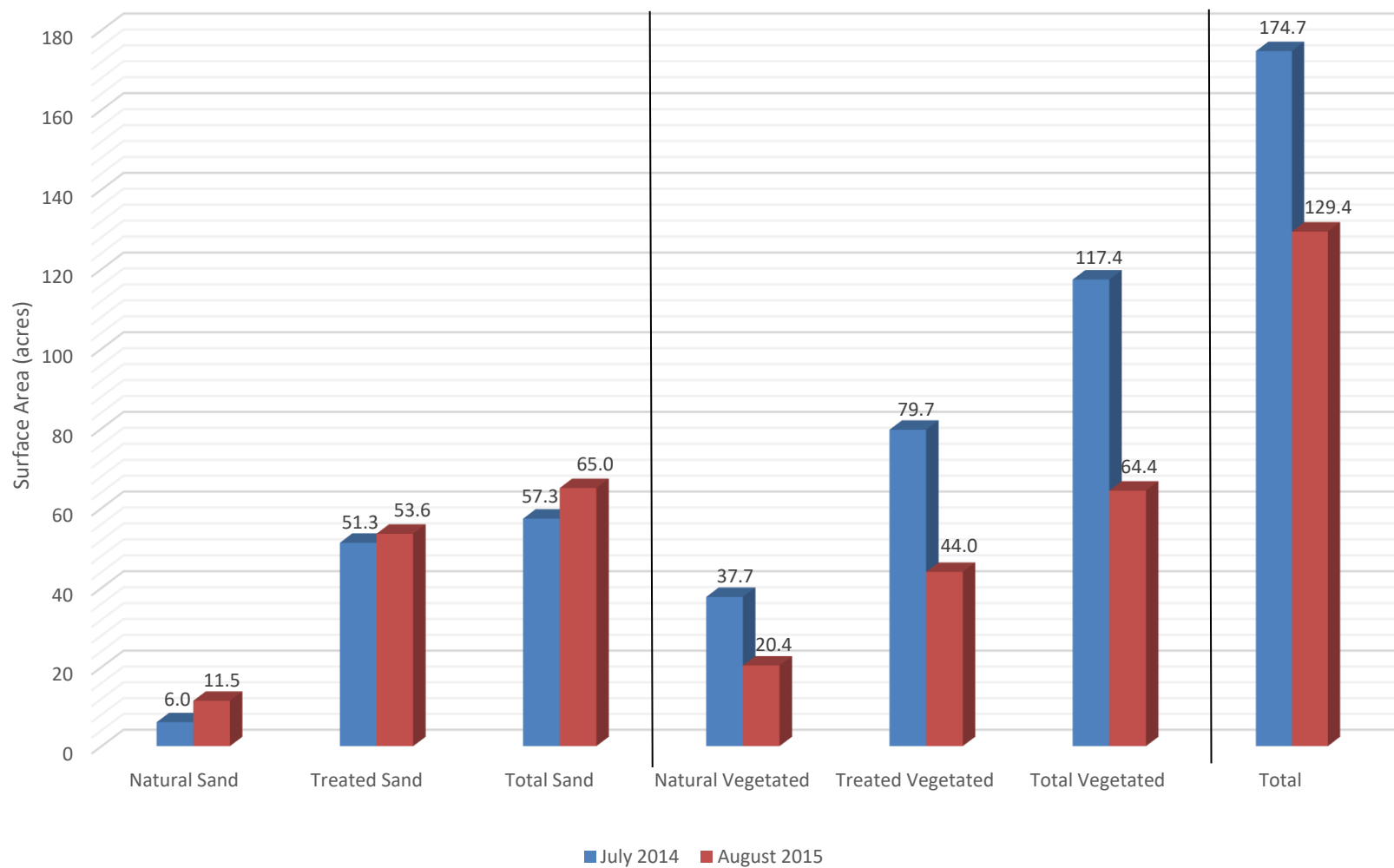




Figure 5-7 Sand Bars Surveyed – July 2014 and August 2015

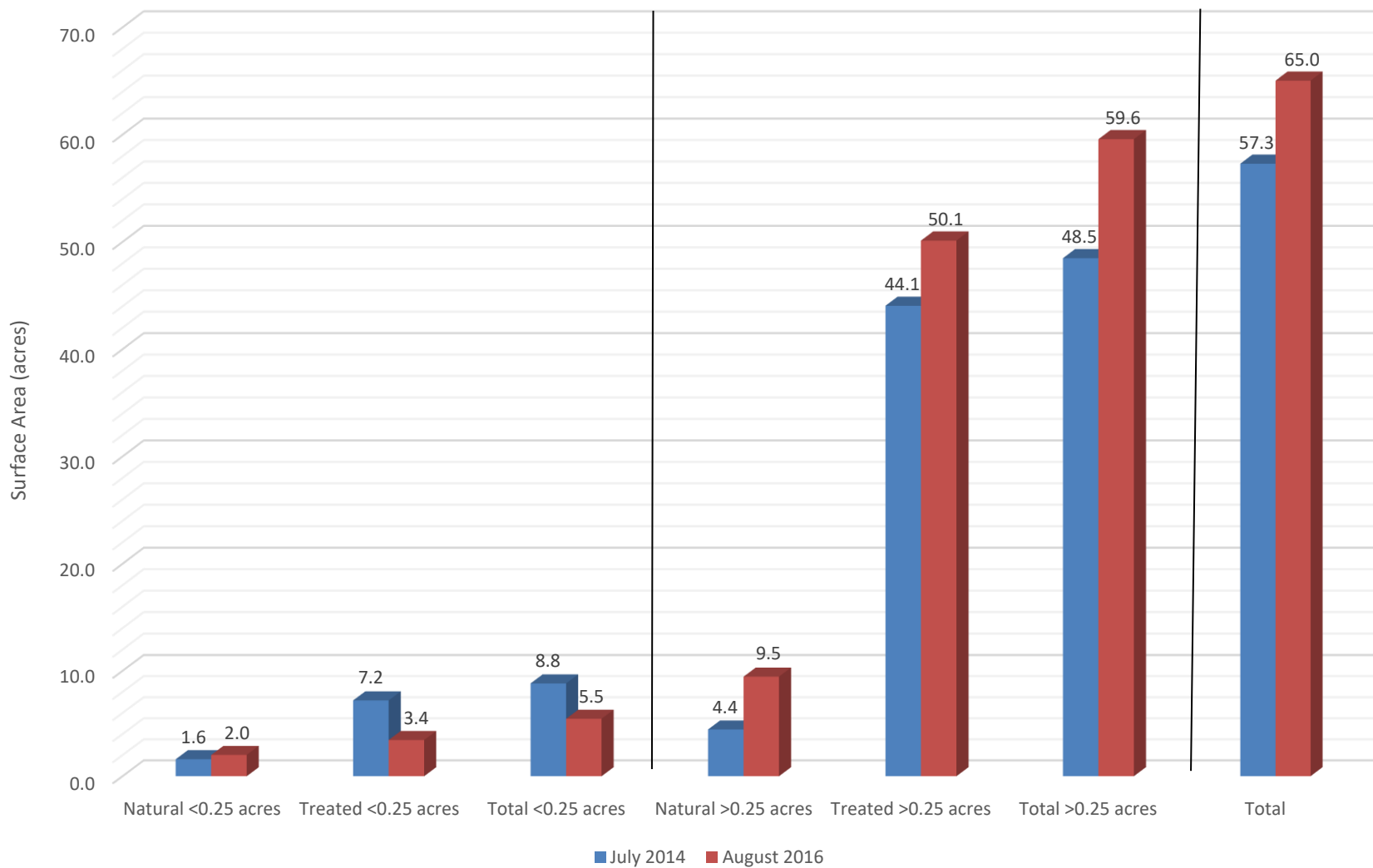




Figure 5-8 Mean Sand Bar Height Above 1,200 cfs TRF Stage - August 2015

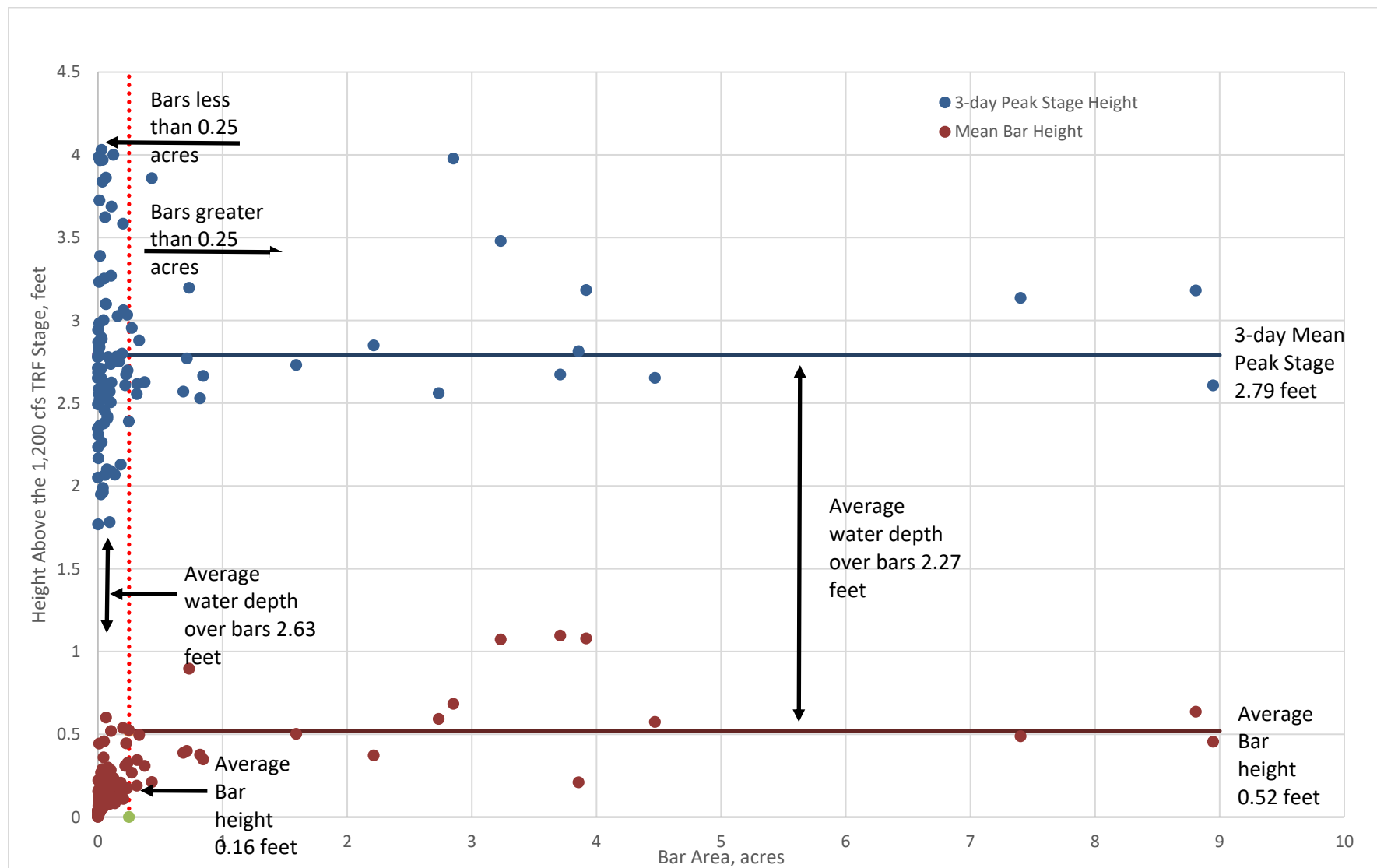




Figure 5-9 Typical Primary Cross Section – Bottom Profile – July 2014 and August 2015

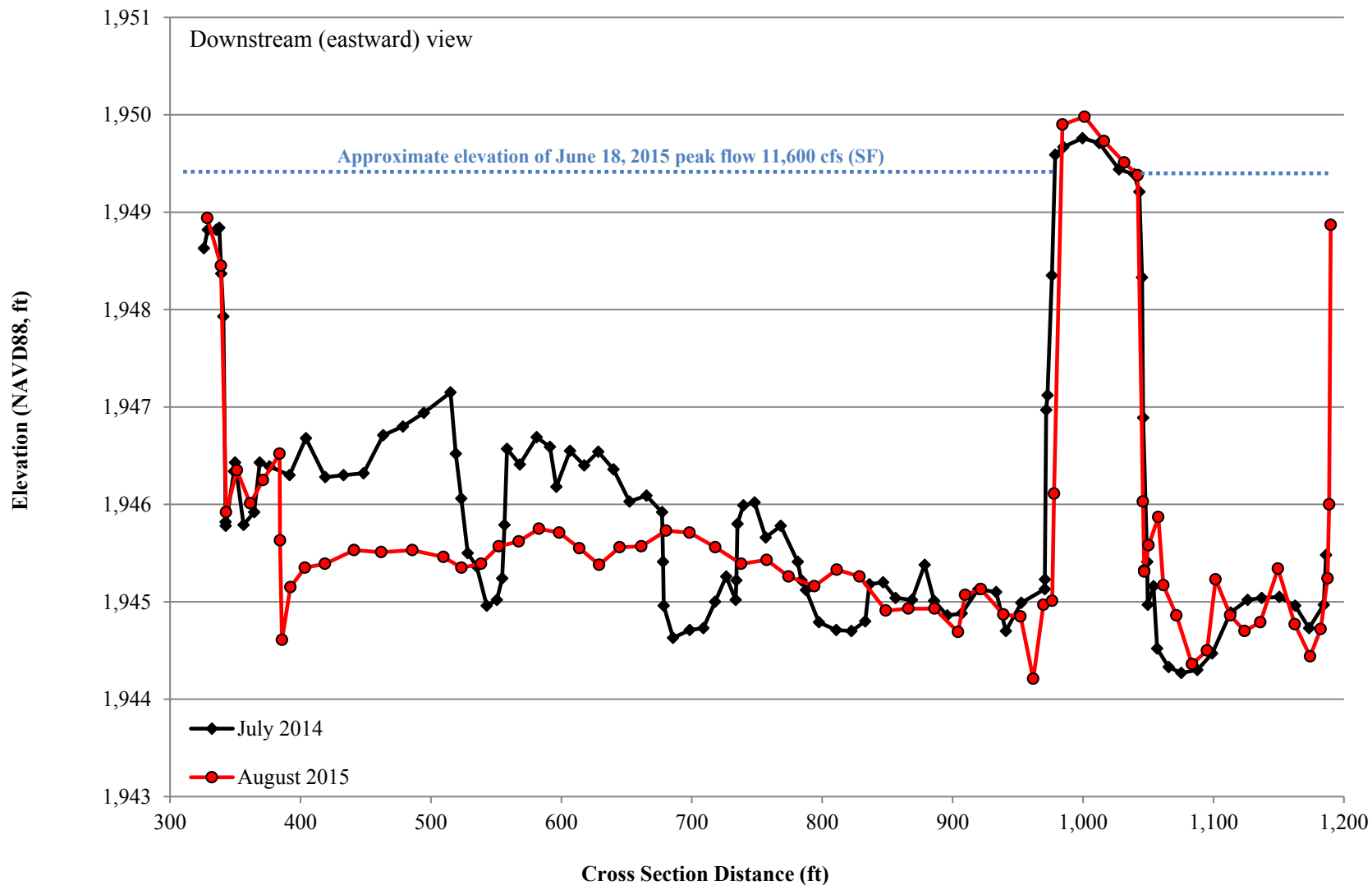




Figure 5-10 Cumulative and Net Volume Change at the 37 Primary and Supplemental Cross Sections – August 2015

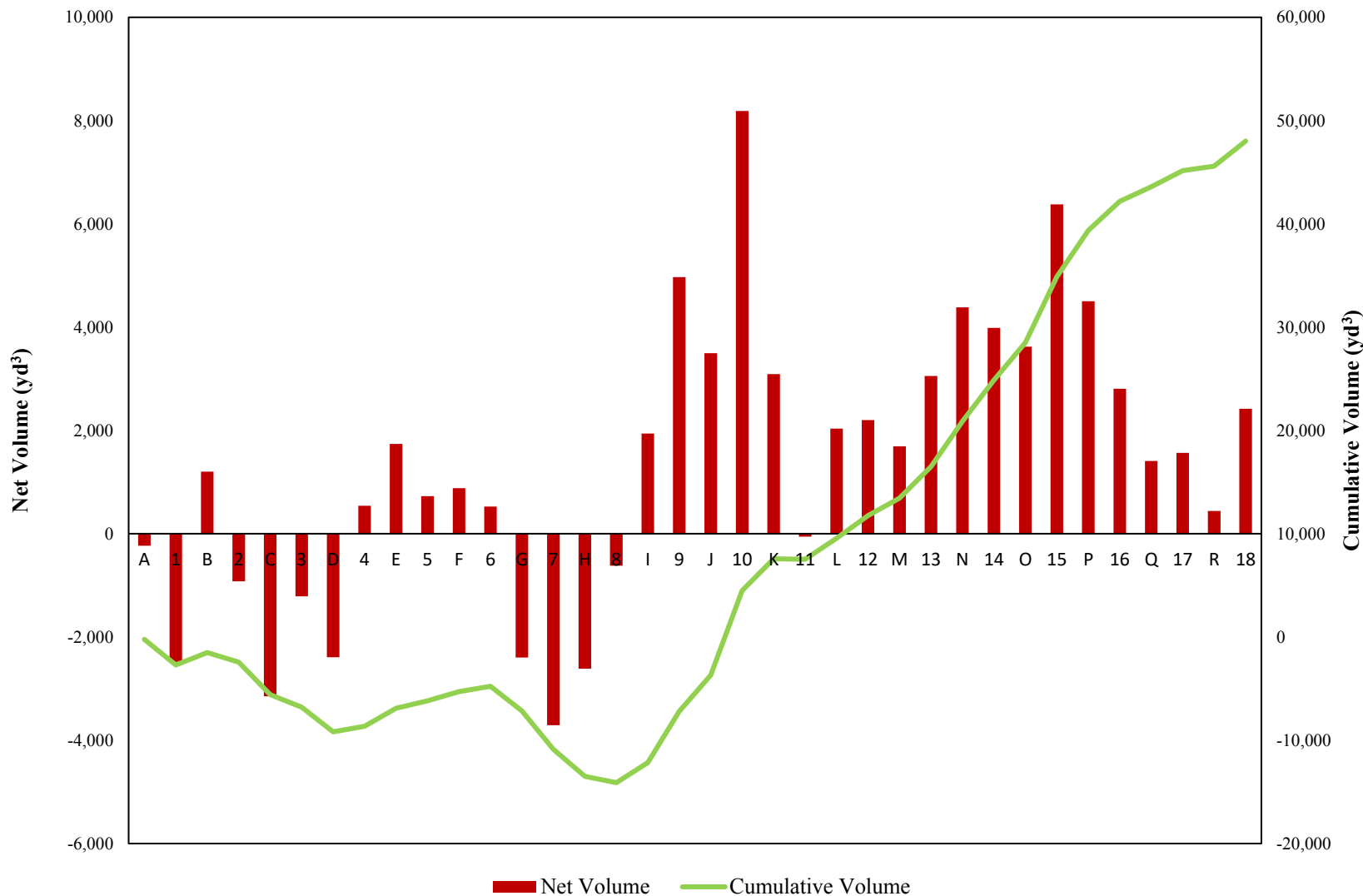
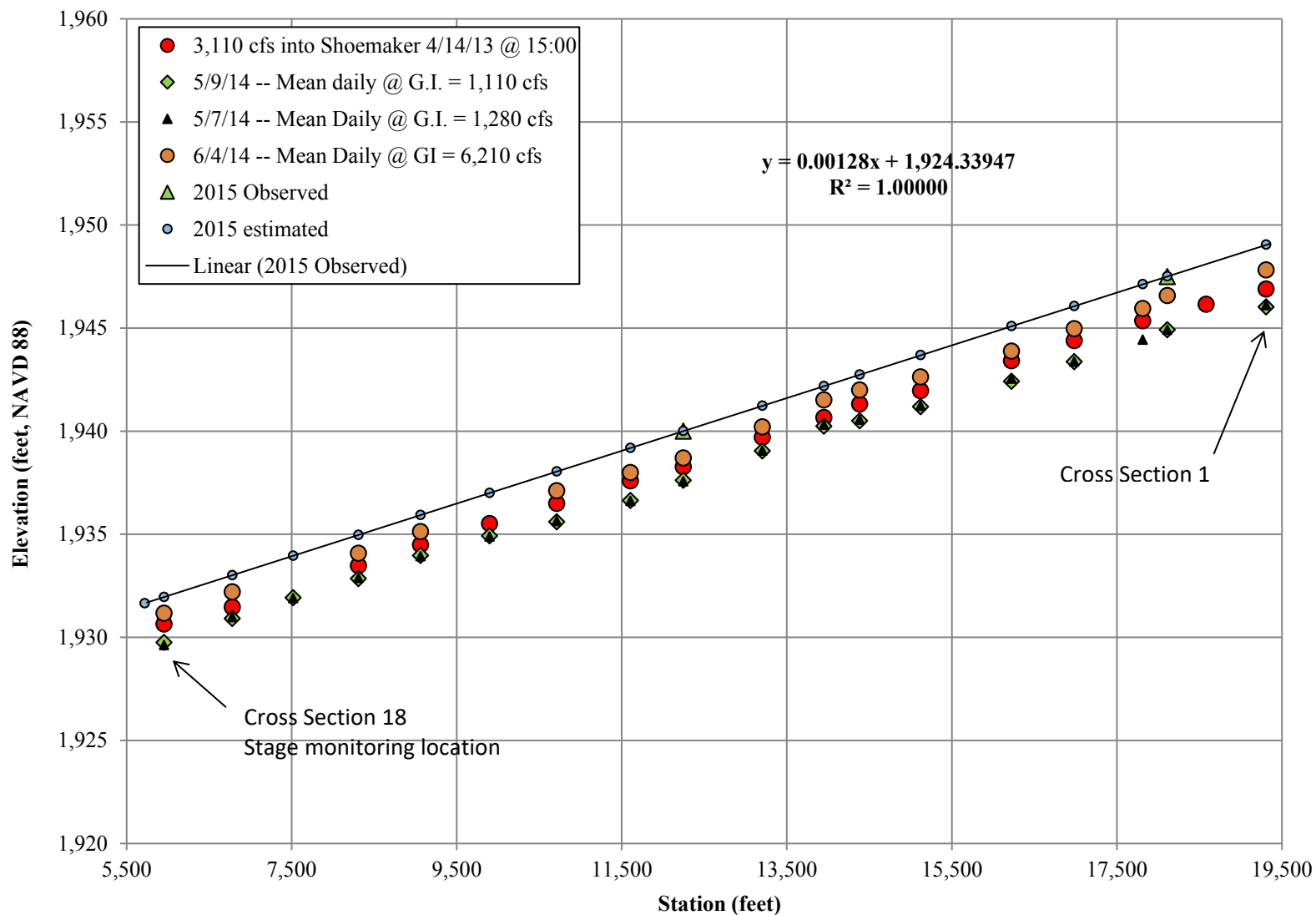




Figure 5-11 Platte River Water Surface Slope Profile Through the Shoemaker Study Reach



2016-08-12 F:\State & Local\Other\Platte River Recovery Program\Projects\1499201 - Shoemaker Island\Figures\MXD\2015\MXD\5-13 - Shoemaker Island-Veg Plots.mxd EA-Lincoln _j.petersen

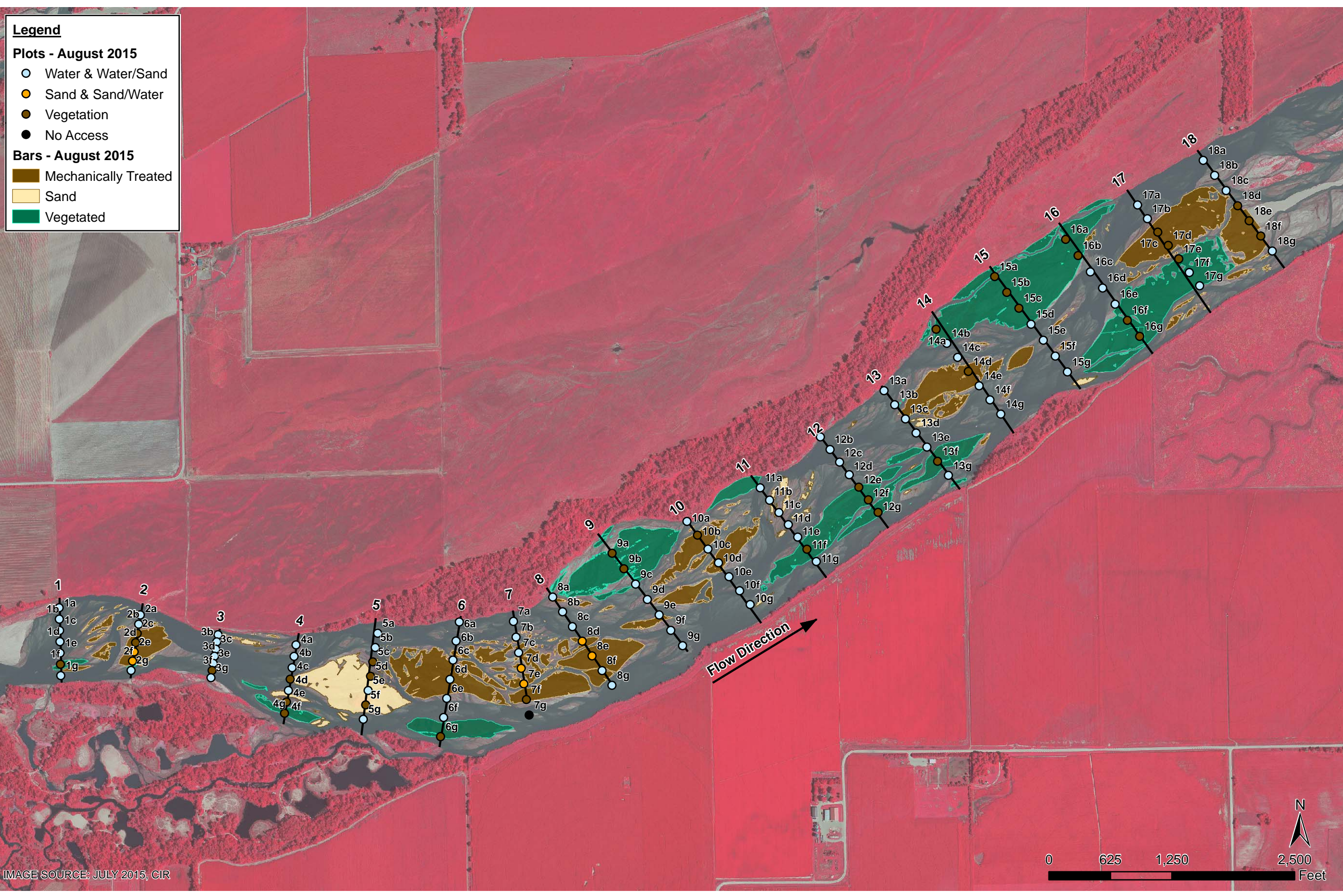


IMAGE SOURCE: JULY 2015, CIR

Legend

Plots - August 2015

- Water & Water/Sand
- Sand & Sand/Water
- Vegetation
- No Access

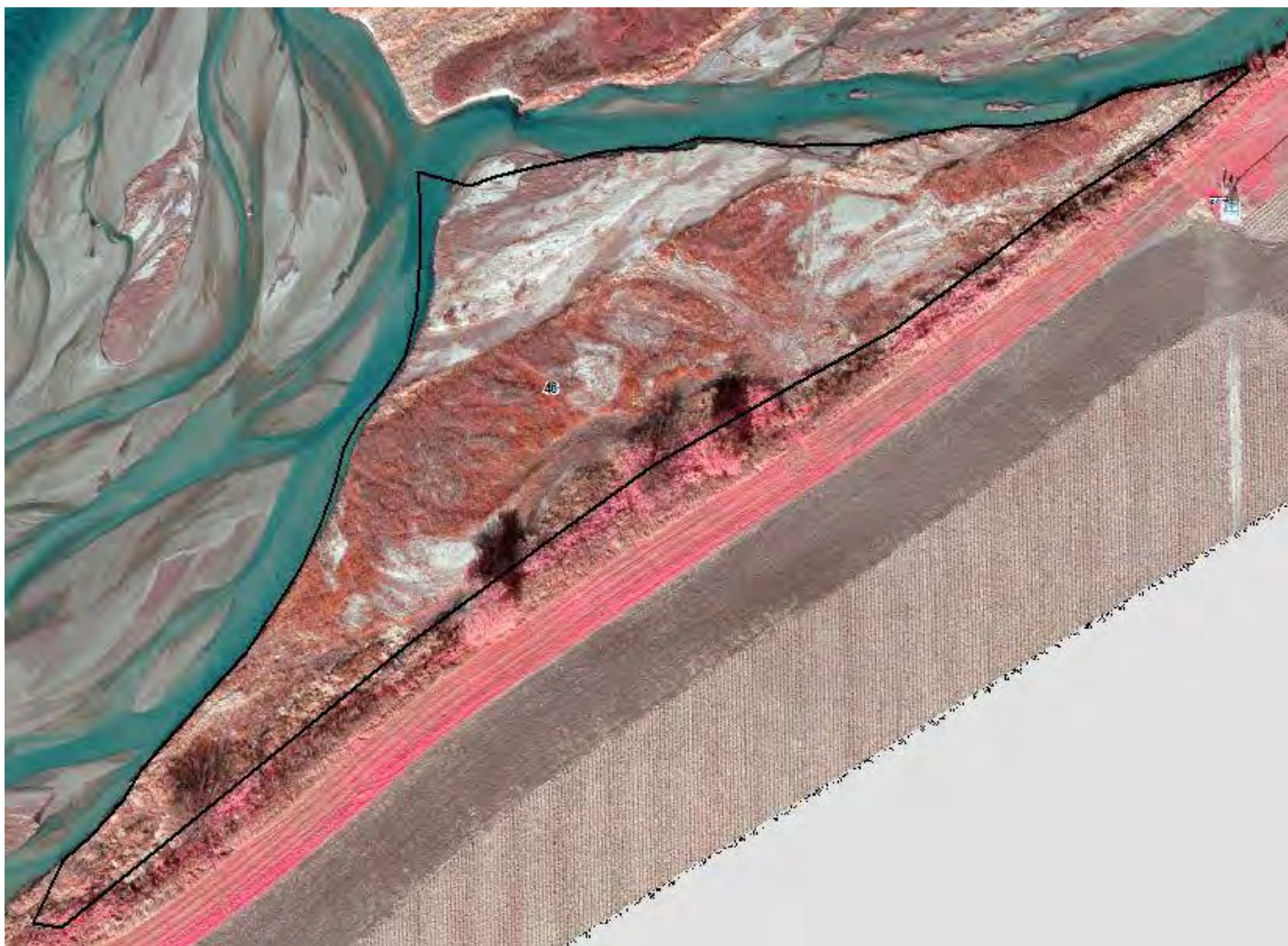
Bars - August 2015

- Mechanically Treated
- Sand
- Vegetated

 PLATTE RIVER RECOVERY IMPLEMENTATION PROGRAM		SHOEMAKER ISLAND FSM PROOF OF CONCEPT <small>HALL COUNTY, NEBRASKA</small>		VEGETATION PLOTS					
		PROJECT MGR. DLB	DESIGNED BY MAW	DRAWN BY MAW	CHECKED BY KMD	DATE JULY 2016	SCALE AS SHOWN	PROJECT NO. 1499201	FILE NAME -



Figure 5-13 Bar 46 in July 2014 (November 2014 Aerial)



The boundary of the bar in July 2014 is outlined in black.

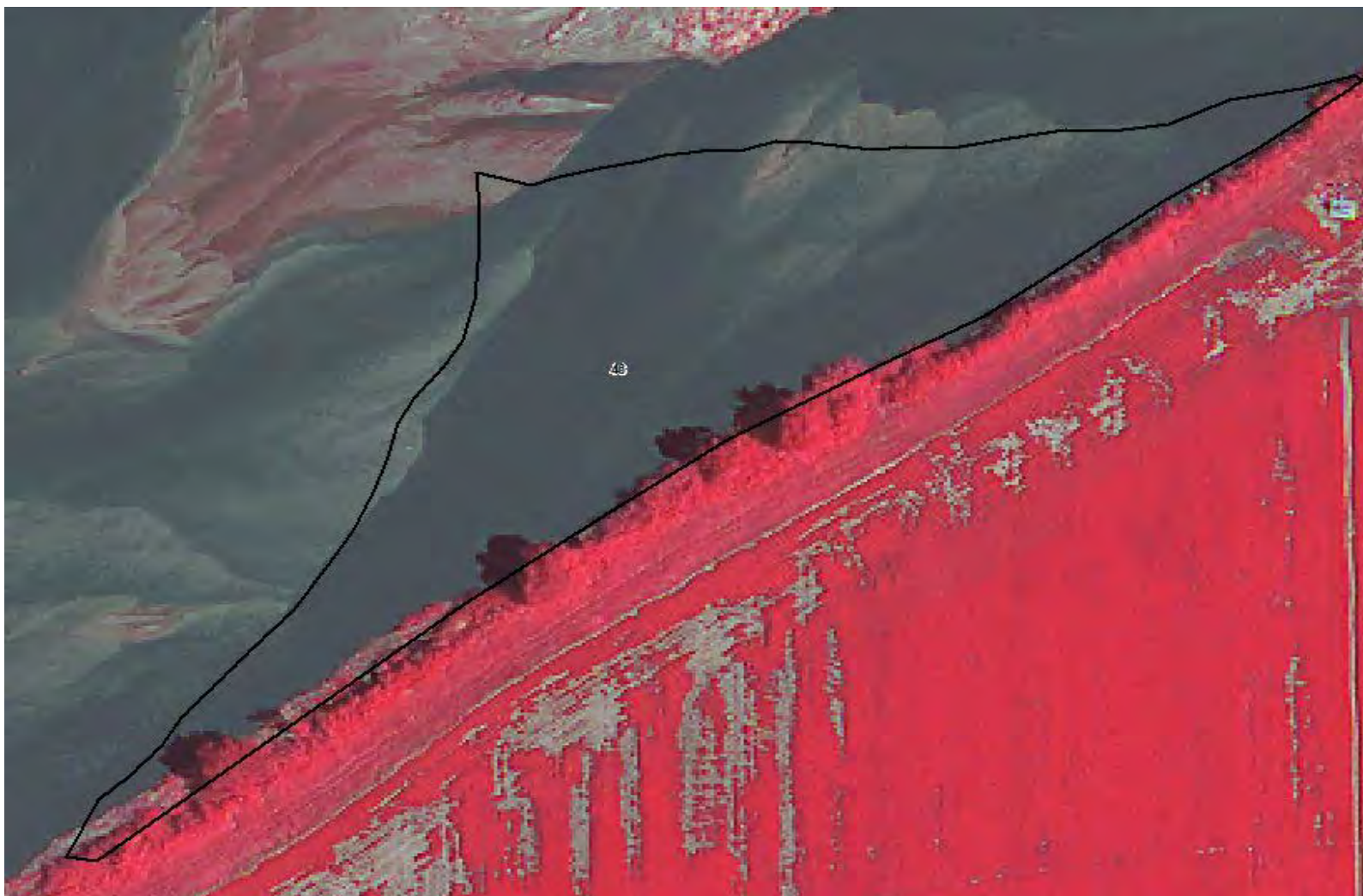


Figure 5-14 Bar 46 in July 2014 – Ground Photo





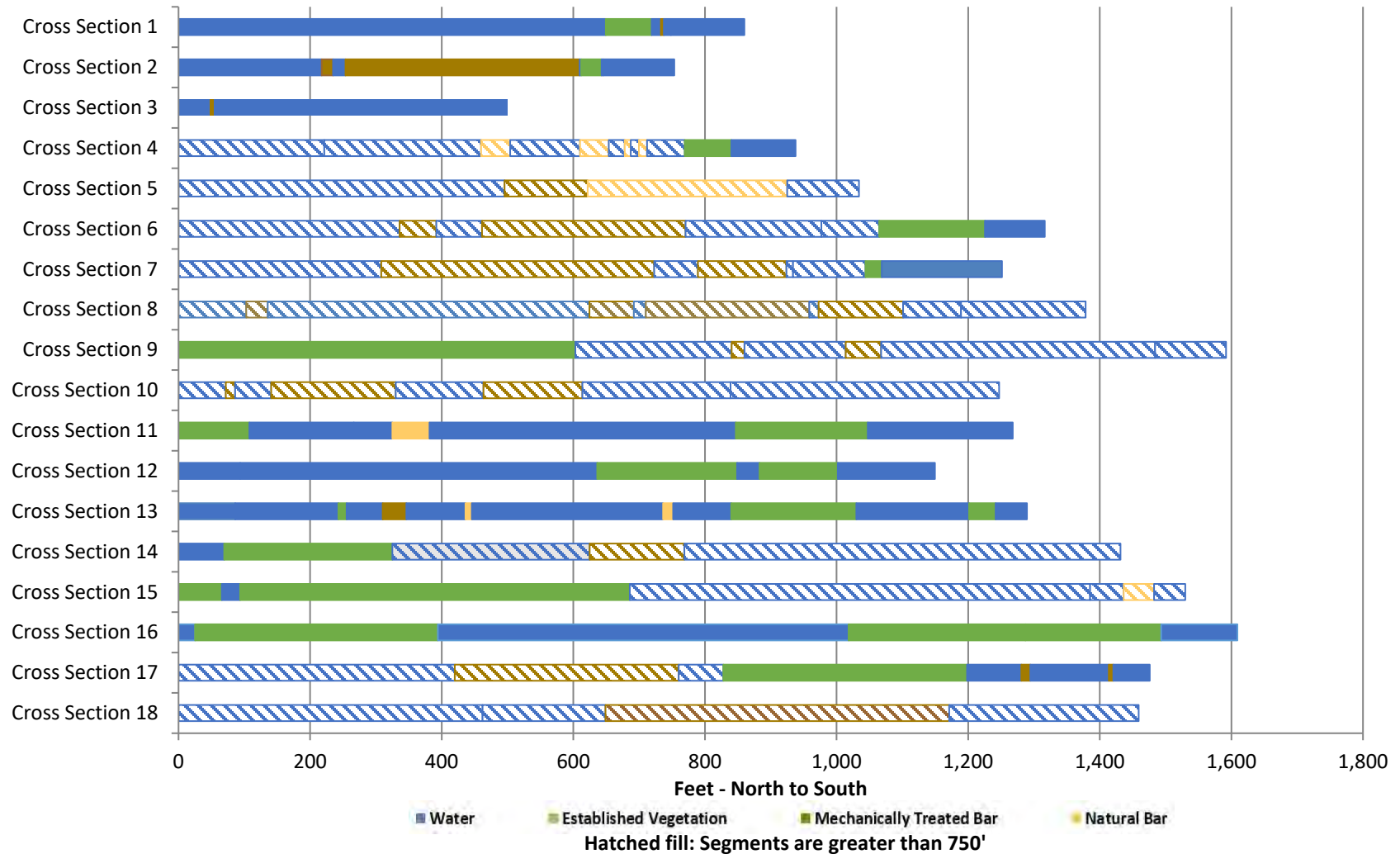
Figure 5-15 Bar 46 in August 2015 (July 2015 Aerial)



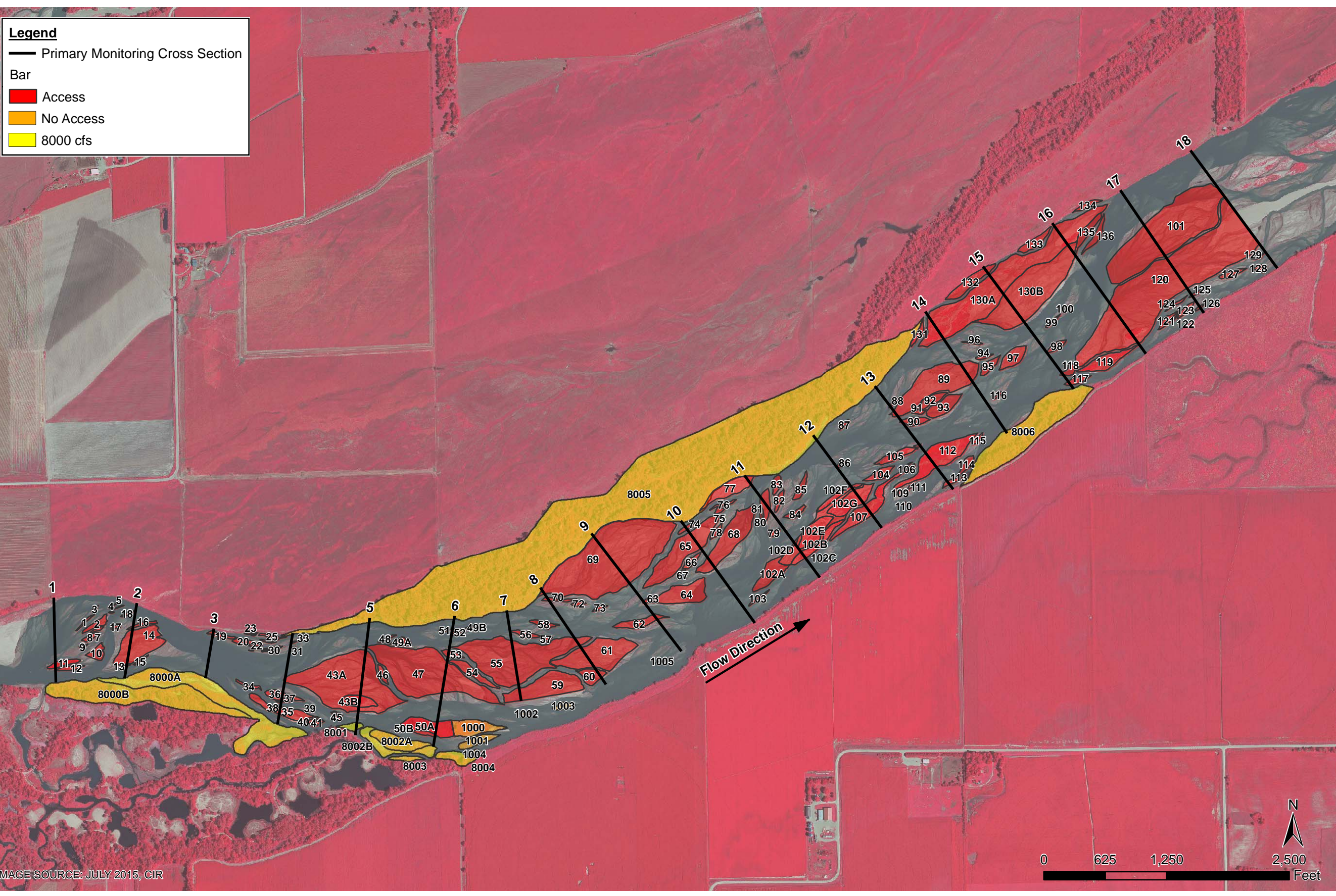
The boundary of the bar in July 2014 is outlined in black.



Figure 5-16 Maximum Un-Vegetated Channel Widths at the 18 Primary Cross Sections – August 2015



2016-08-12 F:\State & Local\OpenPlatte River Recovery Program\Projects\1499201 - Shoemaker FSM Proof of Concept\Figures\MXD\015\MXD\5-15 - Shoemaker Island-Roughness Polygons.mxd EA-Lincoln ,jpetersen



<p>PLATTE RIVER RECOVERY IMPLEMENTATION PROGRAM</p>		<p>SHOEMAKER ISLAND FSM PROOF OF CONCEPT HALL COUNTY, NEBRASKA</p>		<p>VEGETATION ROUGHNESS POLYGONS</p>	
PROJECT MGR.	DESIGNED BY	DRAWN BY	CHECKED BY	DATE	SCALE
DLB	MAW	MAW	KMD	JULY 2016	AS SHOWN
				PROJECT NO.	PROJECT NO.
				1499201	1499201
				FILE NAME	DRAWING NO.
				-	-
				FIGURE	FIGURE
				5-17	5-17



Figure 5-18 Platte River Bedload Discharge – June 2015 High Flow

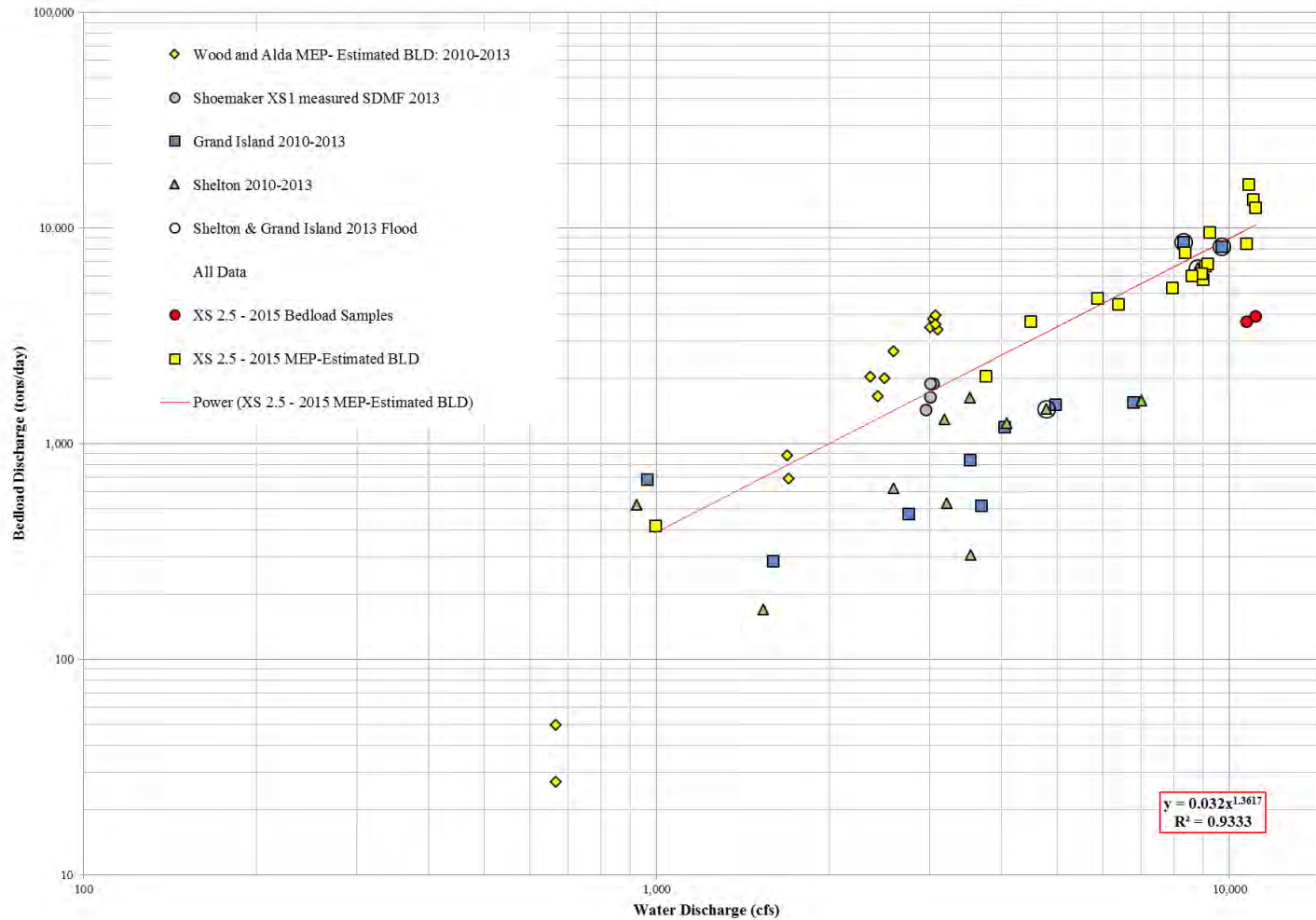




Figure 6-1 Cumulative Distributions of Sand Bar and Vegetated Bar Area Relative to the June 2015 High Flow 3-Day Mean Peak Discharge Stage

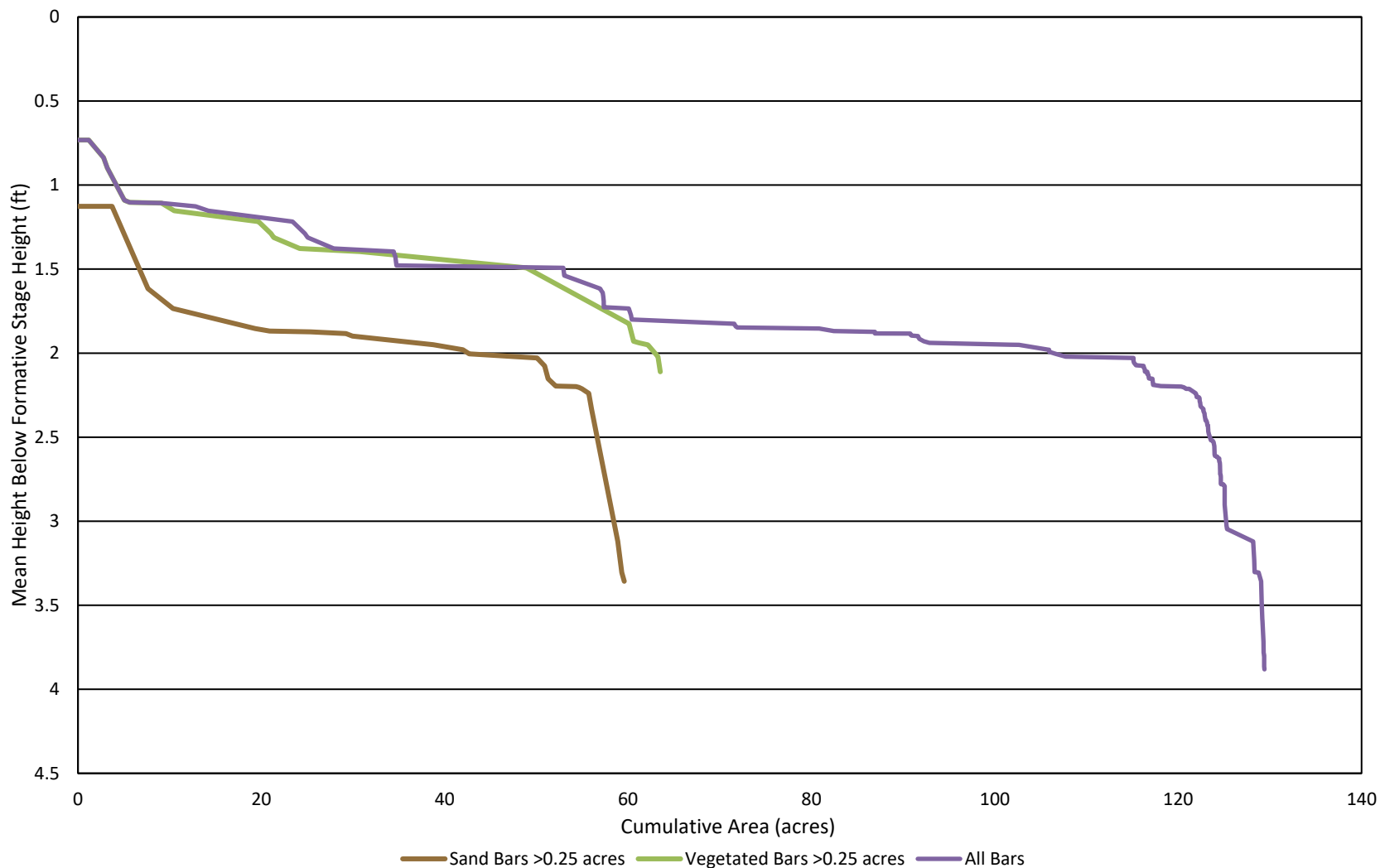
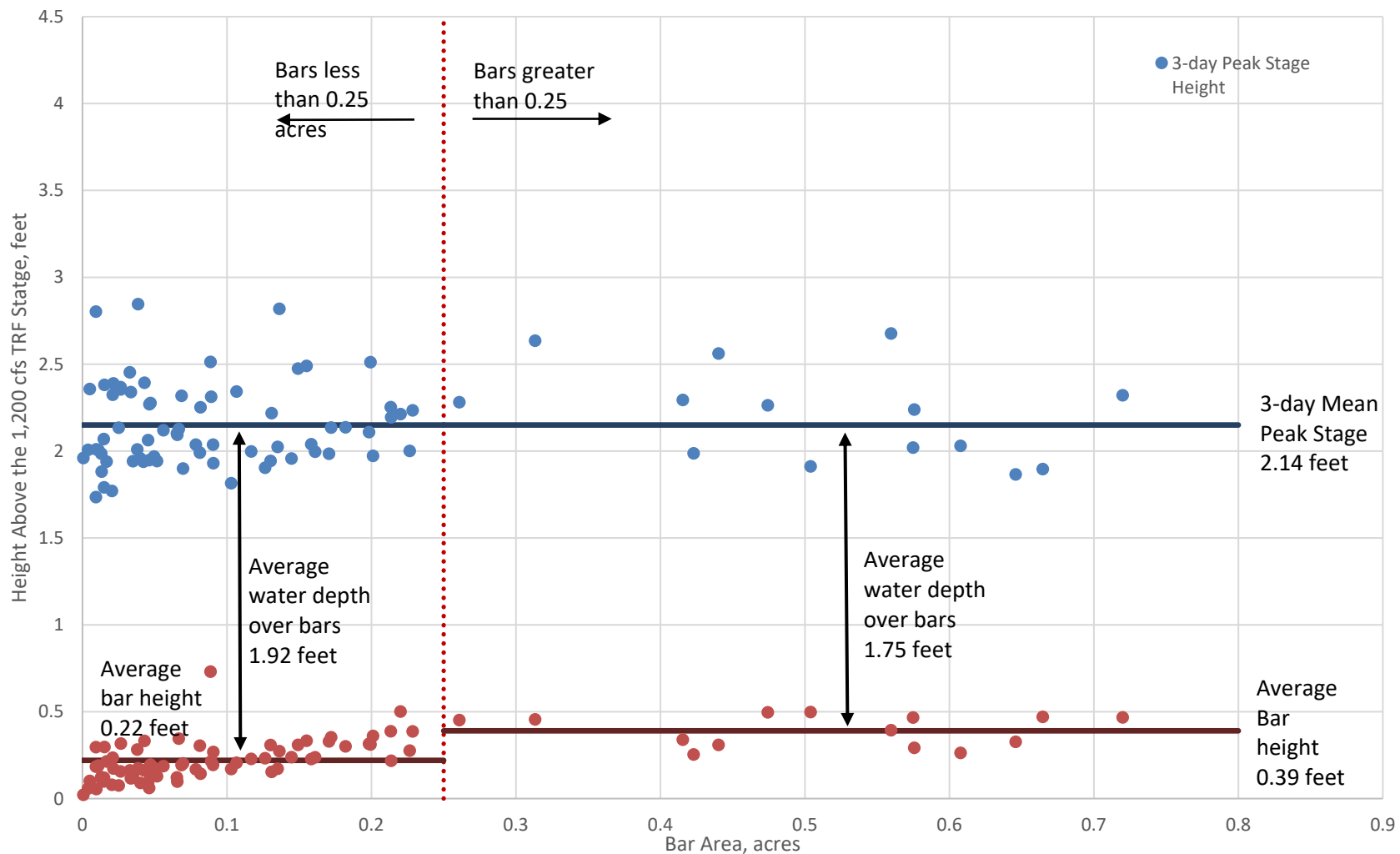
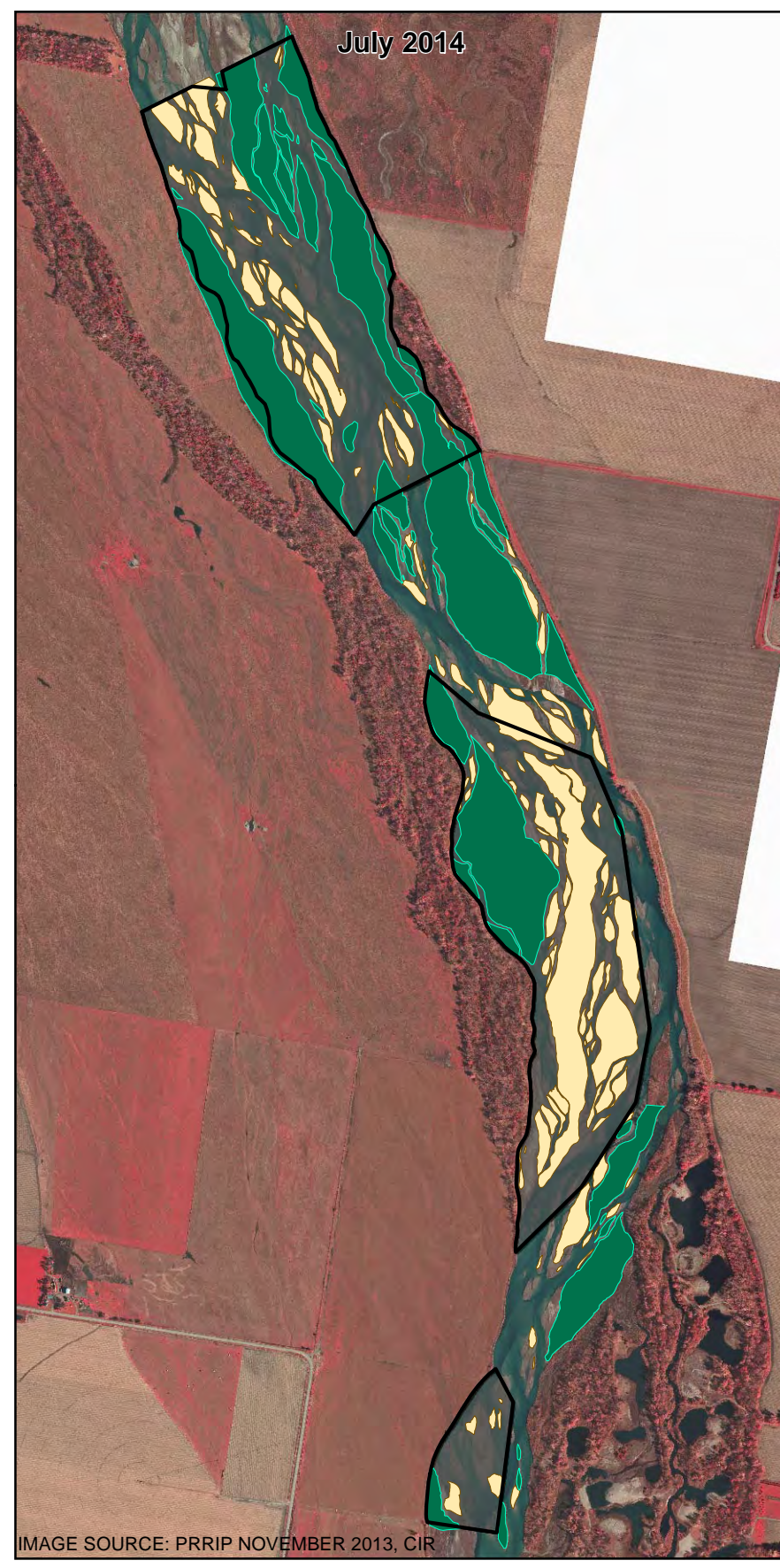




Figure 8-1 Mean Sand Bar Height Above 1,200 cfs TRF Stage – July 2014



2016-08-12 F:\State & Local\Other\Platte River Recovery Program\Projects\1499201 - Shoemaker FSM Proof of Concept\MXD\015\MXD\6-1 - 2013, 2014, 2015.mxd EA-Lincoln jpeterson



<p>PLATTE RIVER RECOVERY IMPLEMENTATION PROGRAM</p>		SHOEMAKER ISLAND FSM PROOF OF CONCEPT HALL COUNTY, NEBRASKA		BAR ATTRIBUTES APRIL 2013, JULY 2014, AND AUGUST 2015					
		PROJECT MGR. DLB	DESIGNED BY ..	DRAWN BY JKP	CHECKED BY KMD	DATE AUG 2016	SCALE AS SHOWN	PROJECT NO. 1499201	FILE NAME -



Figure 8-3 D50 Ranges for 2013 Pre and Post, 2014 Pre and Post, and 2015 Post

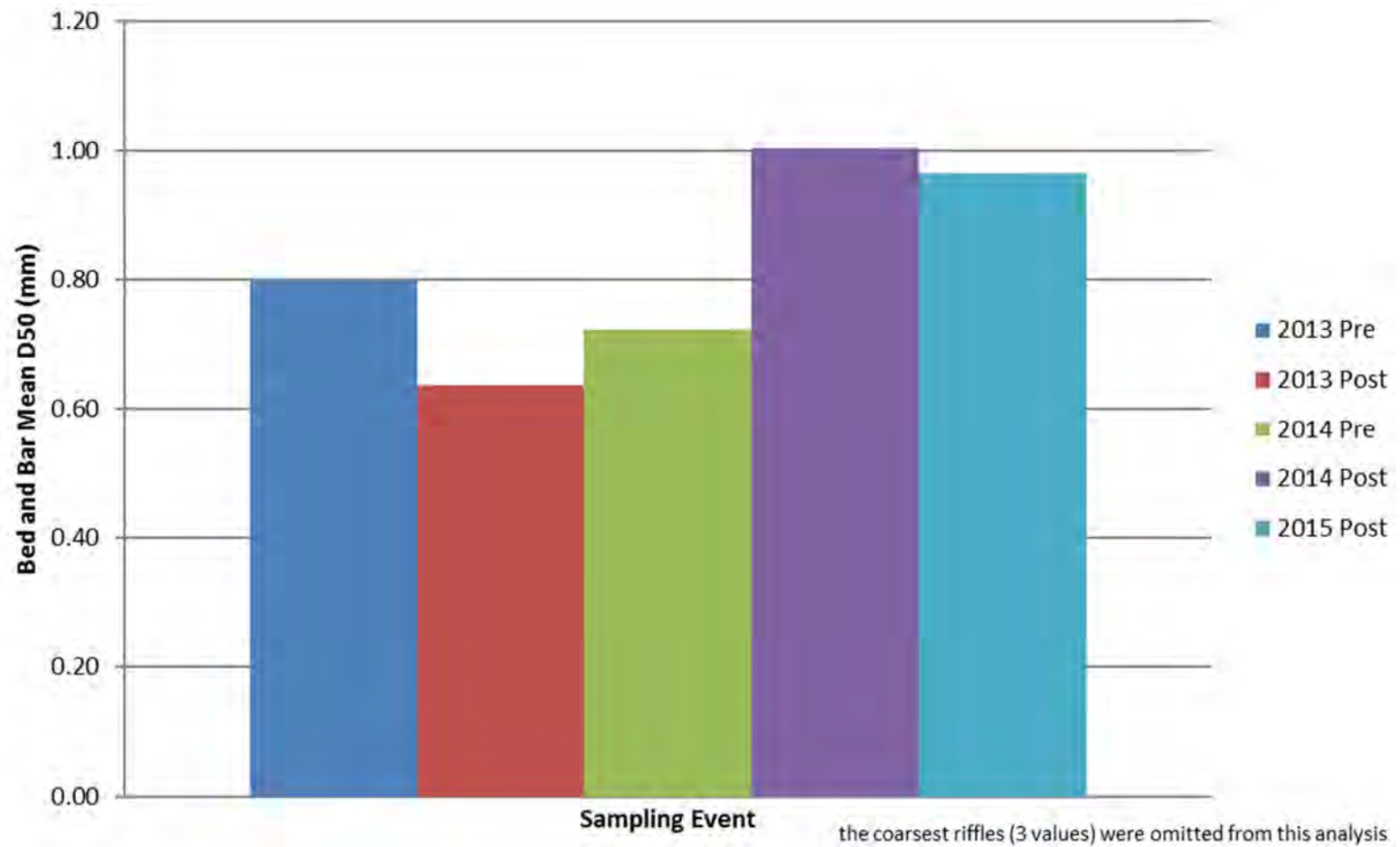
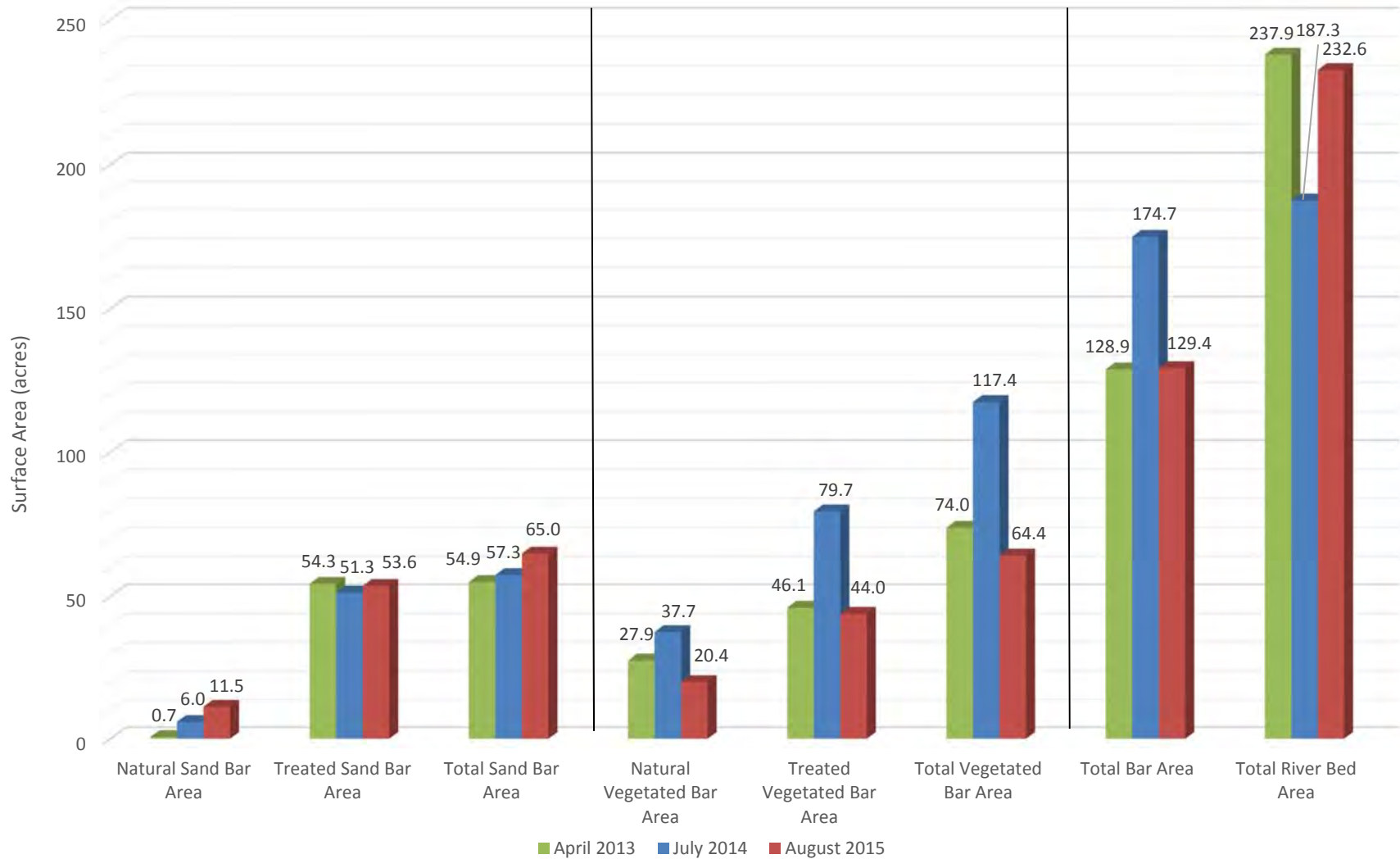




Figure 8-4 Area of All Bars Surveyed – April 2013, July 2014, and August 2015





APPENDIX A
GEOMORPHOLOGY



Table of Contents

Tables

Table A-1. July 2014 and August 2015 Braiding Index	5
Table A-2. Bed and Bar Sample Particle Size Analysis – Sieve Data – August 2015	6
Table A-3. Bed and Bar Density Sample Particle Size Analysis – Grain Size Percentiles – August 2015	7
Table A-4. Bed Sample Particle Size Analysis – Sieve Data – August 2015	8
Table A-5. Bed Sample Particle Size Analysis – Grain Size Percentiles – August 2015	9

Figures

Figure A-1. Geomorphic Monitoring Network – Cross Sections 1-9	11
Figure A-2. Geomorphic Monitoring Network – Cross Sections 7-15	12
Figure A-3. Geomorphic Monitoring Network – Cross Sections 13-18	13
Figure A-4. Planform of Longitudinal Profile Alignment Cross Sections 1-9.....	14
Figure A-5. Planform of Longitudinal Profile Alignment Cross Sections 7-15.....	15
Figure A-6. Planform of Longitudinal Profile Alignment Cross Sections 13-18.....	16
Figure A-7. Primary Cross Section #1 – June 2014 and August 2015.....	17
Figure A-8. Primary Cross Section #2 – June 2014 and August 2015.....	17
Figure A-9. Primary Cross Section #3 – June 2014 and August 2015.....	18
Figure A-10. Primary Cross Section #4 – June 2014 and August 2015.....	18
Figure A-11. Primary Cross Section #5 – June 2014 and August 2015.....	19
Figure A-12. Primary Cross Section #6 – June 2014 and August 2015.....	19
Figure A-13. Primary Cross Section #7 – June 2014 and August 2015.....	20
Figure A-14. Primary Cross Section #8 – June 2014 and August 2015.....	20
Figure A-15. Primary Cross Section #9 – June 2014 and August 2015.....	21
Figure A-16. Primary Cross Section #10 – June 2014 and August 2015.....	21
Figure A-17. Primary Cross Section #11 – June 2014 and August 2015.....	22
Figure A-18. Primary Cross Section #12 – June 2014 and August 2015.....	22
Figure A-19. Primary Cross Section #13 – June 2014 and August 2015.....	23
Figure A-20. Primary Cross Section #14 – June 2014 and August 2015.....	23
Figure A-21. Primary Cross Section #15 – June 2014 and August 2015.....	24



Figure A-22. Primary Cross Section #16 – June 2014 and August 2015	24
Figure A-23. Primary Cross Section #17 – June 2014 and August 2015	25
Figure A-24. Primary Cross Section #18 – June 2014 and August 2015	25
Figure A-25. Supplemental Cross Section A – June 2014 and August 2015	26
Figure A-26. Supplemental Cross Section B – June 2014 and August 2015	26
Figure A-27. Supplemental Cross Section C – June 2014 and August 2015	27
Figure A-28. Supplemental Cross Section D – June 2014 and August 2015	27
Figure A-29. Supplemental Cross Section E – June 2014 and August 2015	28
Figure A-30. Supplemental Cross Section F – June 2014 and August 2015.....	28
Figure A-31. Supplemental Cross Section G – June 2014 and August 2015	29
Figure A-32. Supplemental Cross Section H – June 2014 and August 2015	29
Figure A-33. Supplemental Cross Section I – June 2014 and August 2015	30
Figure A-34. Supplemental Cross Section J – June 2014 and August 2015	30
Figure A-35. Supplemental Cross Section K – June 2014 and August 2015	31
Figure A-36. Supplemental Cross Section L – June 2014 and August 2015	31
Figure A-37. Supplemental Cross Section M – June 2014 and August 2015	32
Figure A-38. Supplemental Cross Section N – June 2014 and August 2015	32
Figure A-39. Supplemental Cross Section O – June 2014 and August 2015	33
Figure A-40. Supplemental Cross Section P – June 2014 and August 2015.....	33
Figure A-41. Supplemental Cross Section Q – June 2014 and August 2015	34
Figure A-42. Supplemental Cross Section R – June 2014 and August 2015	34
Figure A-43. Supplemental Cross Section S – June 2014 and August 2015.....	35
Figure A-44. Longitudinal Profile – Northern Route July 2014 and August 2015 – Cross Sections 1-6.....	36
Figure A-45. Longitudinal Profile – Northern Route July 2014 and August 2015 – Cross Sections 7-12.....	37
Figure A-46. Longitudinal Profile – Northern Route July 2014 and August 2015 – Cross Sections 13-18.....	38
Figure A-47. Longitudinal Profile – Southern Route July 2014 and August 2015 – Cross Sections 1-6.....	39
Figure A-48. Longitudinal Profile – Southern Route July 2014 and August 2015 – Cross Sections 7-12.....	40



Figure A-49. Longitudinal Profile – Southern Route July 2014 and August 2015 – Cross Sections 13-18	41
Figure A-50. 0.063mm to 0.25mm Suspended Sediment Transport Curve	42
Figure A-51. 0.25mm – 0.5mm Suspended Sediment Transport Curve	43
Figure A-52. 0.5mm – 1mm Suspended Sediment Transport Curve	44
Figure A-53. 1mm – 2mm Suspended Sediment Transport Curve	45



TABLES



Table A-1. July 2014 and August 2015 Braiding Index

XS	Number of Channels	
	July 2014	August 2015
1	2	2
2	4	2
3	1	2
4	3	4
5	2	3
6	4	6
7	1	5
8	3	2
9	3	3
10	5	3
11	2	4
12	4	4
13	5	5
14	4	4
15	5	6
16	5	4
17	5	4
18	5	5
Mean:	3.5	3.8



Table A-2. Bed and Bar Sample Particle Size Analysis – Sieve Data – August 2015

Field ID	Type	Date	Description	Feature	Sieve Data – Finer Than (mm)																
					45	31.5	22.4	16	11.2	8	5.6	4	2.8	2	1	0.85	0.5	0.25	0.125	0.063	
1	Bulk	8/26/2015	lateral bar lightly vegetated	Bar	100.0%	100.0%	100.0%	100.0%	100.0%	100.0%	100.0%	100.0%	100.0%	100.0%	99.6%	95.2%	92.5%	71.8%	25.0%	0.9%	0.1%
3	Bulk	8/26/2015	unvegetated active bar coarse lens	Bar	100.0%	100.0%	100.0%	100.0%	100.0%	99.6%	94.6%	85.8%	76.8%	68.3%	50.4%	46.6%	34.7%	14.5%	1.2%	0.2%	
4	Bulk	8/26/2015	unvegetated active bar fine lens	Bar	100.0%	100.0%	100.0%	100.0%	100.0%	99.9%	99.1%	96.9%	94.4%	91.2%	81.1%	77.7%	61.2%	23.9%	3.6%	1.2%	
7	Bulk	8/26/2015	emergent bar - unvegetated	Bar	100.0%	100.0%	100.0%	100.0%	100.0%	99.7%	96.6%	89.5%	82.3%	75.6%	61.2%	57.2%	42.3%	19.4%	1.0%	0.2%	
8	Bulk	8/26/2015	US end of large lightly vegetated bar	Bar	100.0%	100.0%	100.0%	100.0%	96.9%	87.1%	76.4%	66.3%	57.2%	49.6%	40.0%	38.3%	32.0%	16.4%	3.1%	1.1%	
12	Bulk	8/26/2015	lateral bar lightly vegetated below XS13	Bar	100.0%	100.0%	100.0%	100.0%	100.0%	97.6%	88.5%	76.4%	64.6%	54.2%	39.4%	36.9%	29.5%	15.2%	1.8%	0.4%	
13	Bulk	8/26/2015	Fine component of large 1.5' high lateral bar near XS16	Bar	100.0%	100.0%	100.0%	100.0%	99.4%	94.9%	89.4%	83.4%	76.1%	69.0%	56.8%	54.4%	45.2%	22.3%	5.7%	1.7%	
14	Bulk	8/26/2015	Coarse component of large 1.5' high lateral bar near XS16	Bar	100.0%	100.0%	100.0%	100.0%	99.8%	98.8%	93.6%	87.6%	80.6%	71.9%	52.4%	47.6%	32.0%	12.9%	1.3%	0.2%	
19	Bulk	8/26/2015	Fresh lateral bar above XS1	Bar	100.0%	100.0%	100.0%	100.0%	100.0%	100.0%	99.9%	99.2%	96.5%	92.0%	74.7%	69.0%	46.0%	13.0%	1.9%	0.3%	
21	Bulk	8/26/2015	High new bar	Bar	100.0%	100.0%	100.0%	100.0%	100.0%	98.8%	94.8%	87.8%	79.0%	69.7%	52.1%	48.1%	35.1%	16.8%	2.3%	0.2%	
33	Bulk	8/27/2015	Bar near XS6	Bar	100.0%	100.0%	100.0%	100.0%	100.0%	99.9%	99.1%	98.0%	95.8%	92.4%	76.1%	69.5%	43.0%	11.5%	1.0%	0.2%	
2	Bulk	8/26/2015	active dune field in north channel	Bed	100.0%	100.0%	100.0%	100.0%	100.0%	99.9%	99.3%	98.2%	96.6%	93.9%	83.6%	79.2%	58.6%	19.8%	0.4%	0.0%	
5	Bulk	8/26/2015	Active dune 2° flow channel	Bed	100.0%	100.0%	100.0%	100.0%	99.6%	99.1%	98.6%	98.2%	97.5%	96.6%	90.9%	87.2%	54.3%	6.2%	0.1%	0.0%	
6	Bulk	8/26/2015	Dune 1° flow channel	Bed	100.0%	100.0%	100.0%	100.0%	100.0%	99.3%	97.9%	94.9%	90.4%	84.0%	65.6%	59.8%	37.7%	6.1%	0.1%	0.0%	
9	Bulk	8/26/2015	Dune 2° flow channel	Bed	100.0%	100.0%	100.0%	100.0%	100.0%	100.0%	99.6%	97.8%	94.0%	86.9%	61.0%	52.8%	26.1%	5.0%	0.1%	0.0%	
11	Bulk	8/26/2015	Same-all size classes seem mixed even with fine dune surfaces	Bed	100.0%	100.0%	100.0%	100.0%	98.0%	96.4%	93.6%	90.3%	86.1%	81.1%	64.8%	58.6%	31.8%	5.3%	0.1%	0.0%	
15	Bulk	8/26/2015	Very fine flat dune	Bed	100.0%	100.0%	100.0%	100.0%	100.0%	100.0%	99.9%	98.7%	96.0%	91.7%	76.1%	70.5%	46.7%	11.9%	0.3%	0.1%	
16	Bulk	8/26/2015	Coarser bedform 0.1' above water surface	Bed	100.0%	100.0%	100.0%	100.0%	100.0%	99.2%	97.0%	91.8%	84.6%	76.5%	57.5%	52.8%	37.5%	15.2%	0.5%	0.1%	
17	Bulk	8/26/2015	Submerged bar @ XS17	Bed	100.0%	100.0%	100.0%	100.0%	100.0%	99.8%	99.2%	97.8%	95.5%	92.3%	82.4%	78.9%	61.0%	17.7%	0.3%	0.0%	
18	Bulk	8/26/2015	XS1	Bed	100.0%	100.0%	100.0%	100.0%	100.0%	100.0%	97.8%	94.1%	88.9%	82.1%	63.8%	58.2%	36.9%	8.0%	0.3%	0.0%	
20	Bulk	8/26/2015	Main thread (N) dune	Bed	100.0%	100.0%	100.0%	100.0%	99.4%	96.7%	91.5%	85.7%	77.9%	68.1%	44.6%	38.9%	20.5%	3.8%	0.0%	0.0%	
24	Bulk	8/27/2015	tertiary channel near NB XS3	Bed	100.0%	100.0%	100.0%	100.0%	99.7%	98.4%	92.7%	82.8%	68.3%	51.5%	27.9%	23.5%	14.2%	4.8%	0.6%	0.1%	
27	Bulk	8/27/2015	Main channel	Bed	100.0%	100.0%	100.0%	96.8%	89.0%	79.2%	70.3%	61.4%	52.2%	44.1%	32.8%	30.2%	20.3%	7.0%	0.2%	0.0%	
28	Bulk	8/27/2015	N. channel around Tx Bar complex @XS5	Bed	100.0%	100.0%	100.0%	100.0%	99.8%	98.1%	90.6%	80.8%	69.5%	58.1%	34.8%	29.9%	15.4%	2.4%	0.2%	0.0%	
29	Bulk	8/27/2015	Same channel S side	Bed	100.0%	100.0%	100.0%	100.0%	100.0%	99.5%	97.3%	91.6%	82.5%	73.4%	50.8%	45.4%	28.2%	4.9%	0.1%	0.0%	
31	Bulk	8/27/2015	1° flow channel along south bank near BSTEM XS5	Bed	100.0%	100.0%	100.0%	100.0%	99.9%	97.0%	89.1%	75.0%	60.6%	47.7%	31.1%	28.2%	19.3%	3.1%	0.0%	0.0%	
32	Bulk	8/27/2015	South channel below XS5 near property boundary	Bed	100.0%	100.0%	100.0%	100.0%	100.0%	99.8%	98.9%	96.9%	94.1%	90.2%	78.5%	74.6%	58.4%	26.8%	0.5%	0.0%	
35	Bulk	8/27/2015		Bed	100.0%	100.0%	100.0%	100.0%	100.0%	100.0%	99.9%	99.0%	97.4%	94.6%	84.6%	81.0%	59.2%	11.1%	0.1%	0.0%	
22	BD	8/27/2015	DS end of XS2 bar-unvegetated	Bar	100.0%	100.0%	100.0%	100.0%	100.0%	99.4%	97.2%	93.5%	87.2%	79.1%	58.2%	52.0%	31.0%	8.4%	0.8%	0.1%	
23	BD	8/27/2015	DS end of XS2 bar-lightly vegetated	Bar	100.0%	100.0%	100.0%	100.0%	100.0%	99.5%	96.9%	93.5%	87.4%	79.4%	57.3%	50.4%	24.9%	5.2%	0.4%	0.1%	
25	BD	8/27/2015	fine lobe	Bar	100.0%	100.0%	100.0%	100.0%	100.0%	97.3%	92.5%	85.2%	77.4%	68.2%	49.9%	45.4%	28.5%	9.2%	2.3%	0.5%	
26	BD	8/27/2015	coarser lobe	Bar	100.0%	100.0%	100.0%	100.0%	97.5%	89.8%	78.3%	69.7%	59.1%	50.1%	38.3%	35.8%	25.3%	6.3%	0.8%	0.1%	
30	BD	8/27/2015	Mid channel new bar on XS5	Bar	100.0%	100.0%	100.0%	100.0%	100.0%	97.8%	92.5%	87.0%	79.5%	71.4%	52.6%	47.8%	32.2%	12.6%	0.9%	0.1%	
34	BD	8/27/2015	Near XS8-highly braided 1.5' above WSE	Bar	100.0%	100.0%	100.0%	100.0%	99.3%	99.0%	96.4%	90.0%	80.8%	71.1%	52.7%	49.0%	29.2%	8.4%	1.1%	0.1%	
Total: 34				mean	100.0%	100.0%	100.0%	99.9%	99.4%	97.7%	94.1%	89.0%	82.6%	75.5%	59.4%	54.9%	37.4%	11.8%	1.0%	0.2%	
				min	100.0%	100.0%	100.0%	96.8%	89.0%	79.2%	70.3%	61.4%	52.2%	44.1%	27.9%	23.5%	14.2%	2.4%	0.0%	0.0%	
				max	100.0%	100.0%	100.0%	100.0%	100.0%	100.0%	100.0%	100.0%	100.0%	99.6%	95.2%	92.5%	71.8%	26.8%	5.7%	1.7%	



Table A-3. Bed and Bar Density Sample Particle Size Analysis – Grain Size Percentiles – August 2015

Field ID	Type	Date	Description	Feature	Grain Size Percentiles									Mass (g)	Dry Bulk Density (g/cm ³)
					D5	D16	D25	D35	D50	D65	D75	D84	D90		
1	Bulk	8/26/2015	lateral bar lightly vegetated	Bar	0.1 mm	0.2 mm	0.3 mm	0.3 mm	0.4 mm	0.5 mm	0.5 mm	0.7 mm	0.8 mm	1,206	na
3	Bulk	8/26/2015	unvegetated active bar coarse lens	Bar	0.2 mm	0.3 mm	0.4 mm	0.5 mm	1.0 mm	1.8 mm	2.6 mm	3.7 mm	4.7 mm	1,012	na
4	Bulk	8/26/2015	unvegetated active bar fine lens	Bar	0.1 mm	0.2 mm	0.3 mm	0.3 mm	0.4 mm	0.6 mm	0.8 mm	1.2 mm	1.8 mm	995	na
7	Bulk	8/26/2015	emergent bar - unvegetated	Bar	0.1 mm	0.2 mm	0.3 mm	0.4 mm	0.7 mm	1.2 mm	1.9 mm	3.0 mm	4.1 mm	1,872	na
8	Bulk	8/26/2015	US end of large lightly vegetated bar	Bar	0.1 mm	0.2 mm	0.4 mm	0.6 mm	2.0 mm	3.8 mm	5.3 mm	7.2 mm	8.8 mm	1,328	na
12	Bulk	8/26/2015	lateral bar lightly vegetated below XS13	Bar	0.1 mm	0.3 mm	0.4 mm	0.7 mm	1.6 mm	2.8 mm	3.8 mm	4.9 mm	5.9 mm	888	na
13	Bulk	8/26/2015	Fine component of large 1.5' high lateral bar near XS16	Bar	0.1 mm	0.2 mm	0.3 mm	0.4 mm	0.7 mm	1.6 mm	2.7 mm	4.1 mm	5.8 mm	1,090	na
14	Bulk	8/26/2015	Coarse component of large 1.5' high lateral bar near XS16	Bar	0.2 mm	0.3 mm	0.4 mm	0.6 mm	0.9 mm	1.6 mm	2.3 mm	3.3 mm	4.6 mm	1,434	na
19	Bulk	8/26/2015	Fresh lateral bar above XS1	Bar	0.2 mm	0.3 mm	0.3 mm	0.4 mm	0.5 mm	0.8 mm	1.0 mm	1.4 mm	1.8 mm	1,168	na
21	Bulk	8/26/2015	High new bar	Bar	0.1 mm	0.2 mm	0.3 mm	0.5 mm	0.9 mm	1.7 mm	2.4 mm	3.4 mm	4.5 mm	1,126	na
33	Bulk	8/27/2015	Bar near XS6	Bar	0.2 mm	0.3 mm	0.3 mm	0.4 mm	0.6 mm	0.8 mm	1.0 mm	1.4 mm	1.8 mm	976	na
2	Bulk	8/26/2015	active dune field in north channel	Bed	0.1 mm	0.2 mm	0.3 mm	0.3 mm	0.4 mm	0.6 mm	0.8 mm	1.0 mm	1.5 mm	2,438	na
5	Bulk	8/26/2015	Active dune 2° flow channel	Bed	0.2 mm	0.3 mm	0.3 mm	0.4 mm	0.5 mm	0.6 mm	0.7 mm	0.8 mm	1.0 mm	1,690	na
6	Bulk	8/26/2015	Dune 1° flow channel	Bed	0.2 mm	0.3 mm	0.4 mm	0.5 mm	0.7 mm	1.0 mm	1.4 mm	2.0 mm	2.7 mm	1,130	na
9	Bulk	8/26/2015	Dune 2° flow channel	Bed	0.2 mm	0.4 mm	0.5 mm	0.6 mm	0.8 mm	1.1 mm	1.5 mm	1.9 mm	2.3 mm	992	na
11	Bulk	8/26/2015	Same-all size classes seem mixed even with fine dune surfaces	Bed	0.2 mm	0.3 mm	0.4 mm	0.5 mm	0.7 mm	1.0 mm	1.5 mm	2.4 mm	3.9 mm	1,724	na
15	Bulk	8/26/2015	Very fine flat dune	Bed	0.2 mm	0.3 mm	0.3 mm	0.4 mm	0.5 mm	0.8 mm	1.0 mm	1.4 mm	1.9 mm	1,330	na
16	Bulk	8/26/2015	Coarser bedform 0.1' above water surface	Bed	0.2 mm	0.3 mm	0.3 mm	0.5 mm	0.8 mm	1.3 mm	1.9 mm	2.7 mm	3.7 mm	1,016	na
17	Bulk	8/26/2015	Submerged bar @ XS17	Bed	0.2 mm	0.2 mm	0.3 mm	0.3 mm	0.4 mm	0.6 mm	0.8 mm	1.1 mm	1.7 mm	1,202	na
18	Bulk	8/26/2015	XS1	Bed	0.2 mm	0.3 mm	0.4 mm	0.5 mm	0.7 mm	1.0 mm	1.5 mm	2.2 mm	3.0 mm	2,208	na
20	Bulk	8/26/2015	Main thread (N) dune	Bed	0.3 mm	0.4 mm	0.6 mm	0.8 mm	1.2 mm	1.8 mm	2.5 mm	3.7 mm	5.1 mm	2,026	na
24	Bulk	8/27/2015	tertiary channel near NB XS3	Bed	0.3 mm	0.6 mm	0.9 mm	1.2 mm	1.9 mm	2.6 mm	3.3 mm	4.2 mm	5.1 mm	2,322	na
27	Bulk	8/27/2015	Main channel	Bed	0.2 mm	0.4 mm	0.6 mm	1.1 mm	2.6 mm	4.6 mm	6.8 mm	9.4 mm	11.7 mm	1,502	na
28	Bulk	8/27/2015	N. channel around Tx Bar complex @XS5	Bed	0.3 mm	0.5 mm	0.7 mm	1.0 mm	1.6 mm	2.5 mm	3.3 mm	4.5 mm	5.5 mm	1,161	na
29	Bulk	8/27/2015	Same channel S side	Bed	0.3 mm	0.3 mm	0.5 mm	0.6 mm	1.0 mm	1.5 mm	2.1 mm	3.0 mm	3.8 mm	2,142	na
31	Bulk	8/27/2015	1° flow channel along south bank near BSTEM XS5	Bed	0.3 mm	0.4 mm	0.7 mm	1.2 mm	2.1 mm	3.1 mm	4.0 mm	5.0 mm	5.8 mm	2,126	na
32	Bulk	8/27/2015	South channel below XS5 near property boundary	Bed	0.1 mm	0.2 mm	0.2 mm	0.3 mm	0.4 mm	0.6 mm	0.9 mm	1.4 mm	2.0 mm	1,784	na
35	Bulk	8/27/2015		Bed	0.2 mm	0.3 mm	0.3 mm	0.4 mm	0.4 mm	0.6 mm	0.7 mm	1.0 mm	1.5 mm	1,806	na
22	BD	8/27/2015	DS end of XS2 bar-unvegetated	Bar	0.2 mm	0.3 mm	0.4 mm	0.6 mm	0.8 mm	1.3 mm	1.7 mm	2.5 mm	3.3 mm	552	1.79
23	BD	8/27/2015	DS end of XS2 bar-lightly vegetated	Bar	0.2 mm	0.4 mm	0.5 mm	0.6 mm	0.8 mm	1.3 mm	1.7 mm	2.4 mm	3.3 mm	550	1.78
25	BD	8/27/2015	fine lobe	Bar	0.2 mm	0.3 mm	0.4 mm	0.6 mm	1.0 mm	1.8 mm	2.6 mm	3.8 mm	5.0 mm	523	1.69
26	BD	8/27/2015	coarser lobe	Bar	0.2 mm	0.4 mm	0.5 mm	0.8 mm	2.0 mm	3.4 mm	4.9 mm	6.7 mm	8.1 mm	470	1.52
30	BD	8/27/2015	Mid channel new bar on XS5	Bar	0.2 mm	0.3 mm	0.4 mm	0.5 mm	0.9 mm	1.6 mm	2.3 mm	3.5 mm	4.8 mm	589	1.91
34	BD	8/27/2015	Near XS8-highly braided 1.5' above WSE	Bar	0.2 mm	0.3 mm	0.4 mm	0.6 mm	0.9 mm	1.6 mm	2.3 mm	3.2 mm	4.0 mm	539	1.74
				mean	0.19	0.33	0.45	0.62	1.07	1.81	2.60	3.67	4.73		1.74
				min	0.16	0.28	0.39	0.55	0.81	1.25	1.74	2.43	3.26		1.52
				max	0.24	0.37	0.50	0.81	1.98	3.41	4.92	6.68	8.06		1.91



Table A-4. Bed Sample Particle Size Analysis – Sieve Data – August 2015

Field ID	Type	Date	Description	Feature	Sieve Data -- Finer Than (mm)															
					45	31.5	22.4	16	11.2	8	5.6	4	2.8	2	1	0.85	0.5	0.25	0.125	0.063
2	Bulk	8/26/2015	active dune field in north channel	Bed	100.0%	100.0%	100.0%	100.0%	100.0%	99.9%	99.3%	98.2%	96.6%	93.9%	83.6%	79.2%	58.6%	19.8%	0.4%	0.0%
5	Bulk	8/26/2015	Active dune 2° flow channel	Bed	100.0%	100.0%	100.0%	100.0%	99.6%	99.1%	98.6%	98.2%	97.5%	96.6%	90.9%	87.2%	54.3%	6.2%	0.1%	0.0%
6	Bulk	8/26/2015	Dune 1° flow channel	Bed	100.0%	100.0%	100.0%	100.0%	100.0%	99.3%	97.9%	94.9%	90.4%	84.0%	65.6%	59.8%	37.7%	6.1%	0.1%	0.0%
9	Bulk	8/26/2015	Dune 2° flow channel	Bed	100.0%	100.0%	100.0%	100.0%	100.0%	100.0%	99.6%	97.8%	94.0%	86.9%	61.0%	52.8%	26.1%	5.0%	0.1%	0.0%
11	Bulk	8/26/2015	Same-all size classes seem mixed even with fine dune surfaces	Bed	100.0%	100.0%	100.0%	100.0%	98.0%	96.4%	93.6%	90.3%	86.1%	81.1%	64.8%	58.6%	31.8%	5.3%	0.1%	0.0%
15	Bulk	8/26/2015	Very fine flat dune	Bed	100.0%	100.0%	100.0%	100.0%	100.0%	100.0%	99.9%	98.7%	96.0%	91.7%	76.1%	70.5%	46.7%	11.9%	0.3%	0.1%
16	Bulk	8/26/2015	Coarser bedform 0.1' above water surface	Bed	100.0%	100.0%	100.0%	100.0%	100.0%	99.2%	97.0%	91.8%	84.6%	76.5%	57.5%	52.8%	37.5%	15.2%	0.5%	0.1%
17	Bulk	8/26/2015	Submerged bar @ XS17	Bed	100.0%	100.0%	100.0%	100.0%	100.0%	99.8%	99.2%	97.8%	95.5%	92.3%	82.4%	78.9%	61.0%	17.7%	0.3%	0.0%
18	Bulk	8/26/2015	XS1	Bed	100.0%	100.0%	100.0%	100.0%	100.0%	100.0%	97.8%	94.1%	88.9%	82.1%	63.8%	58.2%	36.9%	8.0%	0.3%	0.0%
20	Bulk	8/26/2015	Main thread (N) dune	Bed	100.0%	100.0%	100.0%	100.0%	99.4%	96.7%	91.5%	85.7%	77.9%	68.1%	44.6%	38.9%	20.5%	3.8%	0.0%	0.0%
24	Bulk	8/27/2015	tertiary channel near NB XS3	Bed	100.0%	100.0%	100.0%	100.0%	99.7%	98.4%	92.7%	82.8%	68.3%	51.5%	27.9%	23.5%	14.2%	4.8%	0.6%	0.1%
27	Bulk	8/27/2015	Main channel	Bed	100.0%	100.0%	100.0%	96.8%	89.0%	79.2%	70.3%	61.4%	52.2%	44.1%	32.8%	30.2%	20.3%	7.0%	0.2%	0.0%
28	Bulk	8/27/2015	N. channel around Tx Bar complex @XS5	Bed	100.0%	100.0%	100.0%	100.0%	99.8%	98.1%	90.6%	80.8%	69.5%	58.1%	34.8%	29.9%	15.4%	2.4%	0.2%	0.0%
29	Bulk	8/27/2015	Same channel S side	Bed	100.0%	100.0%	100.0%	100.0%	100.0%	99.5%	97.3%	91.6%	82.5%	73.4%	50.8%	45.4%	28.2%	4.9%	0.1%	0.0%
31	Bulk	8/27/2015	1° flow channel along south bank near BSTEM XS5	Bed	100.0%	100.0%	100.0%	100.0%	99.9%	97.0%	89.1%	75.0%	60.6%	47.7%	31.1%	28.2%	19.3%	3.1%	0.0%	0.0%
32	Bulk	8/27/2015	South channel below XS5 near property boundary	Bed	100.0%	100.0%	100.0%	100.0%	100.0%	99.8%	98.9%	96.9%	94.1%	90.2%	78.5%	74.6%	58.4%	26.8%	0.5%	0.0%
35	Bulk	8/27/2015		Bed	100.0%	100.0%	100.0%	100.0%	100.0%	100.0%	99.9%	99.0%	97.4%	94.6%	84.6%	81.0%	59.2%	11.1%	0.1%	0.0%
				mean	100.0%	100.0%	100.0%	99.8%	99.1%	97.8%	94.9%	90.3%	84.2%	77.2%	60.6%	55.9%	36.8%	9.4%	0.2%	0.0%
				min	100.0%	100.0%	100.0%	96.8%	89.0%	79.2%	70.3%	61.4%	52.2%	44.1%	27.9%	23.5%	14.2%	2.4%	0.0%	0.0%
				max	100.0%	100.0%	100.0%	100.0%	100.0%	100.0%	99.9%	99.0%	97.5%	96.6%	90.9%	87.2%	61.0%	26.8%	0.6%	0.1%



Table A-5. Bed Sample Particle Size Analysis – Grain Size Percentiles – August 2015

Field ID	Type	Date	Description	Feature	Grain Size Percentiles									Mass (g)	Dry Bulk Density (g/cm3)
					D5	D16	D25	D35	D50	D65	D75	D84	D90		
2	Bulk	8/26/2015	active dune field in north channel	Bed	0.1 mm	0.2 mm	0.3 mm	0.3 mm	0.4 mm	0.6 mm	0.8 mm	1.0 mm	1.5 mm	2,438	na
5	Bulk	8/26/2015	Active dune 2° flow channel	Bed	0.2 mm	0.3 mm	0.3 mm	0.4 mm	0.5 mm	0.6 mm	0.7 mm	0.8 mm	1.0 mm	1,690	na
6	Bulk	8/26/2015	Dune 1° flow channel	Bed	0.2 mm	0.3 mm	0.4 mm	0.5 mm	0.7 mm	1.0 mm	1.4 mm	2.0 mm	2.7 mm	1,130	na
9	Bulk	8/26/2015	Dune 2° flow channel	Bed	0.2 mm	0.4 mm	0.5 mm	0.6 mm	0.8 mm	1.1 mm	1.5 mm	1.9 mm	2.3 mm	992	na
11	Bulk	8/26/2015	Same-all size classes seem mixed even with fine dune surfaces	Bed	0.2 mm	0.3 mm	0.4 mm	0.5 mm	0.7 mm	1.0 mm	1.5 mm	2.4 mm	3.9 mm	1,724	na
15	Bulk	8/26/2015	Very fine flat dune	Bed	0.2 mm	0.3 mm	0.3 mm	0.4 mm	0.5 mm	0.8 mm	1.0 mm	1.4 mm	1.9 mm	1,330	na
16	Bulk	8/26/2015	Coarser bedform 0.1' above water surface	Bed	0.2 mm	0.3 mm	0.3 mm	0.5 mm	0.8 mm	1.3 mm	1.9 mm	2.7 mm	3.7 mm	1,016	na
17	Bulk	8/26/2015	Submerged bar @ XS17	Bed	0.2 mm	0.2 mm	0.3 mm	0.3 mm	0.4 mm	0.6 mm	0.8 mm	1.1 mm	1.7 mm	1,202	na
18	Bulk	8/26/2015	XS1	Bed	0.2 mm	0.3 mm	0.4 mm	0.5 mm	0.7 mm	1.0 mm	1.5 mm	2.2 mm	3.0 mm	2,208	na
20	Bulk	8/26/2015	Main thread (N) dune	Bed	0.3 mm	0.4 mm	0.6 mm	0.8 mm	1.2 mm	1.8 mm	2.5 mm	3.7 mm	5.1 mm	2,026	na
24	Bulk	8/27/2015	tertiary channel near NB XS3	Bed	0.3 mm	0.6 mm	0.9 mm	1.2 mm	1.9 mm	2.6 mm	3.3 mm	4.2 mm	5.1 mm	2,322	na
27	Bulk	8/27/2015	Main channel	Bed	0.2 mm	0.4 mm	0.6 mm	1.1 mm	2.6 mm	4.6 mm	6.8 mm	9.4 mm	11.7 mm	1,502	na
28	Bulk	8/27/2015	N. channel around Tx Bar complex @XS5	Bed	0.3 mm	0.5 mm	0.7 mm	1.0 mm	1.6 mm	2.5 mm	3.3 mm	4.5 mm	5.5 mm	1,161	na
29	Bulk	8/27/2015	Same channel S side	Bed	0.3 mm	0.3 mm	0.5 mm	0.6 mm	1.0 mm	1.5 mm	2.1 mm	3.0 mm	3.8 mm	2,142	na
31	Bulk	8/27/2015	1° flow channel along south bank near BSTEM XS5	Bed	0.3 mm	0.4 mm	0.7 mm	1.2 mm	2.1 mm	3.1 mm	4.0 mm	5.0 mm	5.8 mm	2,126	na
32	Bulk	8/27/2015	South channel below XS5 near property boundary	Bed	0.1 mm	0.2 mm	0.2 mm	0.3 mm	0.4 mm	0.6 mm	0.9 mm	1.4 mm	2.0 mm	1,784	na
35	Bulk	8/27/2015		Bed	0.2 mm	0.3 mm	0.3 mm	0.4 mm	0.4 mm	0.6 mm	0.7 mm	1.0 mm	1.5 mm	1,806	na
mean					0.21	0.33	0.45	0.62	0.98	1.49	2.04	2.80	3.66		
min					0.14	0.19	0.24	0.30	0.42	0.56	0.70	0.81	0.96		
max					0.29	0.55	0.90	1.23	2.55	4.58	6.76	9.43	11.71		



FIGURES



Figure A-1. Geomorphic Monitoring Network – Cross Sections 1-9



Figure A-2. Geomorphic Monitoring Network – Cross Sections 7-15



Figure A-3. Geomorphic Monitoring Network – Cross Sections 13-18



Figure A-4. Planform of Longitudinal Profile Alignment Cross Sections 1-9



Figure A-5. Planform of Longitudinal Profile Alignment Cross Sections 7-15



Figure A-6. Planform of Longitudinal Profile Alignment Cross Sections 13-18



Figure A-7. Primary Cross Section #1 – June 2014 and August 2015

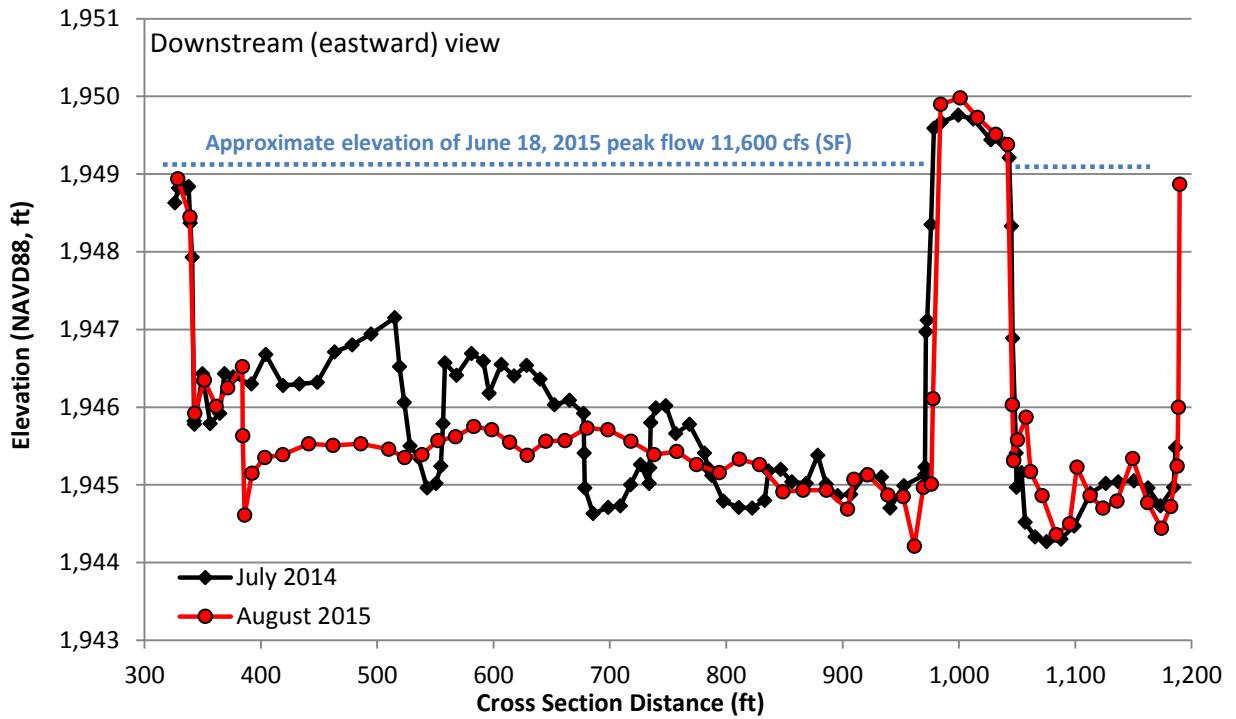


Figure A-8. Primary Cross Section #2 – June 2014 and August 2015

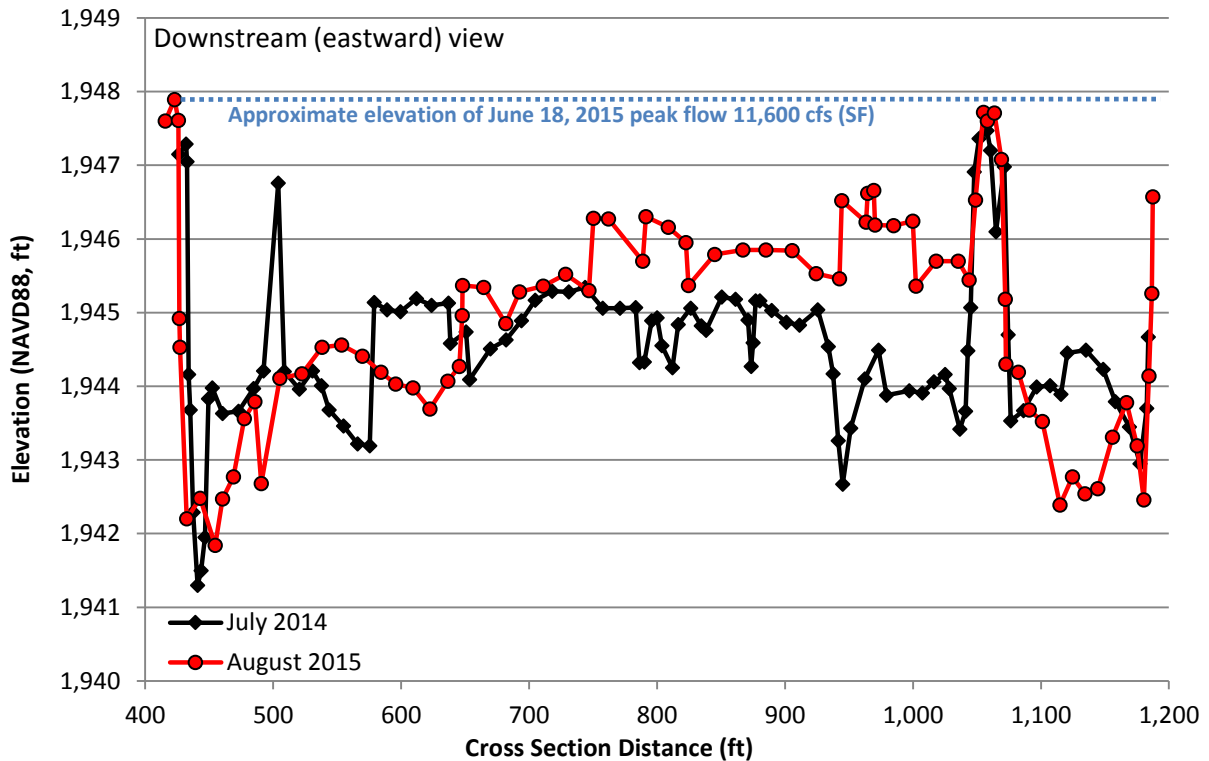




Figure A-9. Primary Cross Section #3 – June 2014 and August 2015

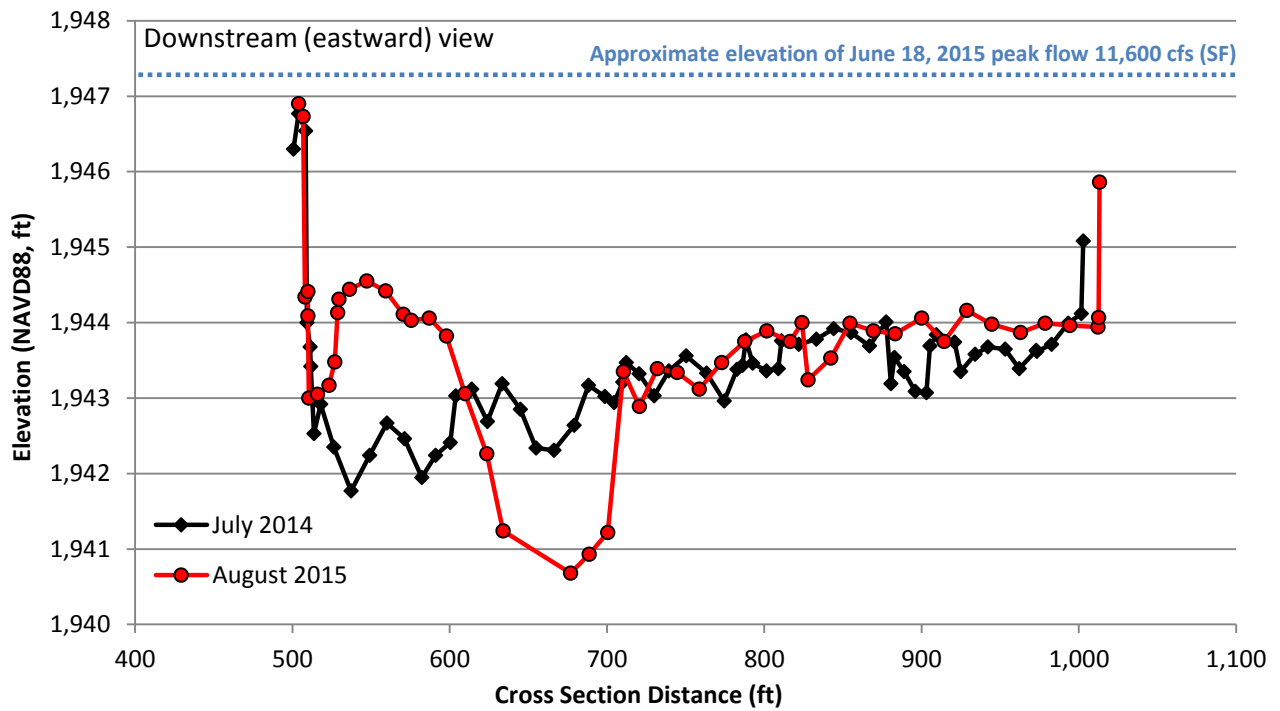


Figure A-10. Primary Cross Section #4 – June 2014 and August 2015

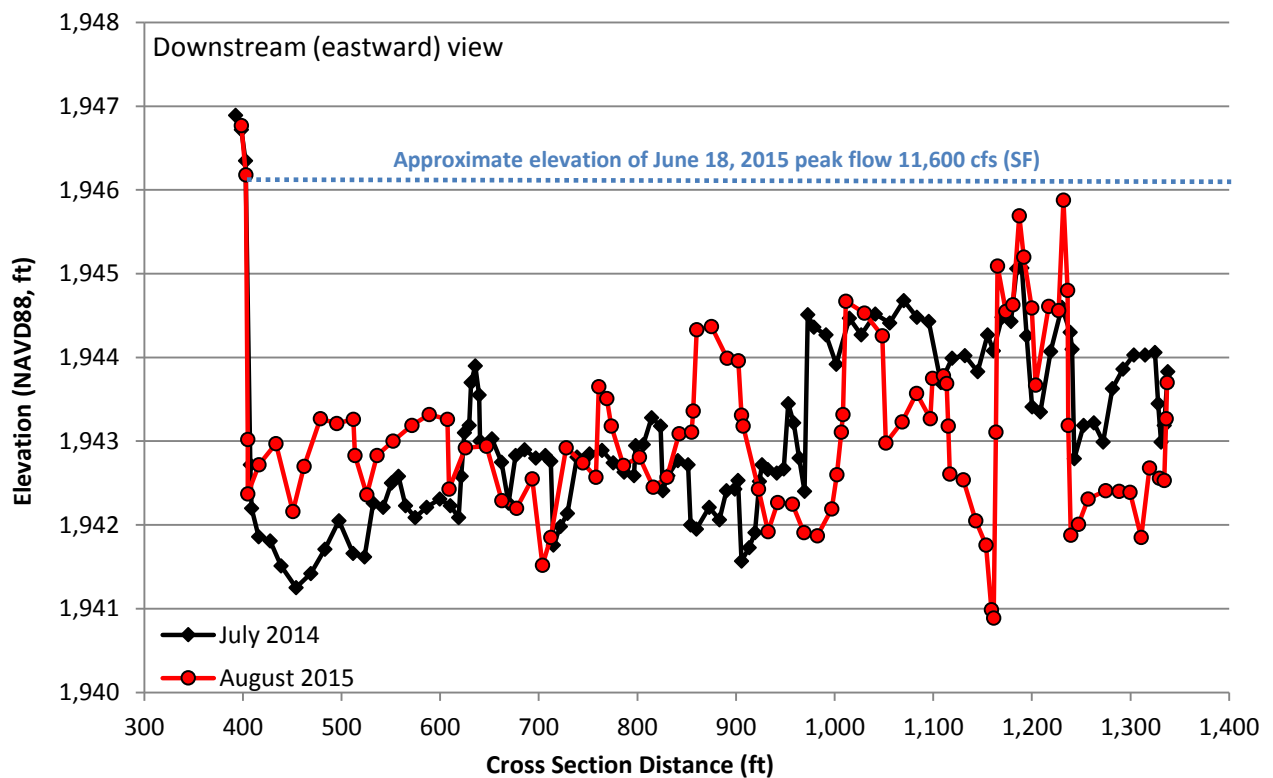




Figure A-11. Primary Cross Section #5 – June 2014 and August 2015

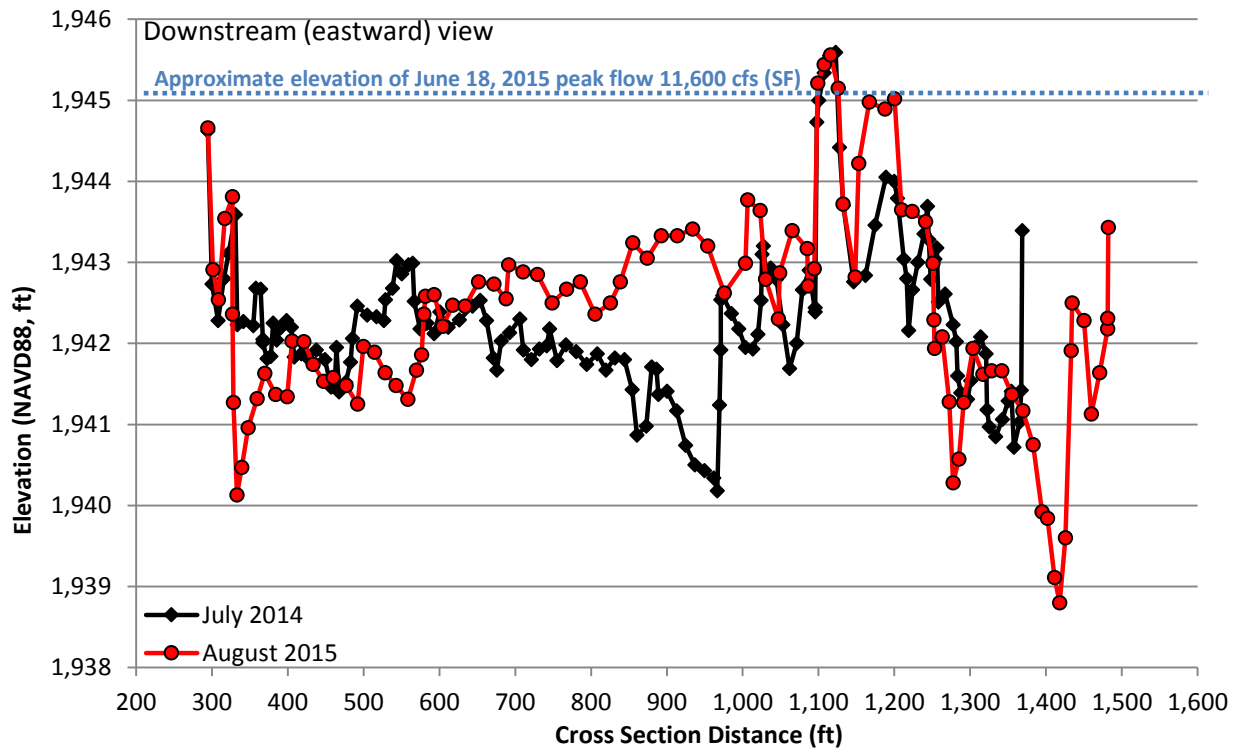


Figure A-12. Primary Cross Section #6 – June 2014 and August 2015

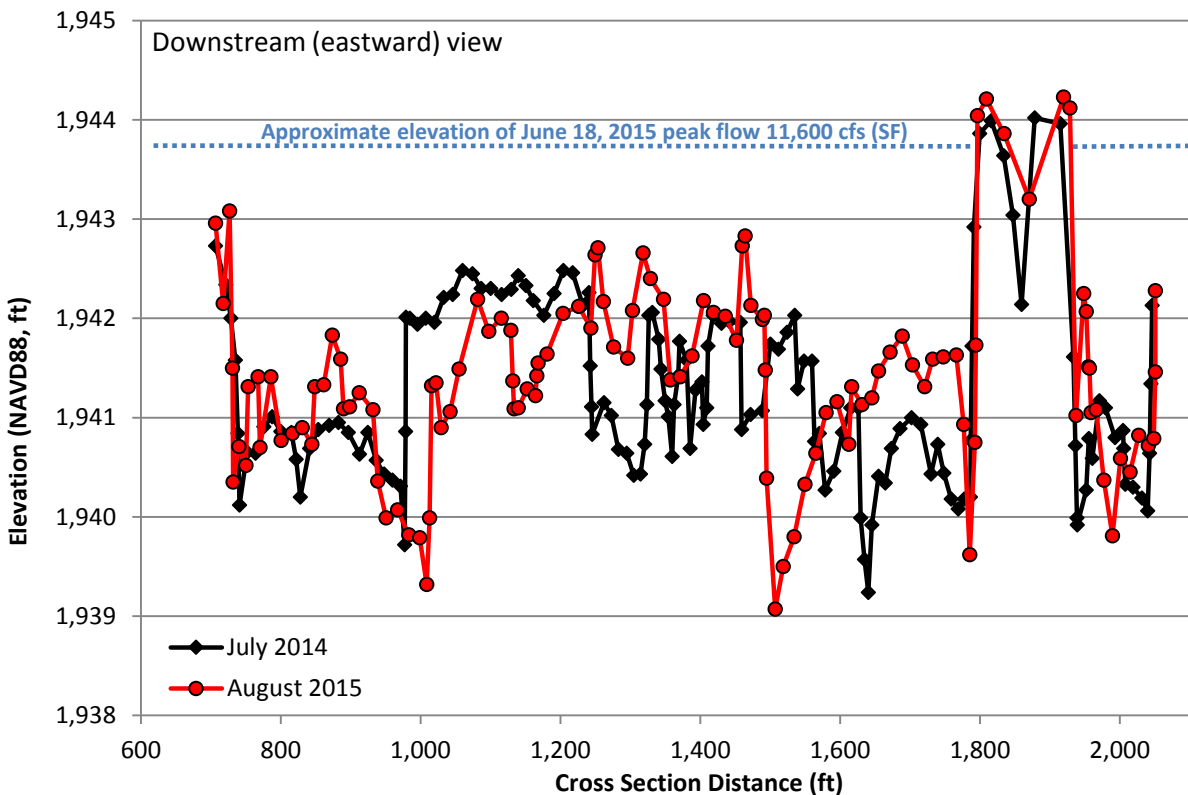




Figure A-13. Primary Cross Section #7 – June 2014 and August 2015

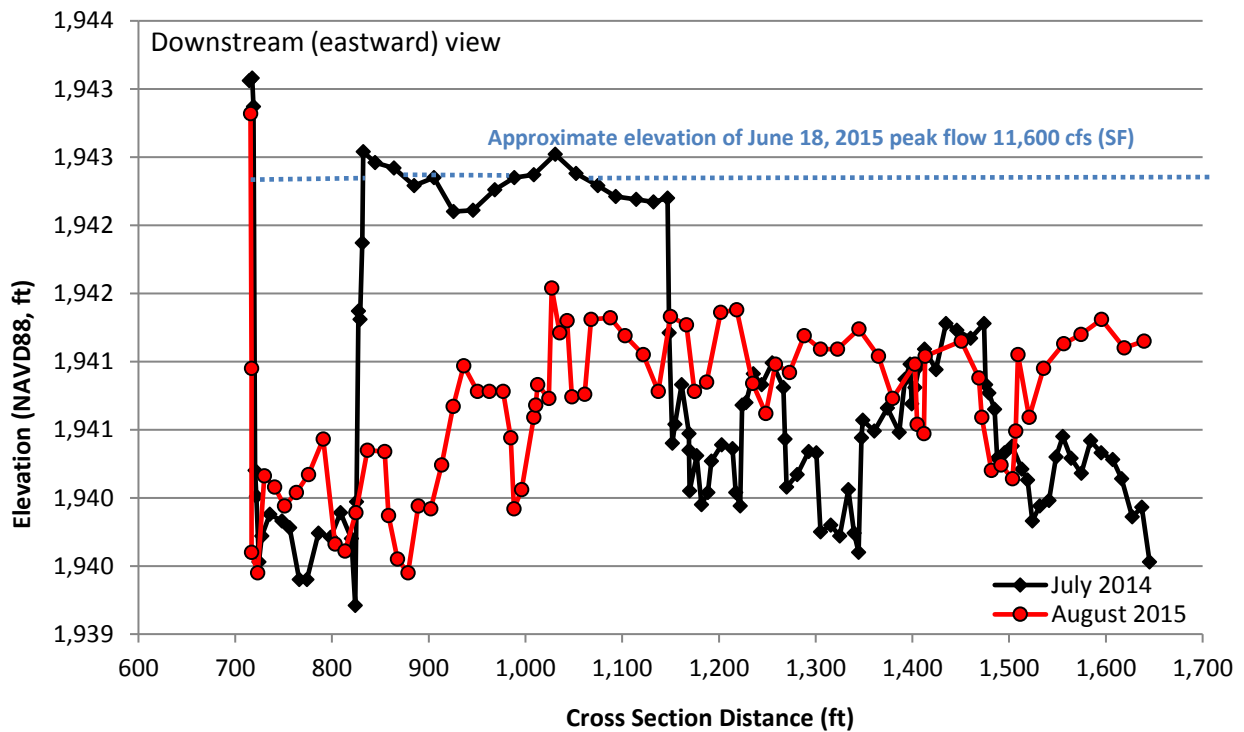


Figure A-14. Primary Cross Section #8 – June 2014 and August 2015

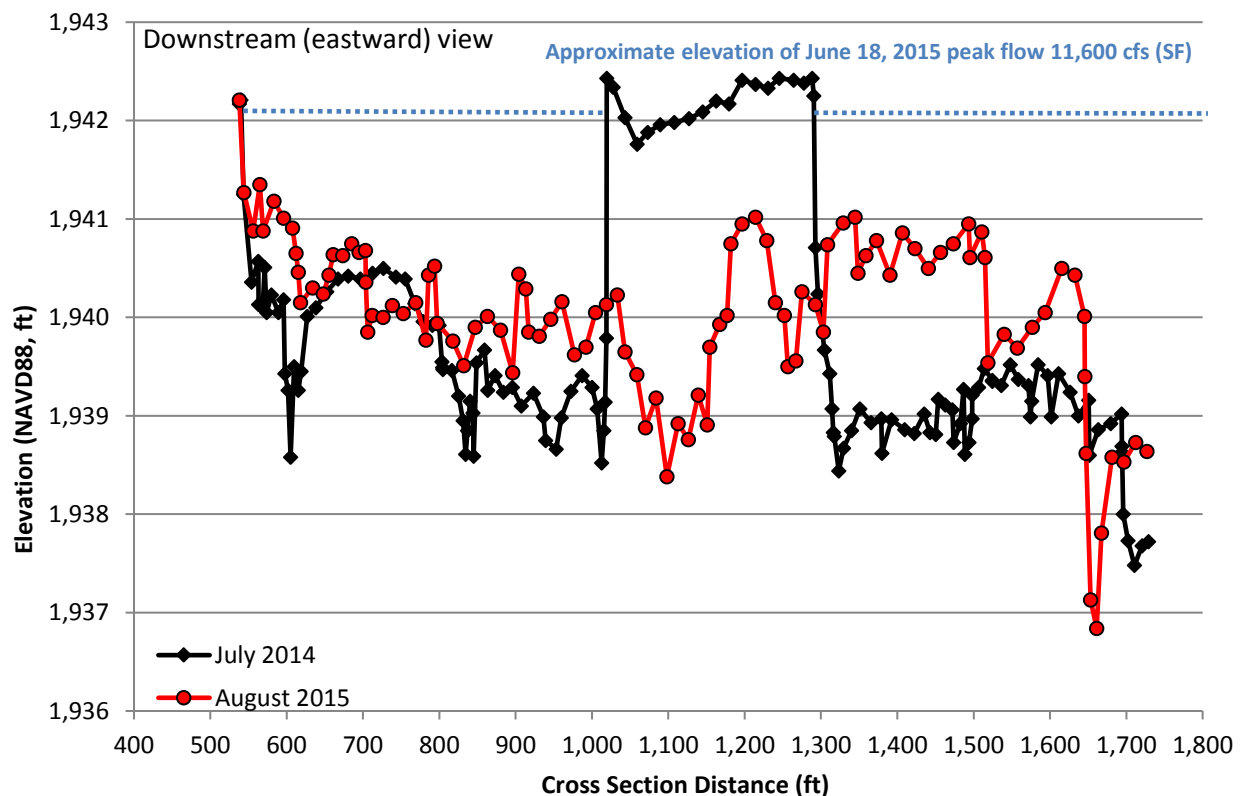




Figure A-15. Primary Cross Section #9 – June 2014 and August 2015

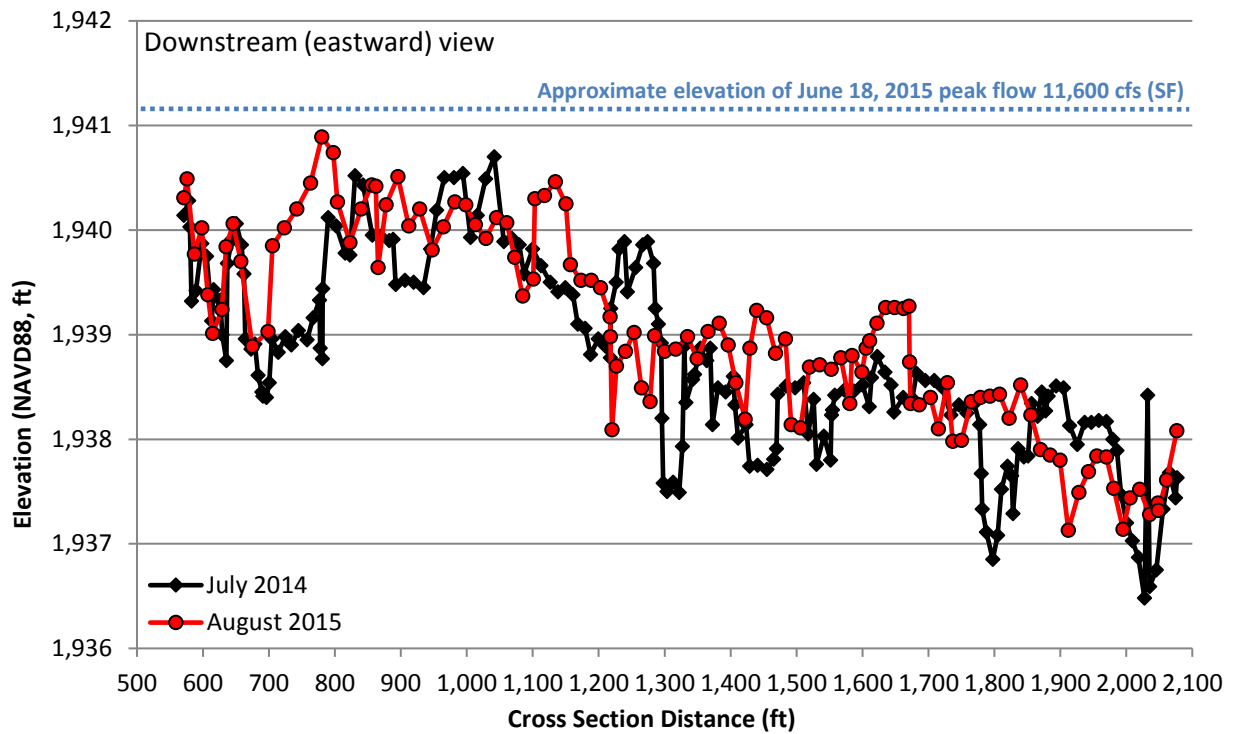


Figure A-16. Primary Cross Section #10 – June 2014 and August 2015

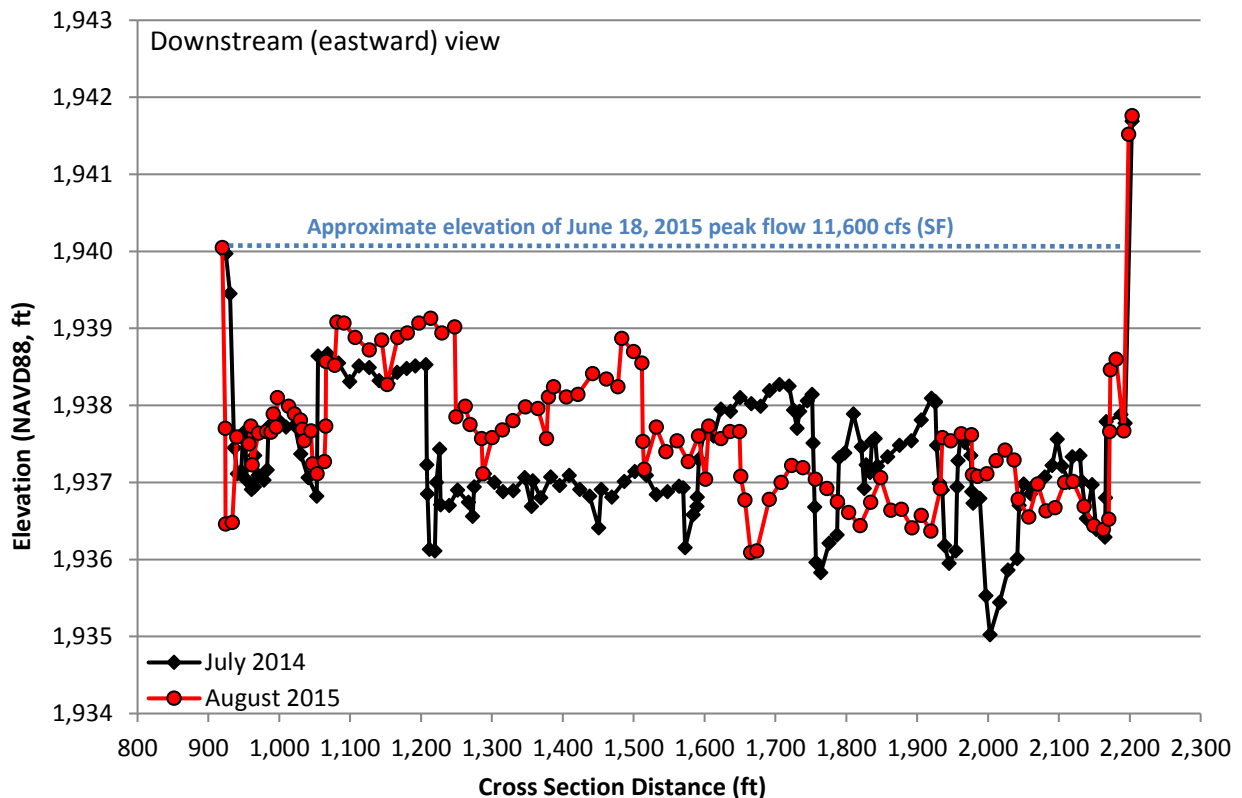




Figure A-17. Primary Cross Section #11 – June 2014 and August 2015

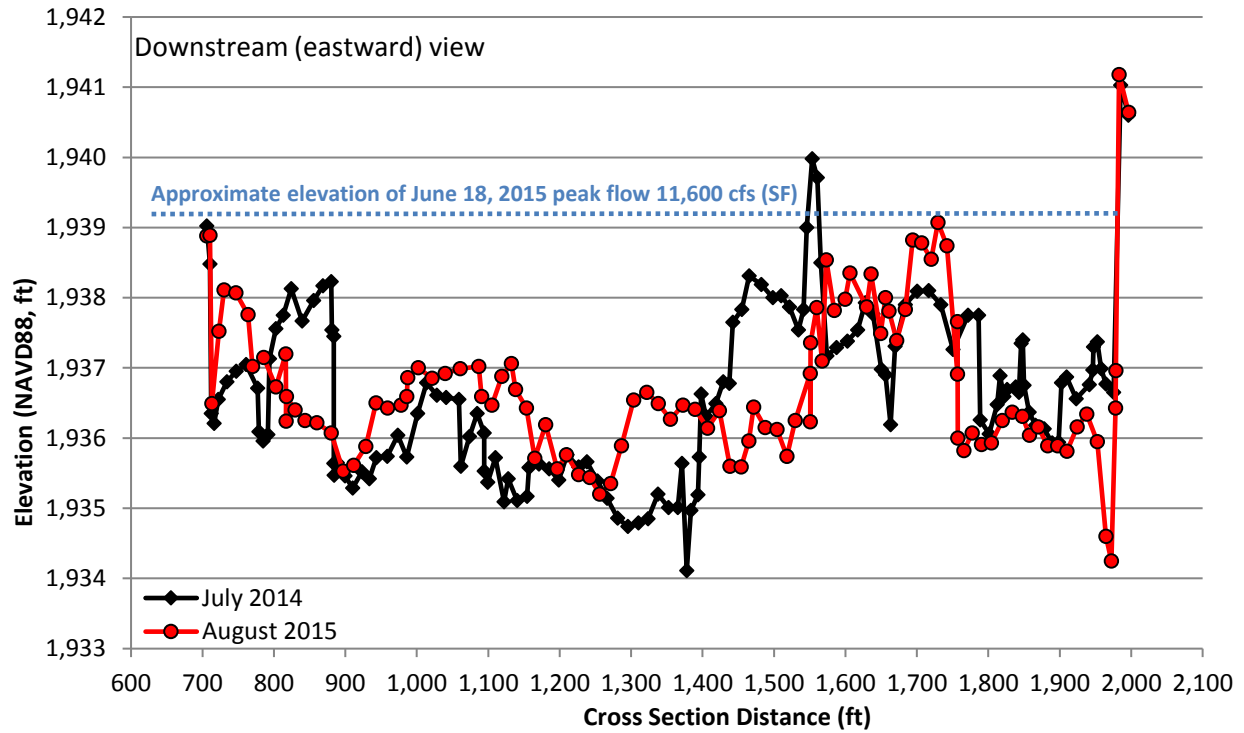


Figure A-18. Primary Cross Section #12 – June 2014 and August 2015

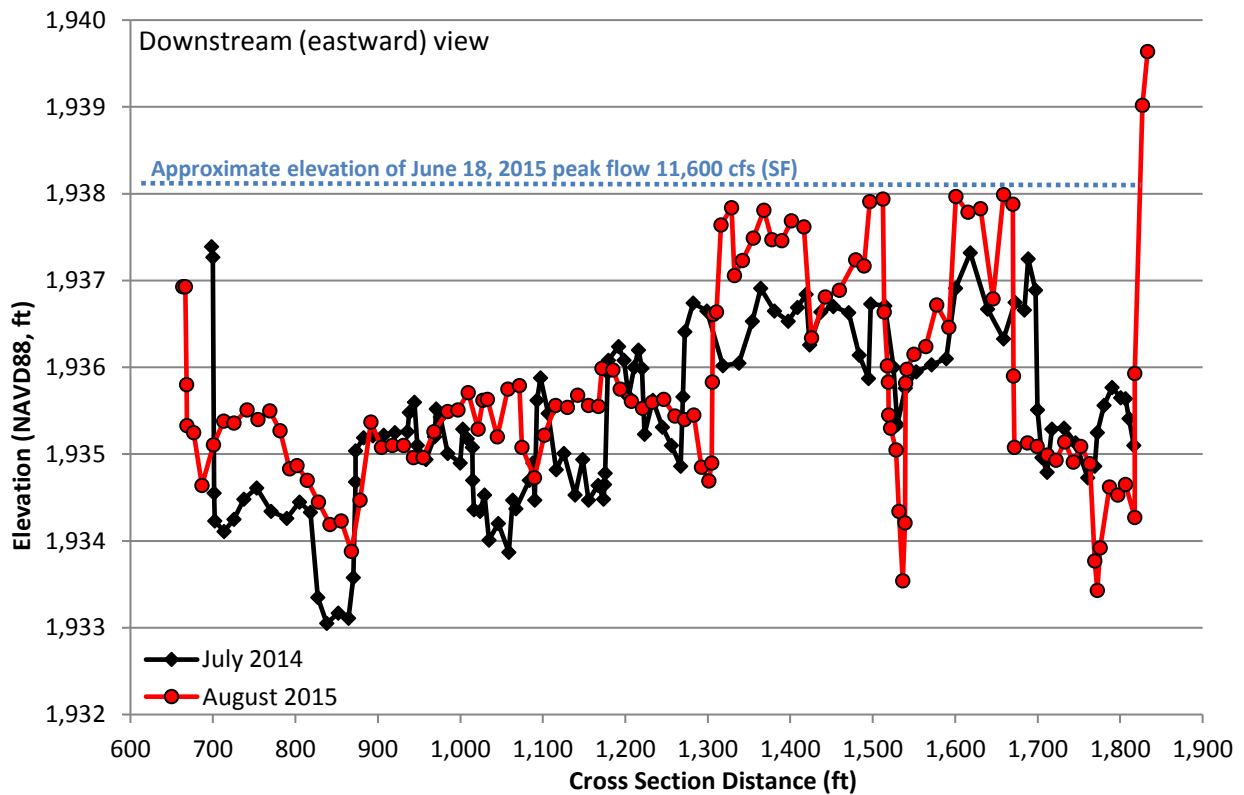




Figure A-19. Primary Cross Section #13 – June 2014 and August 2015

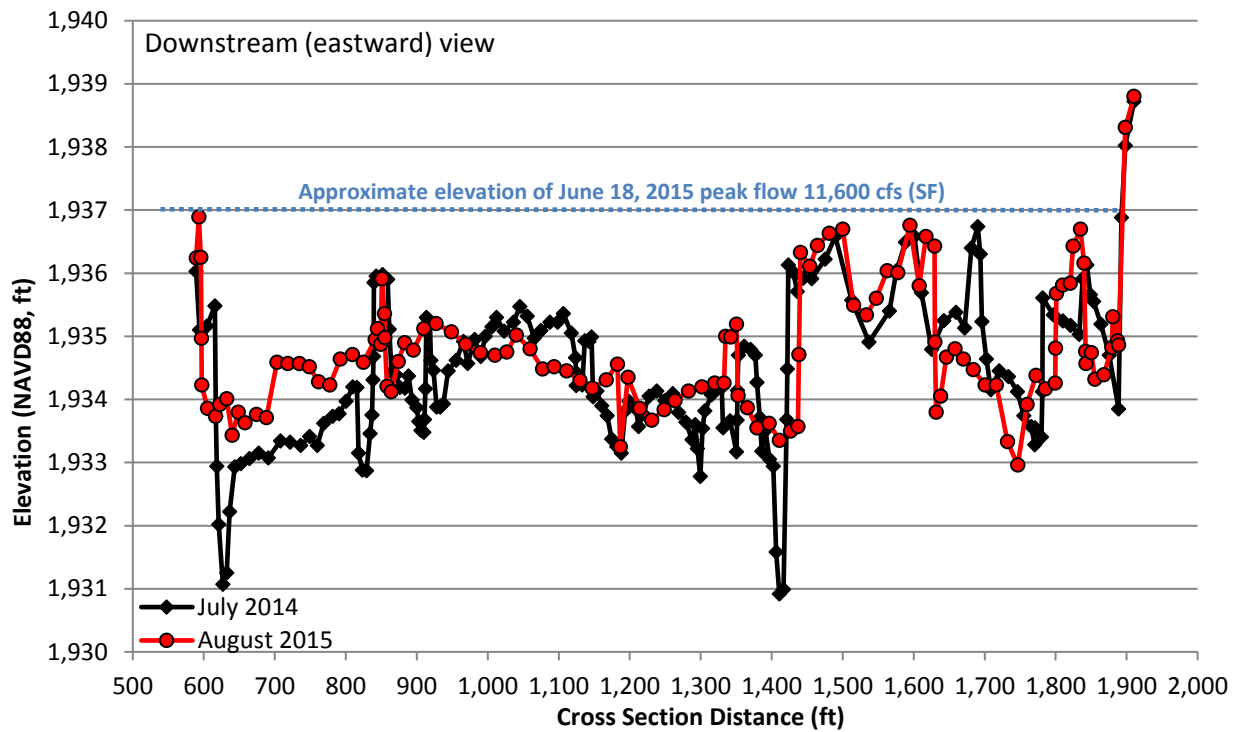


Figure A-20. Primary Cross Section #14 – June 2014 and August 2015

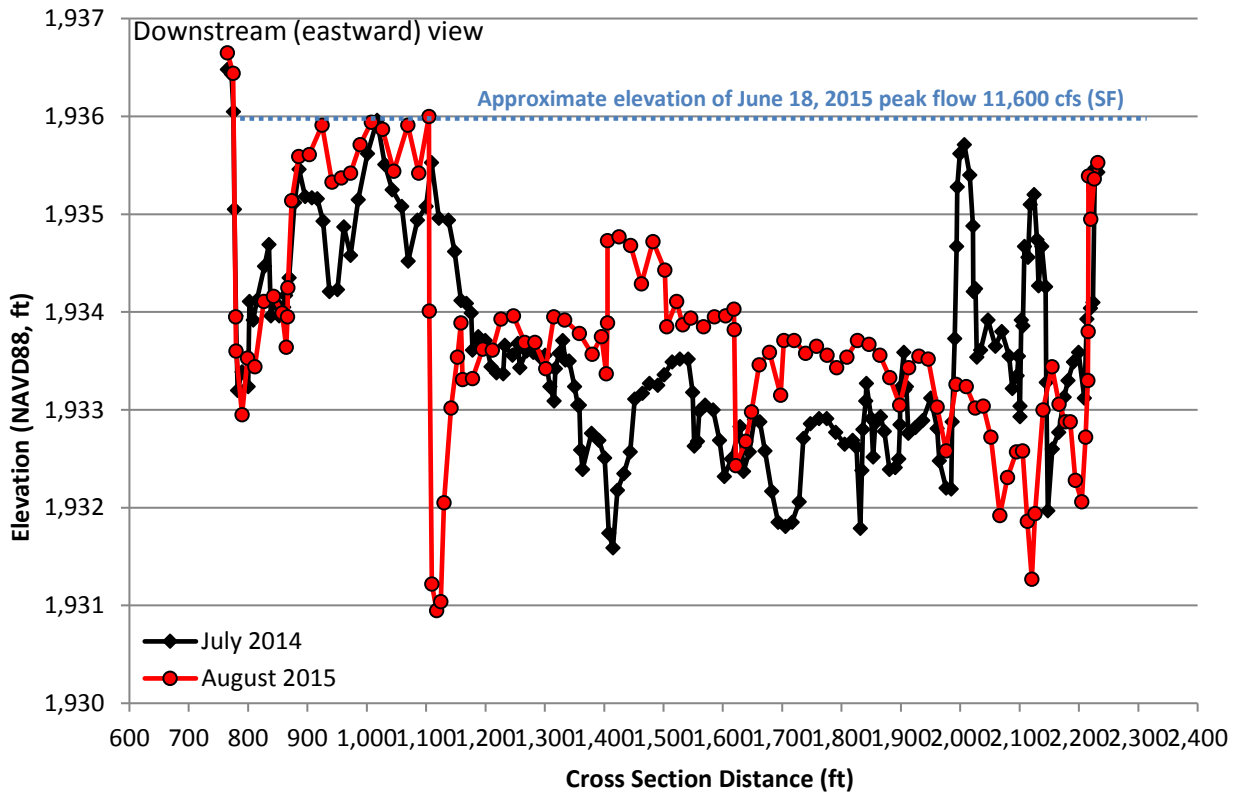




Figure A-21. Primary Cross Section #15 – June 2014 and August 2015

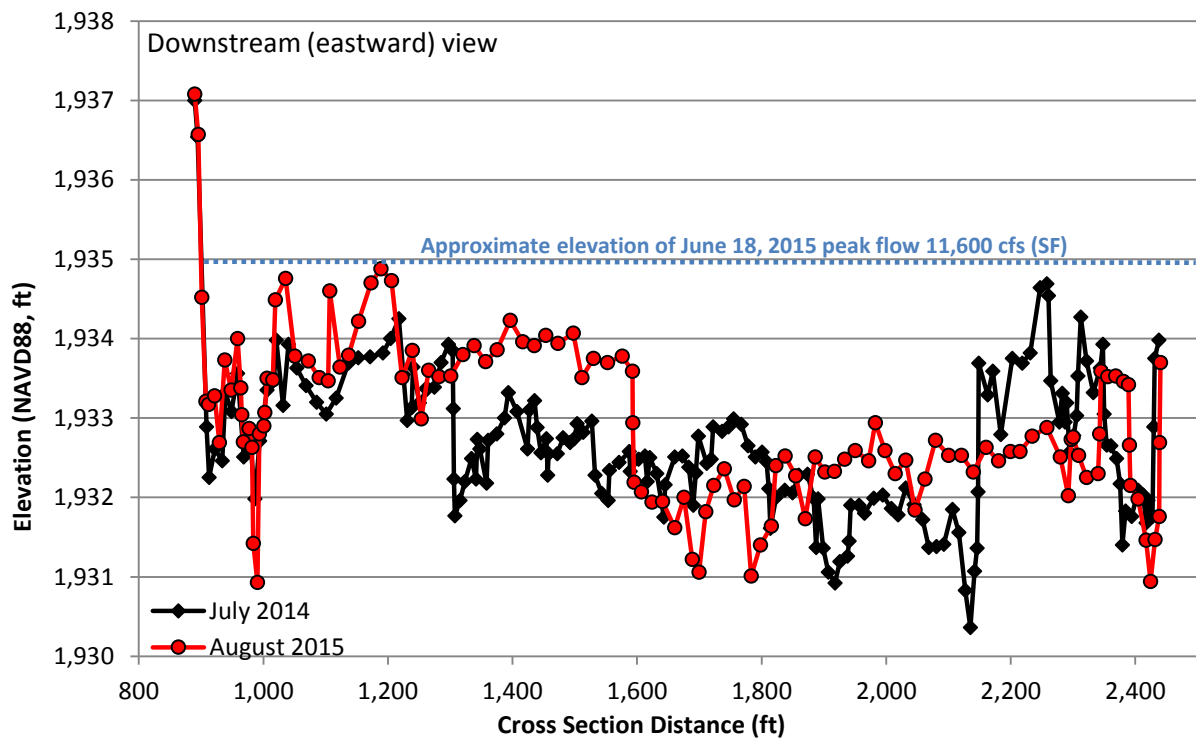


Figure A-22. Primary Cross Section #16 – June 2014 and August 2015

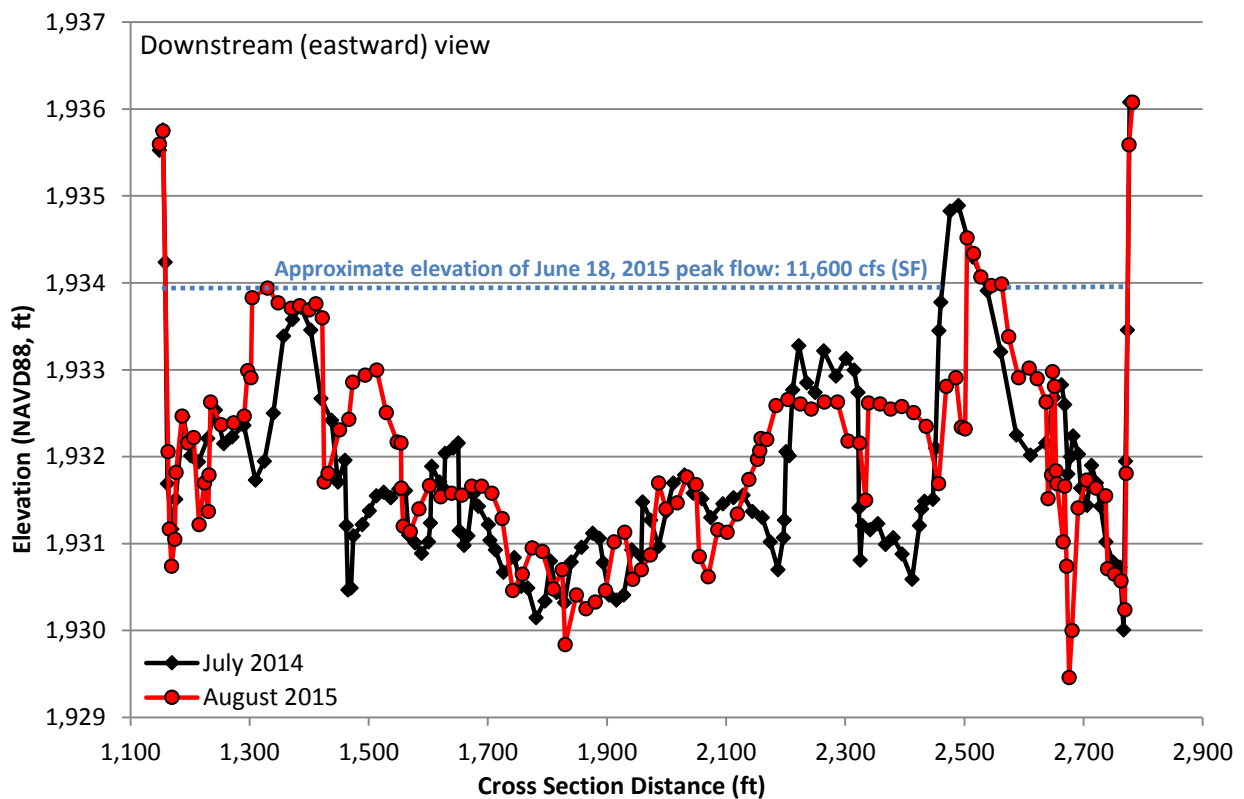




Figure A-23. Primary Cross Section #17 – June 2014 and August 2015

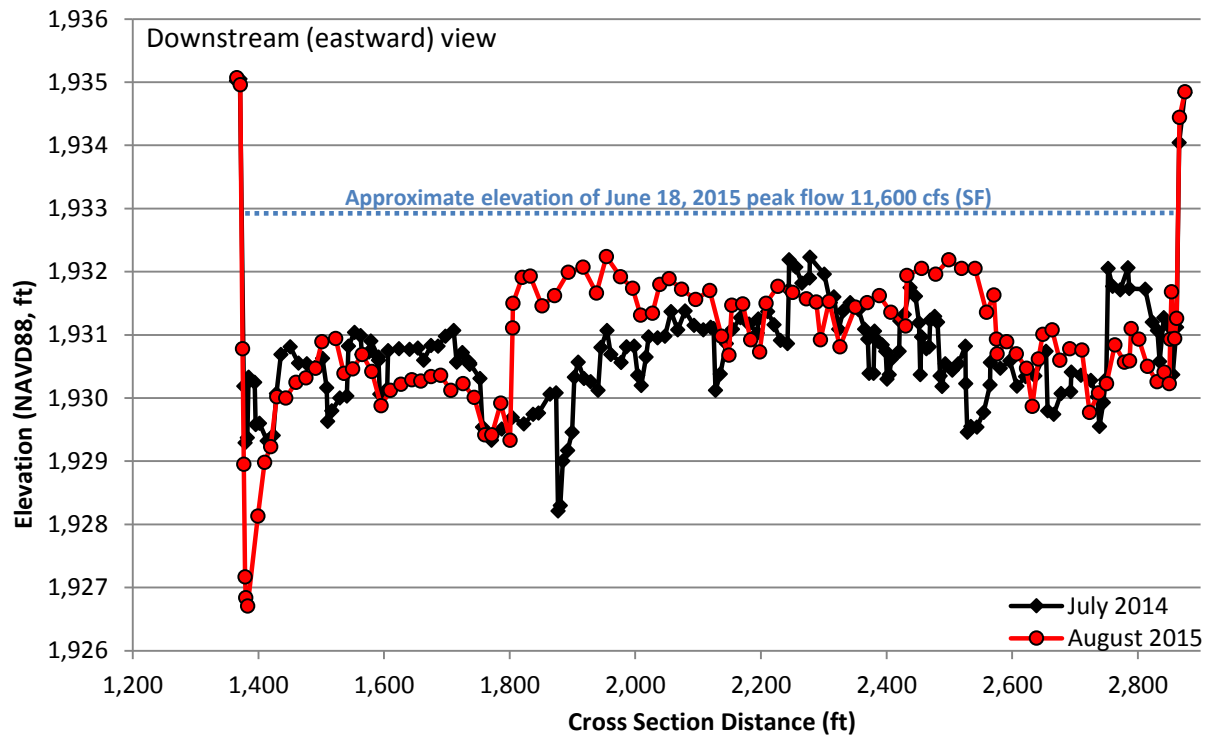


Figure A-24. Primary Cross Section #18 – June 2014 and August 2015

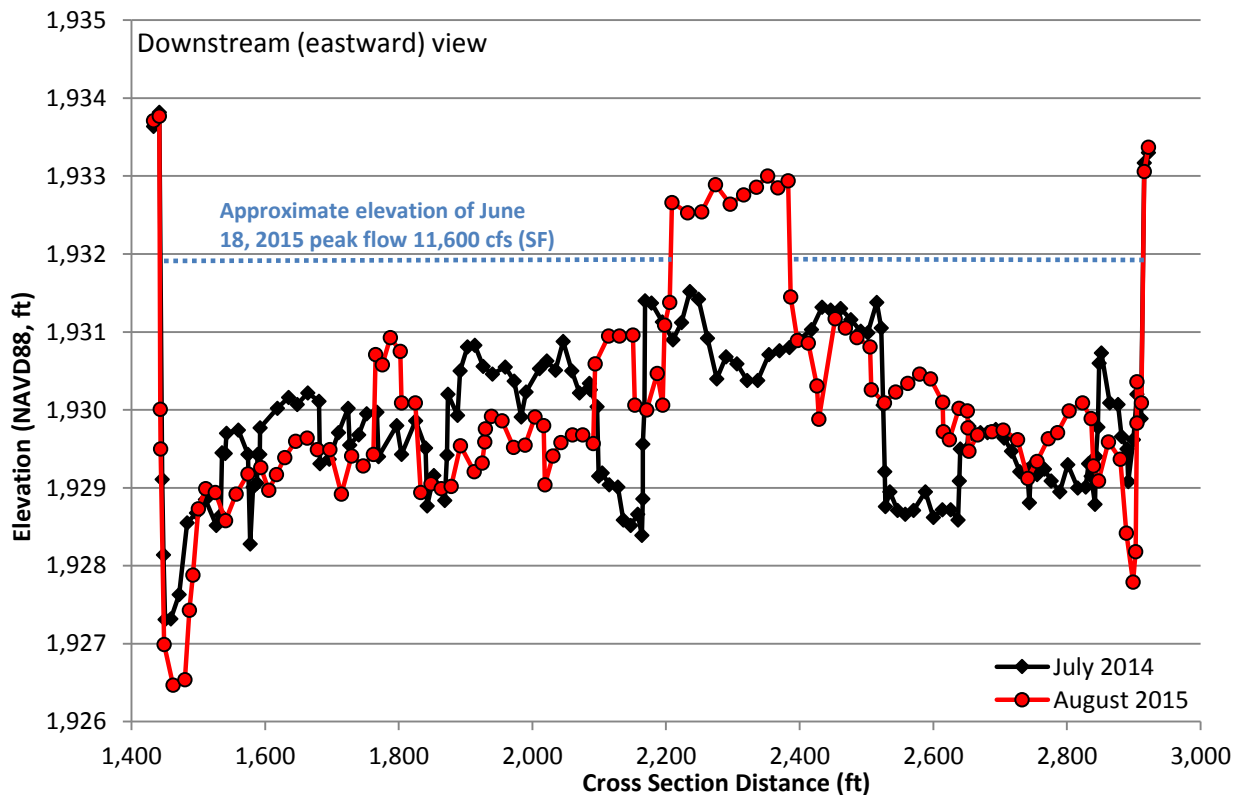




Figure A-25. Supplemental Cross Section A – June 2014 and August 2015

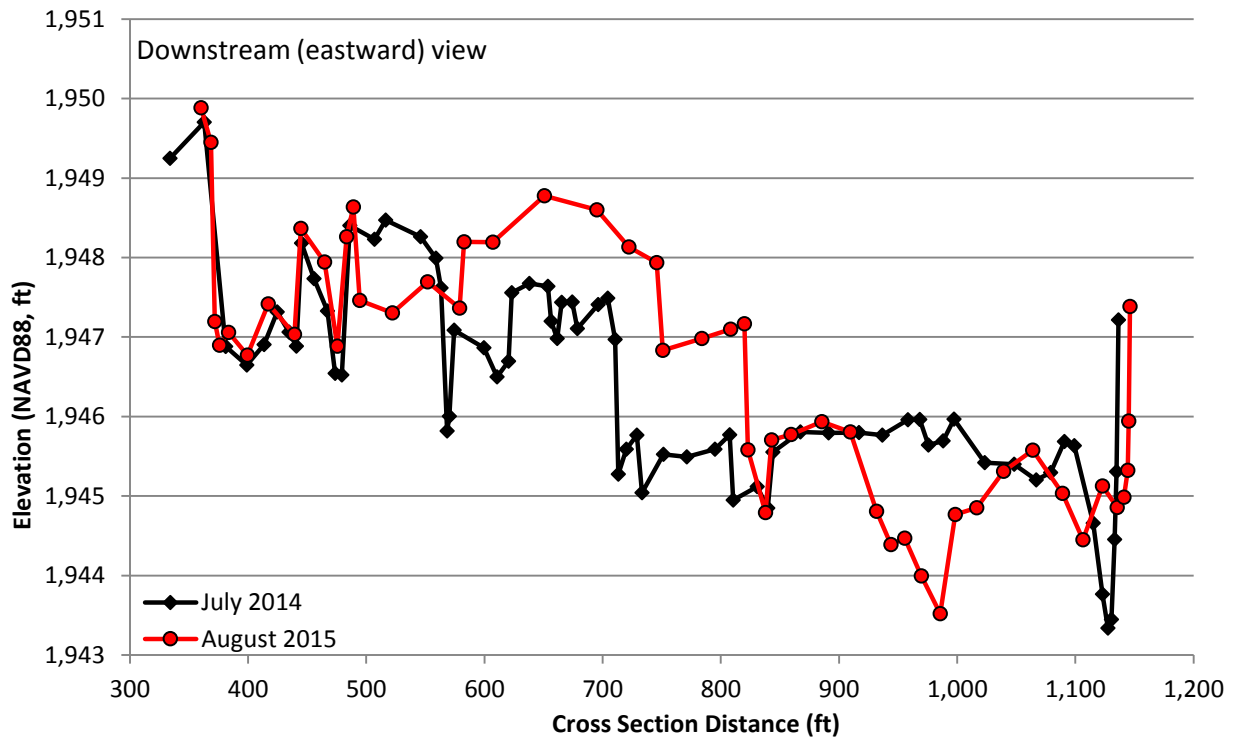


Figure A-26. Supplemental Cross Section B – June 2014 and August 2015

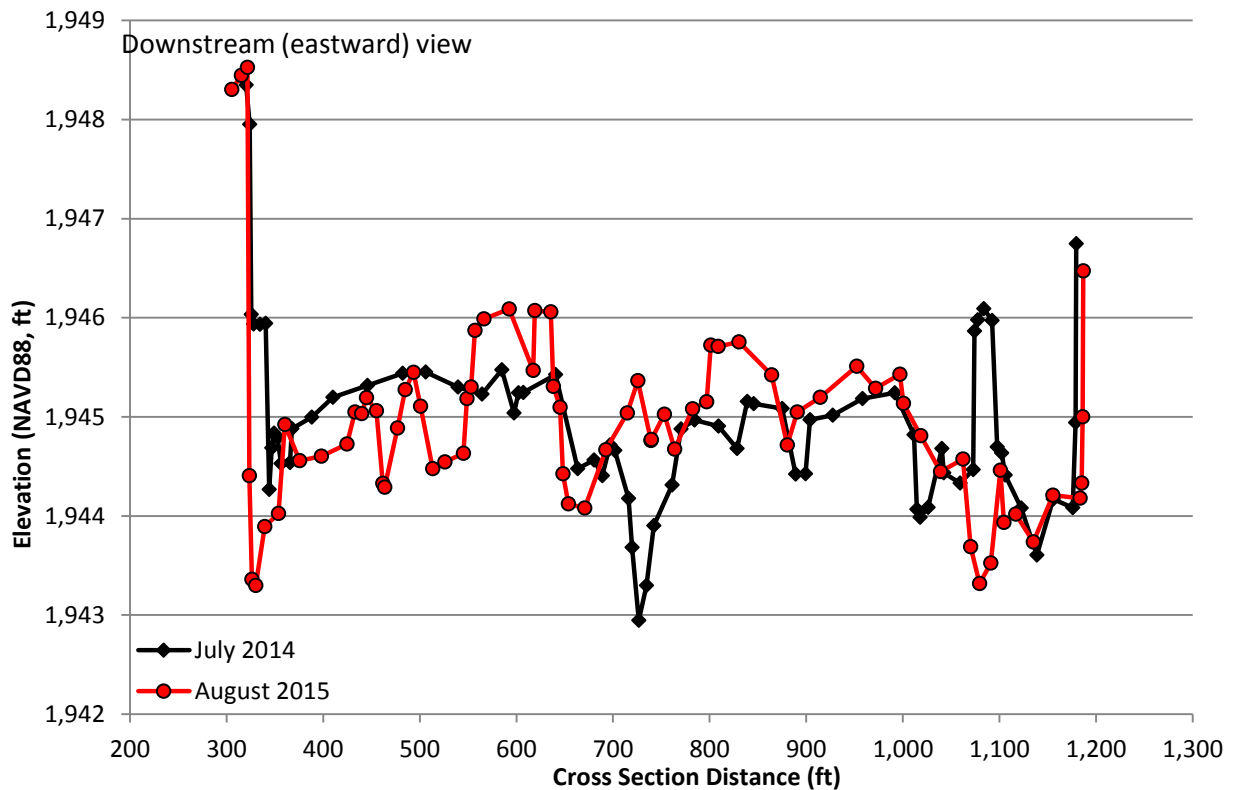




Figure A-27. Supplemental Cross Section C – June 2014 and August 2015

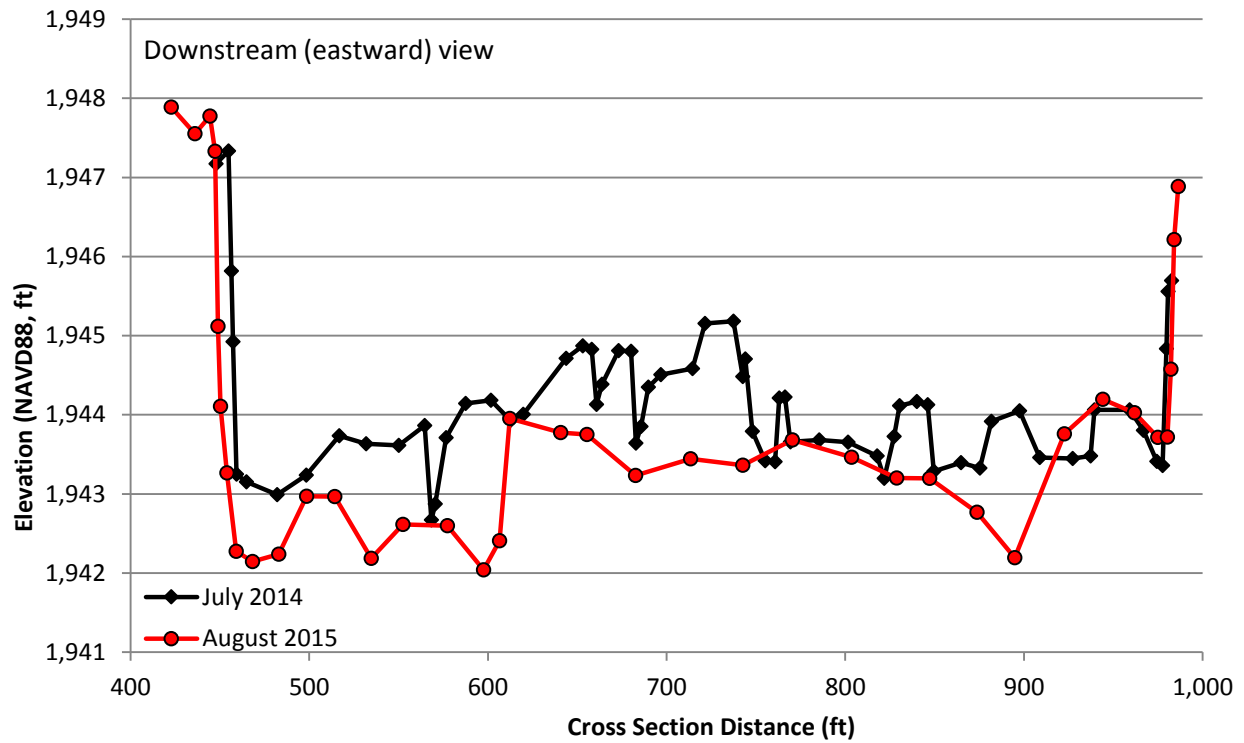


Figure A-28. Supplemental Cross Section D – June 2014 and August 2015

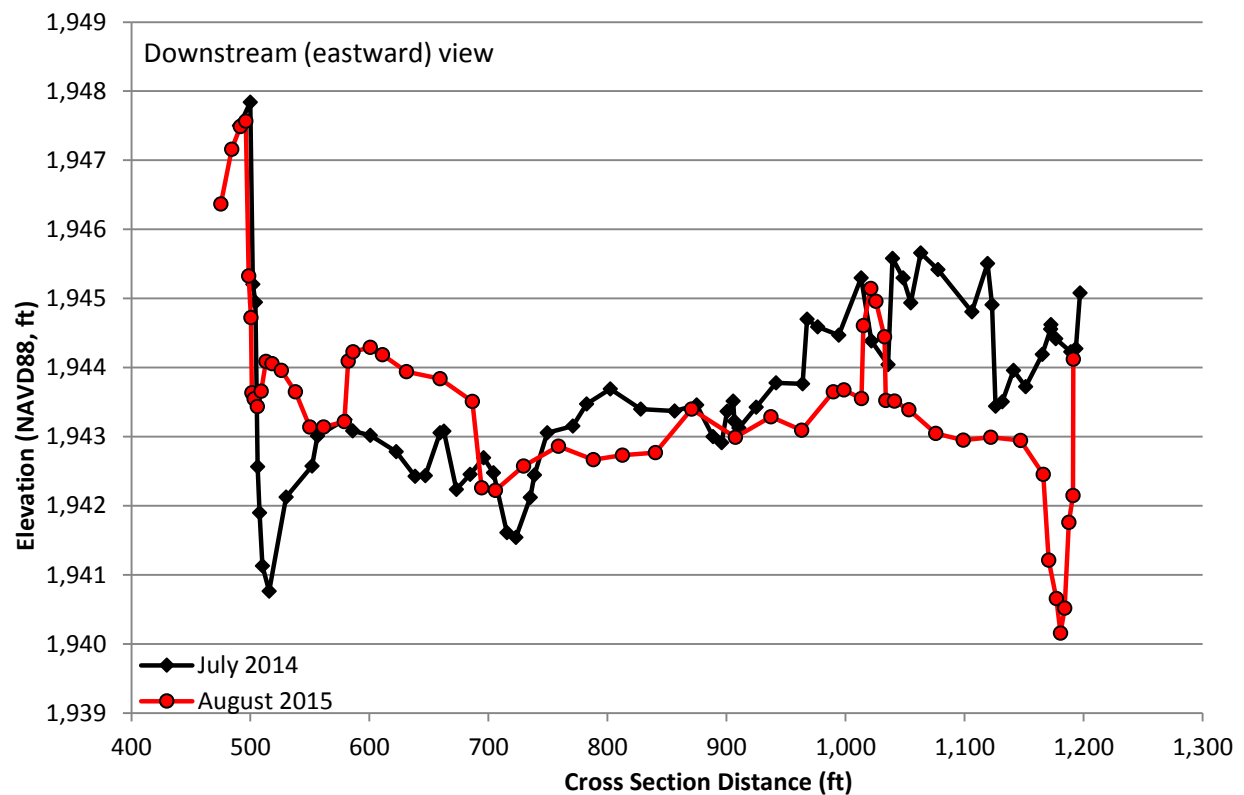




Figure A-29. Supplemental Cross Section E – June 2014 and August 2015

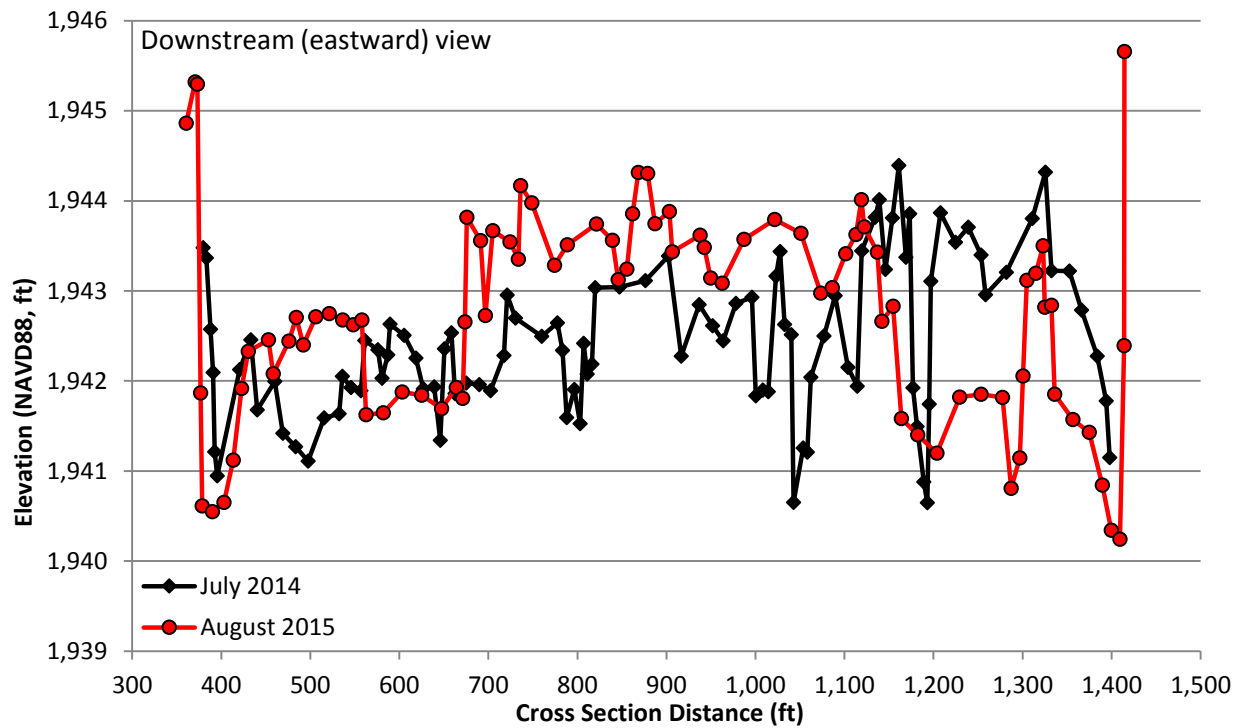


Figure A-30. Supplemental Cross Section F – June 2014 and August 2015

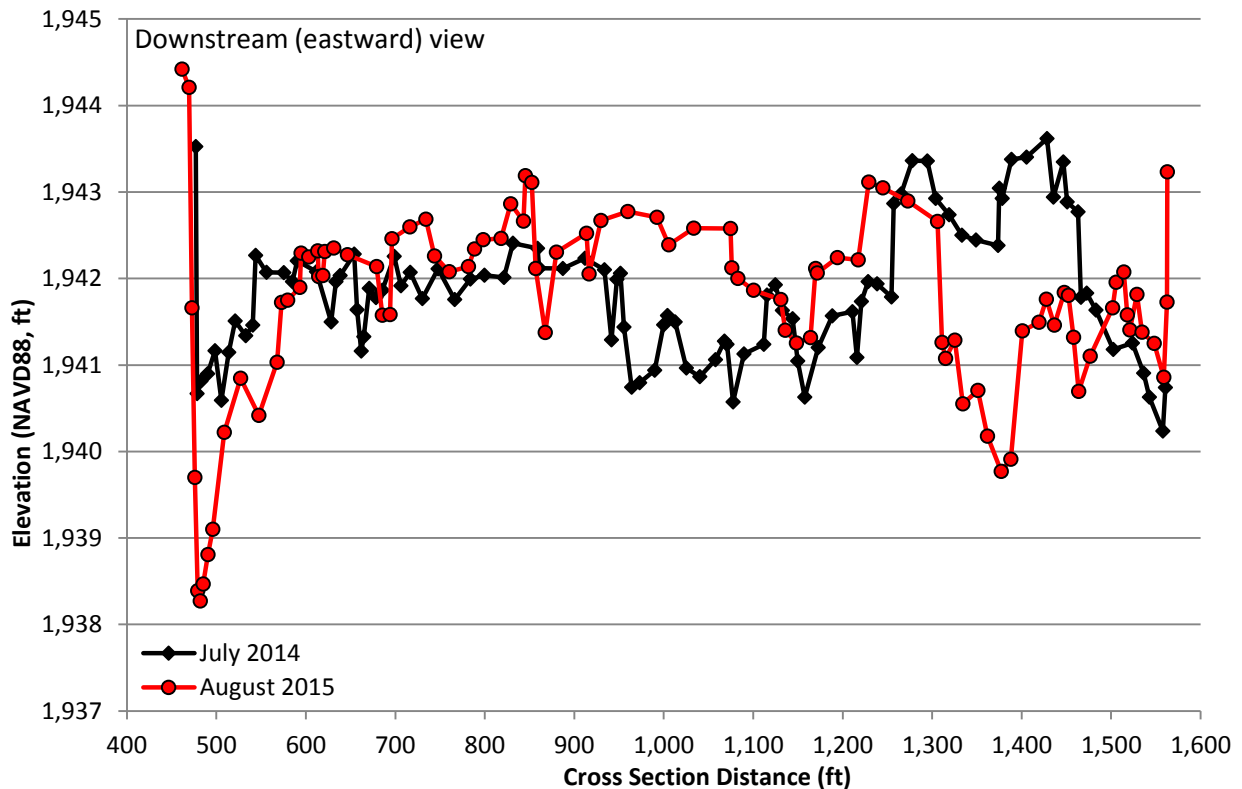




Figure A-31. Supplemental Cross Section G – June 2014 and August 2015

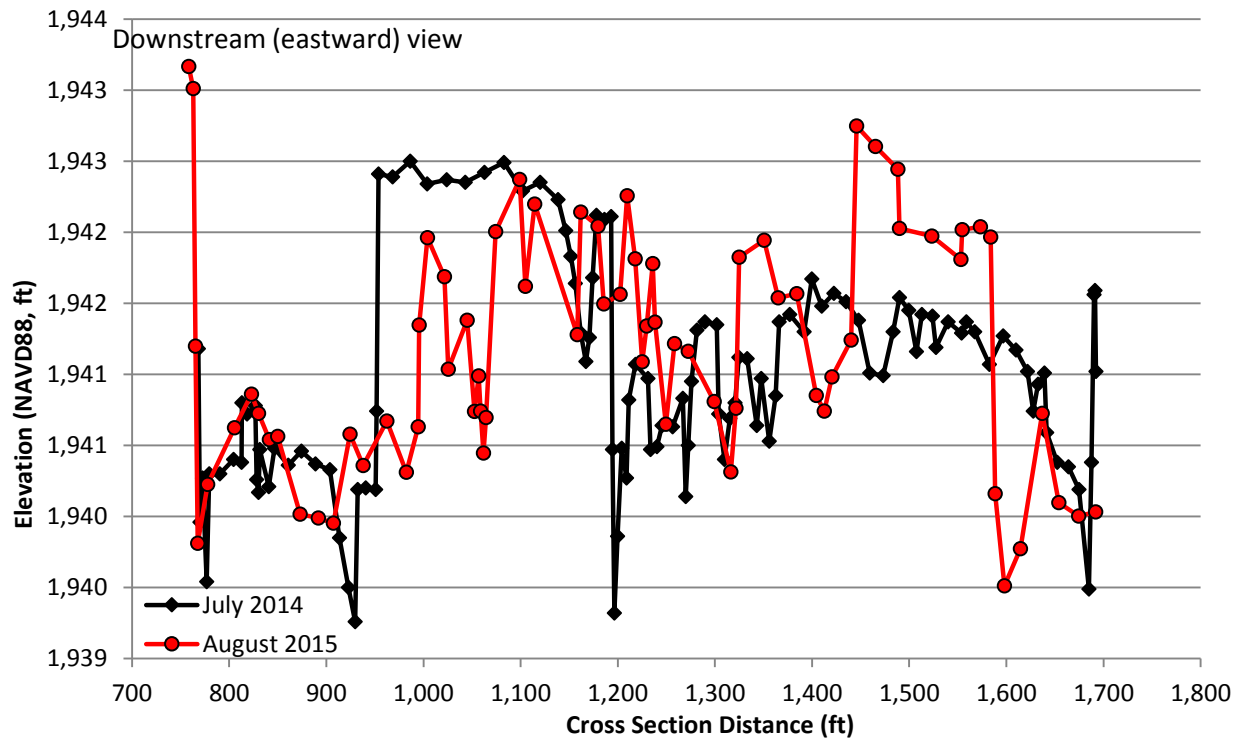


Figure A-32. Supplemental Cross Section H – June 2014 and August 2015

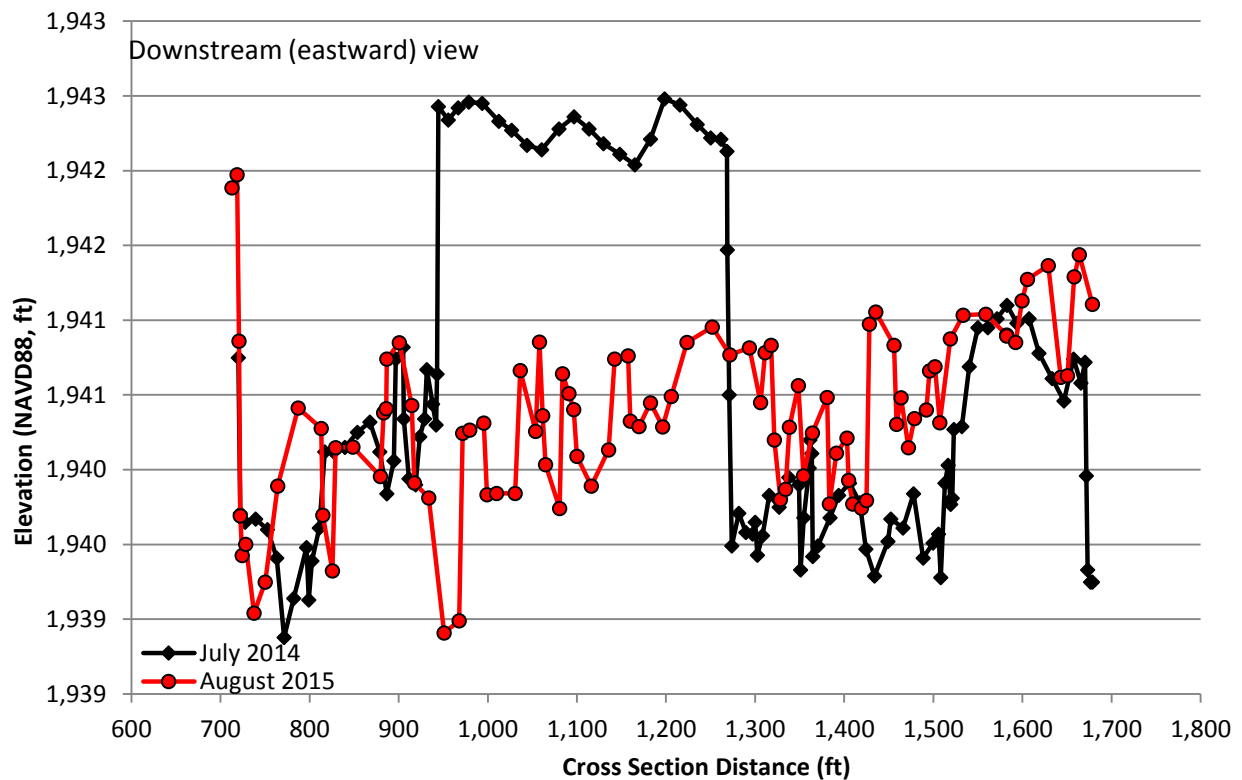




Figure A-33. Supplemental Cross Section I – June 2014 and August 2015

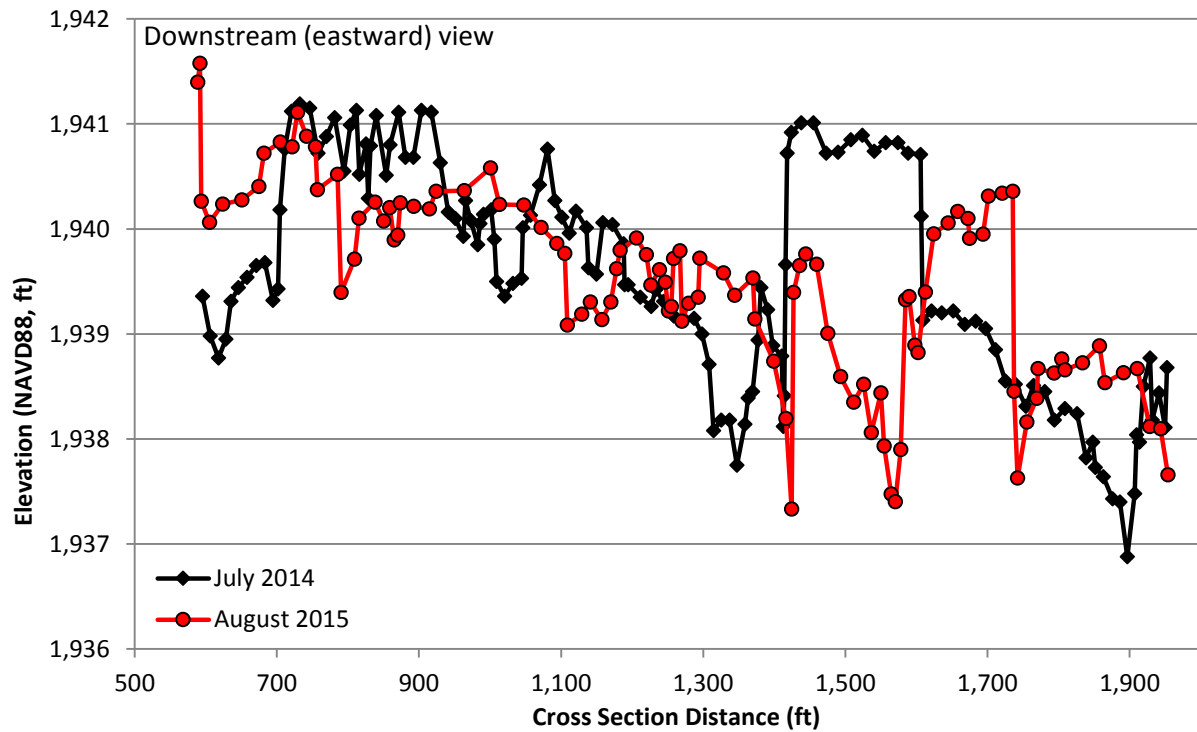


Figure A-34. Supplemental Cross Section J – June 2014 and August 2015

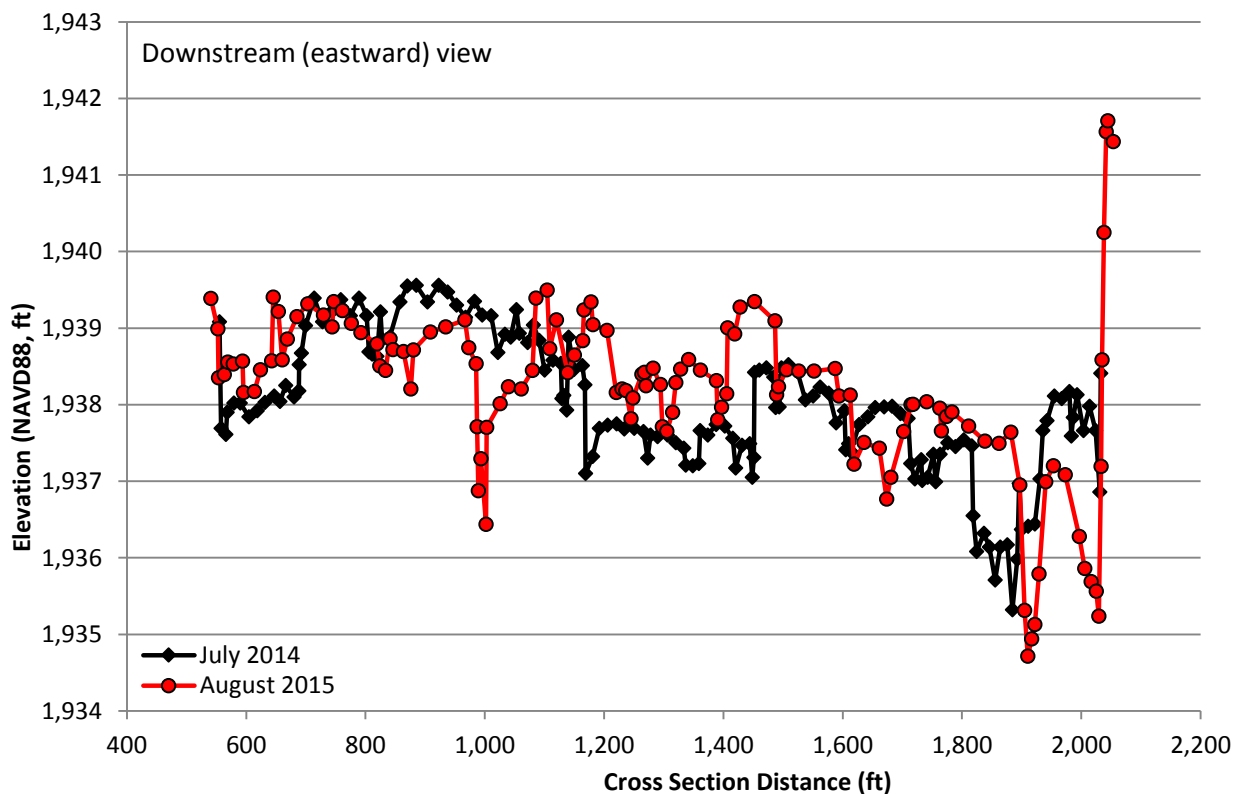




Figure A-35. Supplemental Cross Section K – June 2014 and August 2015

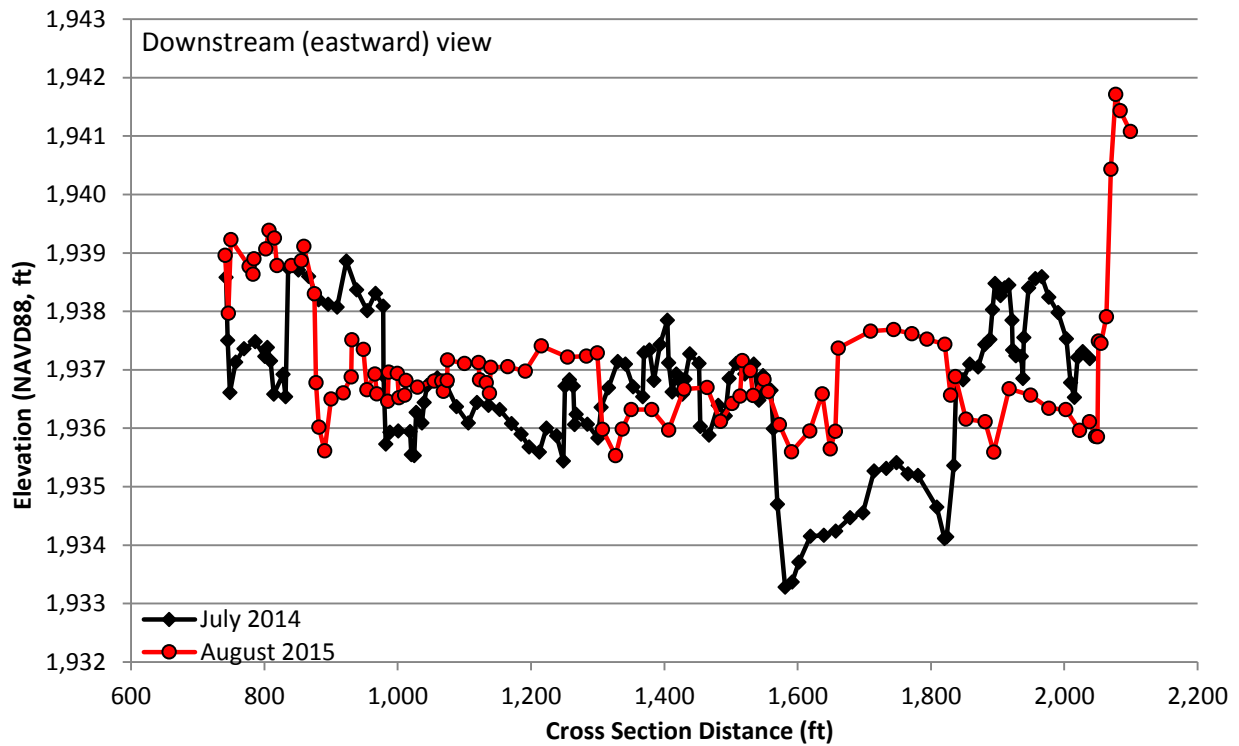


Figure A-36. Supplemental Cross Section L – June 2014 and August 2015

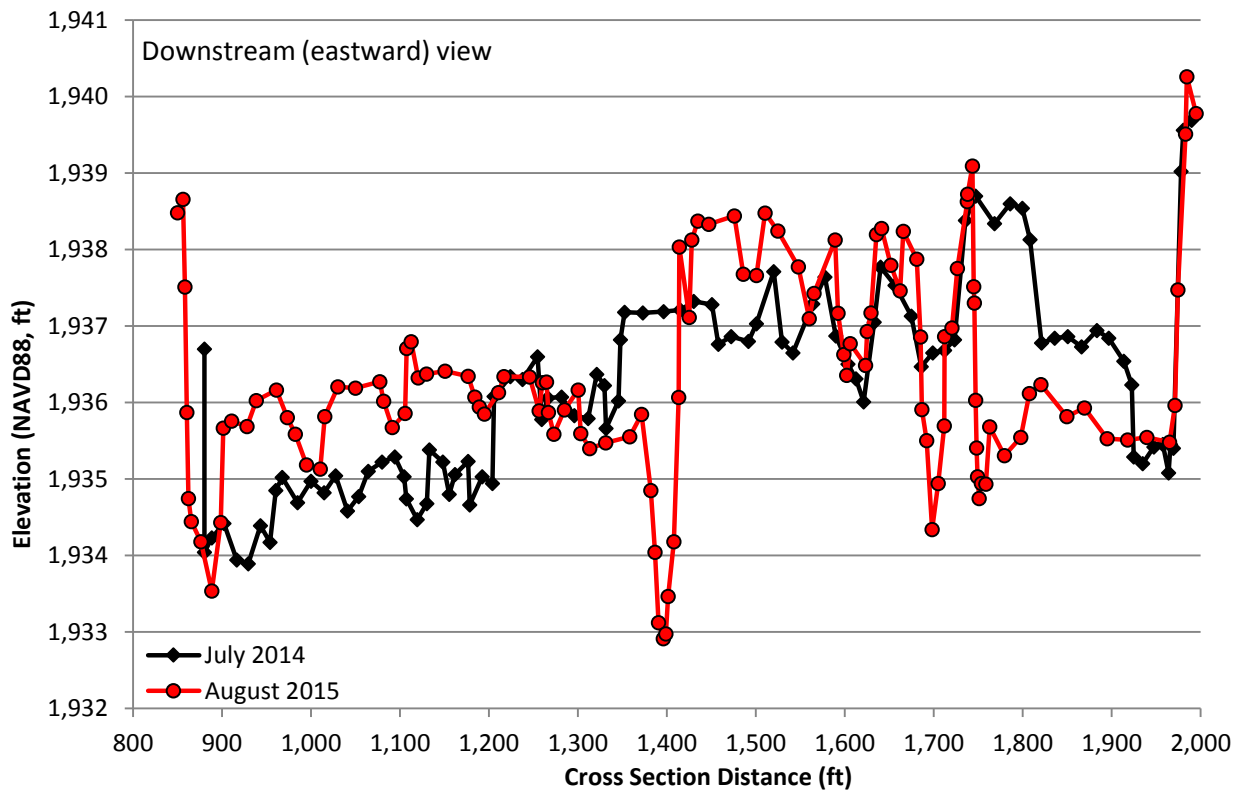




Figure A-37. Supplemental Cross Section M – June 2014 and August 2015

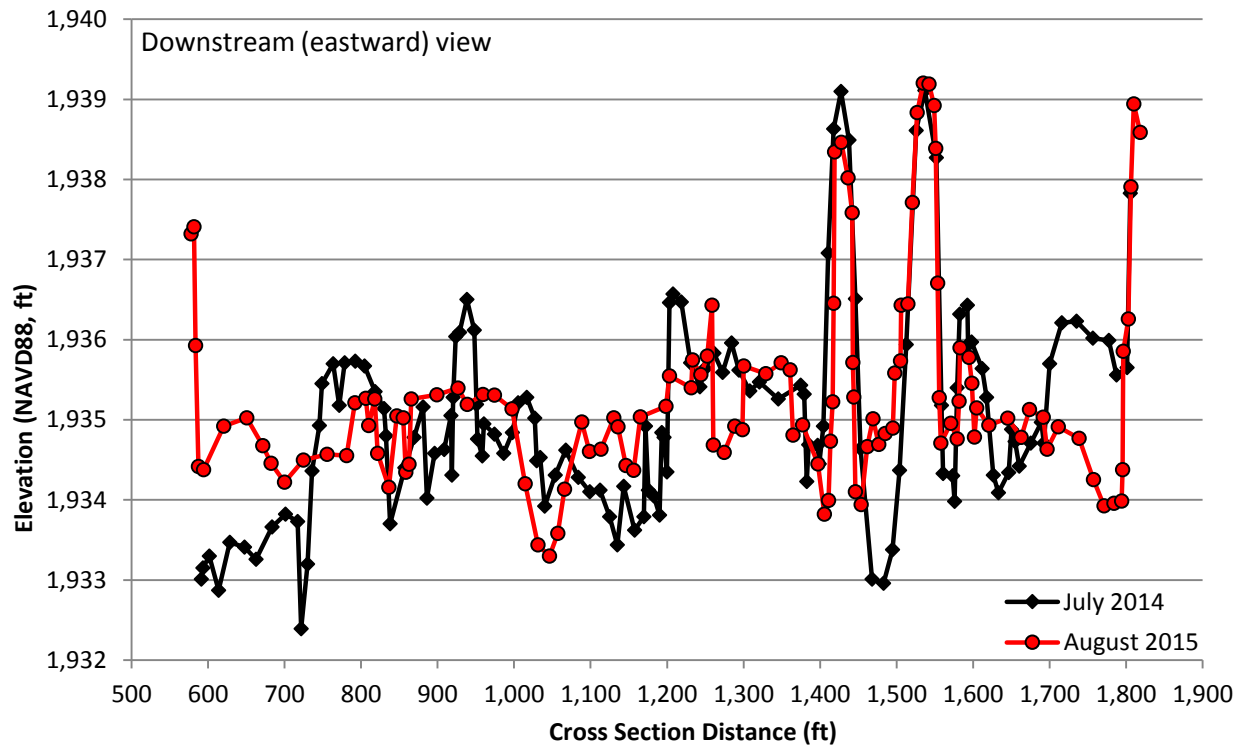


Figure A-38. Supplemental Cross Section N – June 2014 and August 2015

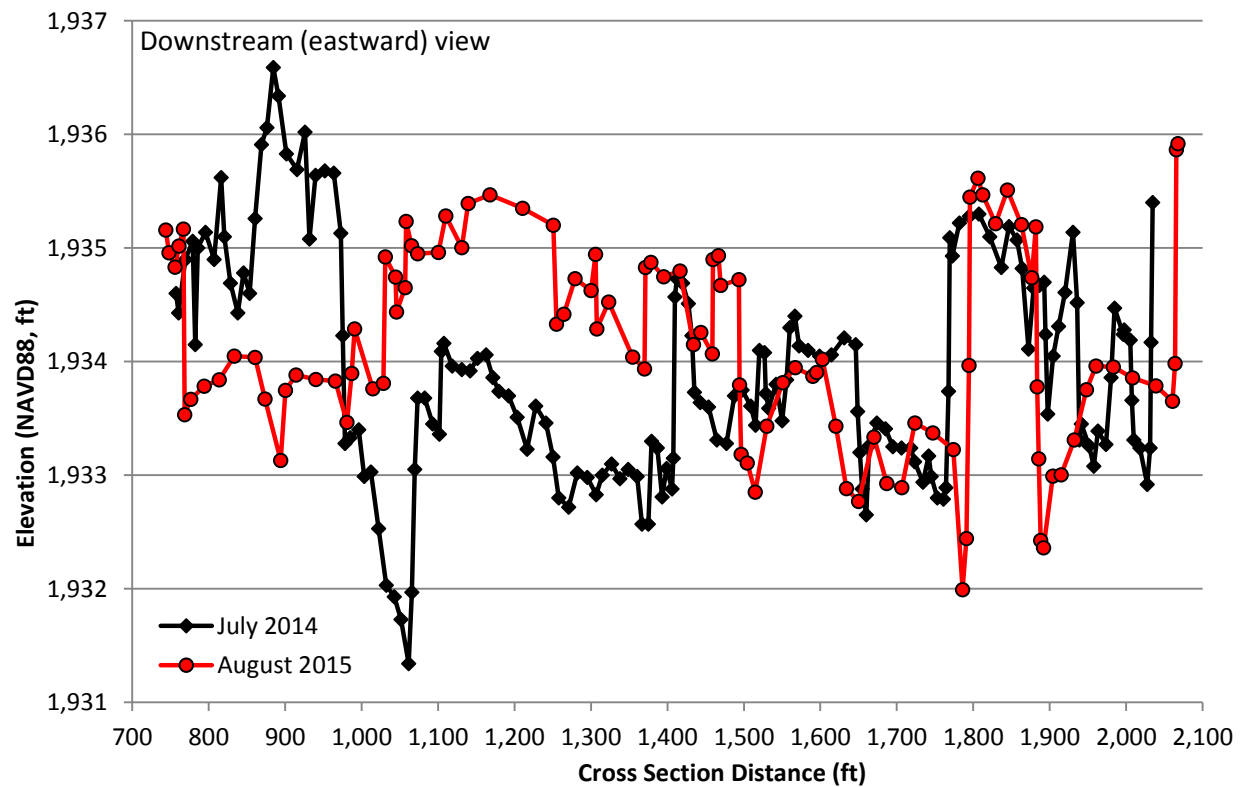




Figure A-39. Supplemental Cross Section O – June 2014 and August 2015

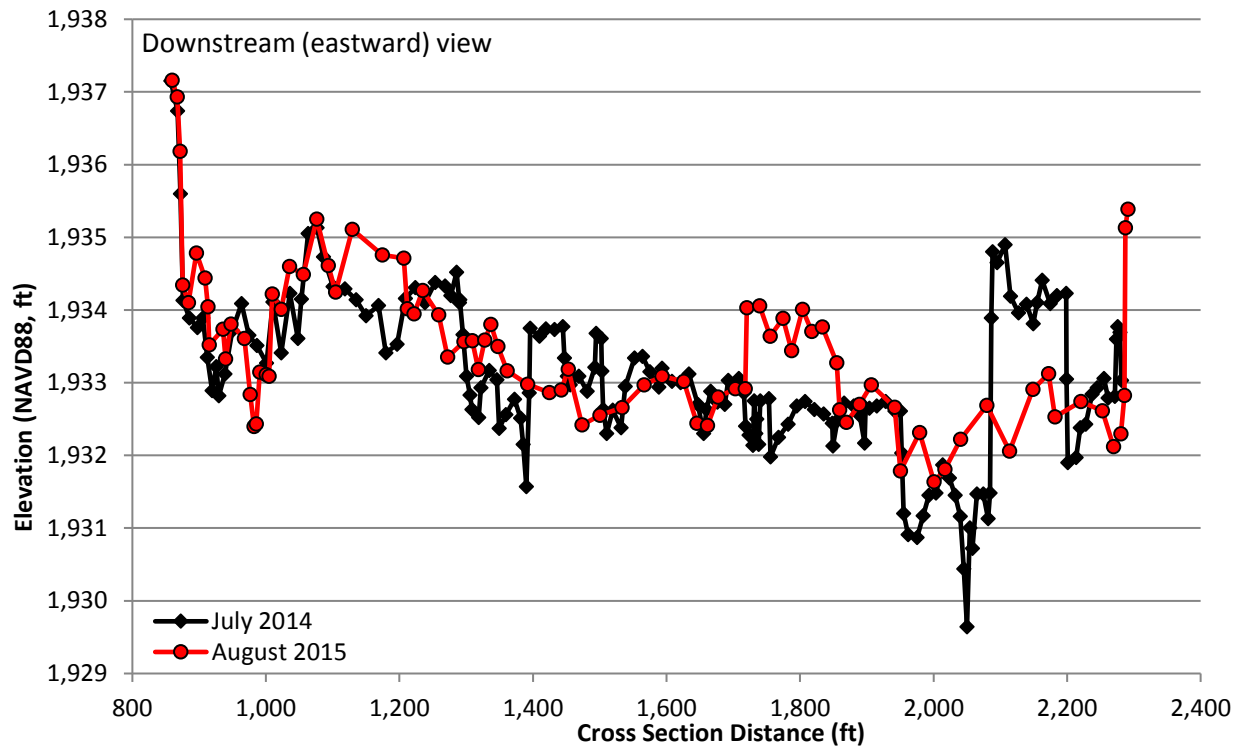


Figure A-40. Supplemental Cross Section P – June 2014 and August 2015

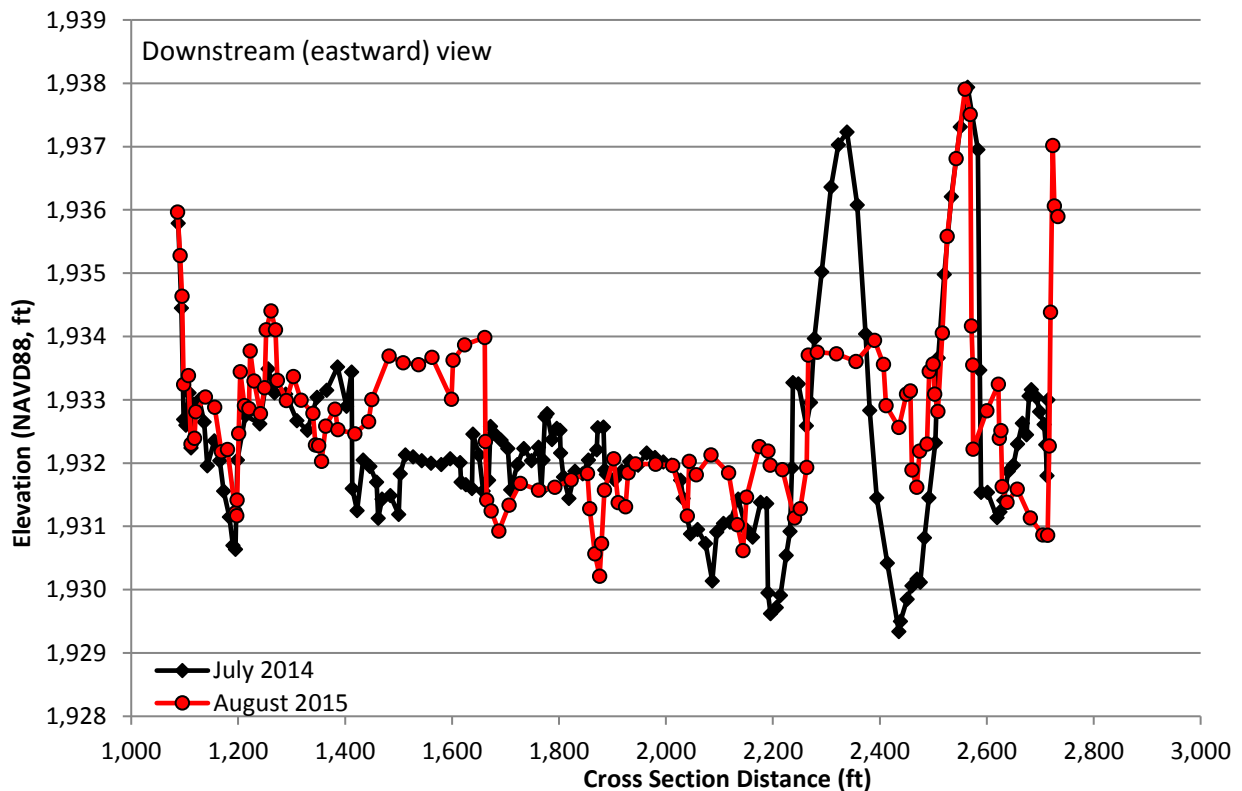




Figure A-41. Supplemental Cross Section Q – June 2014 and August 2015

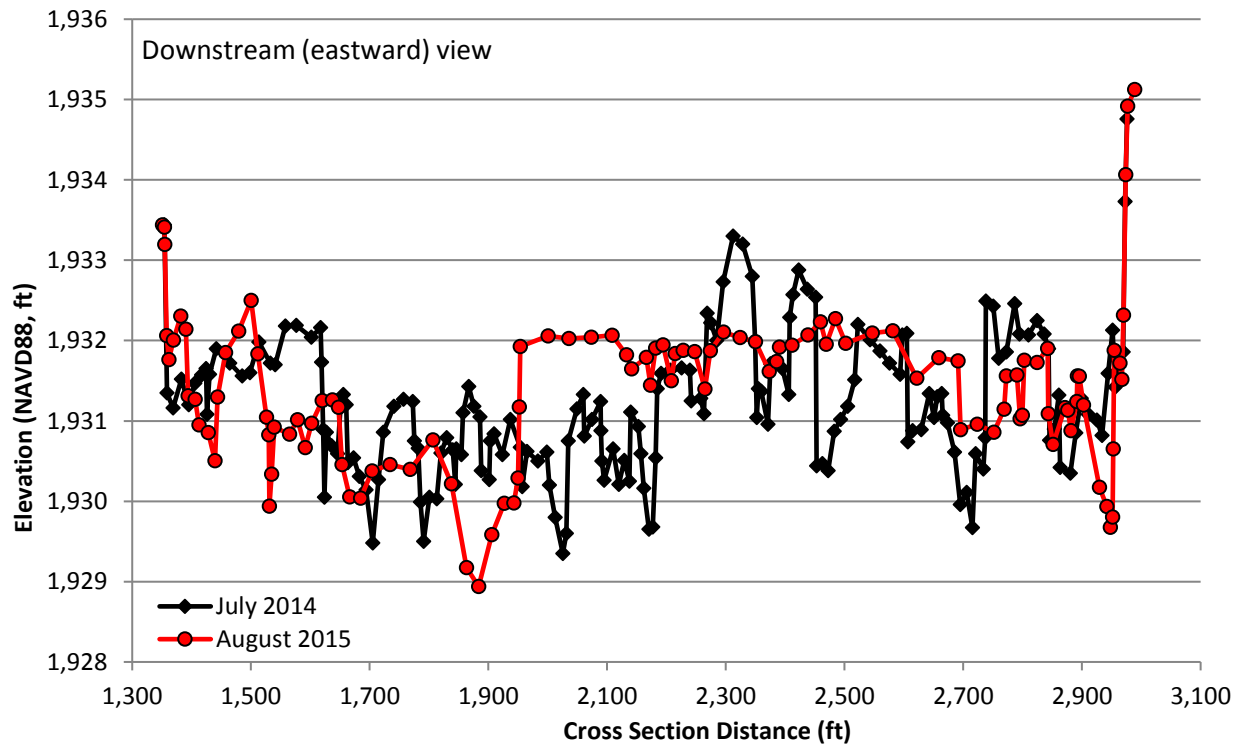


Figure A-42. Supplemental Cross Section R – June 2014 and August 2015

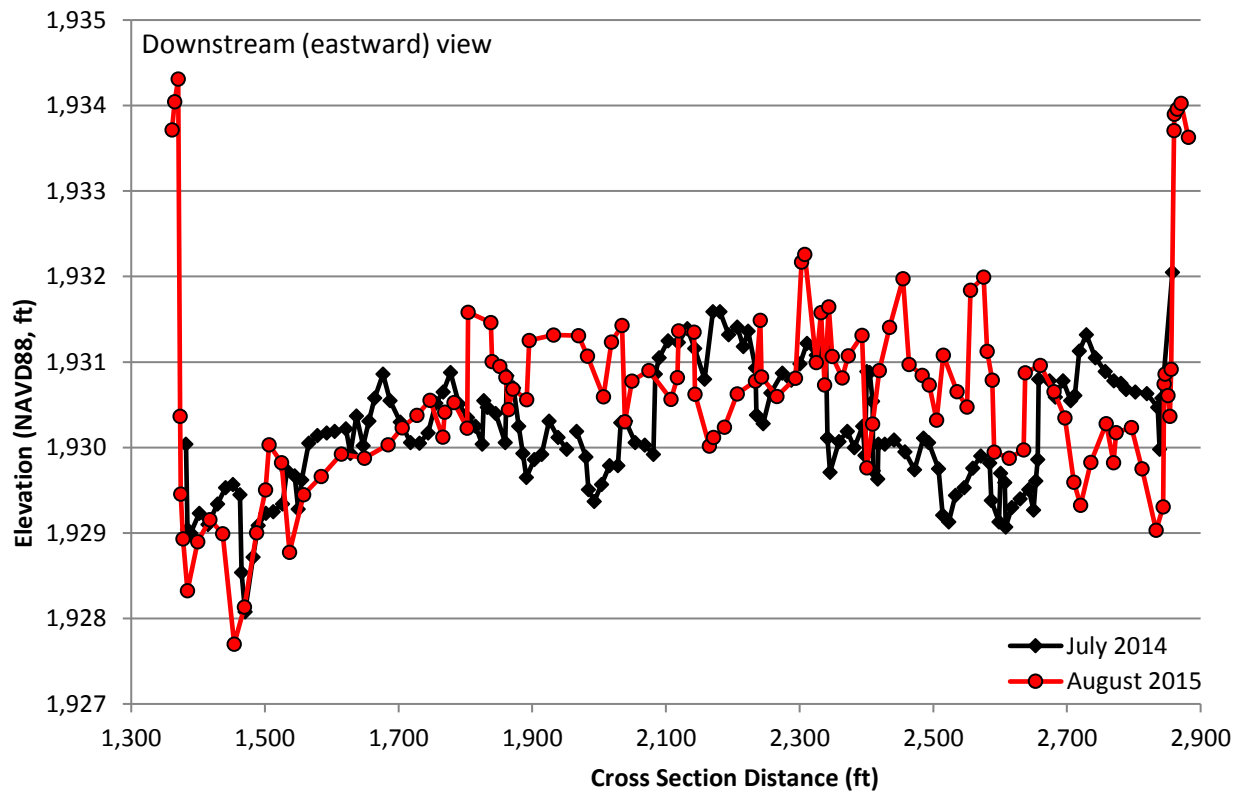




Figure A-43. Supplemental Cross Section S – June 2014 and August 2015

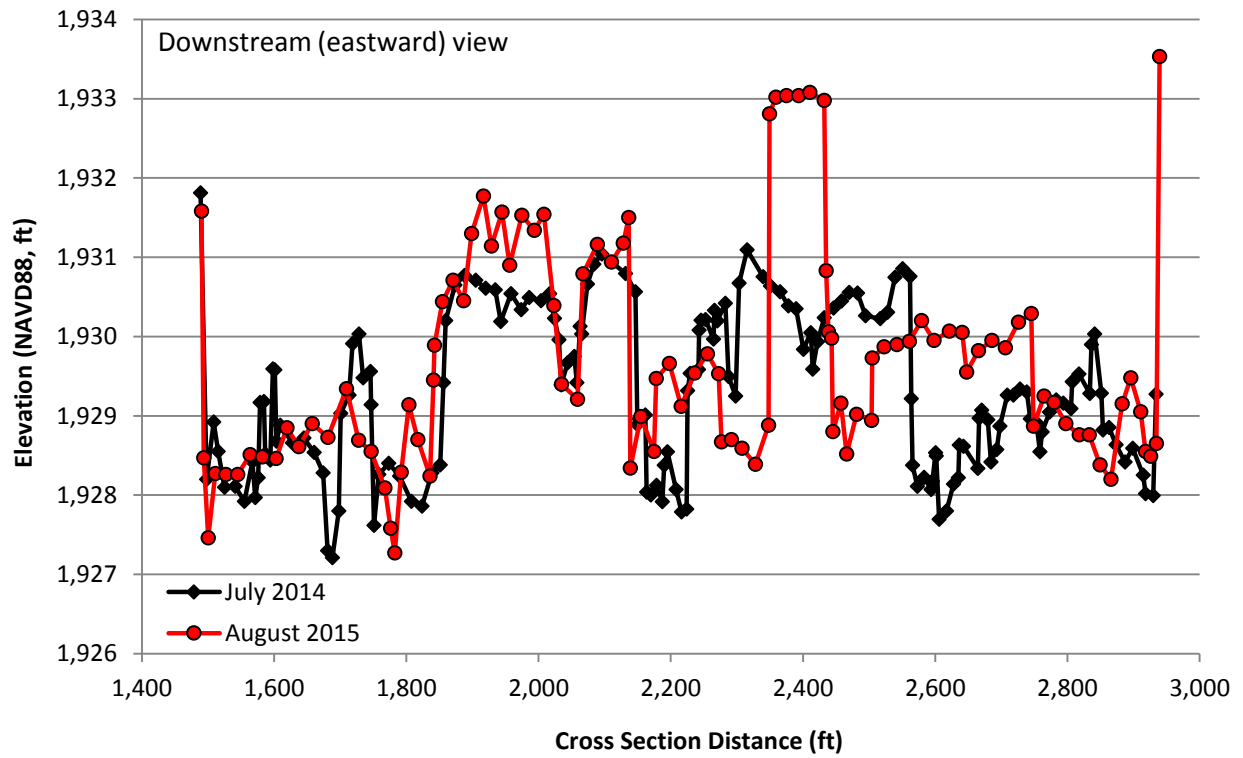




Figure A-44. Longitudinal Profile – Northern Route July 2014 and August 2015 – Cross Sections 1-6

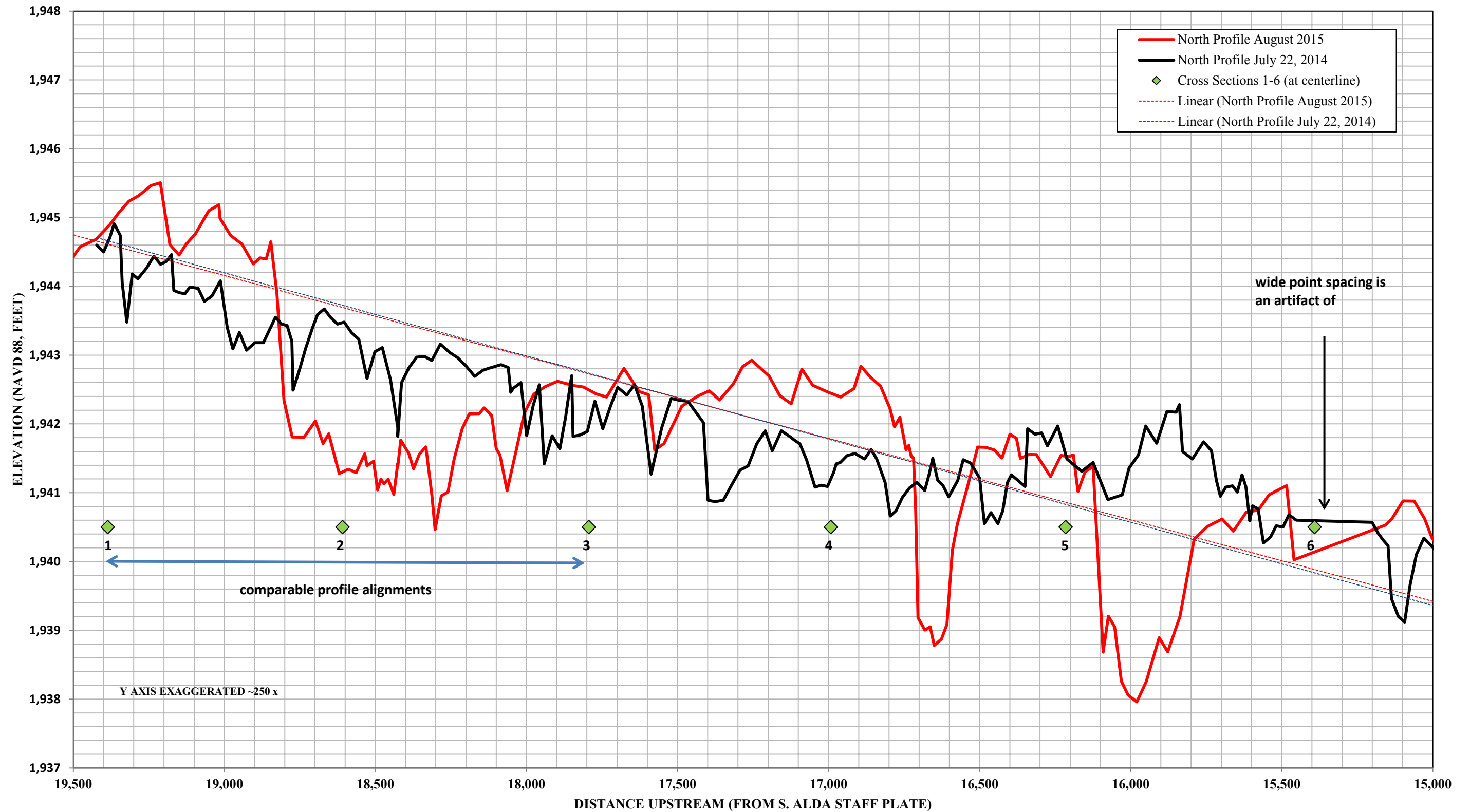




Figure A-45. Longitudinal Profile – Northern Route July 2014 and August 2015 – Cross Sections 7-12

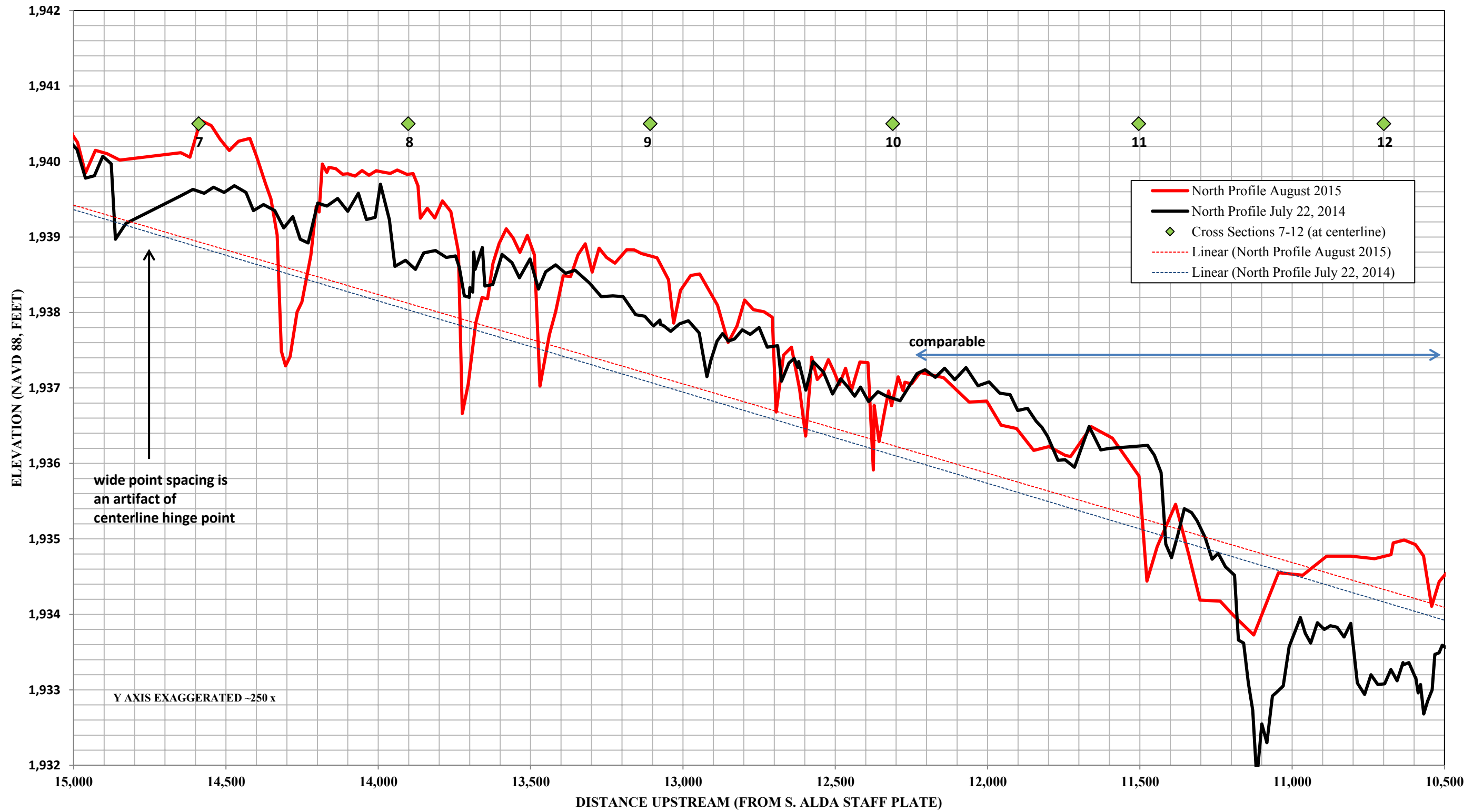




Figure A-46. Longitudinal Profile – Northern Route July 2014 and August 2015 – Cross Sections 13-18

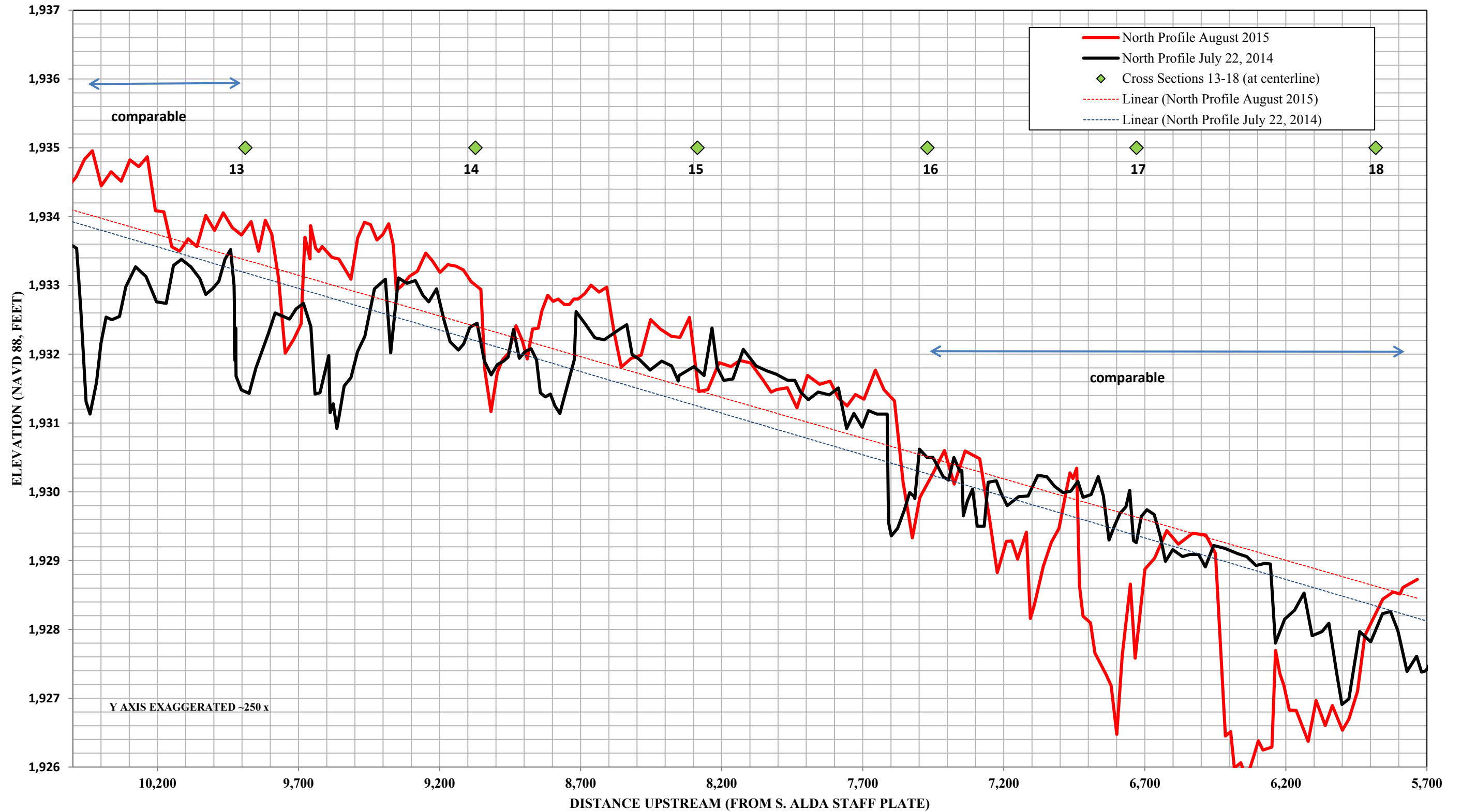




Figure A-47. Longitudinal Profile – Southern Route July 2014 and August 2015 – Cross Sections 1-6

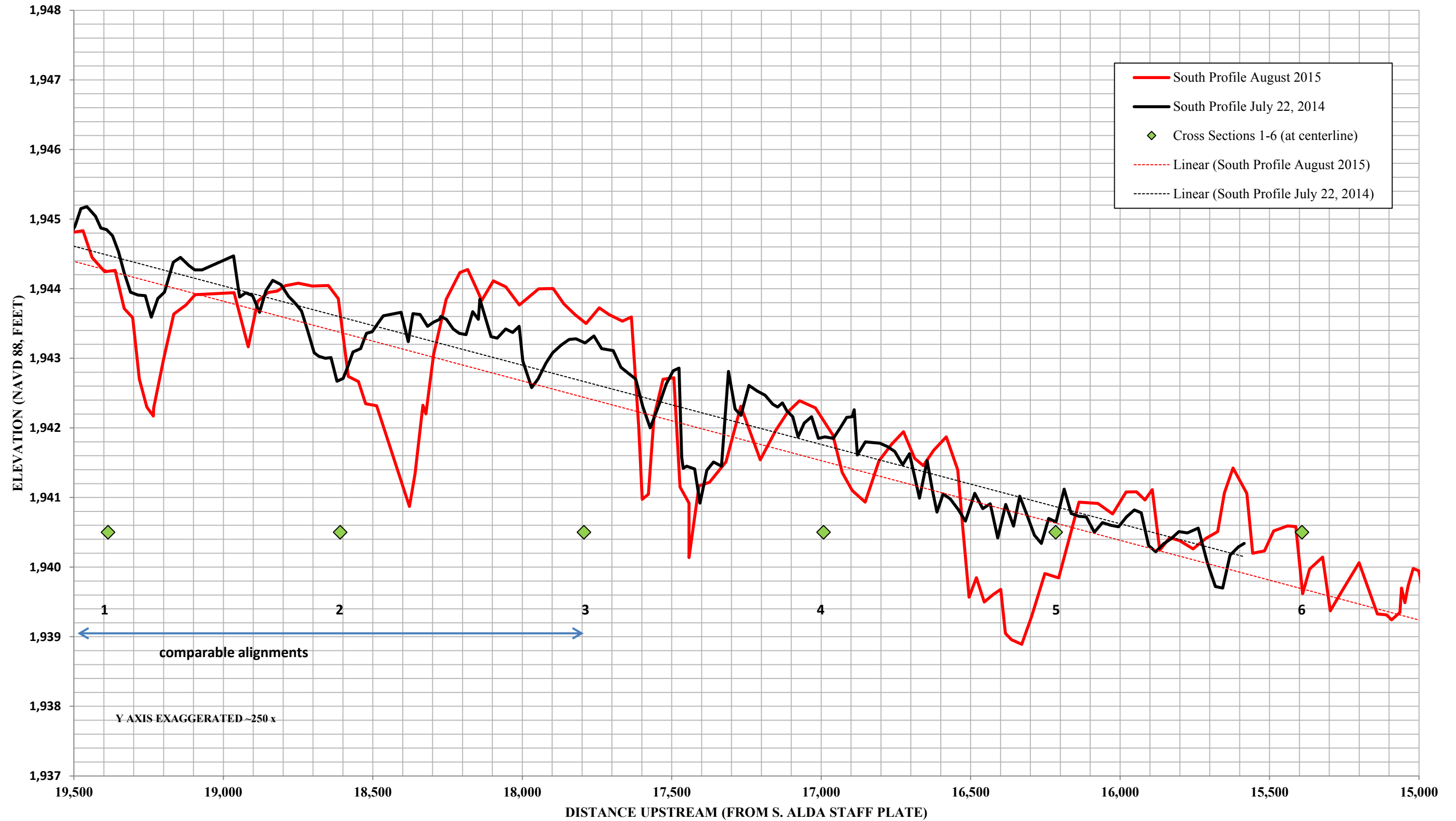




Figure A-48. Longitudinal Profile – Southern Route July 2014 and August 2015 – Cross Sections 7-12

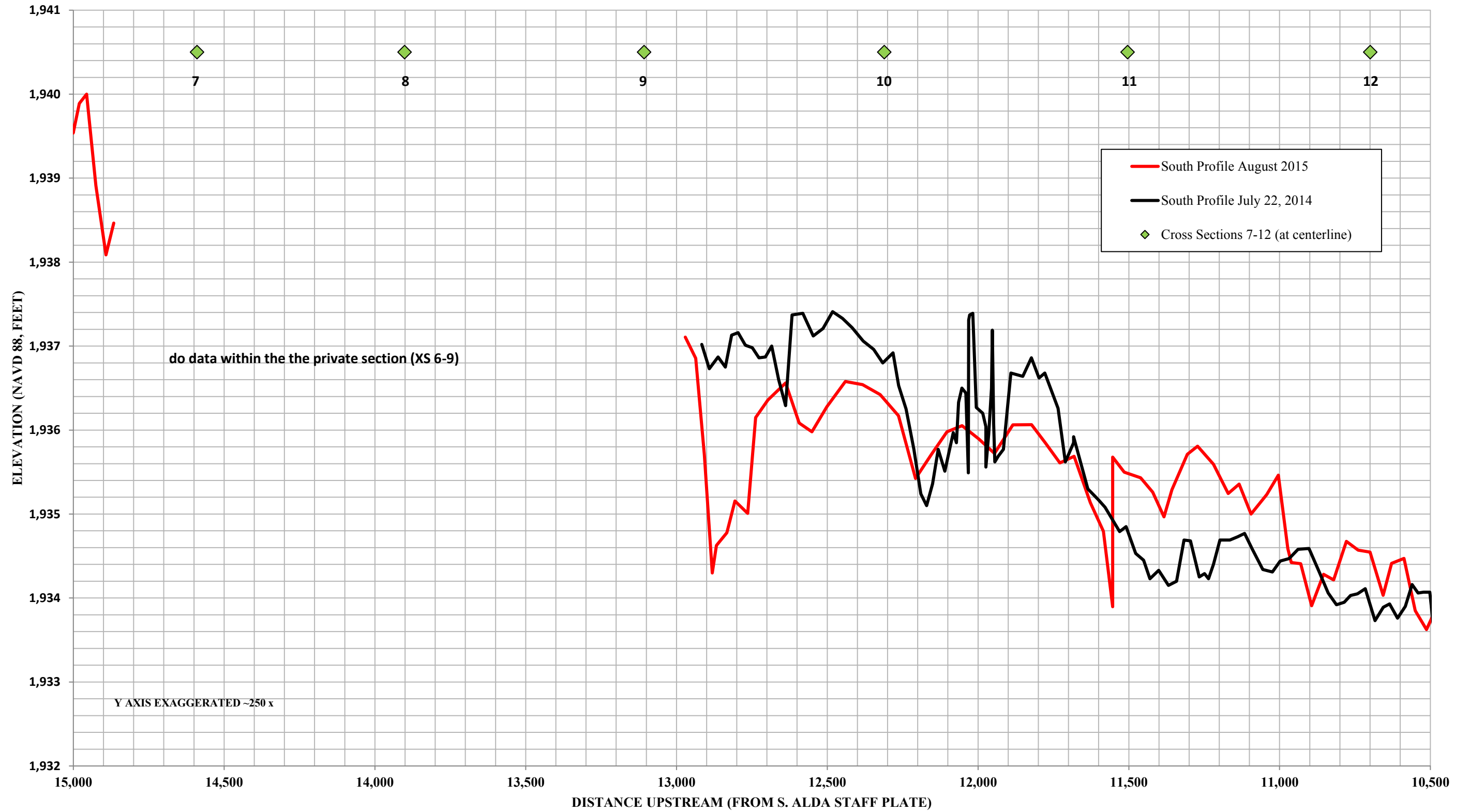




Figure A-49. Longitudinal Profile – Southern Route July 2014 and August 2015 – Cross Sections 13-18

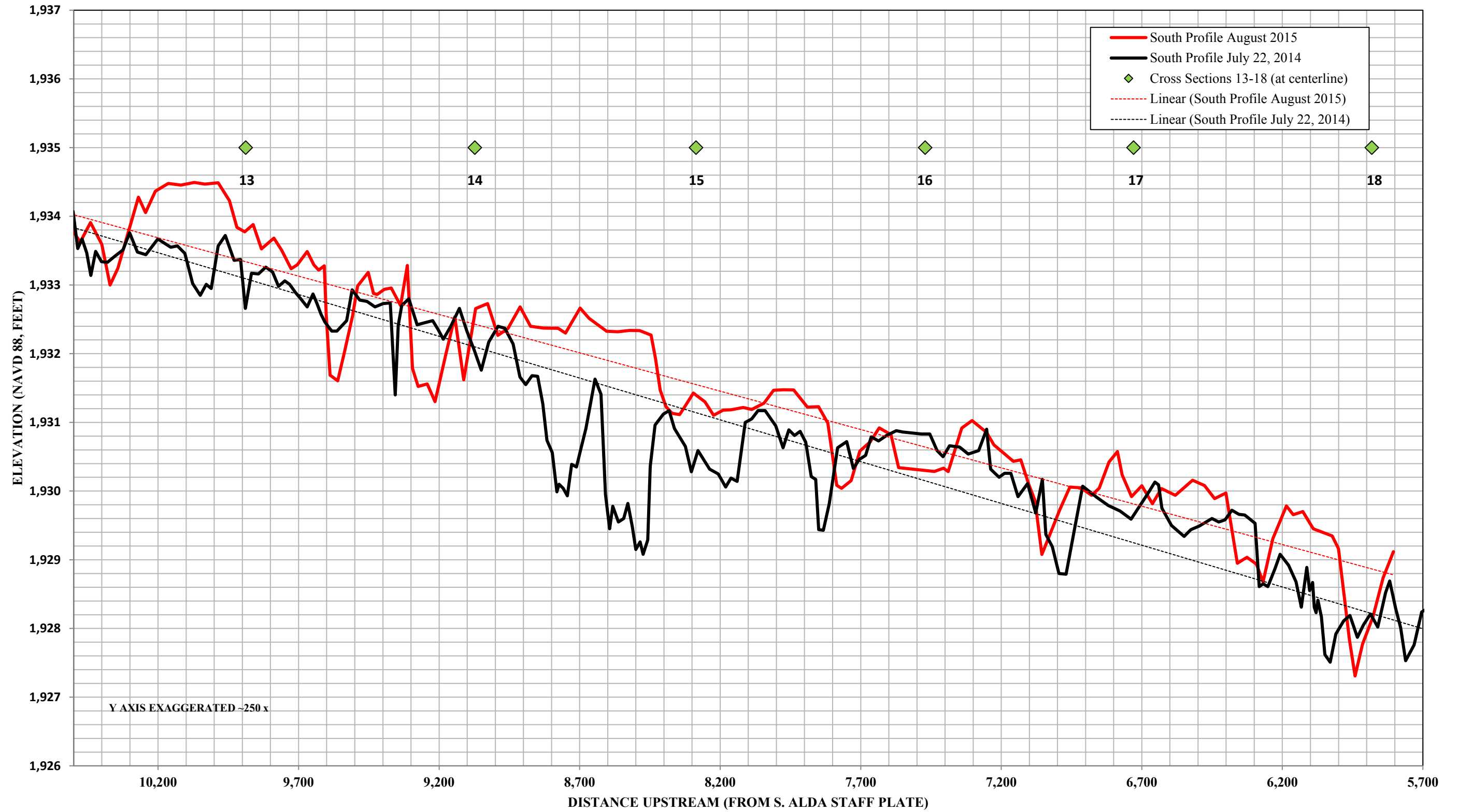




Figure A-50. 0.063mm to 0.25mm Suspended Sediment Transport Curve

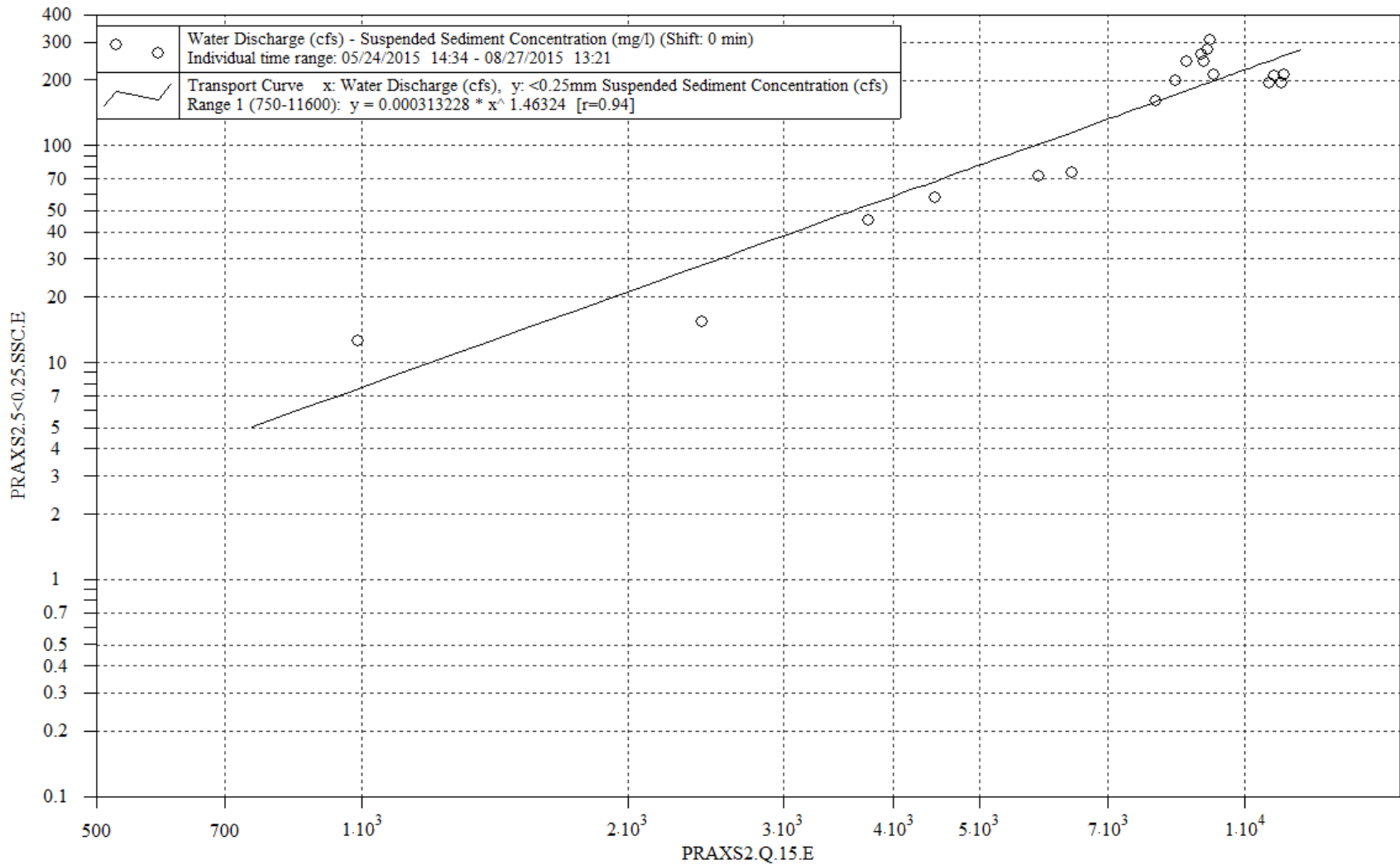




Figure A-51. 0.25mm – 0.5mm Suspended Sediment Transport Curve

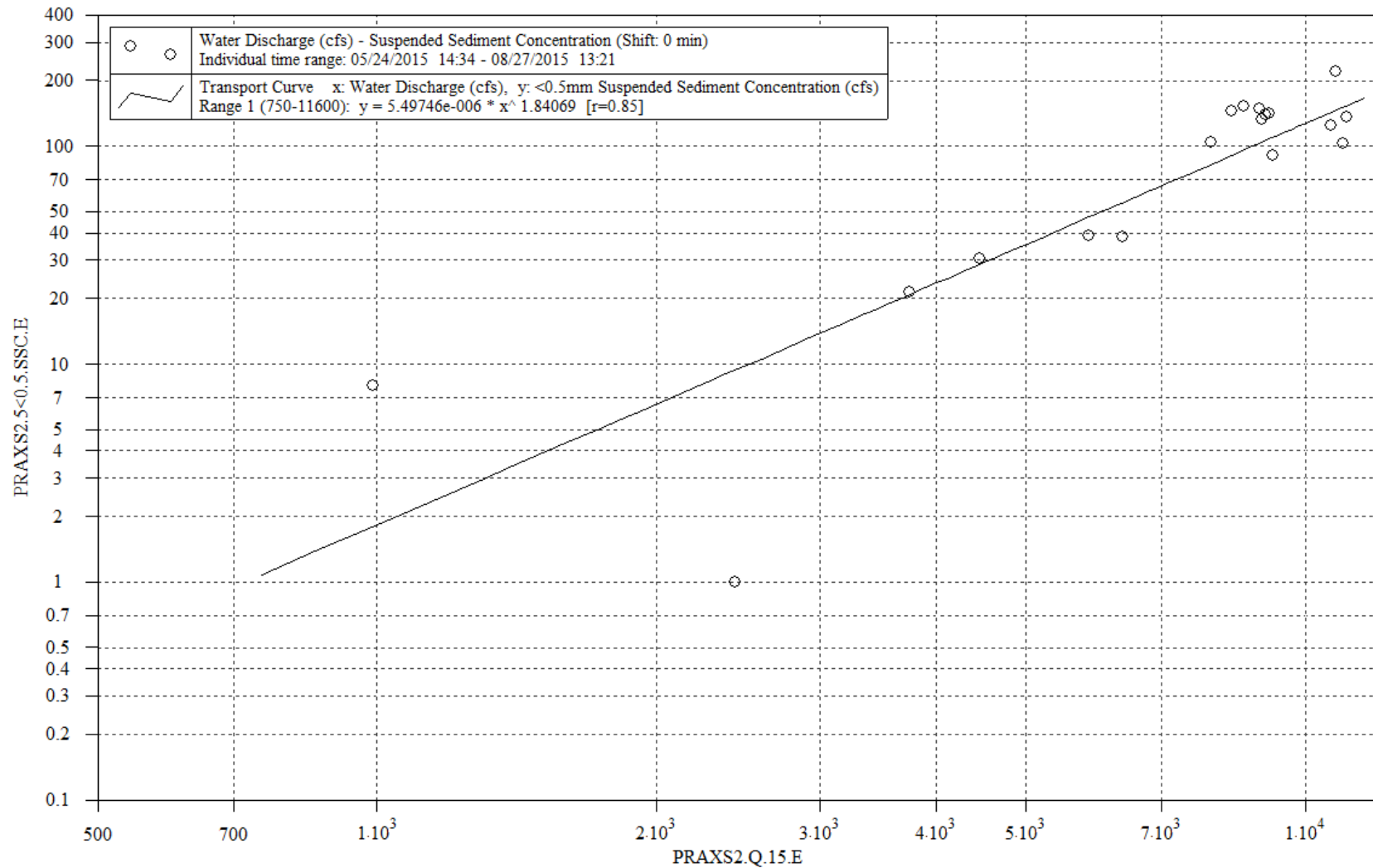




Figure A-52. 0.5mm – 1mm Suspended Sediment Transport Curve

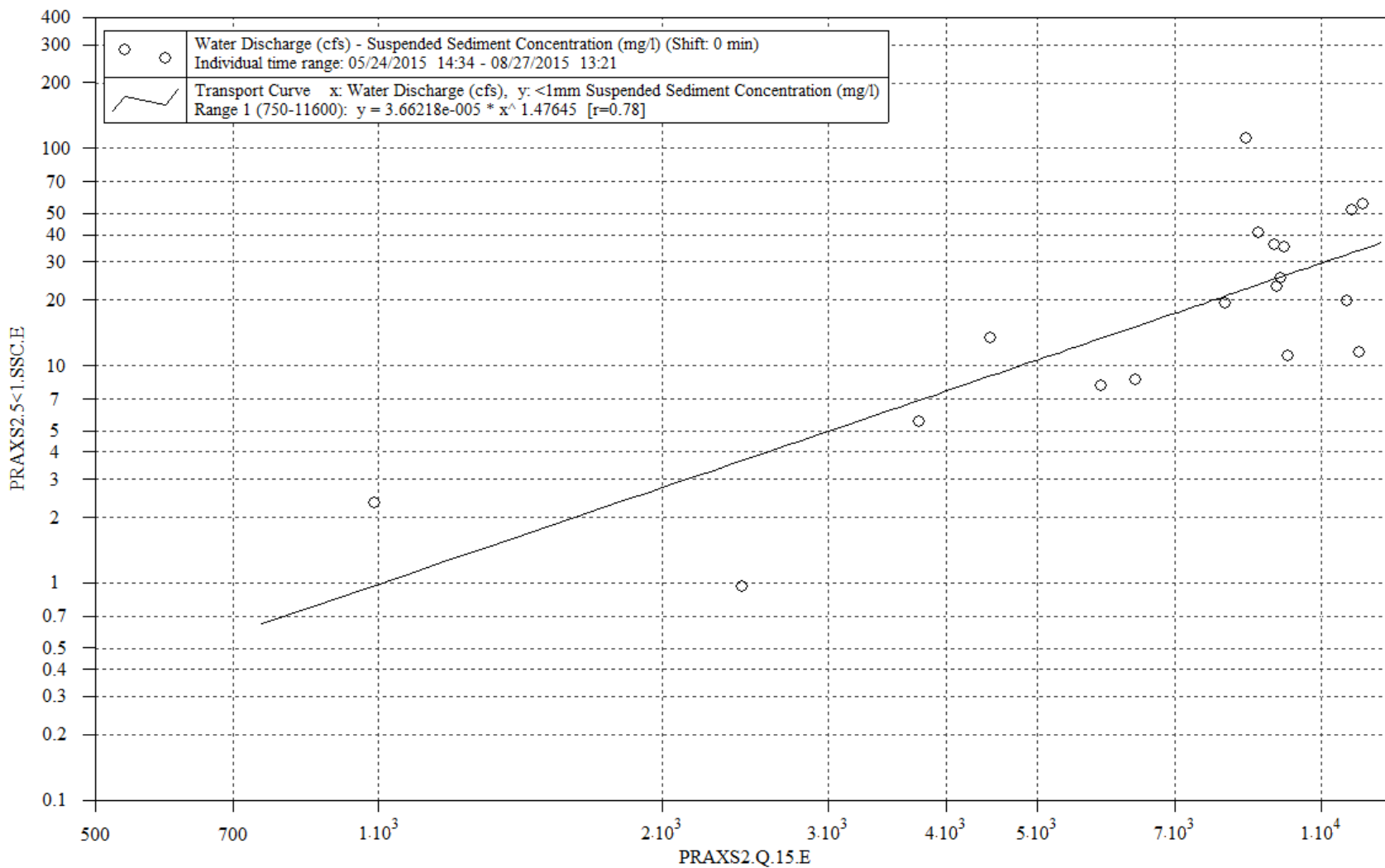
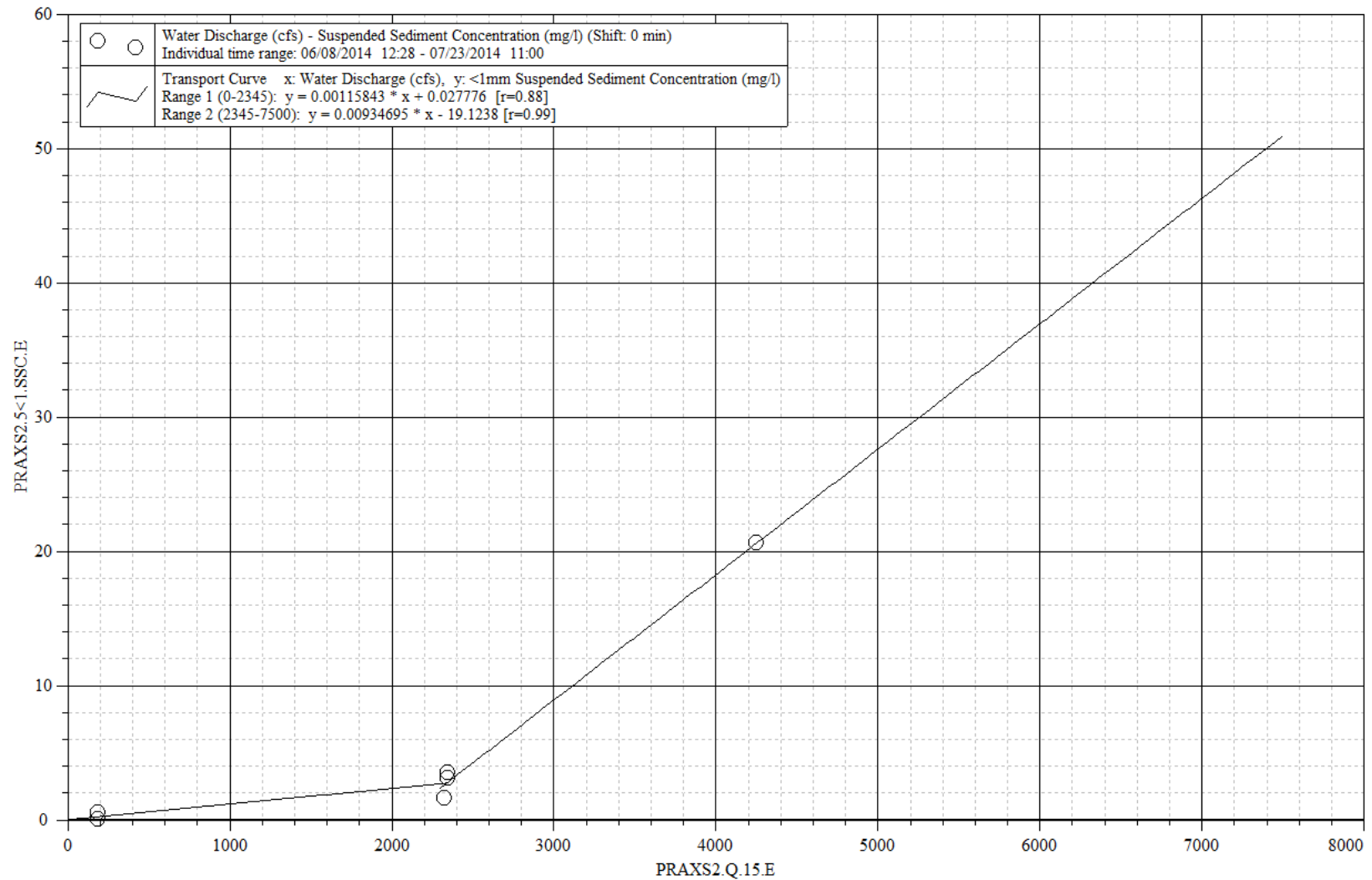




Figure A-53. 1mm – 2mm Suspended Sediment Transport Curve





APPENDIX B
PHOTOS



1. **Bar Topography** - Natural sand bar (108) with less than 20% vegetative cover post June 2015 high flow event.



2. **Bar Topography** - Treated sand bar (64) post June 2015 high flow event.



3. **Bar Topography** - Vegetated natural bar (11) with greater than 20% vegetative cover post June 2015 high flow event.



4. **Bar Topography** - Treated bar with new vegetation (120) with greater than 20% vegetative cover post June 2015 high flow event.



5. **Primary River Cross Sections** – View looking south along the cross section located on the north bank of the Platte River post June 2015 high flow event.



6. **Primary River Cross Sections** – View looking upstream from the cross section located on the north bank of the Platte River post June 2015 high flow event.



7. **Primary River Cross Sections** – View looking downstream from the cross section located on the north bank of the Platte River post June 2015 high flow event.



8. **Primary River Cross Sections** – View looking north along the cross section from the main channel of the Platte River post June 2015 high flow event.



9. **Depth Integrated Sampling** – DIS samples collected from a cataraft between cross sections 2 and 3.



10. **River Stage** – Collection of river stage measurements at the pressure transducer located near cross section 18 during the June 2015 high flow event.



11. **Vegetation Survey** – Collection of vegetation assessment data from a plot pre June 2015 high flow event.



12. **Bar Topography** – Natural bar surveyed prior to the June 2015 high flow event.



APPENDIX C
VEGETATION SURVEY



Table of Contents

Figures

Figure C-1. Comparison of July 2014 and August 2015 Total Percent Cover Across Cross Sections.....	3
Figure C-2. July 2014 and August 2015 % Vegetation Cover – First Half of the Data.....	4
Figure C-3. July 2014 and August 2015 % Vegetation Cover – Second Half of the Data.....	5
Figure C-4. July 2014 Live Frequency Counts	6
Figure C-5. August 2015 Live Frequency Counts	7
Figure C-6. July 2014 Dead Frequency Counts	8
Figure C-7. August 2015 Dead Frequency Counts	9

Tables

Table C-1. Vegetation Plot Results.....	11
Table C-2. Plant Identification Codes.....	15

Photos

Pre and Post Vegetation Plot Photos.....	C-18 to C-59
--	--------------



FIGURES



Figure C-1. Comparison of July 2014 and August 2015 Total Percent Cover Across Cross Sections

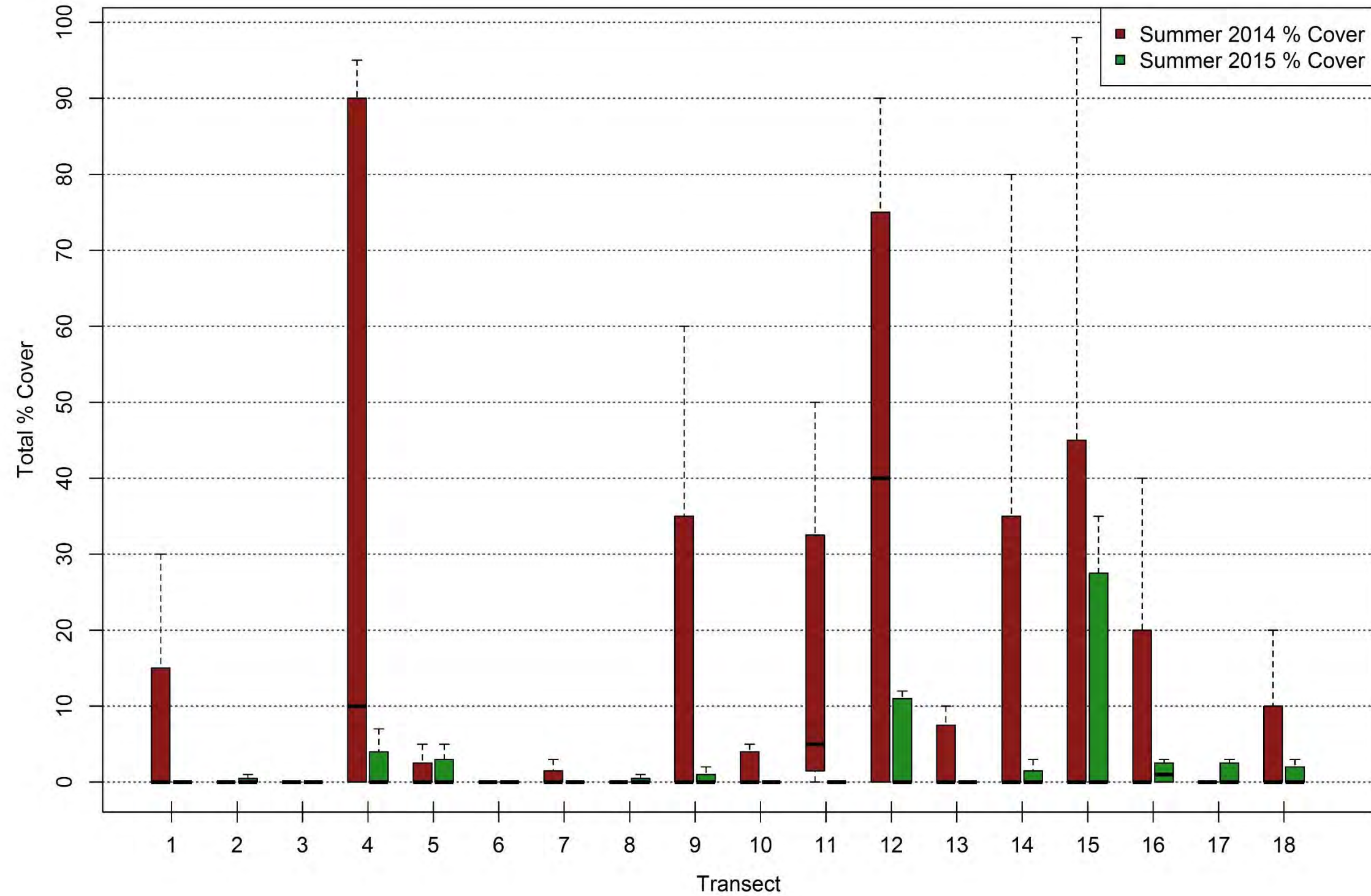




Figure C-2. July 2014 and August 2015 % Vegetation Cover – First Half of the Data

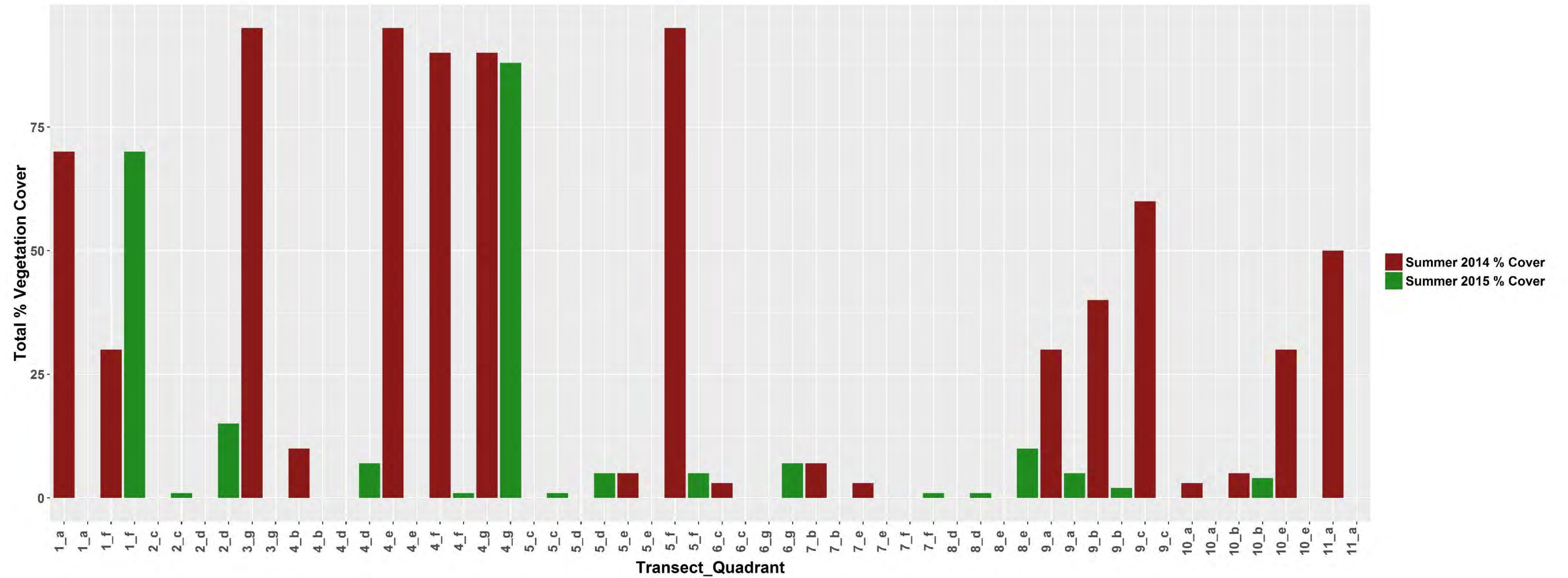




Figure C-3. July 2014 and August 2015 % Vegetation Cover – Second Half of the Data

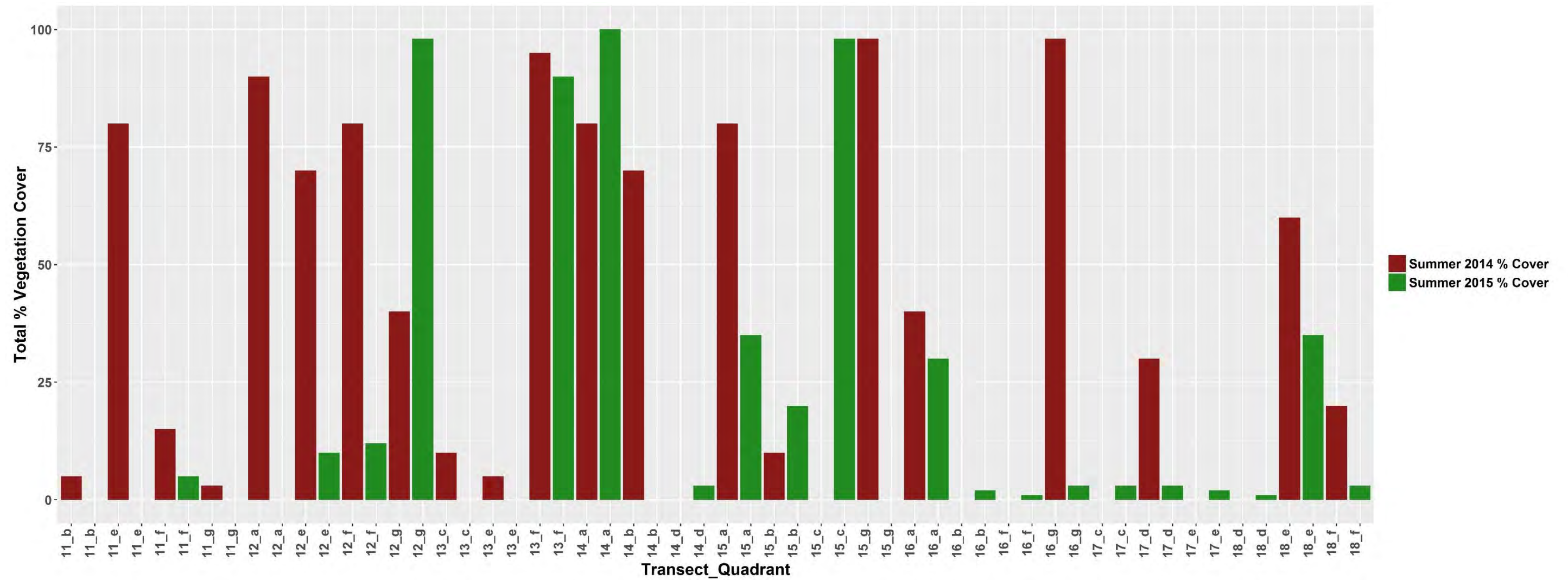




Figure C-4. July 2014 Live Frequency Counts

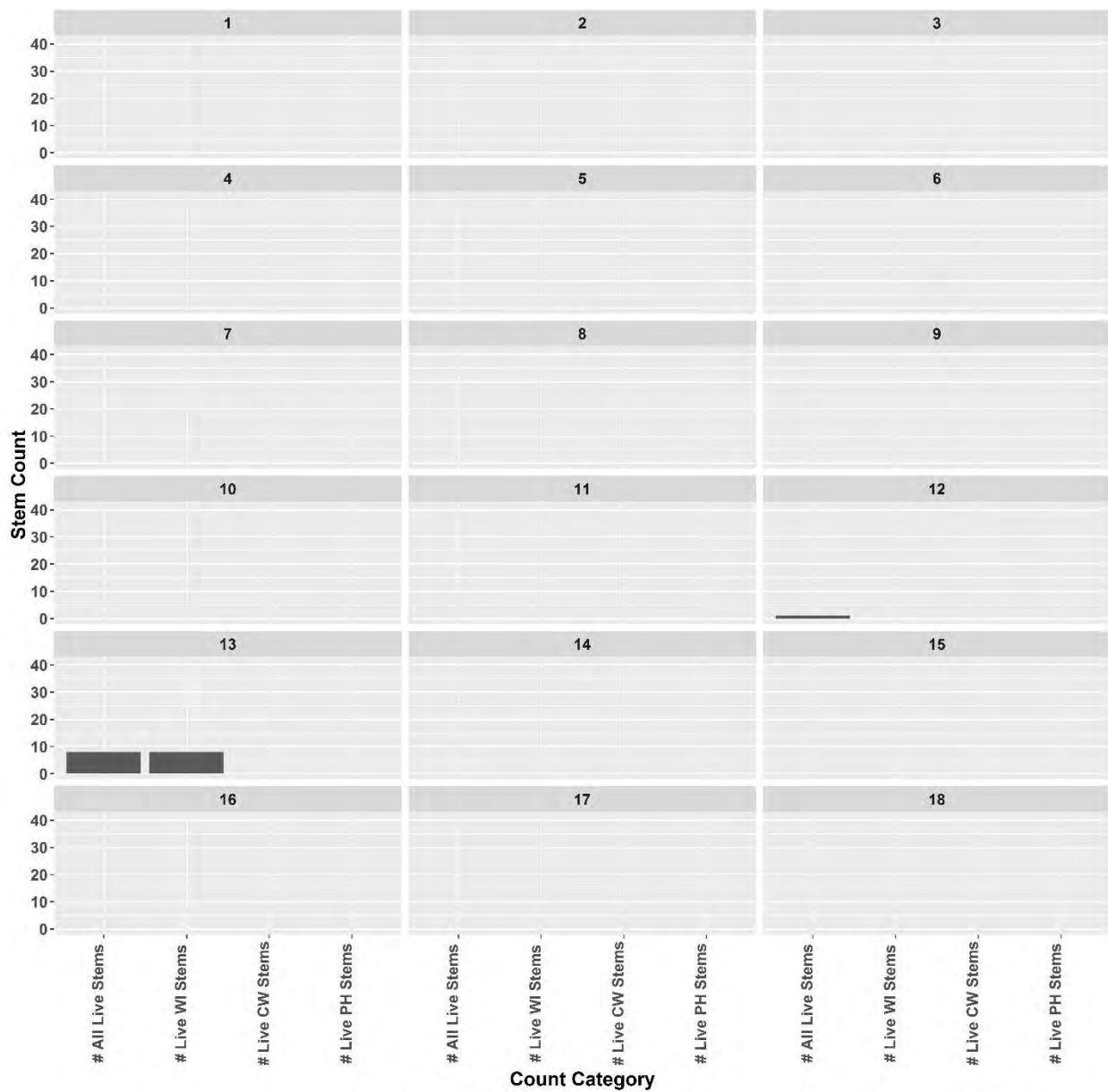




Figure C-5. August 2015 Live Frequency Counts

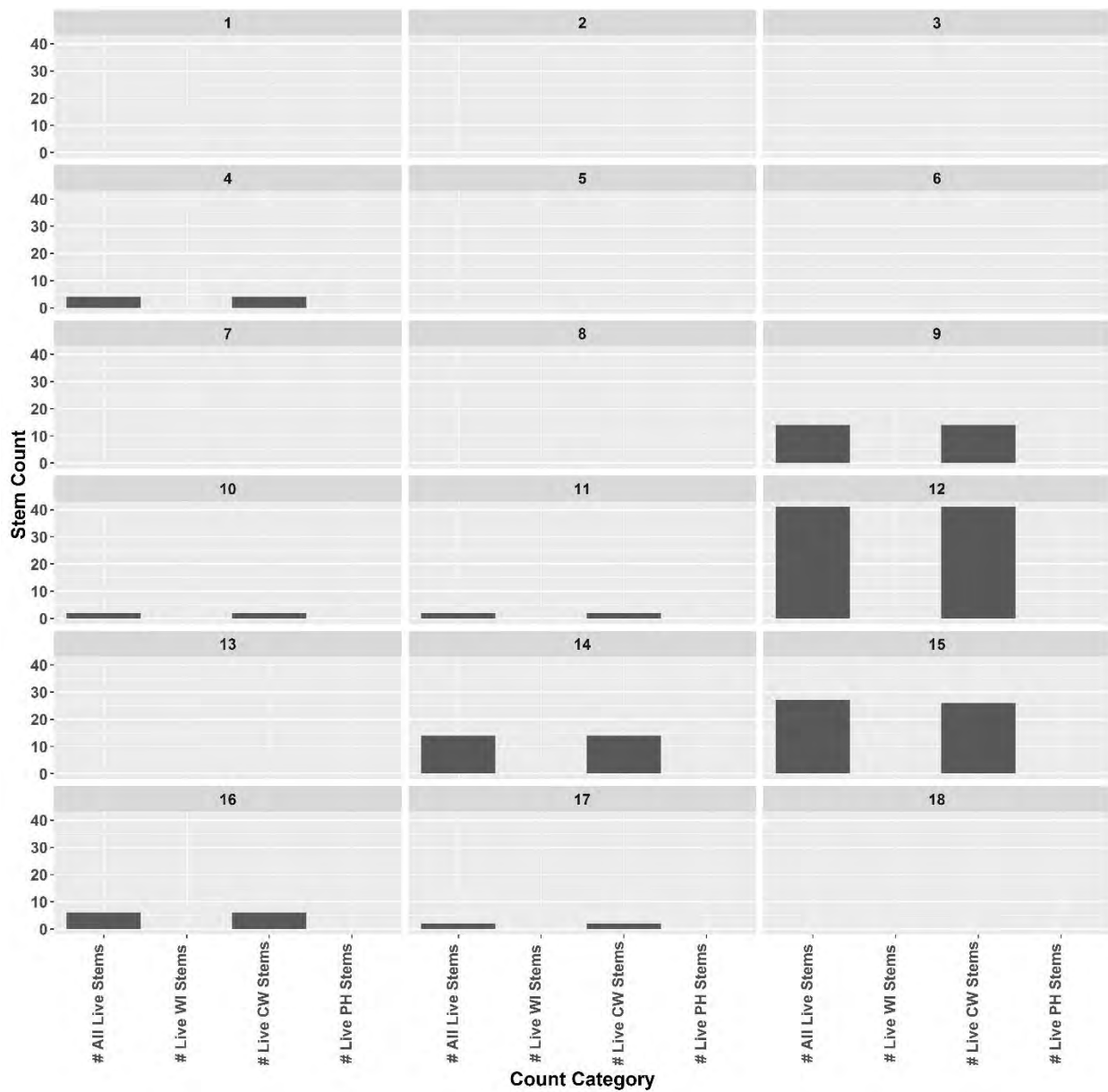




Figure C-6. July 2014 Dead Frequency Counts

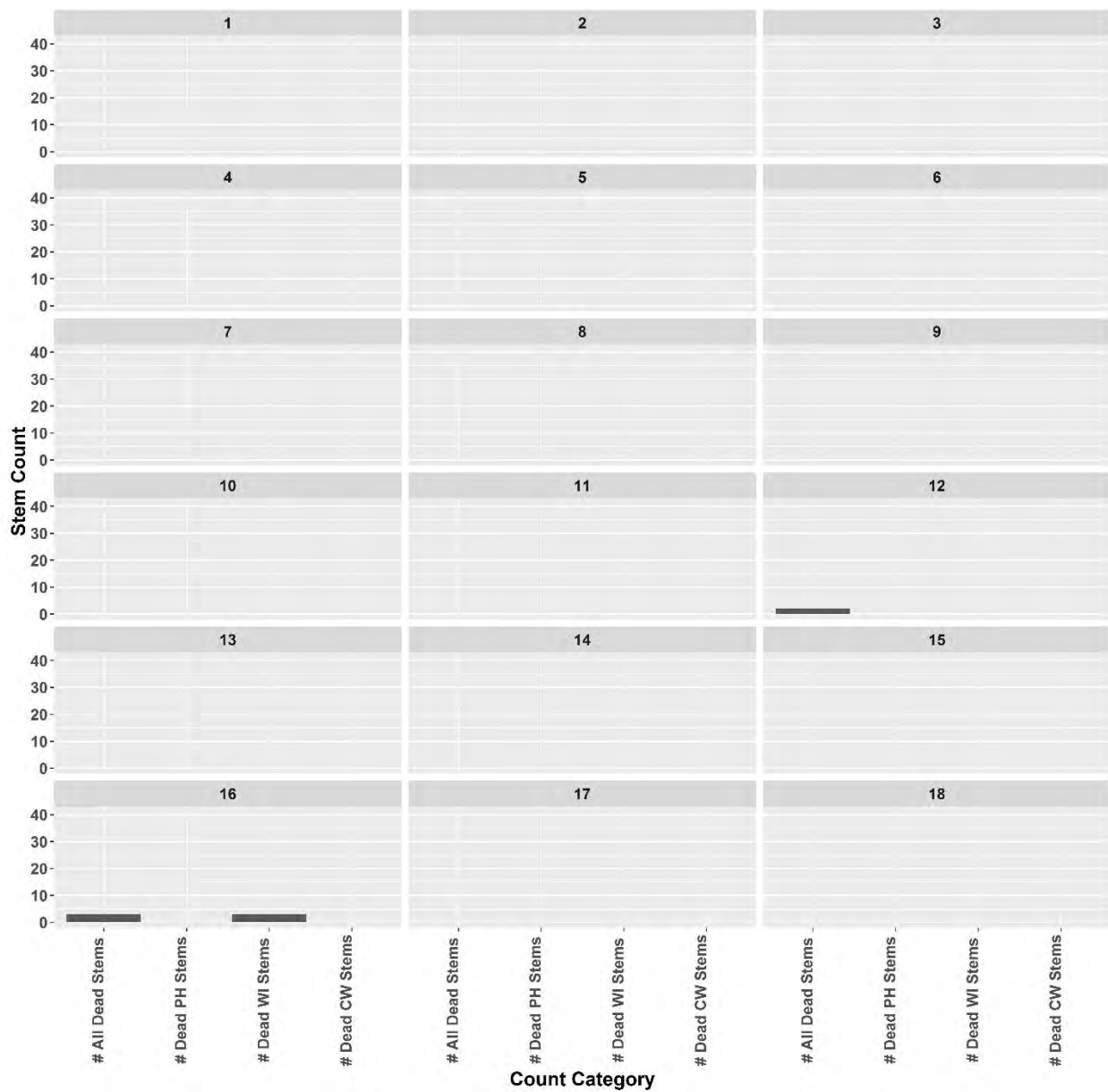
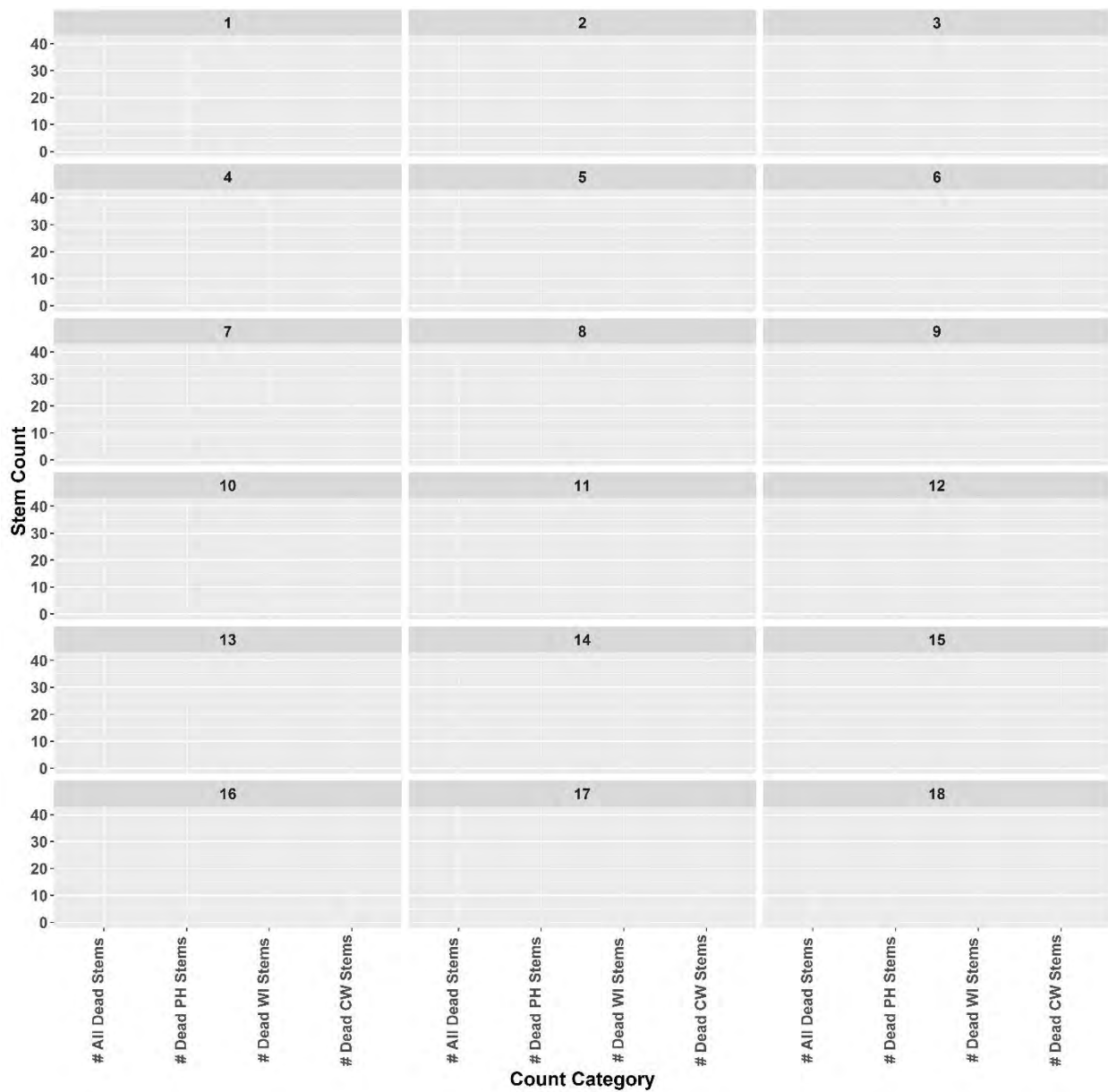




Figure C-7. August 2015 Dead Frequency Counts





TABLES



Table C-1. Vegetation Plot Results

Cross Section	Quadrant	Vegetated Cover		Stem Count July 2014 (PHAU, POPE, SAEX)		Stem Count August 2015 (PHAU, POPE, SAEX)		All Species	Sand/Water Cover	Sand/Water Cover
		July 2014	August 2015	Live Stems	Dead Stems	Live Stems	Dead Stems		July 2014	August 2015
1	a	70%	--	0	0	0	0	RUCR	Sand-30%	Water-100%
1	b	--	--	0	0	0	0	--	Water-100%	Water-100%
1	c	--	--	0	0	0	0	--	Sand-100%	Water-100%
1	d	--	--	0	0	0	0	--	Sand-100%	Water-100%
1	e	--	--	0	0	0	0	--	Water-100%	Water-100%
1	f	30%	70%	0	0	0	0	AMAR, BRJA, ERPE, HESU, LEDE, LEFU, SPCR, VEsp	Sand-70%	Sand-30%
1	g	--	--	0	0	0	0	--	Water-100%	Water-100%
2	a	--	--	0	0	0	0	--	Sand-100%	Water-100%
2	b	--	--	0	0	0	0	--	Sand-100%	Water-100%
2	c	--	1%	0	0	0	0	CYOD, UNK FORB	Sand-100%	Water-99%
2	d	--	25%	0	0	0	0	CYOD, ERPE	Sand-100%	Sand-75%
2	e	--	--	0	0	0	0	--	Sand-100%	Sand-100%
2	f	--	--	0	0	0	0	--	Water-100%	Sand-100%
2	g	--	--	0	0	0	0	--	Water-100%	Water-100%
3	a	--	--	0	0	0	0	--	Water-100%	Water-100%
3	b	--	--	0	0	0	0	--	Water-100%	Water-100%
3	c	--	--	0	0	0	0	--	Sand-90%/Water-10%	Water-100%
3	d	--	--	0	0	0	0	--	Sand-70%/Water-30%	Water-100%
3	e	--	--	0	0	0	0	--	Sand-100%	Water-100%
3	f	--	--	0	0	0	0	--	Sand-100%	Water-100%
3	g	95%	--	0	0	0	0	PHAR, UNK FORB	Sand-5%	Water-100%
4	a	--	--	0	0	0	0	--	Water-100%	Water-100%
4	b	10%	--	0	0	0	0	ECCR, LEFU, POPE, RUCR, XAST	Sand-90%	Water-100%
4	c	--	--	0	0	0	0	--	Sand-100%	Water-100%
4	d	--	7%	0	0	0	0	CYOD, ELPA, POPE, UNK FORB	Water-100%	Sand-93%
4	e	95%	--	0	0	0	0	AMAR, BICE, LEFU, LYSA, POPE, RUCR, UNK FORB	Sand-5%	Water-100%
4	f	90%	1%	0	0	0	0	AMAR, BICE, CYOD, LYSA, POPE, RUCR, XAST, UNK FORB	Sand-10%	Sand-99%
4	g	90%	88%	0	0	4	0	AMAR, AMTU, BICE, CYOD, ECCR, ERPE, POPE, POPE, RUCR, SCFL, THAR, XAST	Sand-10%	Sand-12%
5	a	--	--	0	0	0	0	--	Water-100%	Water-100%
5	b	--	--	0	0	0	0	--	Sand-100%	Water-100%
5	c	--	1%	0	0	0	0	ECCR	Sand-100%	Sand-99%
5	d	--	5%	0	0	0	0	AMAR, CYOD, ECCR, LEFU, VEsp, UNK FORB	Water-100%	Sand-95%
5	e	5%	--	0	0	0	0	ECCR, POPE, UNK FORB	Sand-95%	Water-100%
5	f	95%	5%	0	0	0	0	AMAR, AMTU, BICE, CYOD, ERPE, RUCR, THAR, XAST	Sand-5%	Sand-95%
5	g	--	--	0	0	0	0	--	Water-100%	Water-100%
6	a	--	--	0	0	0	0	--	Water-100%	Water-100%
6	b	--	--	0	0	0	0	--	Water-100%	Water-100%
6	c	3%	--	0	0	0	0	ECCR, LEFU, XAST	Sand-97%	Water-100%
6	d	--	--	0	0	0	0	--	Water-100%	Sand-10%/Water-



Cross Section	Quadrant	Vegetated Cover		Stem Count July 2014 (PHAU, PODE, SAEX)		Stem Count August 2015 (PHAU, PODE, SAEX)		All Species	Sand/Water Cover	Sand/Water Cover
		July 2014	August 2015	Live Stems	Dead Stems	Live Stems	Dead Stems		July 2014	August 2015
										90%
6	e	--	--	0	0	0	0	--	Sand-100%	Water-100%
6	f	--	--	0	0	0	0	--	Water-100%	Sand-20%/Water-80%
6	g	--	7%	0	0	0	0	CYOD, ECCR, LEFU	Water-100%	Water-93%
7	a	--	--	0	0	0	0	--	Water-100%	Water-100%
7	b	7%	--	0	0	0	0	LEFU	Sand-93%	Water-100%
7	c	--	--	0	0	0	0	--	Sand-100%	Sand-5%/Water-95%
7	d	--	--	0	0	0	0	--	Water-100%	Sand-100%
7	e	3%	--	0	0	0	0	ECCR, LEFU, UNK FORB	Sand-97%	Sand-2%/Water-98%
7	f	--	1%	0	0	0	0	CYOD, ECCR, LEFU	Sand-97%/Water-3%	Sand-99%
7	g	--	--	0	0	0	0	--	No Access	No Access
8	a	--	--	0	0	0	0	--	Sand-100%	Water-100%
8	b	--	--	0	0	0	0	--	Water-100%	Water-100%
8	c	--	--	0	0	0	0	--	Sand-25%/Water-75%	Water-100%
8	d	--	1%	0	0	0	0	CYOD, ECCR, LEFU	Sand-100%	Sand-99%
8	e	--	10%	0	0	0	0	CYOD, LEFU	Water-100%	Sand-90%
8	f	--	--	0	0	0	0	--	Sand-100%	Sand-10%/Water-90%
8	g	--	--	0	0	0	0	--	Water-100%	Water-100%
9	a	30%	5%	0	0	10	0	CYOD, ERPE, LEFU, PODE, XAST	Sand-70%	Sand-95%
9	b	40%	2%	0	0	4	0	AMAR, CYOD, ECCR, ERPE, LEFU, PODE	Sand-60%	Sand-98%
9	c	60%	--	0	0	0	0	ECCR, LEFU, XAST, UNK FORB/GRASS	Sand-40%	Water-100%
9	d	--	--	0	0	0	0	--	Sand-60%/Water-40%	Water-100%
9	e	--	--	0	0	0	0	--	Sand-100%	Water-100%
9	f	--	--	0	0	0	0	--	Water-100%	Water-100%
9	g	--	--	0	0	0	0	--	Water-100%	Water-100%
10	a	3%	--	0	0	0	0	PHAR	Sand-97%	Water-100%
10	b	5%	4%	0	0	2	0	CYOD, ECCR, ERPE, LEFU, PODE, RUCR, UNK FORB/GRASS	Sand-95%	Sand-96%
10	c	--	--	0	0	0	0	--	Sand-100%	Water-100%
10	d	--	--	0	0	0	0	--	Water-100%	Sand-50%/Water-50%
10	e	30%	--	0	0	0	0	ECCR, XAST, UNK FORB/GRASS	Sand-70%	Water-100%
10	f	--	--	0	0	0	0	--	Sand-100%	Water-100%
10	g	--	--	0	0	0	0	--	Water-100%	Water-100%
11	a	50%	--	0	0	0	0	AMAR, ECCR, LEFU	Sand-50%	Water-100%
11	b	5%	--	0	0	0	0	ECCR, POPE, XAST, UNK FORB/GRASS	Sand-95%	Sand-10%/Water-90%
11	c	--	--	0	0	0	0	--	Water-100%	Water-100%
11	d	--	--	0	0	0	0	--	Water-100%	Water-100%



Cross Section	Quadrant	Vegetated Cover		Stem Count July 2014 (PHAU, PODE, SAEX)		Stem Count August 2015 (PHAU, PODE, SAEX)		All Species	Sand/Water Cover	Sand/Water Cover
		July 2014	August 2015	Live Stems	Dead Stems	Live Stems	Dead Stems		July 2014	August 2015
11	e	80%	--	0	0	0	0	AMAR, BICE, RUCR	Sand-20%	Water-100%
11	f	15%	5%	0	0	2	0	AMAR, BICE, CYOD, ERPE, LEFU, PODE, RUCR, SCPU, XAST	Sand-85%	Sand-95%
11	g	3%	--	0	0	0	0	ELPA, SCFL	Sand-97%	Water-100%
12	a	90%	--	1	2	0	0	AMAR, CIAR, COCA, CODR, PHAR, SOCA	Sand-10%	Water-100%
12	b	--	--	0	0	0	0	--	Water-100%	Water-100%
12	c	--	--	0	0	0	0	--	Sand-100%	Water-100%
12	d	--	--	0	0	0	0	--	Water-100%	Water-100%
12	e	70%	10%	0	0	34	0	AMRU, BICE, CYOD, ELPA, ERPE, MUVE, PHAR, PODE, RUCR, UNK FORB/GRASS	Sand-30%	Sand-90%
12	f	80%	12%	0	0	1	0	BICE, CYOD, ELPA, ERPE, LEFU, PODE, RUCR, SCPU, XAST, UNK FORB/GRASS	Sand-20%	Sand-88%
12	g	40%	98%	0	0	6	0	AMAR, AMTU, BICE, CYOD, ECCR, ELPA, ERPE, POPE, PODE, RUCR, SCFL, XAST, UNK FORB/GRASS	Sand-60%	Sand-2%
13	a	--	--	0	0	0	0	--	Water -100%	Water-100%
13	b	--	--	0	0	0	0	--	Water-100%	Water-100%
13	c	10%	--	0	0	0	0	ECCR, LEFU, POPE	Sand-90%	Water-100%
13	d	--	--	0	0	0	0	--	Water- 100%	Water-100%
13	e	5%	--	0	0	0	0	SCPU, XAST	Sand-95%	Water-100%
13	f	95%	90%	8	0	0	0	AMAR, BICE, LYSA, SAEX, SCFL	Sand-5%	Sand-10%
13	g	--	--	0	0	0	0	--	Sand-100%	Water-100%
14	a	80%	100%	0	0	13	0	AMAR, AMTR, AMRU, BICE, BRJA, CYOD, ECCR, ERPE, LEFU, PODE, POMO, RUCR, SCFL, XAST	Sand- 20%	None
14	b	70%	--	0	0	0	0	AMRU, BICE, ECCR, JUBU, RUCR	Sand-30%	Water-100%
14	c	--	--	0	0	0	0	--	Sand-100%	Water-100%
14	d	--	3%	0	0	1	0	CYOD, ECCR, ERPE, PODE	Sand-100%	Sand-97%
14	e	--	--	0	0	0	0	--	Water-100%	Water-100%
14	f	--	--	0	0	0	0	--	Sand-80%/Water-20%	Water-100%
14	g	--	--	0	0	0	0	--	Sand-100%	Water-100%
15	a	80%	35%	0	0	0	0	BICE, ECCR, LEFU, POPE, RUCR, SCFL, SCPU, UNK FORB/GRASS	Sand-20%	Sand-65%
15	b	10%	20%	0	0	25	0	AMAR, CYOD, ECCR, ERPE, HEPE, LEFU, PODE, SCPU, RUCR, UNK FORB	Sand- 90%	Sand-80%
15	c	--	98%	0	0	2	0	AMFR, CYOD, ERPE, LEFU, PODE	Sand-100%	Sand-2%
15	d	--	--	0	0	0	0	--	Sand-100%	Water-100%
15	e	--	--	0	0	0	0	--	Water- 100%	Water-100%
15	f	--	--	0	0	0	0	--	Water-100%	Water-100%
15	g	98%	--	0	0	0	0	AMAR	Sand-2%	Water-100%
16	a	40%	30%	0	0	6	0	BICE, ECCR, ELPA, JUBU, LEFU, POMO, RUCR, SCFL, SCPU, SCTA	Sand-60%	Sand-70%
16	b	--	2%	0	0	0	0	CYOD, LEFU	Sand-100%	Sand-98%
16	c	--	--	0	0	0	0	--	Sand-100%	Water-100%
16	d	--	--	0	0	0	0	--	Water -100%	Water-100%
16	e	--	--	0	0	0	0	--	Water- 100%	Water-100%
16	f	--	1%	0	0	0	0	CYOD, ERPE, LEFU	Water- 100%	Sand-99%



Cross Section	Quadrant	Vegetated Cover		Stem Count July 2014 (PHAU, PODE, SAEX)		Stem Count August 2015 (PHAU, PODE, SAEX)		All Species	Sand/Water Cover	Sand/Water Cover
		July 2014	August 2015	Live Stems	Dead Stems	Live Stems	Dead Stems		July 2014	August 2015
16	g	98%	3%	0	3	0	0	AMAR, BICE, COCA, CYOD, ECCR, ERPE, LYSA, MESA, POPE, SAEX, THAR, XAST	Sand-2%	Sand-97%
17	a	--	--	0	0	0	0	--	Sand-100%	Water-100%
17	b	--	--	0	0	0	0	--	Sand-100%	Water-100%
17	c	--	3%	0	0	2	0	CYOD, ERPE, LEFU, PODE, UNK FORB	Water -100%	Sand-97%
17	d	30%	3%	0	0	0	0	CYOD, ECCR, ERPE, LYSA, RUCR, UNK FORB/GRASS	Sand-70%	Sand-97%
17	e	--	2%	0	0	0	0	CYOD, LEFU	Sand-100%	Sand-98%
17	f	--	--	0	0	0	0	--	Sand-100%	Sand-100%
17	g	--	--	0	0	0	0	--	Sand-10%/Water-90%	Water-100%
18	a	--	--	0	0	0	0	--	Sand-100%	Water-100%
18	b	--	--	0	0	0	0	--	Sand-100%	Water-100%
18	c	--	--	0	0	0	0	--	Sand-100%	Sand-10%/Water-90%
18	d	--	1%	0	0	0	0	ERPE, LEFU	Water -100%	Sand-99%
18	e	60%	35%	0	0	0	0	AMAR, ERPE, LEFU, MESA, PACA, POMO, RUCR, XAST	Sand- 40%	Sand-65%
18	f	20%	3%	0	0	0	0	AMAR, AMRU, CYOD, ECCR, ERPE, JUBU, LEFU, MESA, UNK FORB/GRASS	Sand-80%	Sand-97%
18	g	--	--	0	0	0	0	--	Sand-100%	Water- 100%



Table C-2. Plant Identification Codes

Abbreviation	Scientific	Common
ACNE	<i>Acer negundo</i>	box elder
AMAR	<i>Ambrosia artemisiifolia</i>	common ragweed
AMFR	<i>Amorpha fruticosa</i>	false indigo
AMPS	<i>Ambrosia psilostachya</i>	western ragweed
AMTU	<i>Amaranthus tuberculatus</i>	common waterhemp
AMTR	<i>Ambrosia trifida</i>	giant ragweed
APCA	<i>Apocynum cannabinum</i>	Indianhemp
ASSY	<i>Asclepias syriaca</i>	common milkweed
BICE	<i>Bidens cernua</i>	bur marigold
BRIN	<i>Bromus inermis</i>	smooth brome
BRJA	<i>Bromus japonicus</i>	japanese brome
CASA	<i>Cannabis sativa</i>	Marijuana
CASP	<i>Catalpa speciosa</i>	northern catalpa
CELO	<i>Cenchrus longispirus</i>	field sandbur
CIAR	<i>Cirsium arvense</i>	canada thistle
CIVU	<i>Cirsium vulgare</i>	bull thistle
COCA	<i>Conyza canadensis</i>	horseweed
CODR	<i>Cornus drummondii</i>	rough-leaved dogwood
CYOD	<i>Cyperus odoratus</i>	fragrant sedge
CYsp	<i>Cyperus sp.</i>	sedge
ECCR	<i>Echinochloa crus-galli</i>	barnyard grass
ELPA	<i>Eleocharis palustris</i>	common spikerush
ERPE	<i>Eragrostis pectinacea</i>	Carolina lovegrass
FRPE	<i>Fraxinus pennsylvanica</i>	green ash
GAAP	<i>Galium aparine</i>	sticky willy
HEAN	<i>Helianthus annuus</i>	common sunflower
HEGR	<i>Helianthus grosseserratus</i>	sawtooth sunflower
HEPE	<i>Helianthus petiolaris</i>	prairie sunflower
HESU	<i>Heterotheca subaxillaris</i>	camphor weed
HILA	<i>Hibiscus laevis</i>	marsh mallow
JUBU	<i>Juncus bufonius</i>	toad rush
JUTO	<i>Juncus torreyi</i>	Torrey's rush
KOSC	<i>Kochia scoparia</i>	kochia
LEDE	<i>Lepidium densiflorum</i>	common pepperweed
LEFU	<i>Leptochloa fusca</i>	malabar sprangletop
LYSA	<i>Lythrum salicaria</i>	purple loosestrife
MESA	<i>Medicago sativa</i>	alfalfa
MOAL	<i>Morus alba</i>	white mulberry
MUVE	<i>Mulugo verticillata</i>	carpetweed
PACA	<i>Panicum capillare</i>	witchgrass
PHAR	<i>Phalaris arundinacea</i>	reed canary grass
PHAU	<i>Phragmites australis</i>	common reed
PODE	<i>Populus deltoides</i>	eastern cottonwood
POLA	<i>Polypogon lapathifolium</i>	pale smartweed
POMO	<i>Polypogon monspeliensis</i>	rabbit's foot grass
POPE	<i>Polygonum persicaria</i>	lady's thumb
POsp	<i>Polygonum sp.</i>	smartweed
RUCR	<i>Rumex crispus</i>	curly dock



Abbreviation	Scientific	Common
RUST	<i>Rumex stenophyllus</i>	narrowleaf dock
SAAM	<i>Salix amygdalodes</i>	peachleaf willow
SAEX	<i>Salix exigua</i>	sandbar willow
SALA	<i>Sagittaria latifolia</i>	arrowhead
SCFL	<i>Schoenoplectus fluviatilis</i>	river bulrush
SPCR	<i>Sporobolus cyptandrus</i>	sand dropseed
SCPU	<i>Schoenoplectus pungens</i>	threesquare bulrush
SCTA	<i>Schoenoplectus tabernaemontani</i>	softstem bulrush
SEsp	<i>Setaria sp.</i>	foxtail/bristlegrass
SOCA	<i>Solidago canadensis</i>	Canada goldenrod
SPPE	<i>Spartina pectinata</i>	prairie cordgrass
SYLA	<i>Symphotrichum lanceolatum</i>	panicked aster
THAR	<i>Thlaspi arvense</i>	field pennycress
TORA	<i>Toxicodendron radicans</i>	poison ivy
TYAN	<i>Typha angustifolia</i>	narrowleaf cattail
TYLA	<i>Typha latifolia</i>	broadleaf cattail
ULAM	<i>Ulmus americana</i>	American elm
unk forb	NA	unkown forb
unk grass	NA	unkown grass
VEsp	<i>Veronica sp.</i>	Speedwell
VEHA	<i>Verbena hastata</i>	blue vervain
VETH	<i>Verbascum thapsus</i>	common mullein
VIRI	<i>Vitis riparia</i>	river bank grape
XAST	<i>Xanthium strumarium</i>	cocklebur



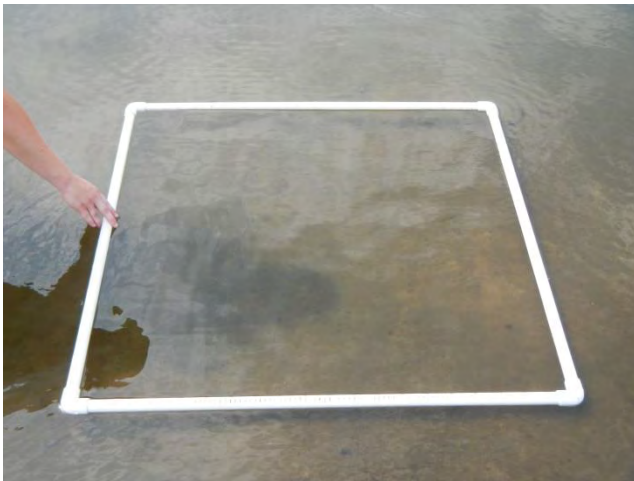
PHOTOS



1 - Plot 1A – July 2014.



2 - Plot 1A – August 2015.



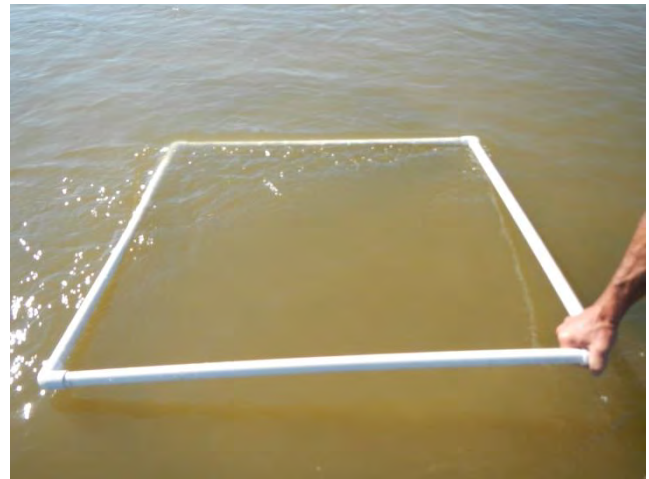
3 - Plot 1B – July 2014.



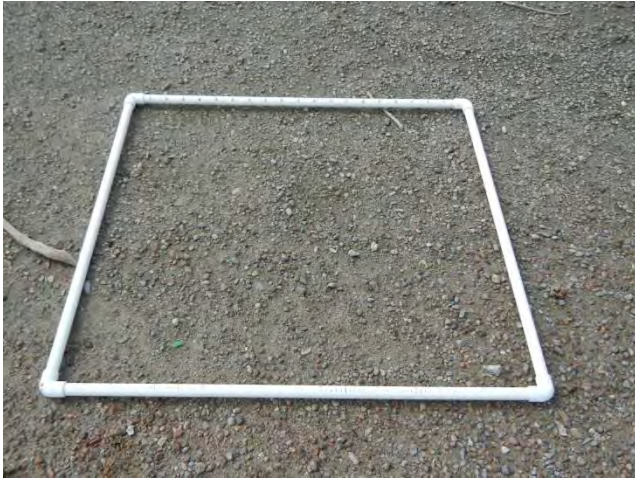
4 - Plot 1B – August 2015.



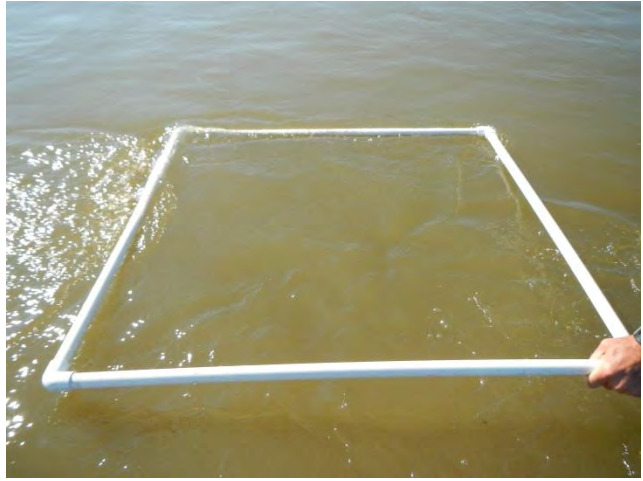
5 - Plot 1C – July 2014.



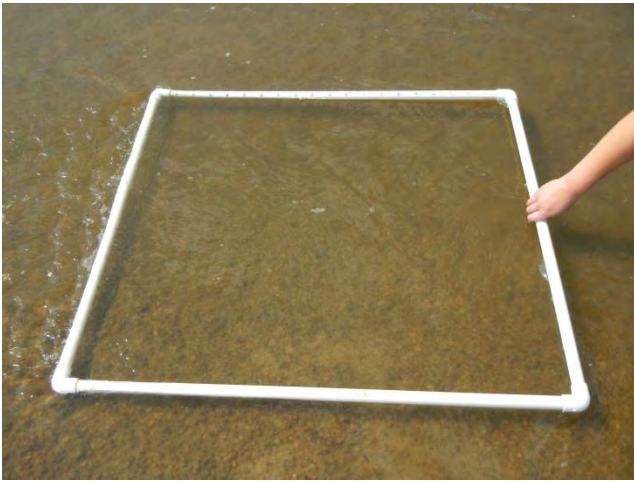
6 - Plot 1C – August 2015.



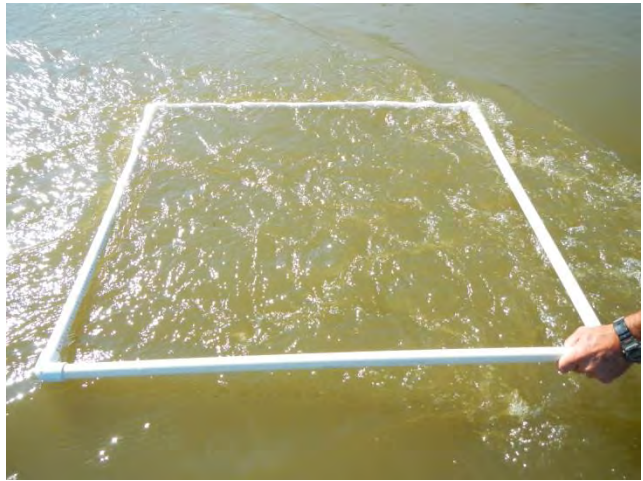
7 - Plot 1D – July 2014.



8 - Plot 1D – August 2015.



9 - Plot 1E – July 2014.



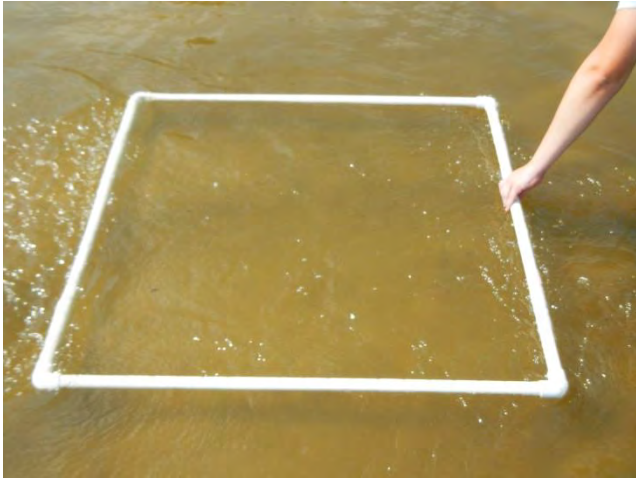
10 - Plot 1E – August 2015.



11 - Plot 1F – July 2014.



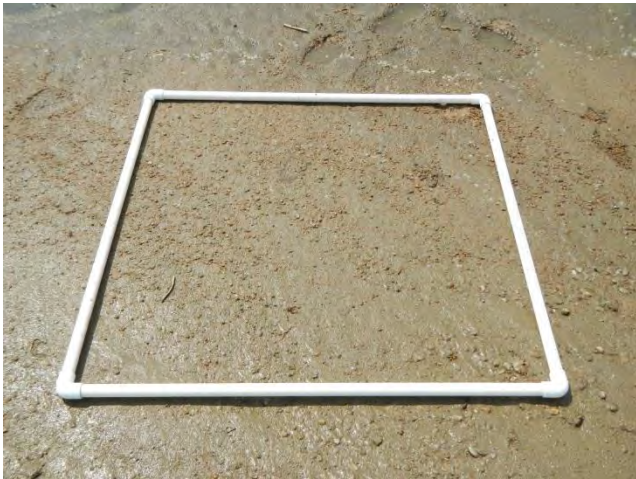
12 - Plot 1F – August 2015.



13 - Plot 1G – July 2014.



14 - Plot 1G – August 2015.



15 - Plot 2A – July 2014.



16 - Plot 2A – August 2015.



17 - Plot 2B – July 2014.



18 - Plot 2B – August 2015.



19 - Plot 2C – July 2014.



20 - Plot 2C – August 2015.



21 - Plot 2D – July 2014.



22 - Plot 2D – August 2015.



23 - Plot 2E – July 2014.



24 - Plot 2E – August 2015.



25 - Plot 2F – July 2014.



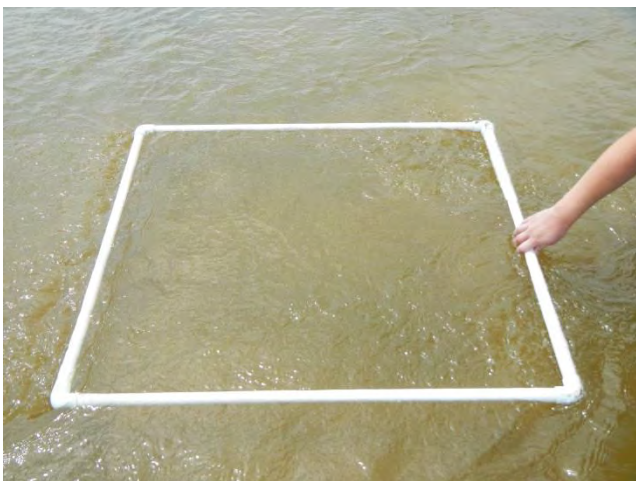
26 - Plot 2F – August 2015.



27 - Plot 2G – July 2014.



28 - Plot 2G – August 2015.



29 - Plot 3A – July 2014.



30 - Plot 3A – August 2015.



31 - Plot 3B – July 2014.



32 - Plot 3B – August 2015.



33 - Plot 3C – July 2014.



34 - Plot 3C – August 2015.



35 - Plot 3D – July 2014.



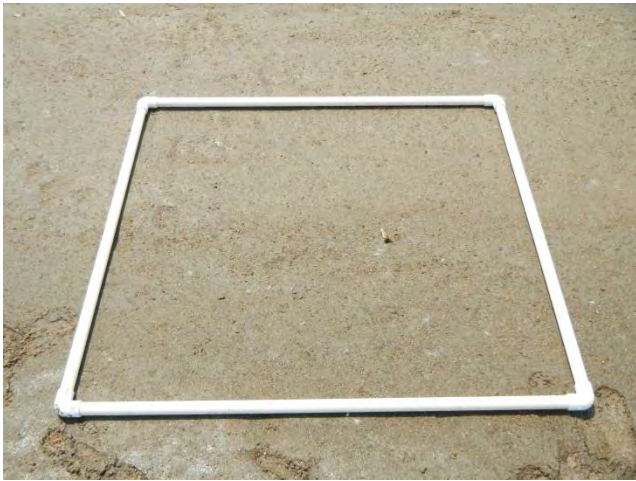
36 - Plot 3D – August 2015.



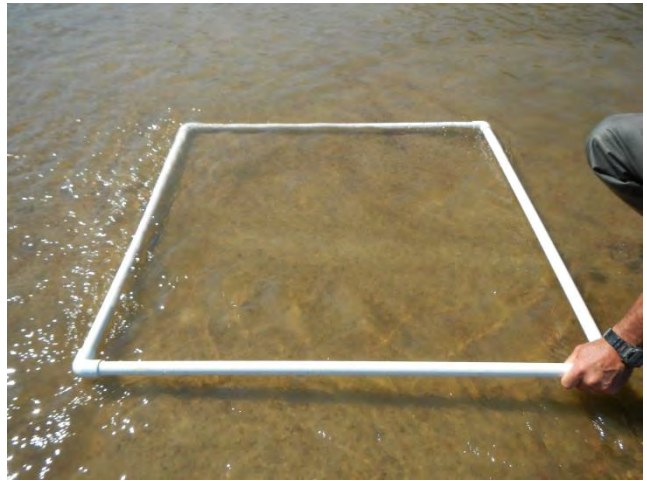
37 - Plot 3E – July 2014.



38 - Plot 3E – August 2015.



39 - Plot 3F – July 2014.



40 - Plot 3F – August 2015.



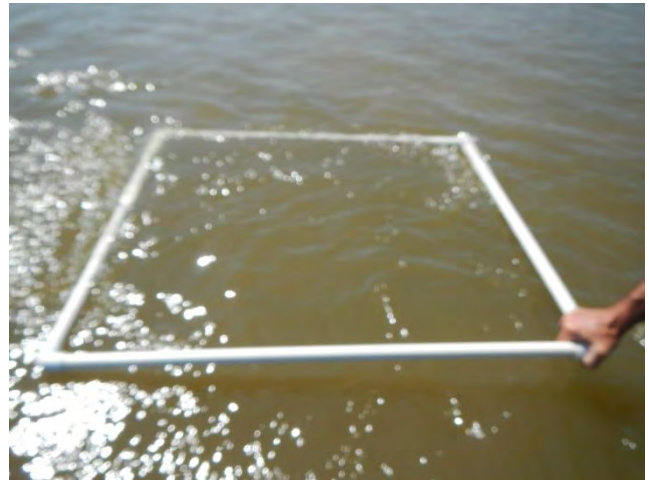
41 - Plot 3G – July 2014.



42 - Plot 3G – August 2015.



43 - Plot 4A – July 2014.



44 - Plot 4A – August 2015.



45 - Plot 4B – July 2014.



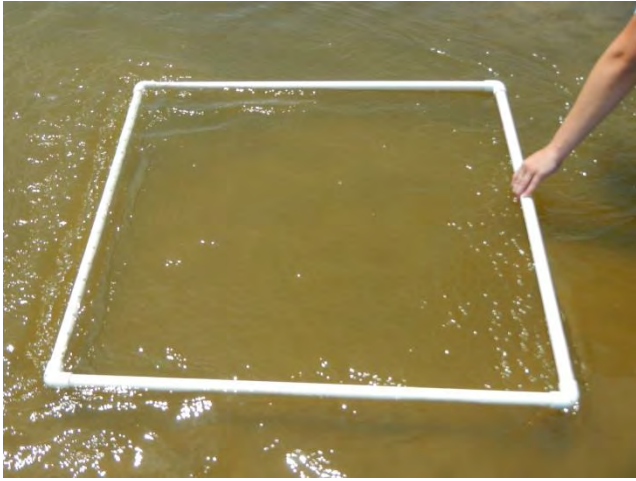
46 - Plot 4B – August 2015.



47 - Plot 4C – July 2014.



48 - Plot 4C – August 2015.



49 - Plot 4D – July 2014.



50 - Plot 4D – August 2015.



51 - Plot 4E – July 2014.



52 - Plot 4E – August 2015.



53 - Plot 4F – July 2014.



54 - Plot 4F – August 2015.



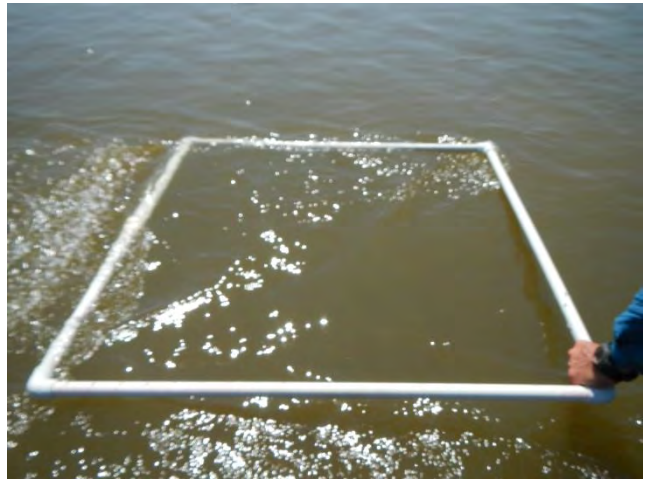
55 - Plot 4G – July 2014.



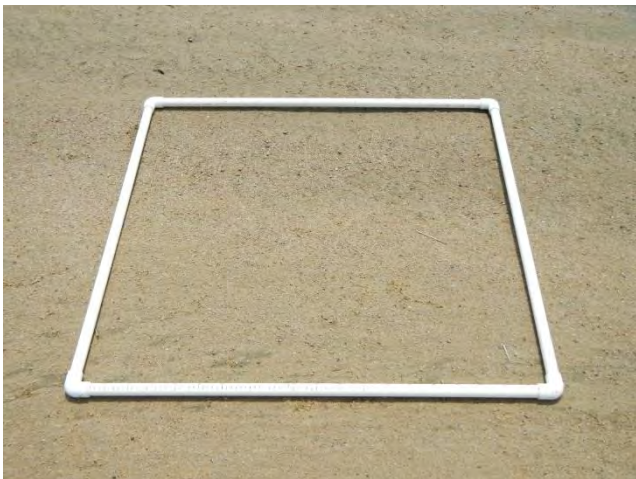
56 - Plot 4G – August 2015.



57 - Plot 5A – July 2014.



58 - Plot 5A – August 2015.



59 - Plot 5B – July 2014.



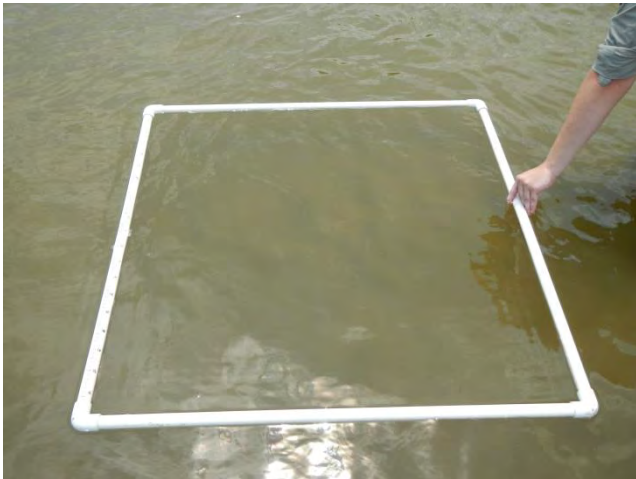
60 - Plot 5B – August 2015.



61 - Plot 5C – July 2014.



62 - Plot 5C – August 2015.



63 - Plot 5D – July 2014.



64 - Plot 5D – August 2015.



65 - Plot 5E – July 2014.



66 - Plot 5E – August 2015.



67 - Plot 5F – July 2014.



68 - Plot 5F – August 2015.



69 - Plot 5G – July 2014.



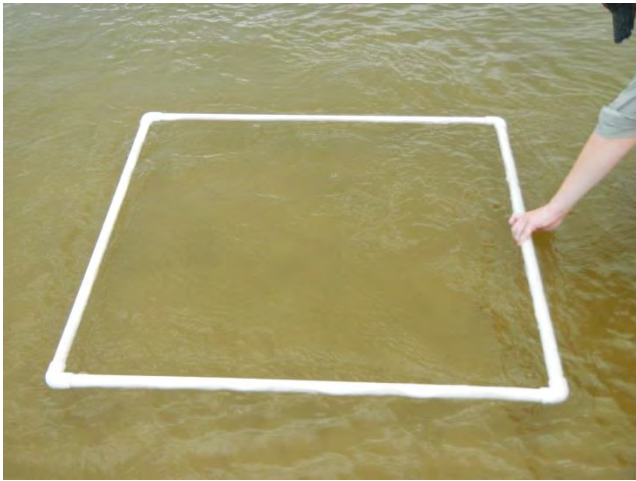
70 - Plot 5G – August 2015.



71 - Plot 6A – July 2014.



72 - Plot 6A – August 2015.



73 - Plot 6B – July 2014.



74 - Plot 6B – August 2015.



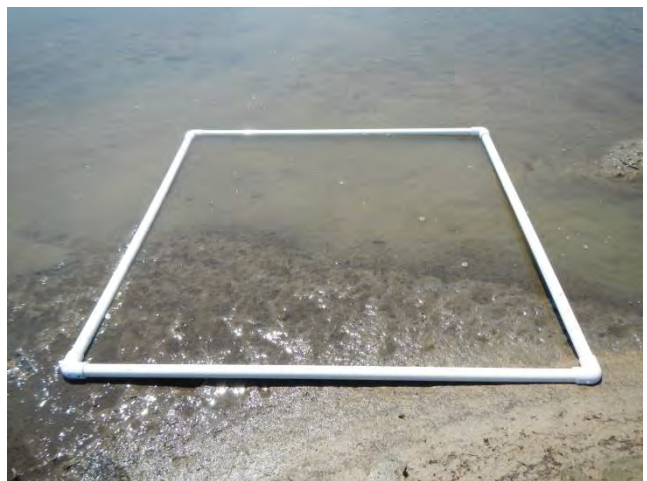
75 - Plot 6C – July 2014.



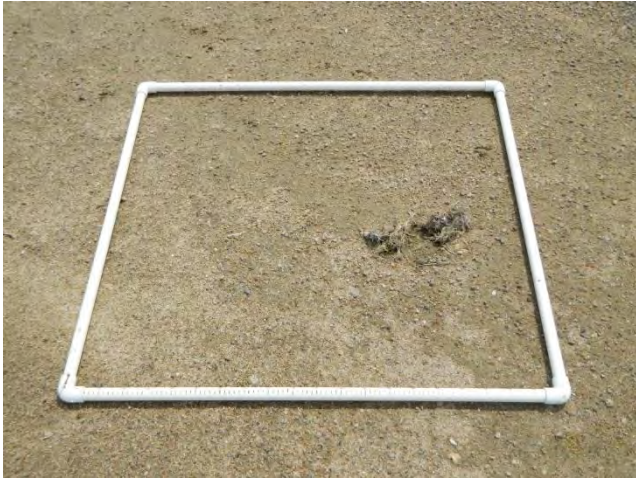
76 - Plot 6C – August 2015.



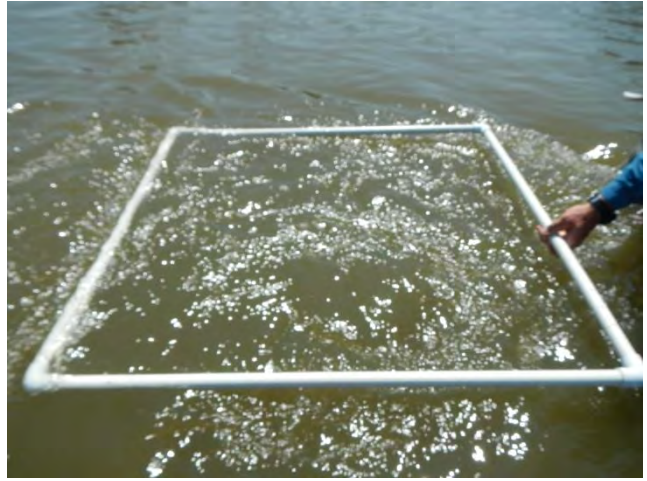
77 - Plot 6D – July 2014.



78 - Plot 6D – August 2015.



79 - Plot 6E – July 2014.



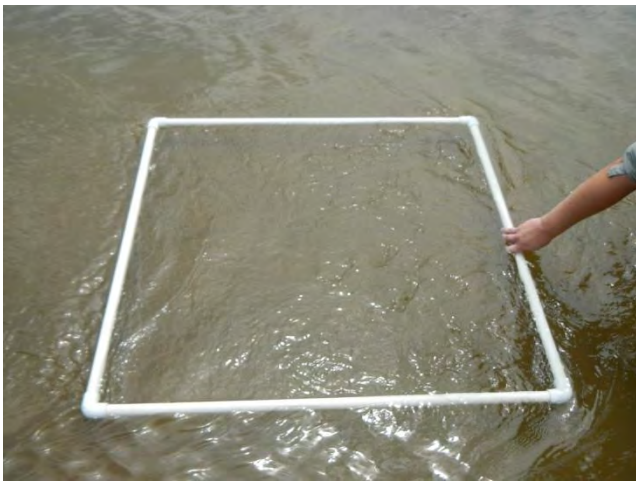
80 - Plot 6E – August 2015.



81 - Plot 6F – July 2014.



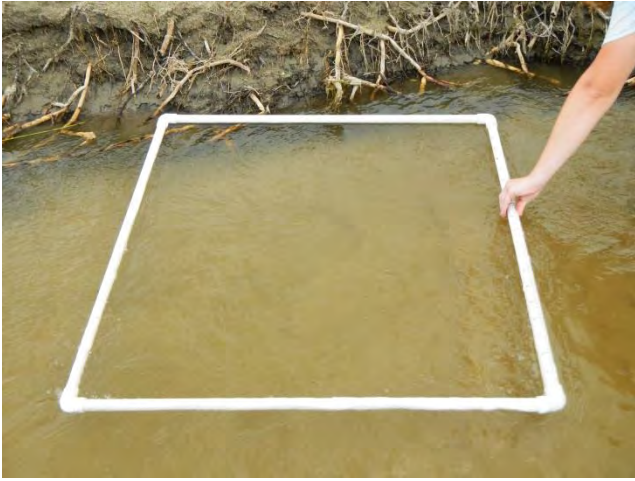
82 - Plot 6F – August 2015.



83 - Plot 6G – July 2014.



84 - Plot 6G – August 2015.



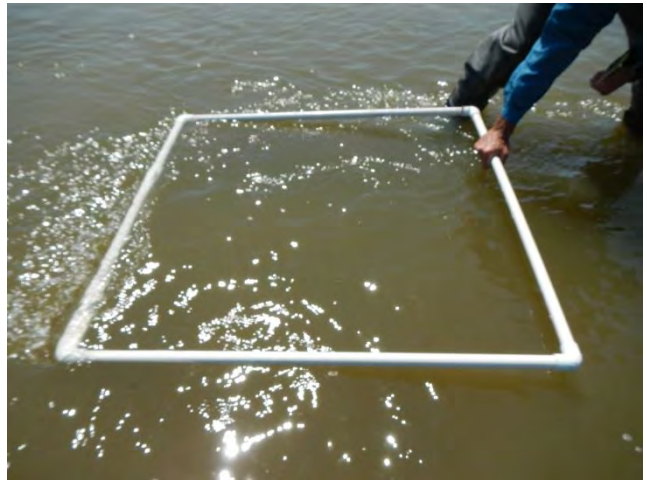
85 - Plot 7A – July 2014.



86 - Plot 7A – August 2015.



87 - Plot 7B – July 2014.



88 - Plot 7B – August 2015.



89 - Plot 7C – July 2014.



90 - Plot 7C – August 2015.



91 - Plot 7D – July 2014.



92 - Plot 7D – August 2015.



93 - Plot 7E – July 2014.



94 - Plot 7E – August 2015.



95 - Plot 7F – July 2014.



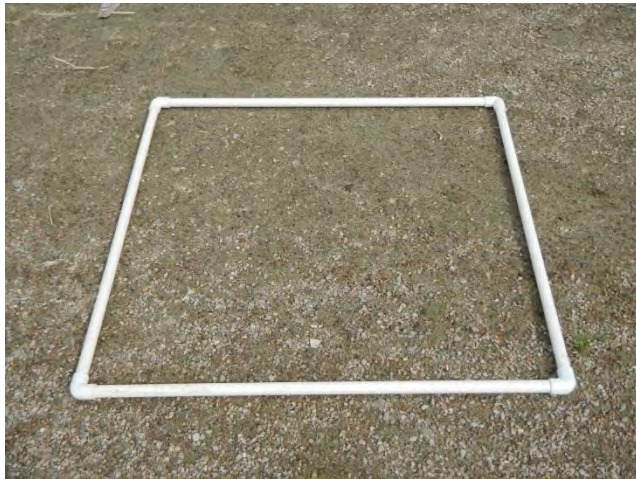
96 - Plot 7F – August 2015.



97 - Plot 7G – July 2014.



98 - Plot 7G – August 2015.



99 - Plot 8A – July 2014.



100 - Plot 8A – August 2015.



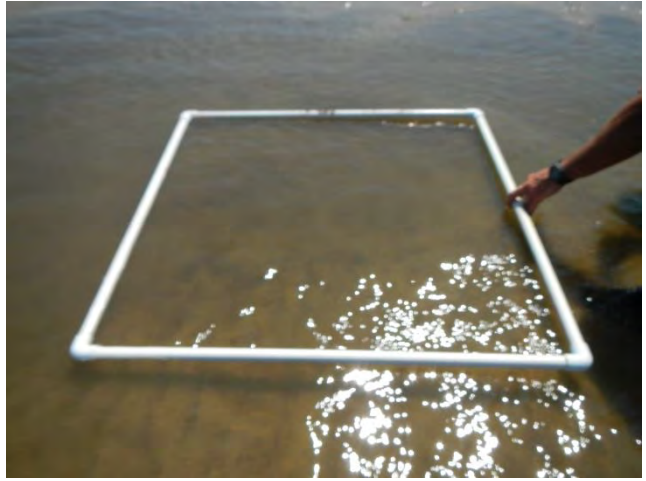
101 - Plot 8B – July 2014.



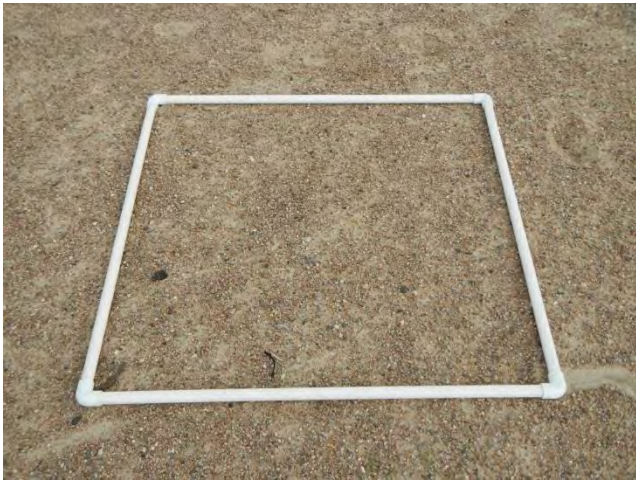
102 - Plot 8B – August 2015.



103 - Plot 8C – July 2014.



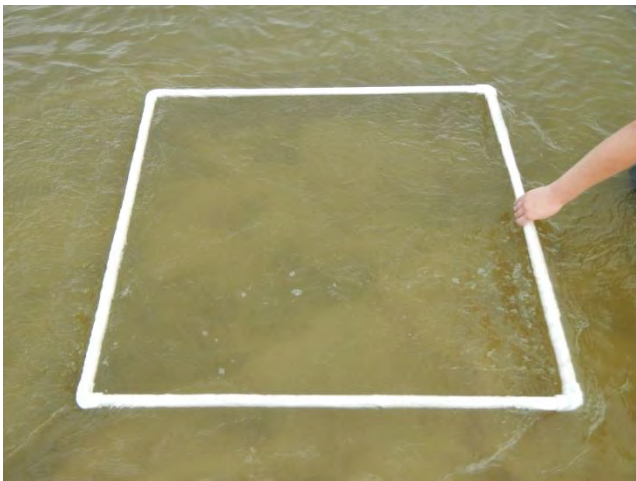
104 - Plot 8C – August 2015.



105 - Plot 8D – July 2014.



106 - Plot 8D – August 2015.



107 - Plot 8E – July 2014.



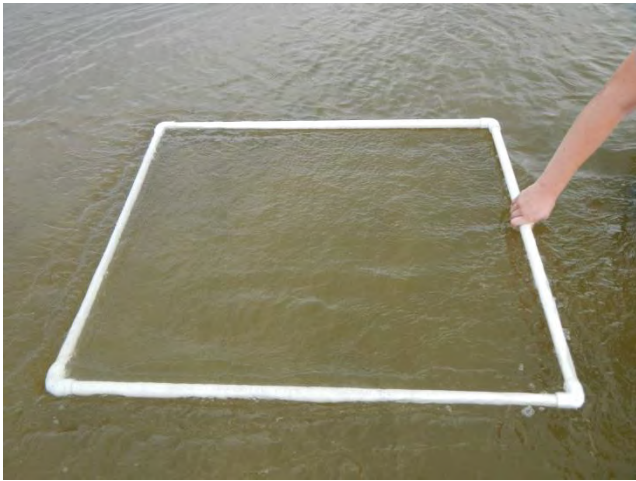
108 - Plot 8E – August 2015.



109 - Plot 8F – July 2014.



110 - Plot 8F – August 2015.



111 - Plot 8G – July 2014.



112 - Plot 8G – August 2015.



113 - Plot 9A – July 2014.



114 - Plot 9A – August 2015.



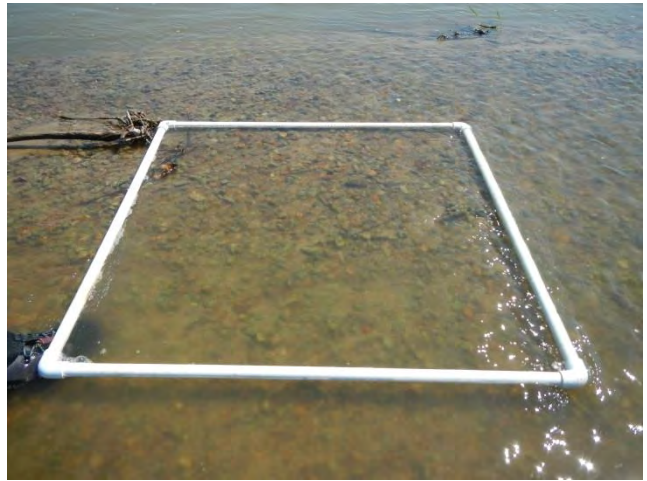
115 - Plot 9B – July 2014.



116 - Plot 9B – August 2015.



117 - Plot 9C – July 2014.



118 - Plot 9C – August 2015.



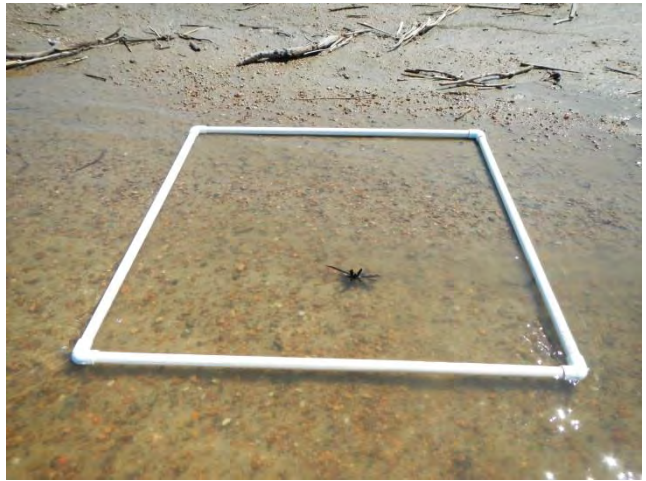
119 - Plot 9D – July 2014.



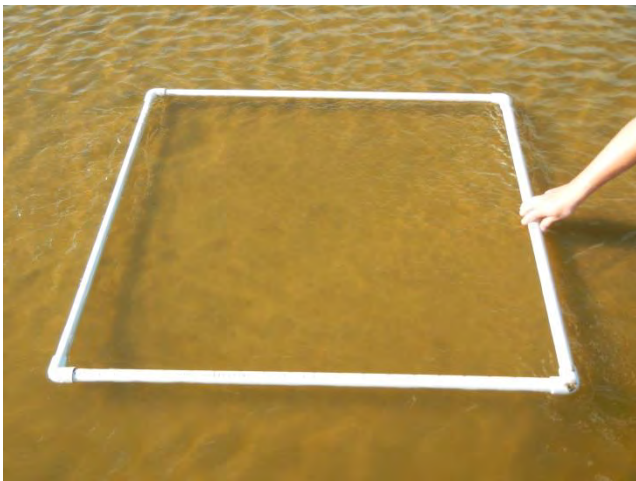
120 - Plot 9D – August 2015.



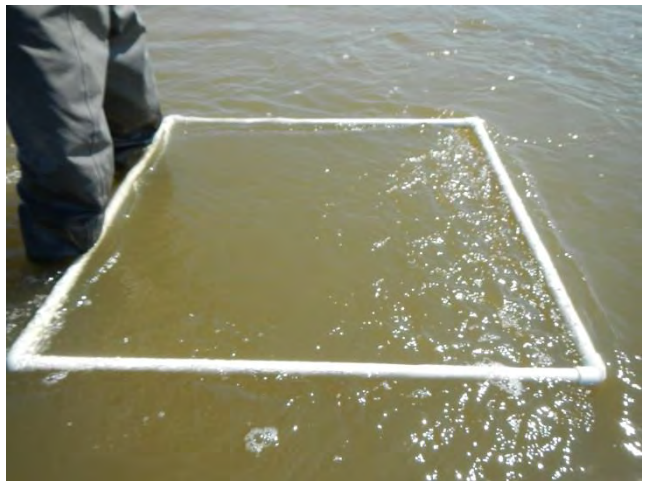
121 - Plot 9E – July 2014.



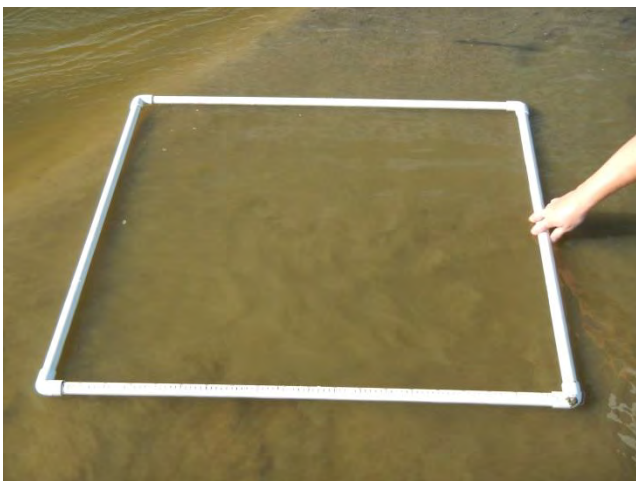
122 - Plot 9E – August 2015.



123 - Plot 9F – July 2014.



124 - Plot 9F – August 2015.



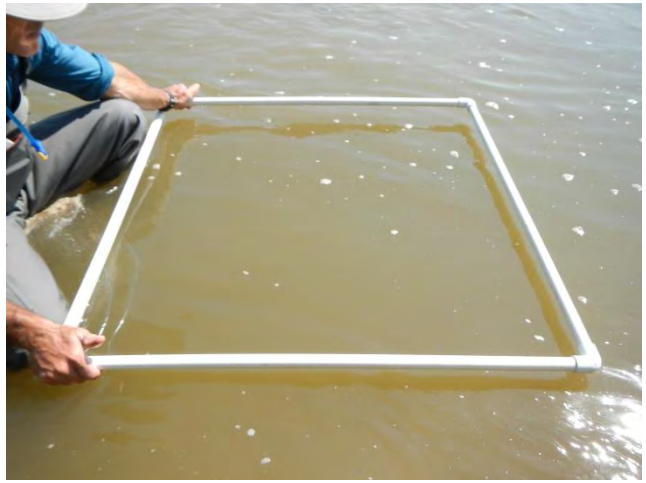
125 - Plot 9G – July 2014.



126 - Plot 9G – August 2015.



127 - Plot 10A – July 2014.



128 - Plot 10A – August 2015.



129 - Plot 10B – July 2014.



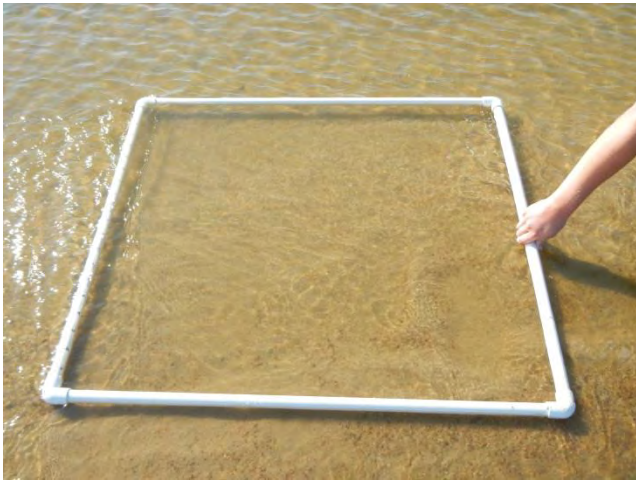
130 - Plot 10B – August 2015.



131 - Plot 10C – July 2014.



132 - Plot 10C – August 2015.



133 - Plot 10D – July 2014.



134 - Plot 10D – August 2015.



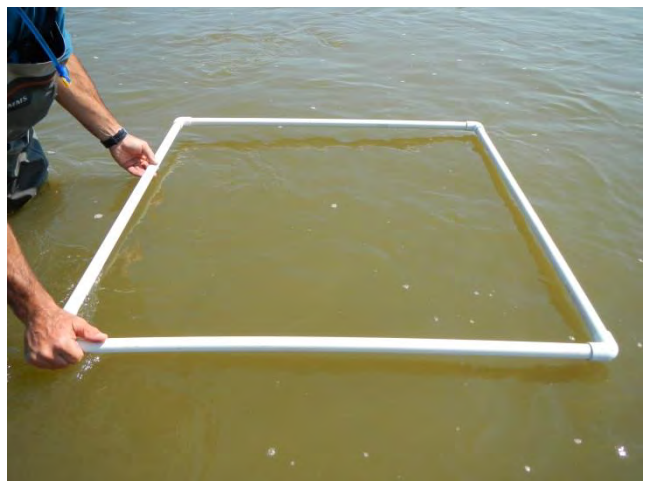
135 - Plot 10E – July 2014.



136 - Plot 10E – August 2015.



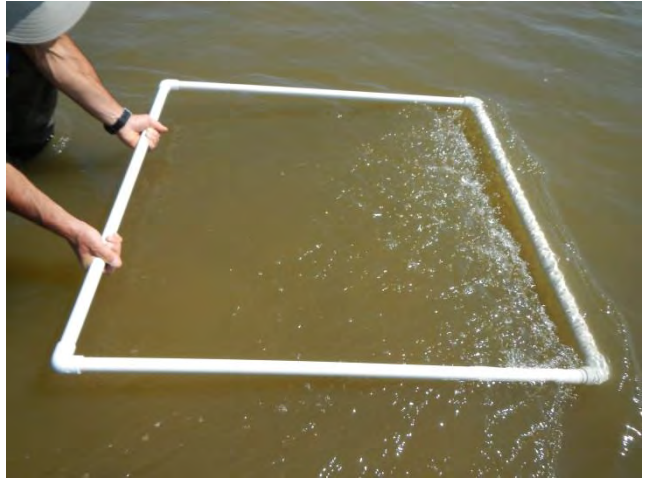
137 - Plot 10F – July 2014.



138 - Plot 10F – August 2015.



139 - Plot 10G – July 2014.



140 - Plot 10G – August 2015.



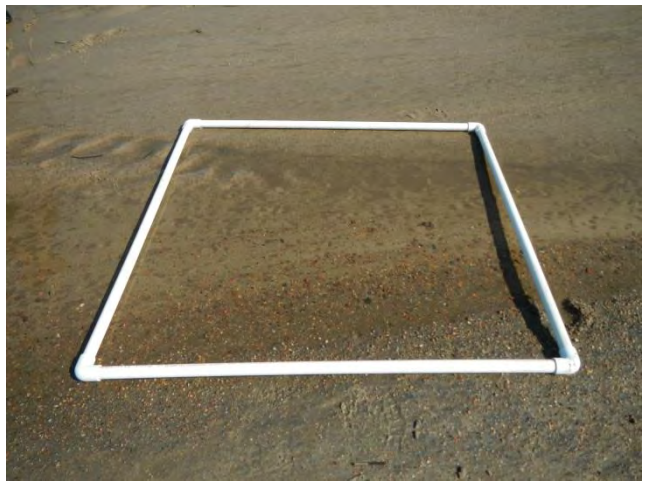
141 - Plot 11A – July 2014.



142 - Plot 11A – August 2015.



143 - Plot 11B – July 2014.



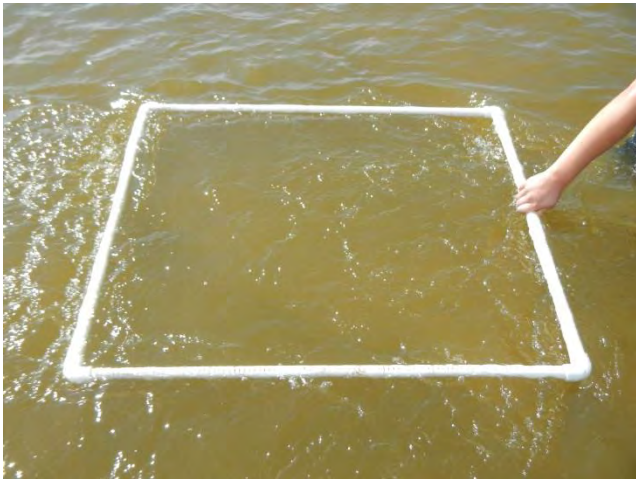
144 - Plot 11B – August 2015.



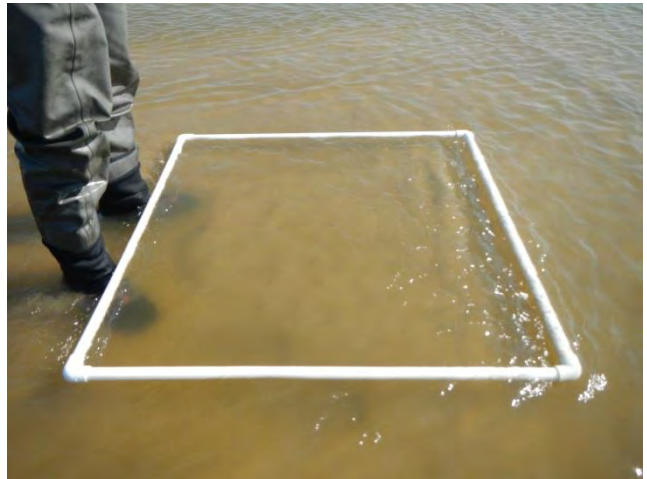
145 - Plot 11C – July 2014.



146 - Plot 11C – August 2015.



147 - Plot 11D – July 2014.



148 - Plot 11D – August 2015.



149 - Plot 11E – July 2014.



150 - Plot 11E – August 2015.



151 - Plot 11F – July 2014.



152 - Plot 11F – August 2015.



153 - Plot 11G – July 2014.



154 - Plot 11G – August 2015.



155 - Plot 12A – July 2014.



156 - Plot 12A – August 2015.



157 - Plot 12B – July 2014.



158 - Plot 12B – August 2015.



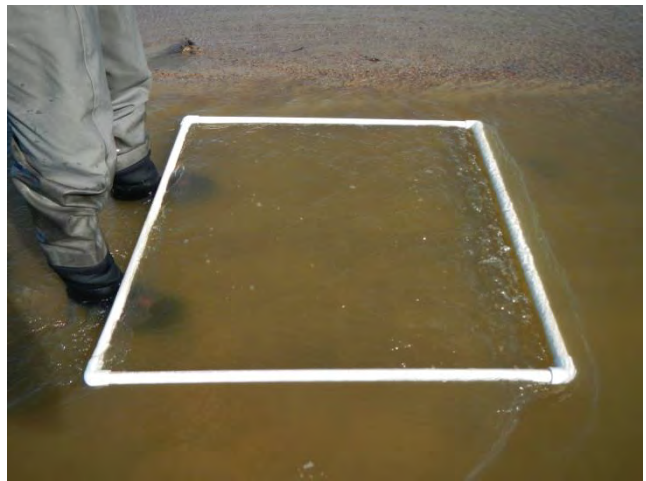
159 - Plot 12C – July 2014.



160 - Plot 12C – August 2015.



161 - Plot 12D – July 2014.



162 - Plot 12D – August 2015.



163 - Plot 12E – July 2014.



164 - Plot 12E – August 2015.



165 - Plot 12F – July 2014.



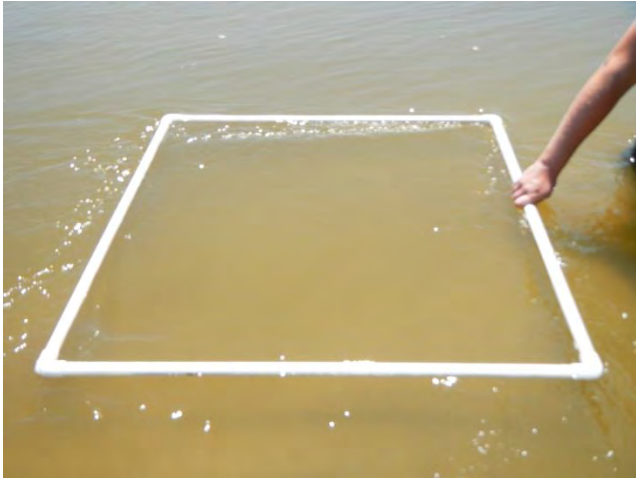
166 - Plot 12F – August 2015.



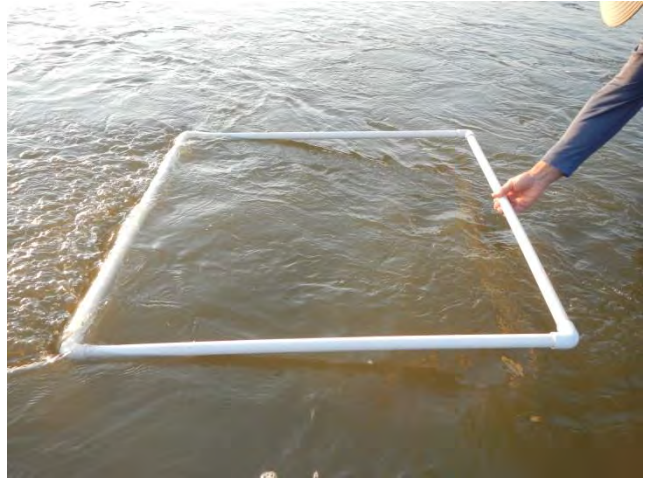
167 - Plot 12G – July 2014.



168 - Plot 12G – August 2015.



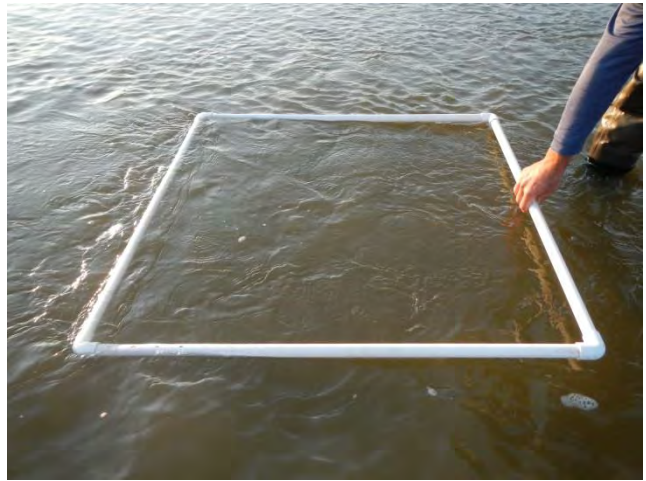
169 - Plot 13A – July 2014.



170 - Plot 13A – August 2015.



171 - Plot 13B – July 2014.



172 - Plot 13B – August 2015.



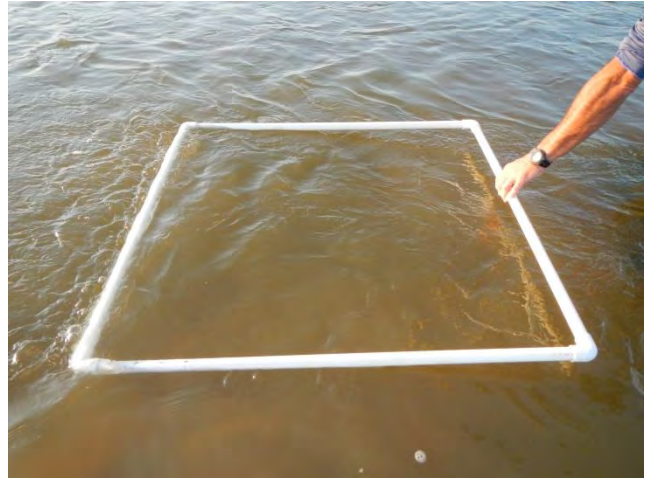
173 - Plot 13C – July 2014.



174 - Plot 13C – August 2015.



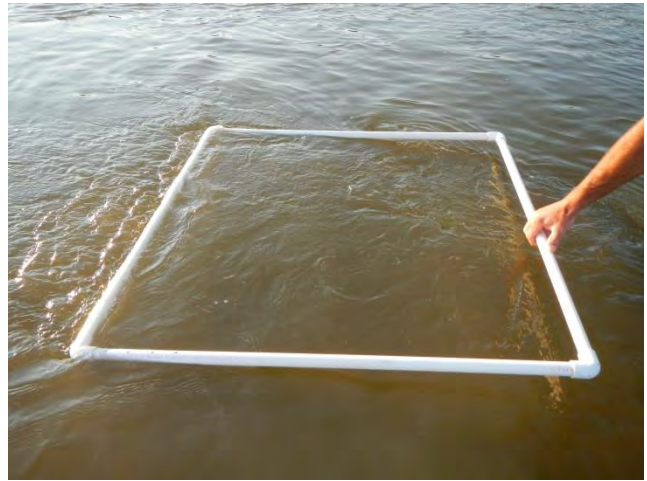
175 - Plot 13D – July 2014.



176 - Plot 13D – August 2015.



177 - Plot 13E – July 2014.



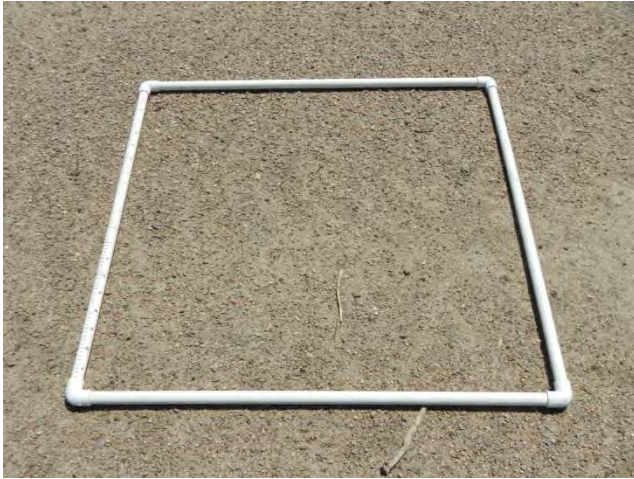
178 - Plot 13E – August 2015.



179 - Plot 13F – July 2014.



180 - Plot 13F – August 2015.



181 - Plot 13G – July 2014.



182 - Plot 13G – August 2015.



183 - Plot 14A – July 2014.



184 - Plot 14A – August 2015.



185 - Plot 14B – July 2014.



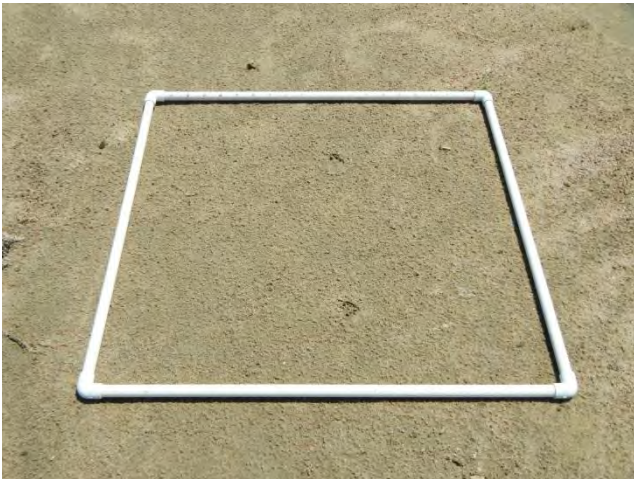
186 - Plot 14B – August 2015.



187 - Plot 14C – July 2014.



188 - Plot 14C – August 2015.



189 - Plot 14D – July 2014.



190 - Plot 14D – August 2015.



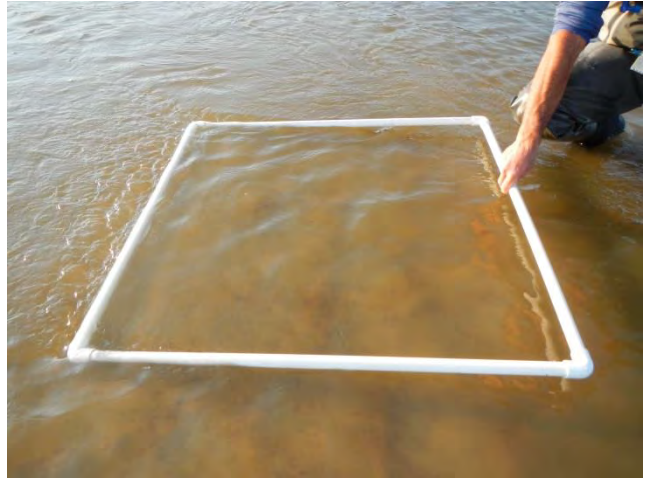
191 - Plot 14E – July 2014.



192 - Plot 14E – August 2015.



193 - Plot 14F – July 2014.



194 - Plot 14F – August 2015.



195 - Plot 14G – July 2014.



196 - Plot 14G – August 2015.



197 - Plot 15A – July 2014.



198 - Plot 15A – August 2015.



199 - Plot 15B – July 2014.



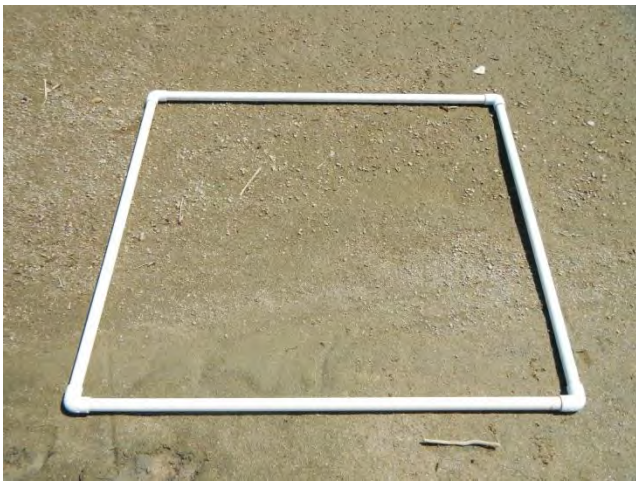
200 - Plot 15B – August 2015.



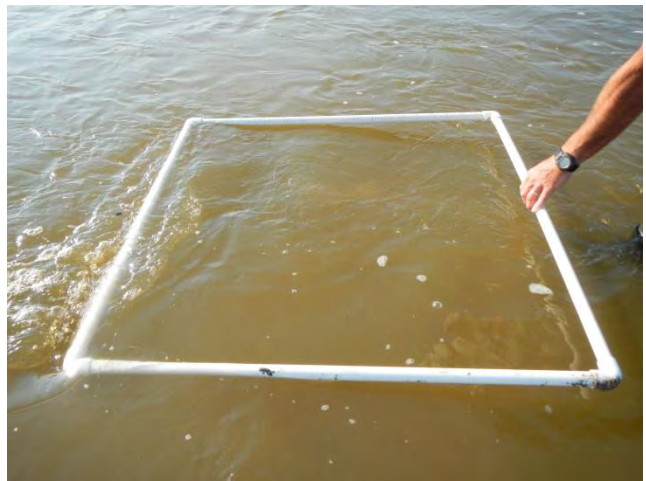
201 - Plot 15C – July 2014.



202 - Plot 15C – August 2015.



203 - Plot 15D – July 2014.



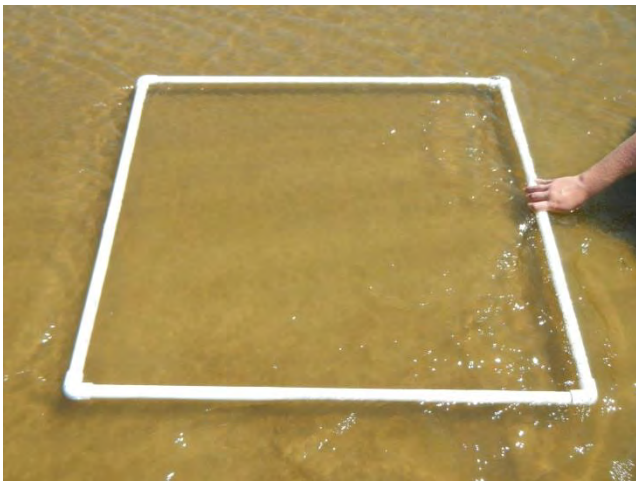
204 - Plot 15D – August 2015.



205 - Plot 15E – July 2014.



206 - Plot 15E – August 2015.



207 - Plot 15F – July 2014.



208 - Plot 15F – August 2015.



209 - Plot 15G – July 2014.



210 - Plot 15G – August 2015.



211 - Plot 16A – July 2014.



212 - Plot 16A – August 2015.



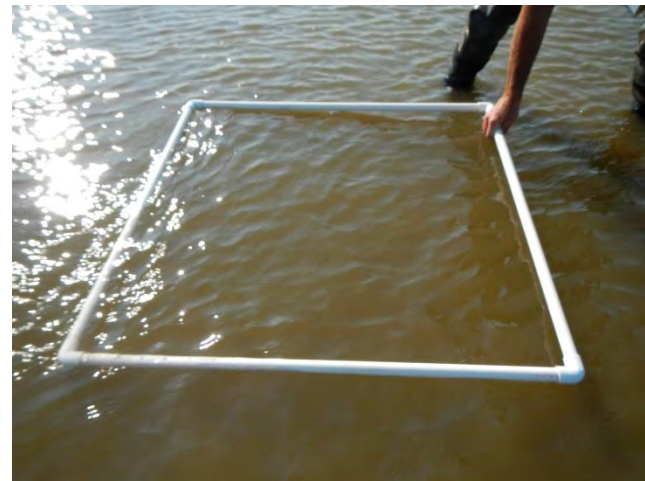
213 - Plot 16B – July 2014.



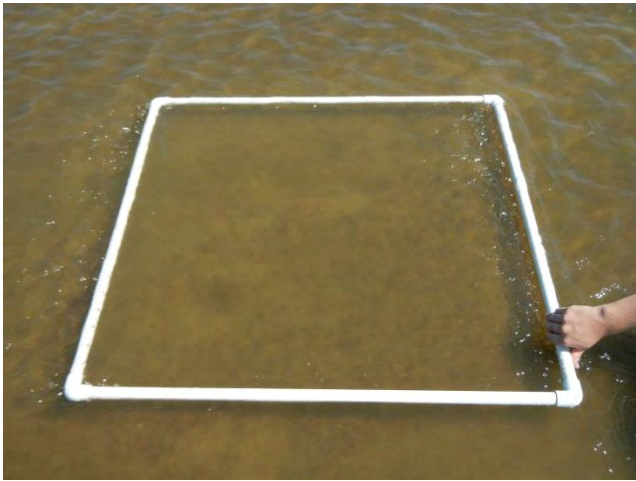
214 - Plot 16B – August 2015.



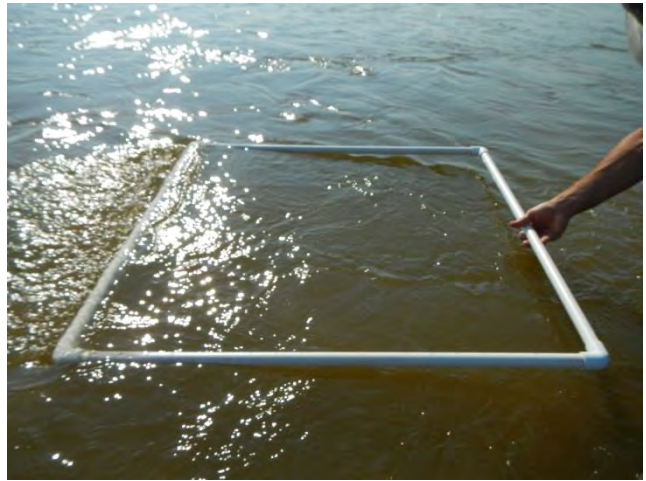
215 - Plot 16C – July 2014.



216 - Plot 16C – August 2015.



217 - Plot 16D – July 2014.



218 - Plot 16D – August 2015.



219 - Plot 16E – July 2014.



220 - Plot 16E – August 2015.



221 - Plot 16F – July 2014.



222 - Plot 16F – August 2015.



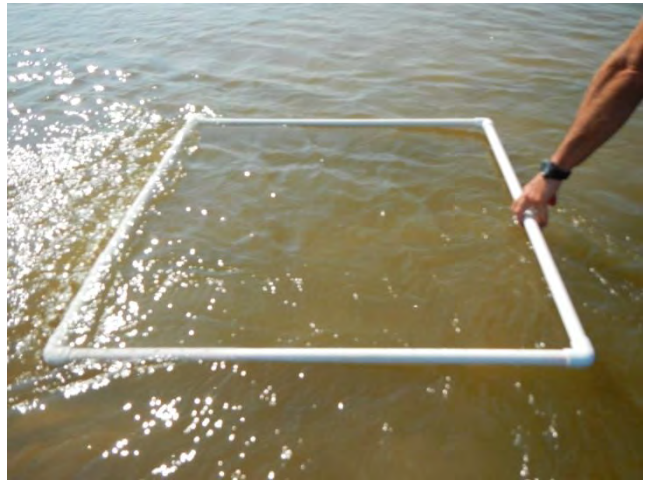
223 - Plot 16G – July 2014.



224 - Plot 16G – August 2015.



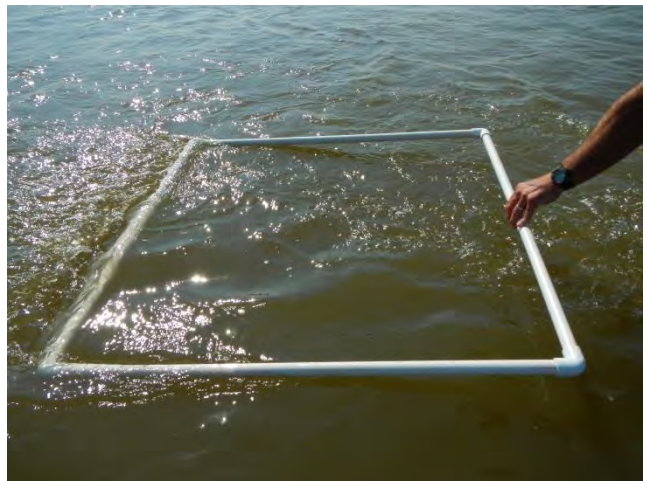
225 - Plot 17A – July 2014.



226 - Plot 17A – August 2015.



227 - Plot 17B – July 2014.



228 - Plot 17B – August 2015.



229 - Plot 17C – July 2014.



230 - Plot 17C – August 2015.



231 - Plot 17D – July 2014.



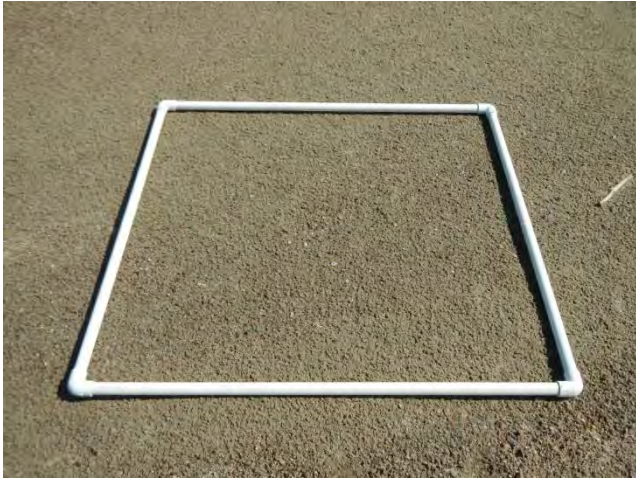
232 - Plot 17D – August 2015.



233 - Plot 17E – July 2014.



234 - Plot 17E – August 2015.



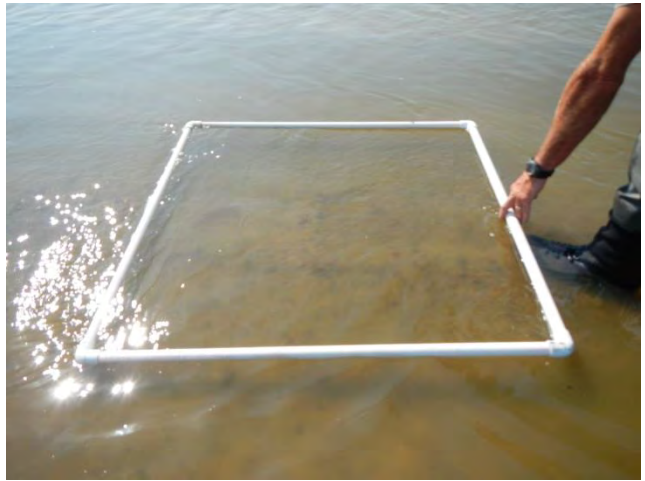
235 - Plot 17F – July 2014.



236 - Plot 17F – August 2015.



237 - Plot 17G – July 2014.



238 - Plot 17G – August 2015.



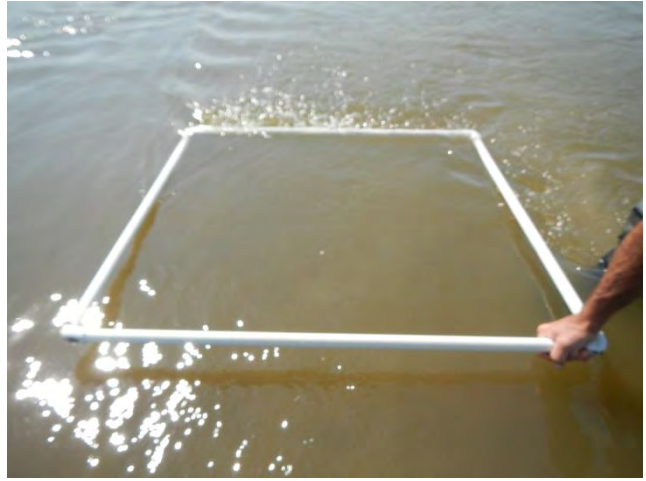
239 - Plot 18A – July 2014.



240 - Plot 18A – August 2015.



241 - Plot 18B – July 2014.



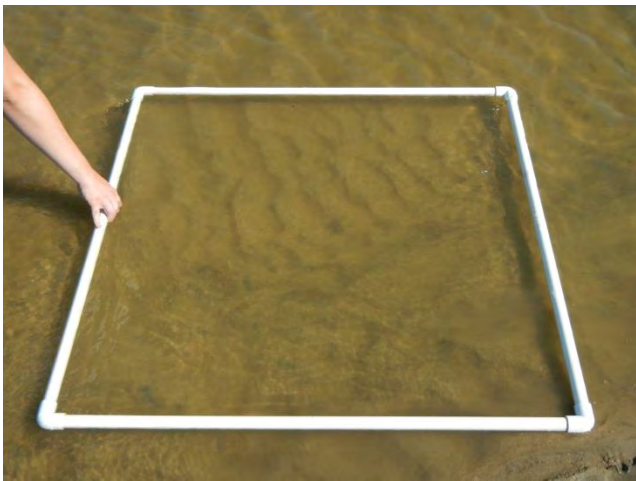
242 - Plot 18B – August 2015.



243 - Plot 18C – July 2014.



244 - Plot 18C – August 2015.



245 - Plot 18D – July 2014.



246 - Plot 18D – August 2015.



247 - Plot 18E – July 2014.



248 - Plot 18E – August 2015.



249 - Plot 18F – July 2014.



250 - Plot 18F – August 2015.



251 - Plot 18G – July 2014.



252 - Plot 18G – August 2015.



PLATTE RIVER RECOVERY IMPLEMENTATION PROGRAM

Shoemaker Island Flow-Sediment-Mechanical “Proof of Concept” Experiment

Fixed Bed Modeling

Attachment I

DRAFT

August 2016

Submitted to:

Platte River Recovery Implementation Program
4111 4th Avenue, Suite 6
Kearney, NE 68845

Submitted by:

Northern Hydrology and Engineering
PO Box 2515
McKinleyville, CA 95519



Table of Contents

I. INTRODUCTION.....	1
II. MODEL DESCRIPTION.....	2
II.A. Model Inputs	2
II.A.1. Flow and Stage Boundary Conditions.....	2
II.A.2. Model Domain and Topography	3
II.A.3. Bed Roughness and Vegetation Drag.....	3
II.A.4. Horizontal Eddy Viscosity and Diffusivity Coefficient.....	3
III. MODEL CALIBRATION/VERIFICATION.....	4
IV. FIXED-BED MODEL RESULTS	4
IV.A. Objective 1: Water Surface Elevation for Measured Bar Changes and Cut/Fill Analyses	4
IV.B. Objective 2: Predict Changes in Vegetation Patches Due to Uprooting of Vegetation.....	4
V. CONCLUSIONS	5
VI. REFERENCES.....	6



I. INTRODUCTION

Several types of models were used to estimate responses of channel morphology and vegetation to potential management actions in the Platte River for SDHF (Short Duration High Flow) releases. These models include two-dimensional fixed-bed hydrodynamic models, a one-dimensional bank erosion model, and two-dimensional mobile-bed sediment transport models.

These models were developed in Year 1 of the study (2013) with a focus on informing the following learning objectives:

1. Evaluate relationships between:
 - a. Sediment supply and frequency of sandbar occurrence
 - b. Grain size and sand bar height
 - c. Hydrograph (shape and duration) and sand bar height
2. Evaluate the relationship between peak flows (magnitude and duration) and riparian plant mortality
3. Evaluate ability of FSM management strategy to create/maintain habitat for whooping cranes, least terns and piping plovers

In Year 1 (2013), the models were calibrated using data collected during the 2013 SDMF (Short Duration Medium Flow) and run for higher flows and durations that would be typical of target SDHF (Short Duration High Flow). The primary limitation of the Year 1 (2013) modeling analysis was a lack of high flow calibration data to confirm model results for the high flow simulations. Two high flows occurred following the 2013 SDMF. One occurred in the fall of 2013 (Fall 2013 High Flow) and a second in June 2014 (June 2014 High Flow). Water surface elevation data was collected by PRRIP (Platte River Recovery Implementation Program) staff for model calibration during the Fall 2013 High Flow and by the EA project team during the June 2014 High Flow. High flow simulations in Year 2 (2014) confirmed that model parameters selected in Year 1 were suitable for high flow fixed-bed simulations. The highest peak flow with the longest duration of the study period occurred in 2015 (Year 3).

The specific objectives of the fixed-bed two-dimensional model for Year 3 included:

1. Predict water surface elevations at 1,200 cfs TRF with updated topography (collected following the June 2015 high flow event) and 3-day average peak flow for the June 2015 high flow for bar area and height computations (see PRRIP 2016) (Learning Objective 1).
2. Predict the velocity during the 3-day average peak flow for the June 2015 high flow event to compare the measured and predicted vegetation patch response (Learning Objective 2).



II. MODEL DESCRIPTION

FaSTMECH (Flow and Sediment Transport with Morphological Evolution of Channels) was selected as the base model to accomplish all fixed-bed modeling objectives. FaSTMECH was selected because the model is computationally efficient and a high grid resolution can be applied to the model domain. The model produced accurate results for the 2013 SDMF and 2014 high flows within the project area. FaSTMECH was developed by Dr. Jonathan Nelson of the U.S. Geological Survey (USGS) and is included within the free software package, IRIC (International River Interface Cooperative) available at <http://i-ric.org/en/introduction>. IRIC is a river flow and riverbed variation analysis software package which combines the functionality of MD_SWMS (Multi-Dimensional Surface Water Modeling System), developed by the USGS (U.S. Geological Survey), and RIC-NAYS2D, developed by the Foundation of Hokkaido River Disaster Prevention Research Center. FaSTMECH is a two-dimensional, vertically averaged model. FaSTMECH contains a sub-model that calculates vertical distribution of the primary velocity as well as the secondary flow about the vertically averaged flow. The vertically averaged equations used in the computational solution are cast in a channel-fitted curvilinear coordinate system. The approach uses the assumptions that (1) the flow is steady (or at least does not vary appreciably over short time scales), (2) the flow is hydrostatic (vertical accelerations are neglected), and (3) the turbulence can be treated adequately by relating Reynolds stresses to shear stresses using an isotropic eddy viscosity. Development of the model equations is described in Nelson and Smith (1989), while the numerical techniques and the streamline-based vertical structure sub-model are discussed by Nelson and McDonald (1996). FaSTMECH has a long track record of accurately predicting local flow conditions and morphological change in a variety of rivers (Andrews and Nelson, 1989; Lisle et al., 2000; Conaway and Moran, 2004; Barton et al., 2005). In addition, FaSTMECH differs from many other mobile-bed models by employing a quasi-steady approximation which enables predictions over longer time frames, finer grid resolutions and longer reaches.

II.A. Model Inputs

Fixed-bed model inputs include flow at the upstream boundary, water surface elevation at the downstream boundary for each flow of interest, topography and roughness.

II.A.1. Flow and Stage Boundary Conditions

The project site is located downstream of a major flow split. The portion of the river that flows through the project site is roughly 80% of the total river flow (TRF). Flows reported at the gaging stations, as well as flow targets developed by PRRIP, reference the total river flow. Thus, when referring to the total river flow, “TRF” is attached to the reported value for clarity.

Continuous stage was measured at the project site at cross-section 18 (near the downstream model boundary). A rating curve was developed from the stage measurements and twelve discharge measurements that ranged from 1,020 to 10,800 cfs (See Figure 5-2 main report). A continuous 15-minute discharge record was estimated from a rating curve developed from the discharge and stage measurements collected during the June 2015 high flow (See Figure 5-3



main report). Model flows are 1,200 cfs TRF (956 cfs in Shoemaker Reach) and the 3-day average peak discharge (15,700 cfs TRF; 11,200 cfs in Shoemaker Reach).

II.A.2. Model Domain and Topography

The model domain covers 2.6 miles of the Platte River (Figure 1). The FaSTMECH model grid is curvilinear with an individual grid cell size of 9.8 feet (3 meters) and a total of 326,433 grid cells. The model domain was not extended laterally to include the adjacent fields and channels that route flow away from the main channel at very high flows. These areas are outside of the focus area of this study.

Model topography for previous years (2013 and 2014) were developed from a combination of LiDAR data to define bar surfaces above the wetted channel and terrestrial data to define the channel geometry (Figure 1). In 2015, both data sets could not be combined, with the exception of limited areas, due to substantial topographic changes that occurred between the LiDAR flight (prior to the June 2015 high flow) and the terrestrial ground surveys (following the June 2015 high flow). Thus, terrestrial data collected following the June 2015 high flow were used as the primary data source to create the model topography. LiDAR data collected during fall 2014 were used on selected bars and to define floodplains adjacent to the channel. The overall topographic data set is highly simplified compared to previous years.

II.A.3. Bed Roughness and Vegetation Drag

The formulation of channel and floodplain roughness varies between models. Roughness was used as a calibration parameter in the fixed-bed runs to match measured water surface elevations.

FaSTMECH utilizes a drag coefficient which was estimated using Manning's roughness coefficient (n), mean flow depth (h) and gravity (g) related by the following equation:

$$C_d = \frac{n^2 g}{h^{1/3}}$$

II.A.4. Horizontal Eddy Viscosity and Diffusivity Coefficient

FaSTMECH requires an input of a lateral eddy viscosity. The lateral eddy viscosity (LEV) is a correction to the eddy viscosity used in the vertically averaged equations to treat lateral separation eddies. LEV can be estimated using the following equation:

$$\text{LEV} = 0.1 \times \text{average depth (meters)} \times \text{average velocity (meters/second)}.$$

Using reach average values, an LEV of 0.05 was estimated. This value was increased to 0.08 to improve model stability.



III. MODEL CALIBRATION/VERIFICATION

Two data points were collected to calibrate the high flow model run. The model over predicted one point by 0.5 feet near cross-section 2.5 and another point by 0.1 feet near cross-section 10. The over-prediction of the water surface elevation may be a result of a combination of containment of flows within the model domain. Complex out of bank flows occurred upstream of the study area (above the upstream model boundary) and beyond the lateral extent of the model domain and were not captured in the model. The over prediction may also be due to inaccurate representation of model topography due to substantial channel geometry changes that occurred during the high flow and/or poor characterization of channel geometry due to widely spaced cross-sections representing the channel.

Low flow calibration was conducted using 96 measurements collected at 18 cross-sections over a period of 2 days (August 31 and September 1, 2015). Discharge during data collection is estimated from the discharge record at the Grand Island Gage. Discharge at Grand Island ranged from 746 to 1,020 cfs with an average value of 915 cfs over the period of 2 days when water surface elevation measurements were collected. Using an assumed value of 82% of the total river flow at Shoemaker, flow at the project site is estimated to be roughly 750 cfs during the data collection. The root mean square error is 0.22 feet (Figure 2)

IV. FIXED-BED MODEL RESULTS

IV.A. Objective 1: Water Surface Elevation for Measured Bar Changes and Cut/Fill Analyses

Fixed-bed model runs were conducted to predict water surface elevations at 1,200 cfs (TRF) and at the 3-day average peak flow (June 2015 high flow) for bar height computations (Figure 3). Only water levels within the bar computational area are provided. Within this area, the average depth increased from 0.9 feet to 2.6 feet between the low flow and high flow; average velocity increased from 1.3 to 2.7 feet/sec and average shear stress increased from 2 Pa to 9.0 Pascals.

IV.B. Objective 2: Predict Changes in Vegetation Patches Due to Uprooting of Vegetation

Relations between velocity and vegetation patch resistance were developed by Pollen-Bankhead et al. (2012) for one-year old cottonwoods, two-year old cottonwoods, reed canarygrass and phragmites. Spatial patterns of velocity within the computational area are shown for the June 2015 high flow (Figure 4).

The 3-day average peak flow velocity results were further processed to match those presented by Pollen-Bankhead et al. (2012) with the exception that the velocity breaks are provided in units of feet/sec rather than meters/sec. The Pollen-Bankhead et al. (2012) color scheme was also adopted for ease in comparison of results to earlier studies. The velocity range in each class is specific to each vegetation type. The classes include no uprooting, uprooting initiated, three



classes of increasing velocity, and finally, a velocity class where all plants are expected to uproot.

The velocities required for initiating uprooting of one-year old cottonwoods are generally predicted within the low flow channels and across all vegetated bars (Figure 5) during the June 2015 high flow. Velocities across all bars are predicted to be within the two lowest uprooting classes (54% in the lowest class and 45% in the next higher class). Only 1% of the bar area did not meet the velocity criteria to initiate uprooting.

Two-year old cottonwoods require higher velocities to initiate uprooting. Similar to 1-year cottonwoods, only 1% of the bar area does not meet the criteria to initiate uprooting. However, 94% of the bar area is in the lowest velocity class for initiation of uprooting and 5% is in the next higher velocity class during the June 2015 high flow.

Velocities are predicted to be too low throughout the reach to initiate uprooting of reed canary grass with the exception of a few small patches identified in higher velocity zones within the main channel during the June 2015 high flow (Figure 5). All predicted velocities are well below that required to initiate uprooting of phragmites (Figure 5).

V. CONCLUSIONS

Velocity predictions at 15,700 cfs (TRF) were used to predict areas where vegetation patches would be uprooted as a result of drag force. Results of the analysis indicate that there are no areas within the Shoemaker Reach where all plants in a patch are expected to be uprooted. Some uprooting is predicted to be initiated for one-year and two-year old cottonwoods across most bars. Initiation of uprooting is not expected for reed canary grass or phragmites on bar surfaces.

Velocity magnitudes were determined to be insufficient for the generation of drag forces capable of uprooting reed canarygrass and phragmites. Thus, hydraulic forces occurring during high flows which exceed the target SDHF are insufficient for managing these vegetation types in the Shoemaker Island Reach (Learning Objective 2).

These results are consistent with Year 1 and 2 results.



VI. REFERENCES

- Andrews, E. D., and J. M. Nelson, 1989. Topographic response of a bar in the Green River, Utah to variation in discharge, in *River Meandering*, Water Resour. Monogr. Ser., vol. 12, edited by S. Ikeda and G. Parker, pp. 463 – 485, AGU, Washington, D. C.
- Barton, G. J., R. R. McDonald, J. M. Nelson, and R. L. Dinehart, 2005. Simulation of flow and sediment mobility using a multidimensional flow model for the white sturgeon critical-habitat reach, Kootenai River near Bonners Ferry, Idaho, U.S. Geol. Surv. Sci. Invest. Rep., 2005-5230, 64 pp.
- Conaway, J. S., and E. H. Moran, 2004. Development and calibration of a two-dimensional hydrodynamic model of the Tanana River near Tok, Alaska, U.S. Geol. Surv. Open File Rep., 1225, 22 pp.
- Lisle, T. E., J. M. Nelson, J. Pitlick, M. A. Madej, and B. L. Barkett, 2000. Variability of bed mobility in natural, gravel-bed channels and adjustments to sediment load at local and reach scales, *Water Resour. Res.*, 36, 3743– 3755, doi:10.1029/2000WR900238.
- Nelson, J. M., and J. D. Smith, 1989. Flow in meandering channels with natural topography, in *River Meandering*, Water Resour. Monogr. Ser., vol. 12, edited by S. Ikeda and G. Parker, pp. 69– 102, AGU, Washington, D. C.
- Nelson, J. M., and R. M. McDonald, 1996. Mechanics and modeling of flow and bed evolution in lateral separation eddies, report, Grand Canyon Environ. Stud., Flagstaff, Ariz.
- Pollen-Bankhead, N., Thomas, R. and A. Simon, 2012. Can short duration high flows be used to remove vegetation from bars on the central Platte River? *Platte River Recovery Implementation Program, Directed Vegetation Research Study* 127pp.
- Platte River Recovery Implementation Program (PRRIP), 2015. Shoemaker Island Flow-Sediment-Mechanical “Proof of Concept” Experiment Annual Report for 2014. May 2015.

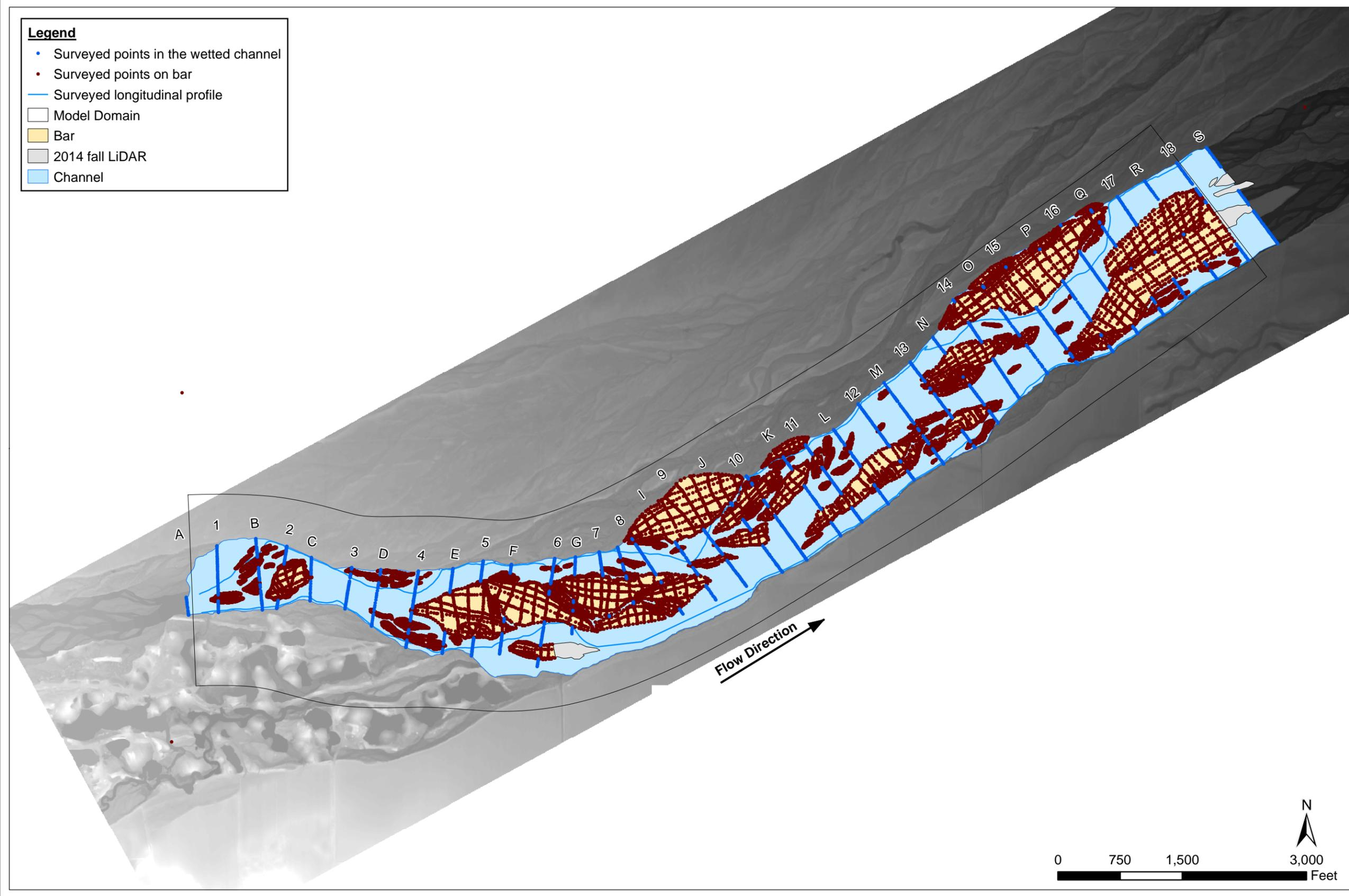


FIGURES

2016-08-18 F:\State & Local\OpenPlate River Recovery Program\Projects\1499201 - Shoemaker FSM Proof of Concept\MXD\2015\Attachment (MXD)\Figure 1 - Shoemaker Study Reach Model Topography for the 2015 High Flow.mxd EA-Lincoln .jpetersen

Legend

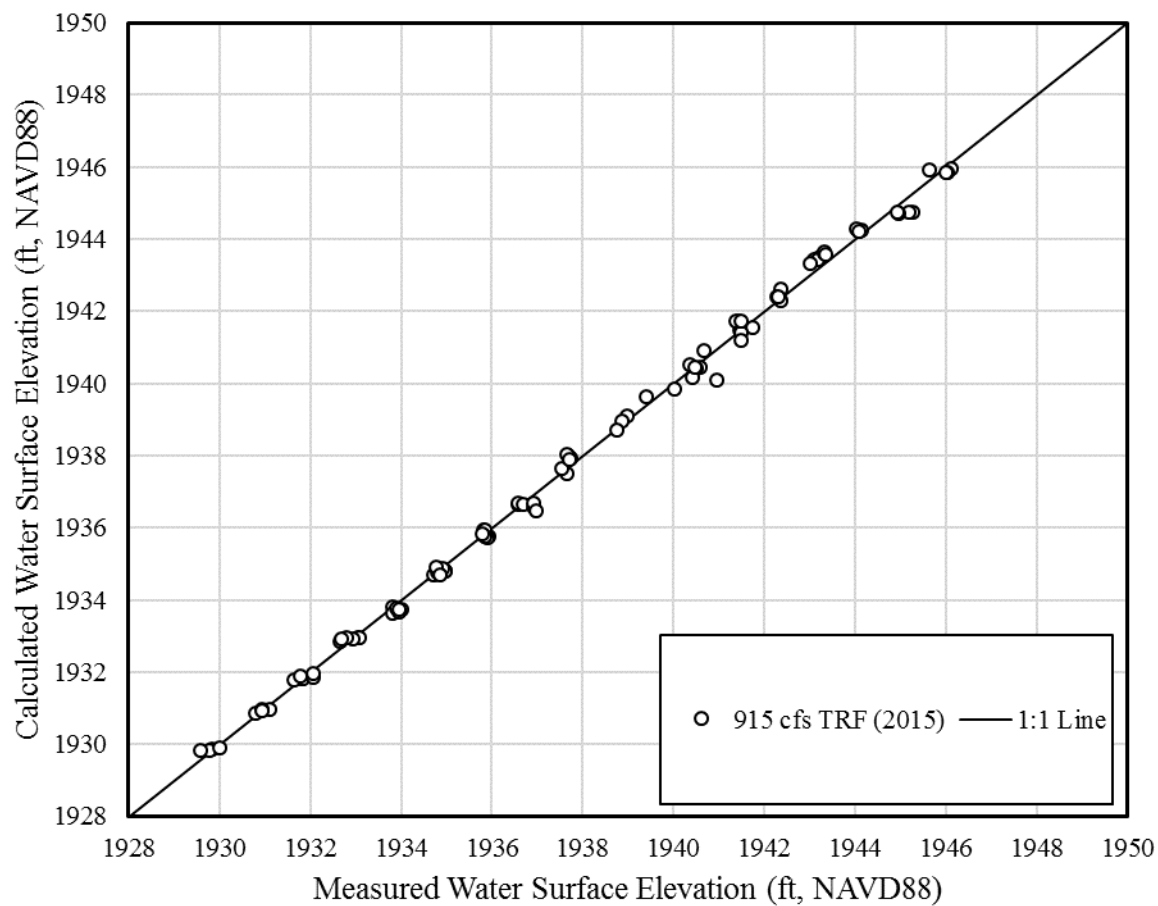
- Surveyed points in the wetted channel
- Surveyed points on bar
- Surveyed longitudinal profile
- Model Domain
- Bar
- 2014 fall LiDAR
- Channel

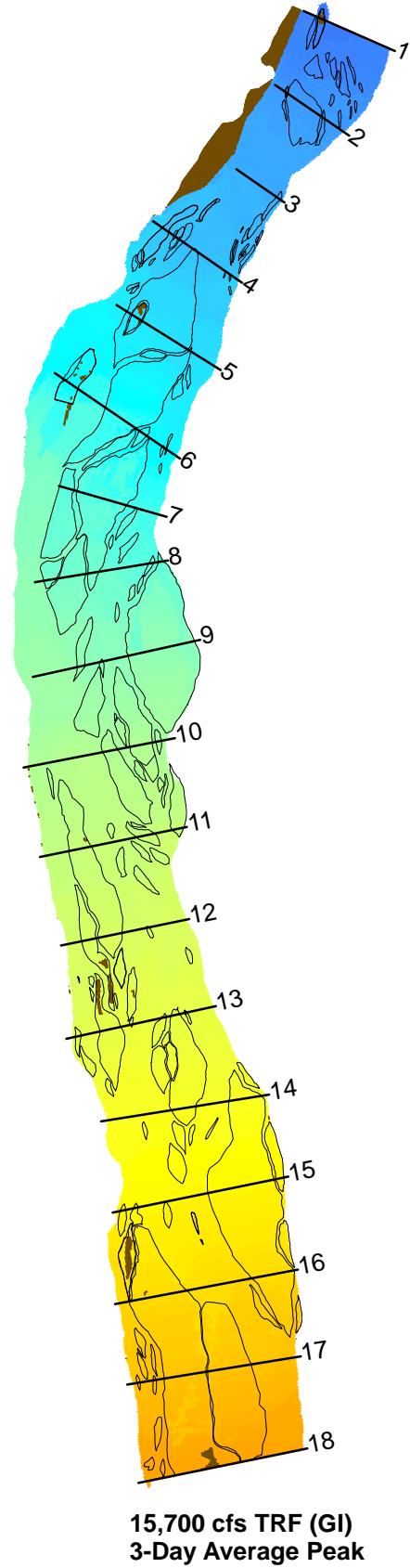
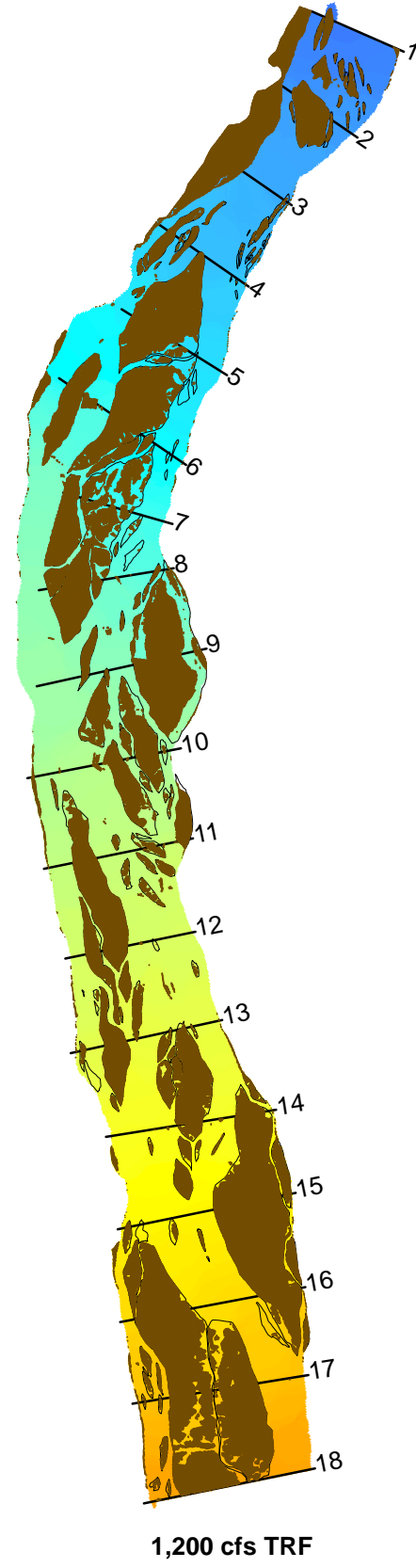


PLATTE RIVER RECOVERY IMPLEMENTATION PROGRAM		SHOEMAKER ISLAND FSM PROOF OF CONCEPT HALL COUNTY, NEBRASKA		JUNE 2015 HIGH FLOW MODEL TOPOGRAPHY	
PROJECT MGR. DLB	DESIGNED BY BP	DRAWN BY BP	CHECKED BY KMD	DATE AUG 2016	SCALE AS SHOWN
				PROJECT NO. 1499201	FILE NAME -
				DRAWING NO. -	FIGURE 1



Figure 2. Measured and Predicted Water Surface Elevation at 915 cfs TRF (750 cfs in Shoemaker Reach).



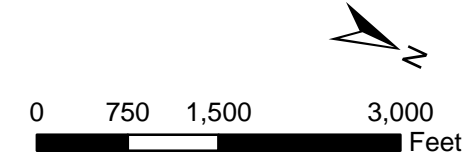
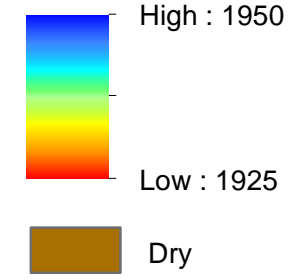


Legend

— Cross Section

□ Bars

Water Surface Elevation (ft, NAVD88)
(clipped to processing boundary)



**PLATTE RIVER RECOVERY
IMPLEMENTATION PROGRAM**

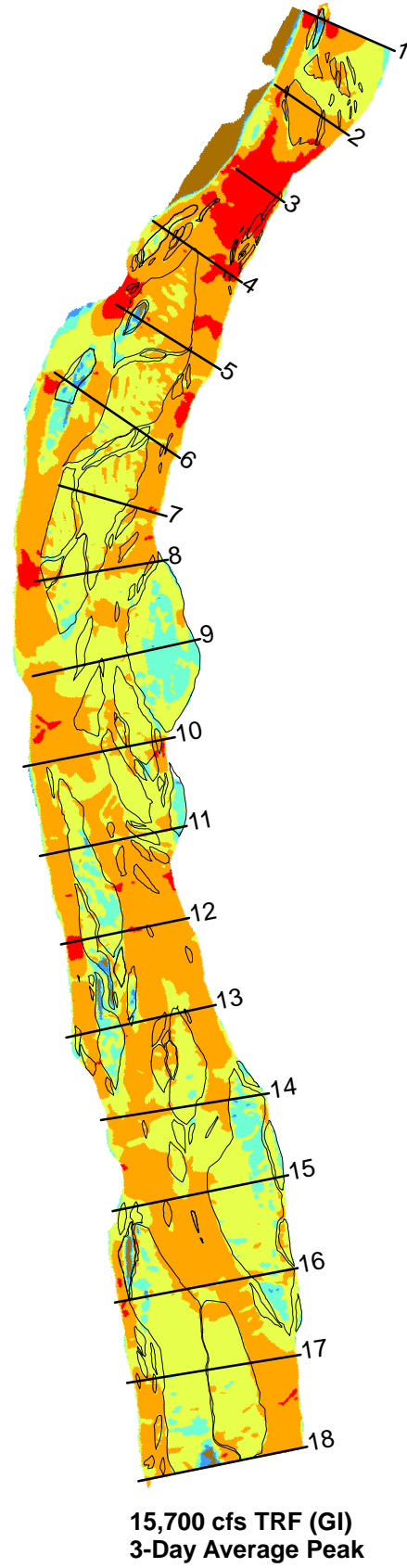
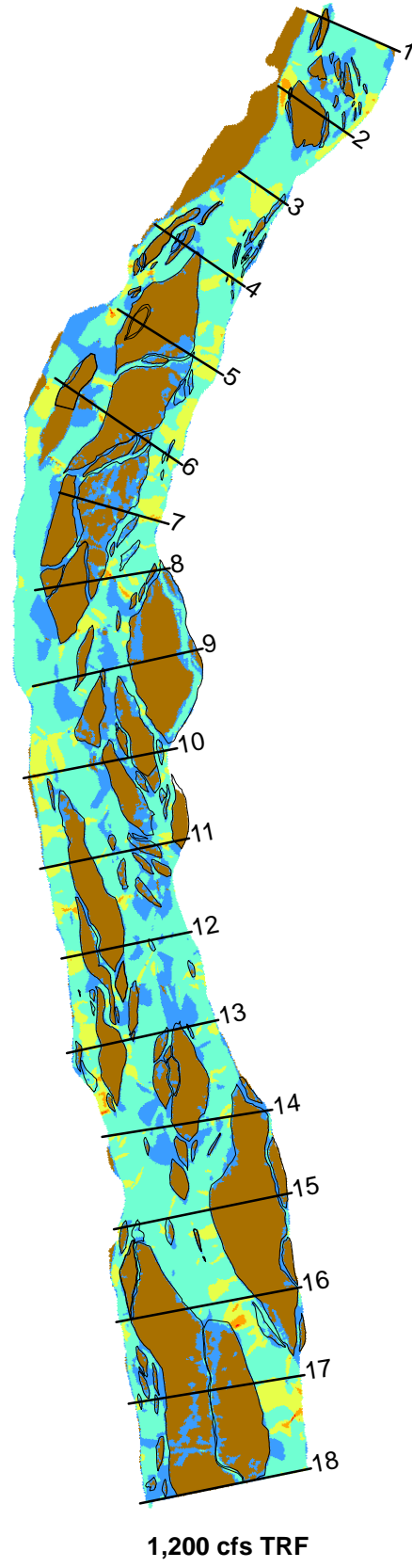
PROJECT MGR.	DESIGNED BY	DRAWN BY	CHECKED BY
DLB	BP	BP	KMD

DATE	SCALE
AUG 2016	AS SHOWN

PROJECT NO.
1499201

**FASTMECH FIXED BED MODEL
RESULTS WATER SURFACE
ELEVATION JUNE 2015 HIGH FLOW**

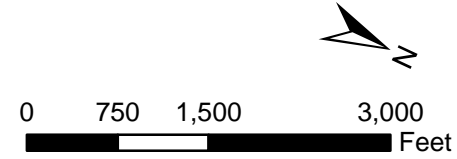
FILE NAME	DRAWING NO.	FIGURE
-	-	3



Legend

Velocity (feet/sec)

- Dry
- 0 - 1
- 1 - 2
- 2 - 3
- 3 - 4
- > 4
- Mapped Bars
- Cross Section



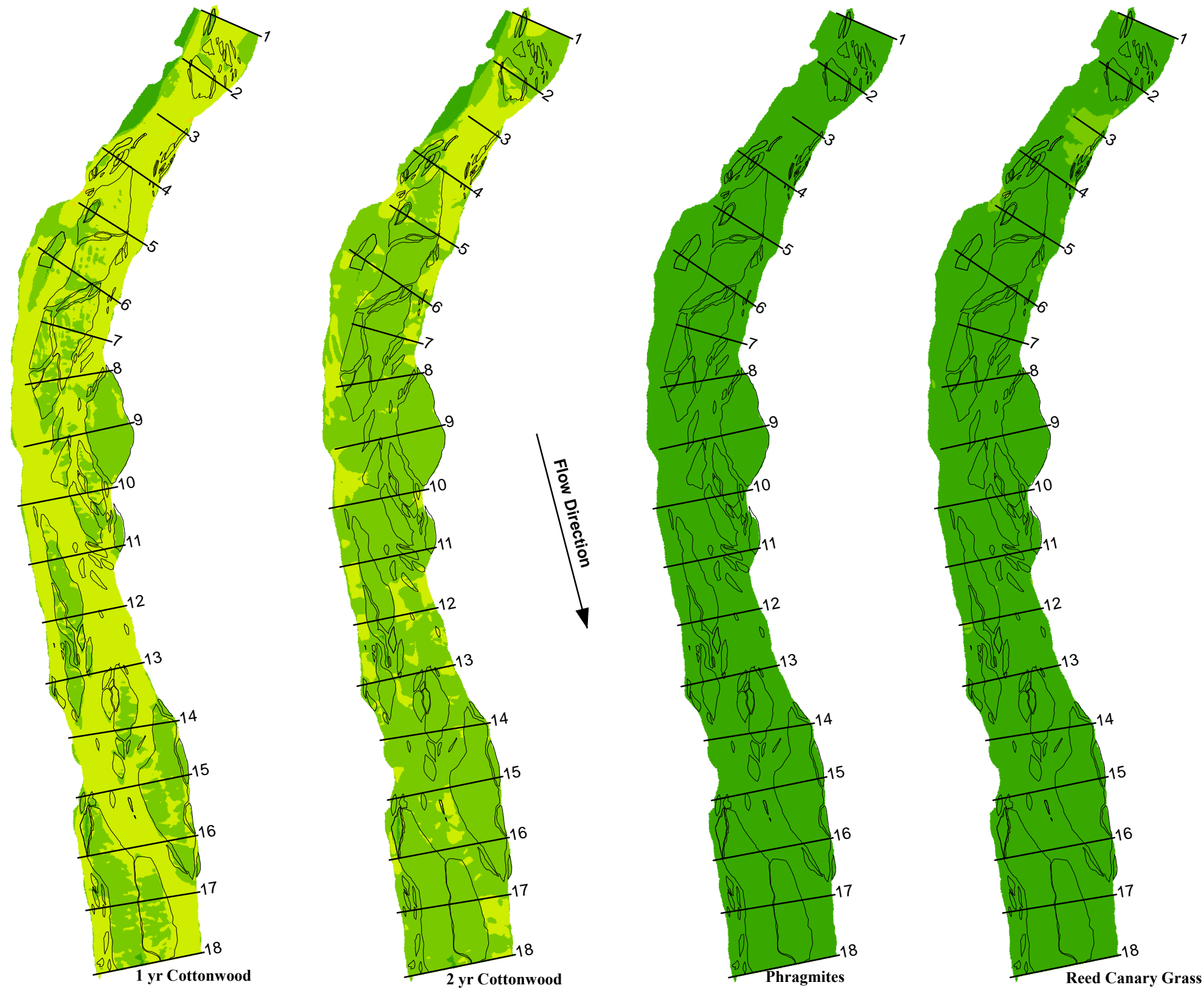
**PLATTE RIVER RECOVERY
IMPLEMENTATION PROGRAM**

**SHOEMAKER ISLAND FSM
PROOF OF CONCEPT**
HALL COUNTY, NEBRASKA

**FaSTMech Fixed Bed Model Results
Velocity June 2015 High Flow**

PROJECT MGR. DLB	DESIGNED BY BP	DRAWN BY BP	CHECKED BY KMD	DATE AUG 2016	SCALE AS SHOWN	PROJECT NO. 1499201	FILE NAME -	DRAWING NO. -	FIGURE 4
---------------------	-------------------	----------------	-------------------	------------------	-------------------	------------------------	----------------	------------------	-------------

2016-08-18 F:\State & Local\Other\Platte River Recovery Program\Projects\1499201 - Shoemaker FSM Proof of Concept\MXD\2015\Attachment\MXD\Figure 5 - Uprooted Vegetation.mxd EA-Lincoln_jpeterson



Legend

- Mapped Bars
- Cross-section

Velocity (feet/sec)

1-yr Cottonwood

- < 0.007 (no uprooting)
- 0.007 - 2.694 (uprooting initiated)
- 2.694 - 5.384
- 5.384 - 8.071
- 8.071 - 10.761
- > 10.761 (all plants uprooted)

2-yr Cottonwood

- < 0.023 (no uprooting)
- 0.023 - 3.507 (uprooting initiated)
- 3.507 - 8.15
- 8.15 - 15.262
- 15.262 - 20.341
- > 20.341 (all plants uprooted)

Phragmites

- < 34.777 (no uprooting)
- 34.777 - 43.389 (uprooting initiated)
- 43.389 - 52.001
- 52.001 - 60.614
- 60.614 - 69.226
- > 69.226 (all plants uprooted)

Reed Canarygrass

- < 4.396 (no uprooting)
- 4.396 - 10.509 (uprooting initiated)
- 10.509 - 16.617
- 16.617 - 22.73
- 22.730 - 28.839
- > 28.839 (all plants uprooted)

Velocities relating to the ability of drag forces to uproot patches of one-year old cottonwoods, two-year old cottonwoods, reed canarygrass, and phragmites. Velocity breaks are identical to research completed in the Elm Creek reach (Pollen-Bankhead et al., 2012), but are converted from meters/second to feet/second. Color scheme is consistent with Pollen-Bankhead et al, 2012 to facilitate direct visual comparisons. Velocities are from the June 2015 High Flow 3-day average peak flow (15,700 cfs TRF at Grand Island) FaSTMECH model.



		SHOEMAKER ISLAND FSM PROOF OF CONCEPT <small>HALL COUNTY, NEBRASKA</small>		FaSTMECH FIXED BED MODEL RESULTS VELOCITY JUNE 2015 HIGH FLOW	
		PROJECT NO. 1499201	DRAWING NO. -	FILE NAME -	FIGURE 5
PROJECT MGR. DLB	DESIGNED BY BP	DRAWN BY BP	CHECKED BY KMD	DATE AUG 2016	SCALE AS SHOWN



PLATTE RIVER RECOVERY IMPLEMENTATION PROGRAM

Shoemaker Island Flow-Sediment-Mechanical “Proof of Concept” Experiment

Mobile Bed Modeling: Year 3

Attachment II

FINAL

March 2017

Submitted to:

Platte River Recovery Implementation Program
4111 4th Avenue, Suite 6
Kearney, NE 68845

Submitted by:

Northern Hydrology and Engineering
PO Box 2515
McKinleyville, CA 95519



Table of Contents

I. INTRODUCTION.....	I-1
II. MODEL DEVELOPMENT	II-1
II.A. Model Domain and Grid	II-3
II.B. Model Inputs	II-3
II.B.1. Flow and Stage Boundary Conditions.....	II-4
II.B.2. Model Topography	II-4
II.B.3. Bed Roughness and Vegetation Drag.....	II-4
II.B.4. Horizontal Eddy Viscosity and Diffusivity Coefficient.....	II-5
II.B.5. Bed Material.....	II-6
II.B.6. Sediment Supply	II-6
II.B.7. Sediment Transport	II-7
II.C. Model Calibration and Evaluation	II-7
III. ANALYSIS METHODOLOGY	III-8
IV. RESULTS AND DISCUSSION	IV-10
IV.A. Effect of a SDHF	IV-10
IV.B. Effect of Hydrograph Shape on Bar Height and Area	IV-11
IV.C. Effect of Sediment Supply on Bar Frequency	IV-12
IV.D. Effect of Grain Size on Bar Height and Area	IV-12
IV.E. Potential for Vertical Erosion of Vegetated Bars	IV-13
V. CONCLUSIONS/SUMMARY.....	V-14
VI. RECOMMENDATIONS FOR FUTURE WORK.....	VI-14
VII. REFERENCES.....	VII-16



I. INTRODUCTION

Two mobile-bed models were developed for the Shoemaker Island reach of the Platte River to evaluate the response of channel morphology and vegetation patterns to a Short Duration High Flow (SDHF) release. The models were developed and calibrated to measured field data in Year 1 and 2 of the study (PRRIP, 2014 and PRRIP, 2015). The calibrated models are applied in Year 3 with a focused on informing following learning objectives:

1. Evaluate relationships between:
 - a. Sediment supply and frequency of sandbar occurrence
 - b. Grain size and sand bar height
 - c. Hydrograph (magnitude and duration) and sand bar height
2. Evaluate the relationship between peak flows (magnitude and duration) and riparian plant mortality.

II. MODEL DEVELOPMENT

The two models applied in the first two years of the study (PRRIP 2013, 2014), were; FaSTMECH (Flow and Sediment Transport with Morphological Evolution of Channels) and EFDC (Environmental Fluid Dynamics Code). The same models were applied in the final year of the study.

FaSTMECH was developed by Dr. Jonathan Nelson of the U.S. Geological Survey (USGS) and is included within the free software package, IRIC (International River Interface Cooperative) available at <http://i-ric.org/en/introduction>. IRIC is a river flow and riverbed variation analysis software package which combines the functionality of MD_SWMS (Multi-Dimensional Surface Water Modeling System), developed by the USGS (U.S. Geological Survey), and RIC-NAYS2D, developed by the Foundation of Hokkaido River Disaster Prevention Research Center. FaSTMECH is a two-dimensional, vertically averaged model. FaSTMECH contains a sub-model that calculates the vertical distribution of the primary velocity as well as the secondary flow about the vertically averaged flow. The vertically averaged equations used in the computational solution are cast in a channel-fitted curvilinear coordinate system. The approach uses the assumptions that: (1) the flow is steady (or at least does not vary appreciably over short time scales), (2) the flow is hydrostatic (vertical accelerations are neglected), and (3) the turbulence can be treated adequately by relating Reynolds stresses to shear stresses using an isotropic eddy viscosity. Several sediment transport equations are included within the model interface. Development of the model equations is described in Nelson and Smith (1989), while the numerical techniques and the streamline-based vertical structure sub-model are discussed by Nelson and McDonald (1996). FaSTMECH has a long record of accurately predicting local flow conditions and morphological change in a variety of rivers (Andrews and Nelson, 1989; Lisle et al., 2000; Conaway and Moran, 2004; Barton et al., 2005). In addition, FaSTMECH differs from many other mobile-bed models by employing a quasi-steady approximation which enables predictions over longer time frames, finer grid resolutions and longer reaches.



Primary strengths of FaSTMECH based on PPRIP (2014):

- FaSTMECH utilizes a computation algorithm that significantly reduces computational time.
- Bed change over a hydrograph is simulated as a series of quasi-steady approximations which significantly reduces computational time.
- Sediment supply is computed at the model boundary with a transport equation, removing the requirement for sediment transport measurements. This feature is particularly useful in areas that do not have a sediment rating curve developed over the range of flows of interest, such as the Shoemaker Reach at the start of the study.
- Sediment supply can be increased or decreased at the model boundary by applying a multiplication factor. This feature allows efficient evaluation of the effects of increasing or decreasing sediment load into the reach (Learning Objective 1).
- Bed changes predicted by FaSTMECH appeared reasonable for the 2013 SDMF.

Primary limitations of FaSTMECH:

- Changes in the grain size distribution of the sediment supply cannot be specifically modeled because the grain size distribution is not specified, however, increases or decreases in the typical grain size can be modeled (Learning Objective 1).
- The grain size distribution of the bed is simplified into a single value. Processes related to variable grain size distributions (e.g. armoring) are not modeled.
- Grain size of the bed and sediment supply cannot be set to different values (e.g. a finer sediment supply cannot be modeled with a coarser initial bed).
- Sediment transport calculations are limited to total load (suspended load + bedload). Thus, direct comparisons with measured data, such as suspended sediment concentrations, cannot be made.
- Lateral erosion and bank collapse are not supported.

EFDC is an Environmental Protection Agency (EPA) supported modeling system for simulating three-dimensional, two-dimensional, or one-dimensional flow, transport and biogeochemical processes in surface waters including rivers, lakes, wetlands, estuaries, and coastal regions. The EFDC model internally links to cohesive and non-cohesive sediment transport sub-models. EFDC solves the three-dimensional (or two-dimensional), vertically hydrostatic, free surface, Reynolds averaged equations of motion for a variable-density fluid. EFDC uses a curvilinear-orthogonal grid in the horizontal domain and a sigma grid in the vertical. EFDC was originally developed at the Virginia Institute of Marine Science by Dr. John Hamrick (Hamrick, 1992), and full documentation of the EFDC model can be found in Tetra Tech (2007a, 2007b and 2007c). Proprietary pre- and post-processing software was used for EFDC model runs (EFDC_Explorer7.1, Craig, 2013).

Primary strengths of EFDC based on PPRIP (2014):

- Specification of sediment supply is user defined, thus, the grain size distribution of the sediment supply can be different than the grain size distribution of the bed material.
- Field measurements of stem diameter, density and height are used to calculate vegetated drag.



- Vegetation resistance is integrated into the momentum equations resulting in reductions to velocity, bed shear stress and diffusion in vegetated areas. Thus, shear stress is correctly partitioned when applying variable roughness due to vegetation.

Primary limitations of EFDC:

- Number of computation grid cells appears to be limited to roughly 100,000 for mobile bed modeling, limiting grid size to about 5-meters. This limitation may be related to our specific version and hardware combination.
- Computational time is limiting even for a relatively coarse model grid (~10-meters). Small time steps (0.2 to 0.4 seconds) are required for mobile-bed model runs. Using a multi-threaded version of EFDC, run times range from approximately 28 to 70 hours to complete depending on the simulation. Run times are likely two to three times longer using the public domain single-threaded version of EFDC.
- Lateral erosion and bank collapse are not supported.

II.A. Model Domain and Grid

EFDC was configured with a two-dimensional curvilinear orthogonal grid consisting of 27,128 grid cells, with an average grid cell measuring 30.05 x 31.48 feet (9.158 x 9.596 meters) in the x and y direction, respectively. The FaSTMECH model grid is curvilinear and grid cell widths are 9.8 feet (3 meters) with 378,873 grid cells. A finer grid resolution can be modeled with FaSTMECH due to the computation efficiency of the program. Differences in grid resolution between the 9.8 feet (3m) and 32.8 feet (10 meters) are shown in Figure 1. The coarser grid applied in EFDC retains the definition of the larger channels, but loses definition of the smaller bars that are defined at the 9.8 feet (3m) grid resolution applied in FaSTMECH.

II.B. Model Inputs

Mobile-bed models require the following inputs: flow at the upstream boundary, water surface elevation at the downstream boundary, topography, roughness, and grain size of the bed material. The level of detail required for specification of the bed material varies between models. Mobile-bed models vary in their requirements for specification of sediment supply. Some models do not require any specification of sediment supply (e.g. FaSTMECH), while others require detailed specifications of quantity and caliber of sediment delivered to the reach (e.g. EFDC). Models that do not require detailed specification rely on transport equations to estimate the incoming sediment supply. Mobile-bed models have more user-specified computational parameters, which slow the speed of the computations. Mobile-bed models employ different smoothing algorithms to predicted bed changes. Representation of the three-dimensional effects of secondary flows are critical for mobile-bed modeling. Input parameters related to the estimation of secondary flows vary between models. Some of these input parameters were adjusted during model calibration. Only the final calibrated or assumed model parameters and boundary condition adjustments are described herein.



II.B.1. Flow and Stage Boundary Conditions

Discharge magnitude is reported as “Total River Flow (TRF)” but the actual flow through the Shoemaker study site is typically around 80 percent of the TRF due to a flow split upstream (Table 1). A rating curve was applied for SDHF runs using paired measurements of stage and discharge during the 2015 high flow. Hydrographs for (1) SDMF 2013, (2) natural high flows in 2014 and (3) 2015, and (4) a hypothetical SDHF are provided in Figure 2.

II.B.2. Model Topography

The model topography is based on the pre-2014 High Flow topography. This data set was developed by combining November 2013 LiDAR, May 2014 ground surveys and estimates of bars that were constructed at the project site (Figure 3). Due to the more complete coverage, the LiDAR data set is used as the base topography, and the ground surveys are used to supplement LiDAR data where no data was captured (within the wetted channel).

LiDAR was flown on November 10, 2013. The average daily flow through the study reach was estimated to be 500 cfs (80% of daily mean discharge at USGS 06770200 Platte River near Kearney, Nebr.). LiDAR derived elevations matched surveyed elevations with sufficient accuracy and no adjustment to the LiDAR elevations was performed. LiDAR data was used in all areas that were dry during the LiDAR flight, except where bars were constructed by PRRIP. The LiDAR contractor provided hydro-breaklines which delineate the interface between water and dry land. Wet areas between these hydro-breaklines consisted of a hydro-flattened surface which approximates the water surface during the LiDAR flight.

Aerial imagery collected during the LiDAR flight indicated that the topography of wetted areas is complex and consist of various sized dunes of different wavelengths, deep areas near channel confluences, and bars of varying sizes and shapes. Ground surveys were used to estimate a simplified channel geometry in the inundated areas. The density of ground survey points varied spatially. Ground survey data consisted of longitudinal profiles through numerous major channels, cross section surveys, and bar topographic surveys, which included the top and toe of the bars. Numerous smaller channels had little to no survey data, while some larger channels were better defined.

In summary, the final model topography consisted primarily of a LiDAR derived digital elevation model (DEM). Within the wetted channel regions of the DEM, ground survey data was used to develop an approximation of the channel bed. The channel topography and constructed bars were added to the LiDAR DEM. This hybrid surface is referred to as “model topography”.

II.B.3. Bed Roughness and Vegetation Drag

The formulation of channel and floodplain roughness varies between models. Roughness was used as a calibration parameter in the fixed bed runs to match measured water surface elevations. Variable roughness due to grain size was not considered because there were not sufficient data to



justify stratification. Roughness variation due to vegetation was not included in FaSTMECH model runs.

FaSTMECH utilizes a drag coefficient which was estimated using Manning's roughness coefficient (n), mean flow depth (h) and gravity (g) using the following relation (FaSTMECH Solver Manual):

$$C_d = \frac{n^2 g}{h^{1/3}}$$

The adjusted parameter for bottom friction in EFDC is the effective bed roughness height (Z_0). This value represents the total roughness due to skin friction and form drag, and is generally represented by bed physical properties. Based on the bed physical data described previously and literature values (Ji, 2008; Tetra Tech, 2007a and 2007b), a constant Z_0 value of 0.016 feet (0.005 meters) was used within the model domain.

Vegetation resistance formulation in EFDC was used (Moustafa and Hamrick, 2000) to account for frictional resistance effects on the flow field from the vegetated islands and floodplain. Data required to incorporate the EFDC vegetation resistance formulation includes plant density, stem diameter and stem height. Required input data for the vegetated islands were measured and consolidated into 11 vegetation community types by similar plant characteristics. The plant density, stem diameter and stem height of the 11 vegetation community types (Table 2) were then assigned to the model grid via vegetation polygons (Figure 4).

Following completion of the June 2014 model runs, an error was identified in the roughness parameters for bars that were inundated at high flows. The inundation of these surfaces is relatively shallow and the errors in the vegetation drag are not expected to substantially change the outcome of the larger scale sedimentation patterns.

II.B.4. Horizontal Eddy Viscosity and Diffusivity Coefficient

Horizontal eddy viscosity and diffusivity were set to zero for the EFDC simulations. It was assumed that the numerical diffusion associated with the EFDC model is likely similar in magnitude to realistic viscosity and diffusivity coefficients due to the fine grid resolution.

FaSTMECH requires an input of a lateral eddy viscosity. The lateral eddy viscosity (LEV) is a correction to the eddy viscosity used in the vertically averaged equations to treat lateral separation eddies. LEV can be estimated using the following equation:

$$\text{LEV} = 0.1 \times \text{average depth (meters)} \times \text{average velocity (meters/second)}.$$

A reach-average value of 0.05 was estimated and applied.



II.B.5. Bed Material

Bed material samples collected throughout the study reach in May 2014 (n=22) were used to parametrize EFDC for the SDHF high flow model runs. A wide range of grain size distributions were measured throughout the reach; however, no systematic variations between bed material samples collected within the low flow channels and on higher bars were detected in the grain size analysis. Thus, the samples were composited into a single grain size distribution that was applied throughout the model domain (Figure 5).

Specification of variable grain size requires the gradation to be divided into size classes and the effective grain size in each class to be specified. Six sediment classes were defined for the EFDC model (Table 3): one cohesive class, and five non-cohesive classes. The effective diameters (d_{eff}) for each class were determined using the average of the weighted median, weighted geometric mean and weighted critical shear velocity methods based on the sediment grain size distributions, as described by Hayter (2006).

The EFDC bed was initially divided into 6 layers. Each layer has the same material properties (grain size distribution, porosity or void ratio and bulk density), but layer thickness varies (Table 4). The layer thickness can affect the tracking of the grain size changes at the surface and within the subsurface as sediment is removed or deposited within a layer. The top (parent) layer thickness (Layer 6) was defined by the thickness of the armor layer (when present) in field samples. Layers 5, 4, 3 and 2 are approximately the size of the bedforms that were observed to be in transport during the SDMF. The final layer (Layer 1) is substantially thicker to ensure that the scour depth did not exceed the bed thickness.

The applied porosity was 0.37, and the wet bulk density of the bed material was 127.3 lb/ft³ (2039 kg/m³) for all model runs.

II.B.6. Sediment Supply

FaSTMECH does not require users to specify the sediment supply. This model internally computes the sediment transport rate at the upstream boundary from the applied transport equation. The sediment transport rate at the boundary, thus sediment supply, can be adjusted within the model interface by multiplying the predicted rate by a factor. The model cannot accept user-specified sediment concentrations and gradations (e.g. field measurements). FaSTMECH uses a single grain size for sediment transport calculations.

EFDC requires a user-specified sediment supply at the upstream boundary. All sediment supplied (bedload and suspended load) is assigned as a suspended sediment concentration (SSC) for each of the user defined sediment classes (Figure 6). Grains that are too coarse to be carried in suspension at the model discharge fall to the bed and are deposited or transported as bedload. Data collection and computational methods to develop the sediment supply (concentrations) for 2015 are provided in the main report (PRRIP, 2017).



II.B.7. Sediment Transport

FaSTMECH has three sediment transport equations: Yalin (bedload equation), Engelund-Hansen (total load) and Wilcock-Kenworthy (two-fraction model). The Engelund-Hansen total load transport equation was selected as it is generally suitable for sand bed rivers. The total boundary shear stress applied in the sediment transport equation is calculated as a combination of skin friction and form drag. The form drag component can be defined using the physical characteristics of the dunes (sand dune height and wavelength). This option essentially reduces the applied shear stress to the bed that is used in the sediment transport calculation. A dune height of 3 feet was applied. A gravitational correction was applied using the pseudo-stress method with a submerged angle of repose set to 12 degrees.

EFDC has numerous sediment transport equations, parameters, and options that can be specified. Key sediment transport model parameters, applied values, and literature sources are provided in Table 5. Bed shear stress was separated into cohesive and non-cohesive fractions within the EFDC model. The Krone (1963) probability of deposition approach using the cohesive grain stress was used for cohesive suspended sediment transport within the EFDC model. The Van Rijn (1984) near-bed equilibrium concentration formulation was used for non-cohesive suspended sediment transport. Non-cohesive settling velocity, critical shear stress and critical Shields stress were determined internal to the EFDC model using the approach of Van Rijn (1984). The modified Engelund-Hansen bedload function (Wu, 2008) was used for non-cohesive bedload transport using default parameters. To reduce computation time, the bed morphology was updated every four time steps.

II.C. Model Calibration and Evaluation

Both mobile-bed models were compared to the measured water surface elevations and channel changes that occurred during the 2013 Short Duration Medium Flow (SDMF) and the June 2014 high flow. The results of the calibration and evaluations were initially reported in PRRIP (2014) and PRRIP (2015) and are summarized below.

FaSTMECH and EFDC were calibrated to the measured water surface elevations. FaSTMECH predicted water surface elevations a root mean square error (RMSE) of 0.18 feet when compared to measured values for higher flows (4366 -7200 cfs) (Figure 7). RMSE is higher for low flow with a value of 0.36 feet. There is a localized area of poor predictions which are likely due to poor representation of topography in the low flow channel. EFDC predictions have a mean bias of 0.30 feet for high flow (7200 cfs).

EFDC provided reasonable estimates of cut and fill for the fall 2013 high flow and excellent results for the June 2014 high flow (PRRIP, 2015). However, EFDC tended to predict the development of longer, deeper pools and a tendency toward incision over much of the reach for both the fall 2013 and June 2014 high flows. The tendency toward incision may be a result of a poor sediment supply boundary condition, inability to predict lateral erosion, or other physical processes governing sediment transport and barform evolution. Recognizable barforms that coalesced and migrated downstream were not predicted by the model. The lack of this type of



barform development is likely due at least in part, to the size of the model grid (10 meters) and/or lack of other physical processes governing sediment transport and barform evolution.

FaSTMECH provided reasonable estimates of cut and fill during the June 2014 high flow, but predicted a net fill, rather than a minor net cut as measured. FaSTMECH predicted a bed profile that closely matched the scale of the measured bar forms and maintained the overall grade of the channel. Barforms within the wetted channel were formed over the course of the model run in a similar spatial scale and vertical amplitude to those observed from aerial photography (Figure 8), measured during the 2013 SDMF (PRRIP, 2014), and measured prior to the June 2014 high flow (PRRIP, 2015).

FaSTMECH also provided a reasonable estimate of the total bar area compared to measured values following the June 2014 high flow; however, the frequency of new bars and new bar area was under-predicted by FaSTMECH (PRRIP, 2015). This result is contrary to the initial hypothesis in 2013 that FaSTMECH may be over predicting bar formation. This change may be due to differences in post-processing model results of the 2013 SDMF and the June 2014 high flow or due to modifications to the June 2014 high flow model parameters. A gravitational correction factor was applied in the June 2014 high flow model run which resulted in the widespread formation of bar forms that migrated downstream. In the 2013 SDMF model run, recognizable barforms did not occur. In addition to the potential effects of changes to model parameters, the inability of FaSTMECH to laterally erode limits channel widening and new bar development within the widened channel. Examples of channel widening and new bar development (Figure 9) occurred in the middle treatment reach during the June 2014 high flow (PRRIP, 2015). Predicted bar height was generally within 0.5 feet of the measured values which is within the reported error of the LiDAR data.

Lateral erosion predictions conducted with BSTEM in PRRIP (2014) indicated that flow duration has a particularly strong effect on lateral erosion which is a known limitation of the mobile-bed models. Thus, the mobile-bed models used in this study (EFDC and FaSTMECH) are expected to perform better over shorter durations when lateral erosion has less of an effect on channel change.

III. ANALYSIS METHODOLOGY

Model runs in 2015 focused on estimating the channel response to SDHF and sensitivity to changes in hydrograph shape (magnitude and duration), grain size and sediment supply. The effect of hydrograph shape is analyzed using hydrographs that have the same volume of water (60,000 acre-feet), but have different peak magnitude and flow duration. A peak flow of 8,000 cfs, for 3-days is compared to a peak flow of 5,000 cfs for ~6.5 days using FaSTMECH. The effect of grain size is estimated using grain sizes of 0.75 mm, 1 mm, and 2 mm using FaSTMECH. The effect of sediment supply is estimated using twice the equilibrium sediment supply (2x), equilibrium sediment supply (1x), and half the equilibrium sediment supply (0.5x) using FaSTMECH. The effect of sediment supply is also estimated with EFDC using grain-size specific sediment rating curves derived from direct measurements at the project site using EFDC. Effects of these variables (sediment supply, grain size and hydrograph shape) are evaluated for:



1. Populations of all bars (sand and vegetated) following the SDHF. This analysis is intended to demonstrate reach wide effects on all bars (Figure 10).
2. Populations of sand bars following the SDHF. This analysis removes the influence of vegetated bars which may be less sensitive to the variables due to higher stability. The analysis is focused on the response of sand bars, which is the target bar type to meet biological objectives.
3. Populations of new sand bars. This analysis focuses on new sand bars created during the high flow, which are expected to be most responsive to changes in variables.

Bars are portions of the river channel that are higher than the 1,200 cfs TRF water level. Bar area is computed as the two-dimensional area of the bar surface. New bars are defined as bars that are present at the end of the event that were not present at the beginning of the event. No portion of a new bar may intersect any portion of a pre-existing (old) bar. New depositional areas that are adjacent to an existing bar are simply added to the pre-existing bar even if they do not share the same cover type. For example, if a sand bar is deposited at the toe of an existing vegetated bar, the new deposition will be reported as an increase in area of the vegetated bar. This methodology is equivalent to analyses conducted in the Year 2 (PRRIP, 2015), but differs from the Year 1 (PRRIP, 2014) report.

In FaSTMECH, bars are composed of 3-meter grid cells, while in EFDC bars are composed of 10-meter grid cells, thus the number of bars, particularly small bars, will vary due to model grid resolution.

Bar statistics are computed on a cell by cell basis, then averaged for each bar. Height at each grid cell is computed by subtracting the elevation of the cell from the predicted water surface elevation at 1,200 cfs TRF at the same location. Height is a positive value. Mean bar height is computed by averaging the height of all cells in each polygon. Mean bar height can change by changes to the bar such as: (1) direct erosion of an existing bar (e.g. vertical erosion), (2) deposition on top of an existing bar, and/or (3) deposition adjacent to the existing bar. Mean bar height may increase without deposition on the bar if lower areas of the bar are eroded. Mean bar height may decrease without erosion of the bar if deposition occurs that has a lower elevation than the rest of the bar.

The depth of each cell is computed by subtracting the predicted water level at the peak stage at each cell from the elevation of each cell. If the elevation of a cell is lower than the peak stage height the depth is recorded as a negative value, if the height is above the peak stage, depth is recorded as a positive number. Mean bar depth is computed by averaging the depth of all the cells within each polygon.

Each of the data sets (bar height and area) were tested for normality with the Shapiro–Wilk test. None of the data sets are normally distributed. Thus, a non-parametric test was applied to determine whether there was a statistical difference between bar height and bar area following the SDHF. Statistical tests were applied to “all bars” which include sand and vegetated bars, “sand bars” which excludes vegetated bars and “new bars” which were formed during the SDHF.



When two data sets were compared, Mann-Whitney-Wilcoxon test was applied and when three or more data sets were tested, Kruskal-Wallis test was applied. Both methods test whether samples originate from populations with the same distribution. The null hypothesis is that it is equally likely that a randomly selected value from one sample will be less than or greater than a randomly selected value from a second sample. The significance level is set at a p-value of 0.05.

All boxplots presented in this study were generated using R's default boxplot code, in which upper whisker lengths are extended to the maximum data value when no outliers present, or to the 75th percentile value plus 1.5 times the interquartile range when outliers present. Likewise, lower whisker lengths are extended the minimum data value when no outliers present, or to the 25th percentile value minus 1.5 times the interquartile range (when outliers present). The bottom of the box is the 25th percentile, the top of the box is the 75th percentile and the line through the box is the median (50th percentile).

IV. RESULTS AND DISCUSSION

The effects of hydrograph shape, bed material grain size and sediment supply on the bar frequency, height and area were evaluated for the hypothetical SDHF. A hydrograph with a 3-day peak of 8,000 cfs that contains ~60,000 acre-feet of water, a bed material grain size of 1 mm, and a sediment supply that is equivalent to an “equilibrium” supply is used as the basis for comparison of FaSTMECH runs. FaSTMECH is used to evaluate effects of hydrograph shape, bed material grain size and sediment supply.

The same hydrograph applied to the FaSTMECH runs is also used in the EFDC runs. Bed material grain size differs within the EFDC model because it is defined by multiple grain size classes which more closely matches the measured bed material. Grain size specific sediment rating curves developed from paired measurements of sediment concentrations and flow is used to define the sediment supply, rather than an equilibrium supply in EFDC. EFDC is only used to verify effect of sediment supply.

IV.A. Effect of a SDHF

A hypothetical SDHF with a peak flow of 8,000 cfs for 3 days with a total volume of water of ~60,000 acre-feet, a bed material grain size of 1 mm and a sediment supply equivalent to an “equilibrium” sediment supply is used as a basis for comparison for effects of hydrograph shape, grain size and sediment supply. This run is referred to as the “base case”.

FaSTMECH predicted a total cut of 90,000 CY and fill of 94,000 CY with a net fill of 4,000 CY during the SDHF, indicating the reach is roughly at equilibrium (Table 6). The net fill is likely due to low relief bar formation on the otherwise plane bed channel present in the initial topography (Figure 8). The overall acreage of bars declined slightly from 175 acres before the SDHF to 169 acres after the SDHF.

The total number of bars decreased substantially from 303 bars before the SDHF to 177 bars following the SDHF (Figure 11). Bar frequency declined primarily due to direct erosion of very



small bars or translation of these small bars far enough downstream that they did not intersect with the original bar location (126 bars), accounting for a total of 2.5 acres of change. Many bars merge with adjacent bars which accounts for the decline of an additional 35 bars. A statistically significant (p -value = 0.04) increase in individual bar areas occurred due to erosion of the smaller bars and merging of adjacent bars (Table 7). Total new bar area was 0.9 acres following the 8,000 cfs SDHF. New bars were generally small. Only one bar was close to reaching the biological target of 0.25 acres.

A very small (<0.1 feet), but statistically significant (p -value=0.03), increase in mean bar height occurred following the SDHF. The maximum mean bar height of new bars was less than 0.6 feet (Figure 12 and Figure 13) which does not meet the biological objective of 1.5 feet.

IV.B. Effect of Hydrograph Shape on Bar Height and Area

The effect of hydrograph shape is evaluated using hydrographs that have the same volume of water (~60,000 acre-feet), but have different peak magnitude and flow duration. A peak flow of 8,000 cfs for 3 days (base case) is compared to a peak flow of 5,000 cfs for ~6.5 days using FaSTMECH.

The SDHF hydrographs both produce a large amount of cut and fill throughout the study reach (Table 6). The 8,000 cfs hydrograph produces roughly 17% more cut and 19% more fill than the 5,000 cfs hydrograph. Both hydrographs result in a small net fill, which was likely due to low relief bar formation on the otherwise plane bed channel present in the initial topography as stated earlier.

The total number of bars increased by 3 following a 5,000 cfs SDHF compared to the 8,000 cfs SDHF (Figure 11). Total bar area decreases from 175 acres, to 166 acres and 169 acres, respectively, following a 5,000 cfs and 8,000 cfs TRF SDHF. The results of the statistical tests indicate there is not a statistically significant difference between populations of bar heights or bar areas due to the hydrograph shape of the SDHF (Table 7).

The difference in sand bar frequency following a 5,000 cfs and 8,000 cfs is small (140 bars following a 5,000 cfs peak flow versus 134 bars following an 8,000 cfs peak flow). While the median bar height appears slightly higher following an 8,000 cfs peak flow, the populations are not statistically different between the two flows (Figure 14 and Table 7)

The difference in number of new bars formed is minor, with 32 new bars formed following the 5,000 cfs SDHF and 30 bars formed following the 8,000 cfs SDHF. Total new bar area is 0.5 acres following the 5,000 cfs SDHF and 0.9 acres following the 8,000 cfs SDHF. New sand bars are less than 0.07 acres following the 5,000 cfs SDHF, and less than 0.23 acres following the 8,000 cfs SDHF (Figure 13 and Figure 14). In both cases, no bars met the biological target of 0.25 acres. Mean new sand bar heights are less than 0.5 foot above the 1,200 cfs water surface elevation for both hydrographs. These heights are substantially less than the biological target of 1.5 feet. Although there appears to be a tendency for higher bar heights and larger bar areas associated with a higher peak discharge, the populations are not statistically different (Table 7).



New bars are formed 0.4 to 1.7 feet below the peak stage with a median depth of 1.2 feet at 5,000 cfs, while bars that formed during the 8,000 cfs SDHF formed 0.6 to 2.3 feet below the peak stage with a median value of 1.7 feet (Figure 15).

New bars formed during the 5,000 cfs and 8,000 cfs TRF SDHF were all lower and smaller than needed to achieve biological objectives of 0.25 acres and 1.5 feet above the 1,200 cfs TRF water level. Overall, bars on the reach scale did not change substantially with a single SDHF. It is possible that multiple events could produce a statistically significant difference in bar height and area, however; the results of the field study indicate the potential differences are relatively small. Hydrographs within the range of the target SDHF do not appear to be sufficient to achieve biological objectives.

IV.C. Effect of Sediment Supply on Bar Frequency

The effect of sediment supply on bar frequency was evaluated with FaSTMECH and EFDC during a SDHF with a peak flow of 8,000 cfs TRF for 3 days. Sediment supply was doubled and reduced by half compared to the base case. Sediment supply was adjusted in FaSTMECH by modifying the equilibrium sediment supply and in EFDC by modifying the measured sediment concentrations.

Both models predicted negligible changes to bar frequency, height, and area in response to a change in the upstream sediment supply during one SDHF. FaSTMECH predicted a difference of 1 bar between the cases of half and double the equilibrium supply during a SDHF (Figure 16) and a difference of 4 bars across all cases for sand bars and new sand bars (Figure 17 and Figure 18). Some small differences occur in the total area of bars, lower sediment supply resulting in slightly more new bar area and higher bars (Figure 19 and Figure 20), but these difference are not statistically significant (Table 8).

The most significant changes occurred at the project boundary in EFDC, which resulted in accumulations of sediment in the form of a delta as observed in previous years' model predictions (PRRIP, 2014, 2015). These sediment accumulations were localized and did not translate through the project reach during the SDHF. A significantly longer duration simulation is likely necessary to observe the long-term impacts of changes in sediment supply.

IV.D. Effect of Grain Size on Bar Height and Area

The effect of bed material grain size on bar height and area was evaluated with FaSTMECH during a SDHF with a peak flow of 8,000 cfs TRF for 3 days. Bed material grain sizes of 0.75 mm, 1 mm (base case) and 2 mm were evaluated.

Bed material grain size affects the predicted amount of scour and fill, total number of bars, number of new bars and bar area. Reducing the bed material size from 1 mm to 0.75 mm increases cut by 22% and fill by 21%. Coarsening the bed material from 1 mm to 2 mm decreases cut by 42% and fill by 40% (Table 6).



The total number of bars decreases substantially from the initial condition of 303 bars to 177 bars following an 8,000 cfs TRF SDHF for the base case (grain size = 1 mm). As discussed in the previous section, bar frequency declines due to merging of bars, erosion of smaller bars or downstream translation of bars. The decline in bar frequency for finer bed material (0.75 mm) is less pronounced (a reduction from 303 bars to 215 bars), but there is not a clear trend associated with increasing grain size (Figure 21). In the case of the finer grain size (0.75 mm), the erosion of smaller bars appears to be somewhat offset by new bar development and a more active bed. As grain size is increased, the bed is less active and the higher bar frequency of bars in the coarser bed (188 versus 177) may be a result of a less active bed that resulted in less erosion of the smaller bars.

Total bar area decreases from 175 acres to 169 acres with a bed material grain size of 1 mm. Decreasing the grain size to 0.75 mm results in a bar area of 173 acres, and increasing the grain size to 2 mm results in a decline in bar area to 166 acres. Thus, greater total bar areas result with finer grain sizes, with a total difference in bar area of about 4%.

The populations of average bar height and bar area for all bars (sand bars and vegetated bars), for sand bars with grain sizes ranging between 0.75 and 2mm, are not statistically different (Figure 21, Figure 22, and Table 9)

The number of new bars formed during the SDHF is substantially larger with a finer grain size (74 new bars with a 0.75 mm grain size versus only 9 new bars with a 2 mm grain size) (Figure 23). Total new bar area also increases with finer grain size (1.7 acres for 0.75 mm, 0.89 acres for 1 mm, 0.12 acres for 2 mm grain size) (Figure 24). However, these differences in total area are quite small relative to the total bar area in the project site, representing a change of less than 1% of the total bar area. There appears to be a trend of higher and larger bars with decreasing grain size (Figure 23, Figure 24, and Figure 25); however, the differences between the populations are not statistically significant (Table 8).

In all grain size cases, none of the bars met the biological target of 0.25 acres; however, one bar nearly met the target at 0.23 acres (0.75-mm grain size). Similarly, none of the bars met the height target of 1.5 feet above the 1,200 cfs water level for 1 mm and 2 mm grain size, and only one bar exceeded an average height of 1.5 feet when the bed material was 0.75 mm (Figure 24). Generally, average heights of bars were substantially lower than the target heights, with median heights of 0.1 feet or less.

While grain size appears to have an important effect on sediment transport, reflected in the total cut and fill that occurred throughout the project site and bar frequency, it does not appear to have a significant impact on bar height area during one SDHF.

IV.E. Potential for Vertical Erosion of Vegetated Bars

The potential for riparian plant mortality by drag forces and vertical scour across bars was evaluated in Attachment I. The mobile-bed predictions are generally lower than the empirical



relation (fixed-bed model) because the fixed-bed results represent “scour potential” or the maximum scour observed for a given shear stress during the study period. Mobile-bed predictions are generally lower than the “maximum” scour potential because shear stress is only one factor that contributes to scour in the mobile bed model. Transport from each cell is computed based on an empirical equation (Engelund-Hansen) that is a function of shear stress and a friction factor. The mobile-bed model performs a mass balance calculation between the amount of sediment entering a cell (from upstream cells) and the amount of sediment exiting the cell. If the amount of incoming sediment is less than the amount of sediment transported out of the cell, scour occurs. If the amount of incoming sediment is more than the amount of sediment transported out of the cell, fill occurs. Thus, for any given shear stress the mobile-bed model may predict scour, fill or no change, depending on the amount of sediment delivered from an upstream cell(s).

The results of both analyses (fixed-bed and mobile-bed) indicated that the potential for vertical scour of deeply rooted vegetation is low. Most of the bar area has predicted scour depths of less than 1 foot (Figure 26) and median values are well below 0.5 feet.

V. CONCLUSIONS/SUMMARY

The results of the mobile-bed modeling analysis indicate that SDHF events are not likely to create bars with sufficient height or areas to achieve biological objectives. While there were differences in sediment transport (cut/fill) and total number of bars formed, the relative changes in bar area and height during a SDHF were minor. Differences in peak magnitude (5,000 cfs - 8,000 cfs) and duration of peak flow (3 - 6.5 days), grain size (0.5, 1 mm, 2 mm) and sediment supply changes (0.5 – 2x sediment supply) did not produce statistically significant changes in the bar forms created during the SDHF. These results are limited to the effect of one SDHF event. It is possible that some of these parameters may have a long-term effect that was not captured during this study. The conclusion from the modeling exercise is consistent with field measurements of barform changes following a short duration medium flow and three distinct high flow events (Fall 2013, June 2014 and June 2015) that met or exceeded the target volume, peak flow magnitude and duration for a SDHF.

The mobile-bed analysis also supports conclusions from the fixed-bed analysis (Attachment I) that the potential for widespread scour of deeply rooted riparian plants during a SDHF is low.

VI. RECOMMENDATIONS FOR FUTURE WORK

- The results in this study are focused on the effects of a single SDHF. The variables (grain size, hydrograph shape and sediment supply) did not have a statistically significant effect on barform height and area. However, longer duration flows and/or multiple events may produce measurable differences, particularly with respect to sediment supply. Increasing sediment supply at the model boundary produced localized effects that were not translated through the model domain over the course of a single SDHF.
- The integration of a coupled bed mobility and lateral erosion model is essential for predicting channel response during longer duration runs when lateral erosion is expected



to create significant changes to bar forms. While a suitable model has not been identified to date, new models that integrate these capabilities should be explored as the field of bed evolution modeling advances.

- Barforms in the low flow channels were excluded from the initial model topography due to the limitations of the LiDAR data in wet areas, as discussed in the Model Topography Section. Improved topography within the wetted channel would likely improve model results and should be explored as LiDAR or other similar technologies advance.



VII. REFERENCES

- Andrews, E. D., and J. M. Nelson, 1989. Topographic response of a bar in the Green River, Utah to variation in discharge, in *River Meandering*, Water Resour. Monogr. Ser., vol. 12, edited by S. Ikeda and G. Parker, pp. 463 – 485, AGU, Washington, D. C.
- Barton, G. J., R. R. McDonald, J. M. Nelson, and R. L. Dinehart, 2005. Simulation of flow and sediment mobility using a multidimensional flow model for the white sturgeon critical-habitat reach, Kootenai River near Bonners Ferry, Idaho, U.S. Geol. Surv. Sci. Invest. Rep., 2005-5230, 64 pp.
- Conaway, J. S., and E. H. Moran, 2004. Development and calibration of a two-dimensional hydrodynamic model of the Tanana River near Tok, Alaska, U.S. Geol. Surv. Open File Rep., 1225, 22 pp.
- Craig, Paul M. 2013. User's Manual for EFDC_Explorer7.1: A Pre/Post Processor for the Environmental Fluid Dynamics Code (Rev 00). Dynamic Solutions-International, LLC, Knoxville, TN. June, 2013.
- Engelund, F. and Hansen, E., 1967. *A Monograph on Sediment Transport in Alluvial Streams*. Danish Technical (Teknisk Forlag).
- Hamrick, J.M. 1992. *A Three-Dimensional Environmental Fluid Dynamics Computer Code: Theoretical and Computational Aspects*. The College of William and Mary, Virginia Institute of Marine Science, Special Report 317.
- Hayter, E.J. 2006. *Evaluation of the State-of-the-Art Contaminated Sediment Transport and Fate Modeling System*. U.S. Environmental Protection Agency, Ecosystems Research Division, Athens, GA. EPA/600/R-06/108.
- Ji, Z. G. 2008. *Hydrodynamics and Water Quality, Modeling Rivers, Lakes, and Estuaries*. John Wiley & Sons, Inc., Hoboken, New Jersey.
- Krone, R.B. 1963. *A Study of the Rheologic Properties of Estuarial Sediments*. SERL Report No. 63-8, Hydraulic Engineering Laboratory and Sanitary Engineering Research Laboratory, University of California, Berkeley.
- Lisle, T. E., J. M. Nelson, J. Pitlick, M. A. Madej, and B. L. Barkett, 2000. Variability of bed mobility in natural, gravel-bed channels and adjustments to sediment load at local and reach scales, *Water Resour. Res.*, 36, 3743– 3755, doi:10.1029/2000WR900238.
- Moustafa, M.Z. and J.M. Hamrick. 2000. Calibration of the wetland hydrodynamic model to the Everglades nutrient removal project. *Water Quality and Ecosystem Modeling*, 1, 141-167.



- Nelson, J. M., and J. D. Smith, 1989. Flow in meandering channels with natural topography, in *River Meandering*, Water Resour. Monogr. Ser., vol. 12, edited by S. Ikeda and G. Parker, pp. 69– 102, AGU, Washington, D. C.
- Nelson, J. M., and R. M. McDonald, 1996. Mechanics and modeling of flow and bed evolution in lateral separation eddies, report, Grand Canyon Environ. Stud., Flagstaff, Ariz.
- NHE, 2014b. Attachment III: One-Dimensional Bank Erosion Analysis. Technical Memorandum. Shoemaker Island Flow-Sediment-Mechanical “Proof-of-Concept” Experiment. March 2014.
- Northern Hydrology and Engineering (NHE), 2014a. Attachment II: Fixed Bed Modeling. Technical Memorandum. Shoemaker Island Flow-Sediment-Mechanical “Proof-of-Concept” Experiment. March 2014.
- Platte River Recovery Implementation Program (PRRIP), 2014. Shoemaker Island Flow-Sediment-Mechanical “Proof of Concept” Experiment Annual Summary Report for 2013. April 2014.
- PRRIP, 2015. Shoemaker Island Flow-Sediment-Mechanical “Proof of Concept” Experiment Annual Summary Report for 2014. December 2015.
- PRRIP, 2017. Shoemaker Island Flow-Sediment-Mechanical “Proof of Concept” Experiment Annual Report for 2015. March 2017.
- Tetra Tech. 2007a. The Environmental Fluid Dynamics Code, User Manual, USEPA Version 1.01. Tetra Tech, Inc., Fairfax, VA.
- Tetra Tech. 2007b. The Environmental Fluid Dynamics Code, Theory and Computation, Volume 2: Sediment and Contaminant Transport and Fate. Tetra Tech, Inc., Fairfax, VA.
- Tetra Tech. 2007c. The Environmental Fluid Dynamics Code, Theory and Computation, Volume 3: Water Quality Module. Tetra Tech, Inc., Fairfax, VA.
- van Rijn, L.C., 1984. Sediment transport, part II: suspended sediment load transport, *J. Hydr. Engr.*, ASCE, 110(11): 1613-1638.
- Wilcock P.R., and S. T. Kenworthy, 2002. A two-fraction model for the transport of sand/gravel mixtures, *Water Resour. Res.*, 38(10), 1194, doi:10.1029/2001WR00684.
- Wu, W. 2008. *Computational River Dynamics*. Taylor & Francis 494p.
- Yalin, M. S. 1963: An expression for bed-load transportation. *J. Hydraul. Eng.*, ASCE, 89, 3, 221-250.



TABLES AND FIGURES



Table 1. Flow characteristic of high flow events relative to target Short Duration High Flow (SDHF)

Model Run	Total Platte River Flow (cfs)		Estimate of Shoemaker Reach Flow (cfs)
	Grand Island USGS Gage	Kearney USGS Gage	
Fall 2013			
3-day Average Peak Flow	9,700	12,100	8,950
Peak Flow	10,600	13,100	10,700
June 2014			
3-day Average Peak Flow	7,320	6,420	5,580
Peak Flow	8,800	6,730	6,280
Target SDHF			
3-day Average Peak Flow	5000-8000	5000-8000	~4000-6400



Table 2. Vegetation community type and physical characteristics used in the EFDC model for the Platte River Shoemaker Reach for the SDHF high flow event

Vegetation Type	Number of Bars	Average Density (stems/sq m)	Average Diameter (mm)	Average Height (cm)
1	Open Water	-	-	-
2	1	0.7	7.1	86.0
3	0	-	-	-
4	2	7.1	8.1	92.0
5	2	13.1	8.7	175.5
6	12	21.7	8.0	56.8
7	3	20.4	8.6	146.0
8	0	-	-	-
9	4	30.7	11.6	164.0
10	16	40.3	8.3	103.1
11	1	62.3	9.4	159.0
12	13	66.3	7.2	100.2
13	4	67.1	5.4	94.3
14	0	-	-	-



Table 3. Sediment particle size classes used in the June 2014 high flow EFDC sediment transport model for the Platte River Shoemaker reach

Sediment Classes	Particle Size Range (mm)	Effective Diameter (mm)			
		Weighted Median	Weighted Geometric Mean	Weighted Critical Shear Velocity	Value used in EFDC Model
Cohesive 1 (coarse silt to very fine clay)	$0.004 < d_{\text{eff}} \leq 0.0625$	-	-	-	0.016
Non-Cohesive 1 (fine to very fine sand)	$0.0625 < d_{\text{eff}} \leq 0.25$	0.175	0.175	0.176	0.175
Non-Cohesive 2 (medium sand)	$0.25 < d_{\text{eff}} \leq 0.5$	0.354	0.354	0.353	0.353
Non-Cohesive 3 (coarse sand)	$0.5 < d_{\text{eff}} \leq 1$	0.713	0.705	0.715	0.711
Non-Cohesive 4 (very coarse sand)	$1 < d_{\text{eff}} \leq 2$	1.414	1.414	1.414	1.414
Non-Cohesive 5 (medium to very fine gravel)	$2 < d_{\text{eff}} \leq 16$	3.852	3.502	3.762	3.705



Table 4. Sediment bed initial conditions used in SDHF EFDC sediment transport model for the Platte River Shoemaker Island Reach

Sediment Bed Parameter	Sediment Bed Layers					
	Layer 6 (a)	Layer 5 (b)	Layer 4 (b)	Layer 3 (b)	Layer 2 (b)	Layer 1 (c)
Thickness (ft)	0.066	1.58	1.64	1.64	1.64	6.56
Cohesive 1 (%)	0	0	0	0	0	0
Non-Cohesive 1 (%)	9	9	9	9	9	9
Non-Cohesive 2 (%)	32.3	32.3	32.3	32.3	32.3	32.3
Non-Cohesive 3 (%)	29.5	29.5	29.5	29.5	29.5	29.5
Non-Cohesive 4 (%)	16.4	16.4	16.4	16.4	16.4	16.4
Non-Cohesive 5 (%)	12.8	12.8	12.8	12.8	12.8	12.8
Wet Bulk Density (lb/ft ³)	127.3	127.3	127.3	127.3	127.3	127.3
Porosity (%)	37	37	37	37	37	37

- (a) top layer
- (b) subsurface layer
- (c) bottom layer



Table 5. Key parameters and EFDC model options used in the SDHF sediment transport model for the Platte River Shoemaker Island reach

Model Parameter/Option	Value/Description	Source
Suspended sediment anti-diffusion correction	On	EFDC option
Suspended sediment flux limitation correction	Off	EFDC option
Maximum sediment bed layer thickness before new layer added to sediment bed model	1.64 ft (0.5 m)	EFDC option, estimate
Non-cohesive roughness grain size for stress separation	d ₉₀	EFDC option, estimate
Cohesive 1 settling velocity	3.3E-05 ft/s (0.00001 m/s)	Estimated from range of literature values (Ji 2008, Tetra Tech 2007b)
Cohesive 1 critical shear stress for deposition	0.01 N/m ²	Estimated from range of literature values (Ji 2008, Tetra Tech 2007b)
Cohesive 1 critical shear stress for erosion	0.012 N/m ²	Estimated from range of literature values (Ji 2008, Tetra Tech 2007b)
Reference surface erosion rate	2.04E-05 lb/ft ² /s (0.1 g/m ² /s)	Calibrated within range of literature values (Ji 2008, Tetra Tech 2007b)
Constant bed porosity (θ) for depositing non-cohesive sediment (%)	37	Estimated from sediment bed samples
Void ratio (ϵ) of depositing cohesive sediment	0.587	Estimated based on bed porosity by equation: $\epsilon = \theta / (1 - \theta)$
Non-cohesive bed armoring with active-parent layer (top layer) constant thickness	0.066 ft (0.02 m)	EFDC option, thickness based on sediment bed field observations
Maximum adverse slope for bedload transport	0.1	EFDC option, estimated
Number of time steps to allow bed elevation change	4	EFDC option, estimated



Table 6. Cut and fill volumes for SDHF simulations

Flow	Grain Size	Sediment Supply	Cut (CY)	Fill (CY)	Net (CY)	
Hydrograph Shape						
8,000 cfs (TRF)	1 mm	Equilibrium	-90,000	94,000	4,000	Fill
5,000 cfs (TRF)	1 mm	Equilibrium	-77,000	79,000	2,000	Fill
Grain Size						
8,000 cfs (TRF)	0.75 mm	Equilibrium	-110,000	114,000	4,000	Fill
8,000 cfs (TRF)	1 mm	Equilibrium	-90,000	94,000	4,000	Fill
8,000 cfs (TRF)	2 mm	Equilibrium	-52,000	56,000	4,000	Fill
Sediment Supply						
8,000 cfs (TRF)	1 mm	0.5x Equilibrium	-89,000	93,000	4,000	Fill
8,000 cfs (TRF)	1 mm	Equilibrium	-90,000	94,000	4,000	Fill
8,000 cfs (TRF)	1 mm	2x Equilibrium	-90,000	94,000	4,000	Fill



Table 7. Results of statistical tests that test differences in populations of sand bar heights and areas resulting from a change in hydrograph shape of a SDHF

Data Sets	Null Hypothesis	Test Used	p-value	Interpretation
All bars (sand and veg) present at the end of the 8,000 cfs and 5,000 cfs SDHF	All bar heights (sand and veg) are equal	Wilcoxon	0.33	No significant difference
	All bar areas (sand and veg) are equal	Wilcoxon	0.42	No significant difference
Sand bars present at the end of the 8,000 cfs and 5,000 cfs SDHF	New sand bar heights are equal	Wilcoxon	0.37	No significant difference
	New sand bar areas are equal	Wilcoxon	0.33	No significant difference
New sand bars present at the end of the 8,000 cfs and 5,000 cfs SDHF	New sand bar heights are equal	Wilcoxon	0.20	No significant difference
	New sand bar areas are equal	Wilcoxon	0.68	No significant difference



Table 8. Results of statistical tests that test differences in populations of sand bar heights and areas resulting from a change in sediment supply

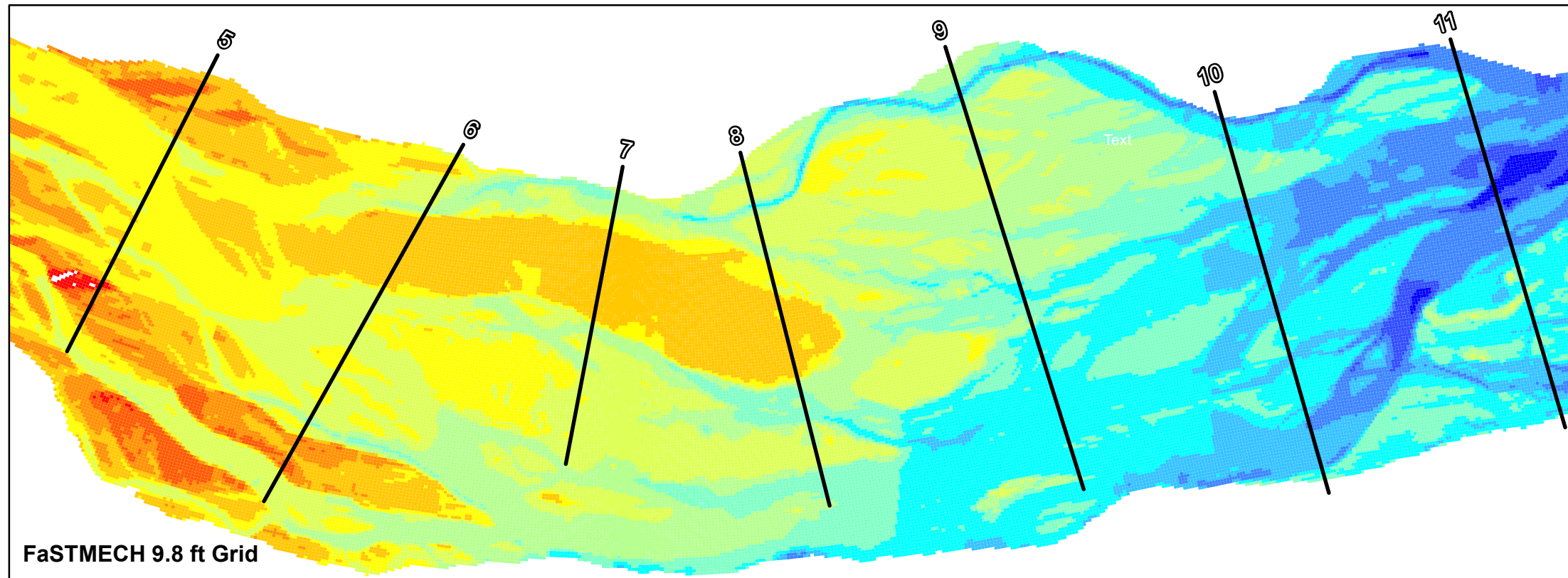
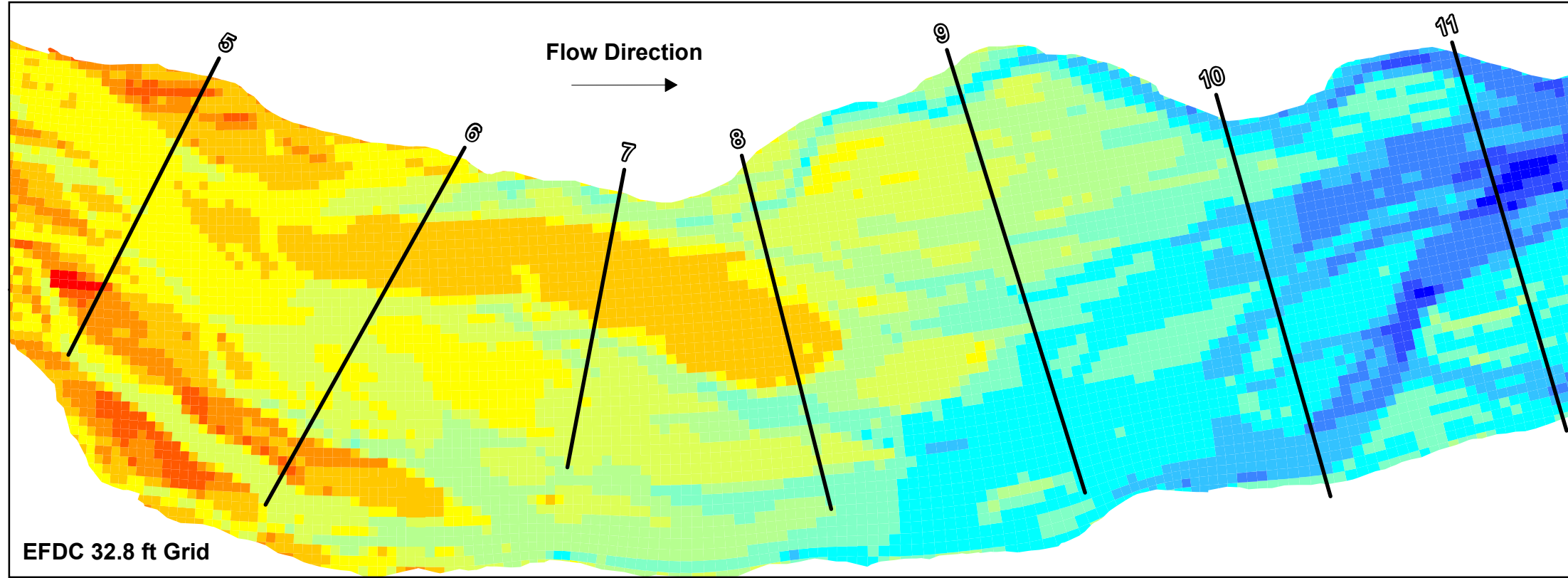
Data Sets	Null Hypothesis	Test Used	p-value	Interpretation
All bars (sand and veg) present at the end of the SDHF with sediment supply equal to 2x equilibrium, equilibrium and ½ equilibrium.	All bar heights (sand and veg) are equal	Kruskal-Wallis	0.68	No significant difference
	All bar areas (sand and veg) are equal	Kruskal-Wallis	0.99	No significant difference
Sand bars present at the end of the SDHF with sediment supply equal to 2x equilibrium, equilibrium and ½ equilibrium.	All sand bar heights are equal	Kruskal-Wallis	0.66	No significant difference
	All sand bar areas are equal	Kruskal-Wallis	0.92	No significant difference
New sand bars present at the end of the SDHF with sediment supply equal to 2x equilibrium, equilibrium and ½ equilibrium.	New sand bar heights are equal	Kruskal-Wallis	0.65	No significant difference
	New sand bar areas are equal	Kruskal-Wallis	0.97	No significant difference



Table 9. Results of statistical tests that test differences in populations of sand bar heights and areas resulting from a change in the grain size of the bed material

Data Sets	Null Hypothesis	Test Used	p-value	Interpretation
All bars (sand and veg) present at the end of the SDHF with bed material grain sizes of: 0.75 mm, 1mm and 2mm	All bar heights (sand and veg) are equal	Kruskal-Wallis	0.23	No significant difference
	All bar areas (sand and veg) are equal	Kruskal-Wallis	0.51	No significant difference
Sand bars present at the end of the SDHF with bed material grain sizes of: 0.75mm, 1mm and 2mm	All sand bar heights are equal	Kruskal-Wallis	0.20	No significant difference
	All sand bar areas are equal	Kruskal-Wallis	0.36	No significant difference
New sand bars present at the end of the SDHF with bed material grain sizes of: 0.75mm, 1mm and 2mm	New sand bar heights are equal	Kruskal-Wallis	0.31	No significant difference
	New sand bar areas are equal	Kruskal-Wallis	0.19	No significant difference

2017-01-04 F:\State & Local\Other\Plate River Recovery Program\Projects\1499201 - Shoemaker FSM Proof of Concept\Figures\MXD\2015\Attachment 1\IMXD\Figure 2 - Model Topography Reis.mxd EA-Uncin_jpetersen



Legend

— Cross Section

Elevation (feet, NAVD88)

- >1945
- 1944 - 1945
- 1943 - 1944
- 1942 - 1943
- 1941 - 1942
- 1940 - 1941
- 1939 - 1940
- 1938 - 1939
- 1937 - 1938
- 1936 - 1937
- 1935 - 1936
- 1934 - 1935
- <1934



**PLATTE RIVER RECOVERY
IMPLEMENTATION PROGRAM**

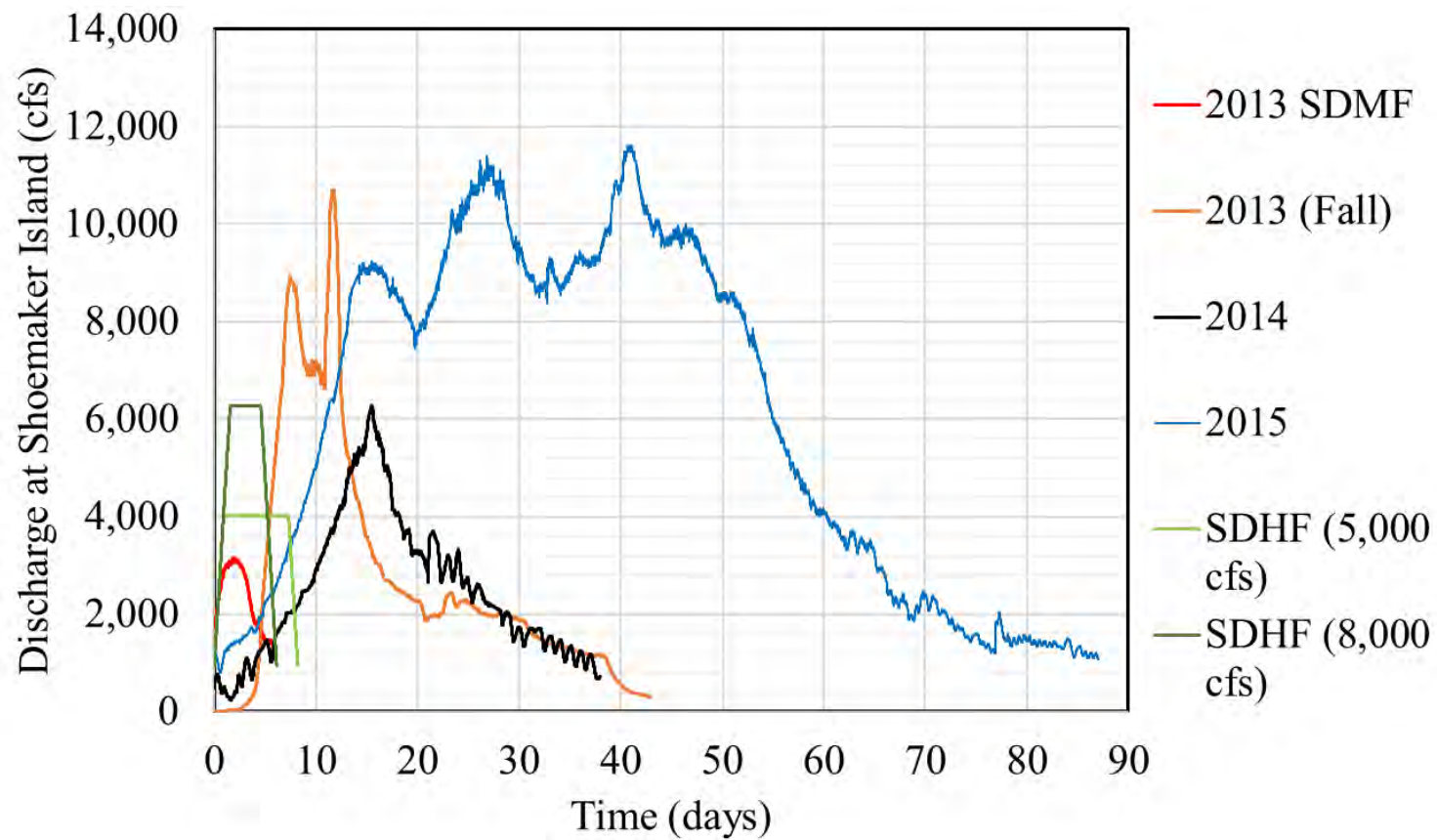
**SHOEMAKER ISLAND FSM
PROOF OF CONCEPT**
HALL COUNTY, NEBRASKA

**COMPARISON OF MODEL TOPOGRAPHY
FOR VARIOUS GRID CELL SIZES**

PROJECT MGR. DLB	DESIGNED BY BP	DRAWN BY BP	CHECKED BY KMD	DATE JAN 2017	SCALE AS SHOWN	PROJECT NO. 1499201	FILE NAME -	DRAWING NO. -	FIGURE 1
---------------------	-------------------	----------------	-------------------	------------------	-------------------	------------------------	----------------	------------------	-------------



Figure 2. Observed and simulated hydrographs (2013-2015)



2017-01-06 F:\Site & Local\Other\Platte River Recovery Program\Projects\1499201 - Shoemaker FSM Proof of Concept\Figures\MXD\2015\Attachment 1\MXD\Figure 3 - Model Topography for June 2014 High Flow.mxd EA-Lincoln_jpetersen

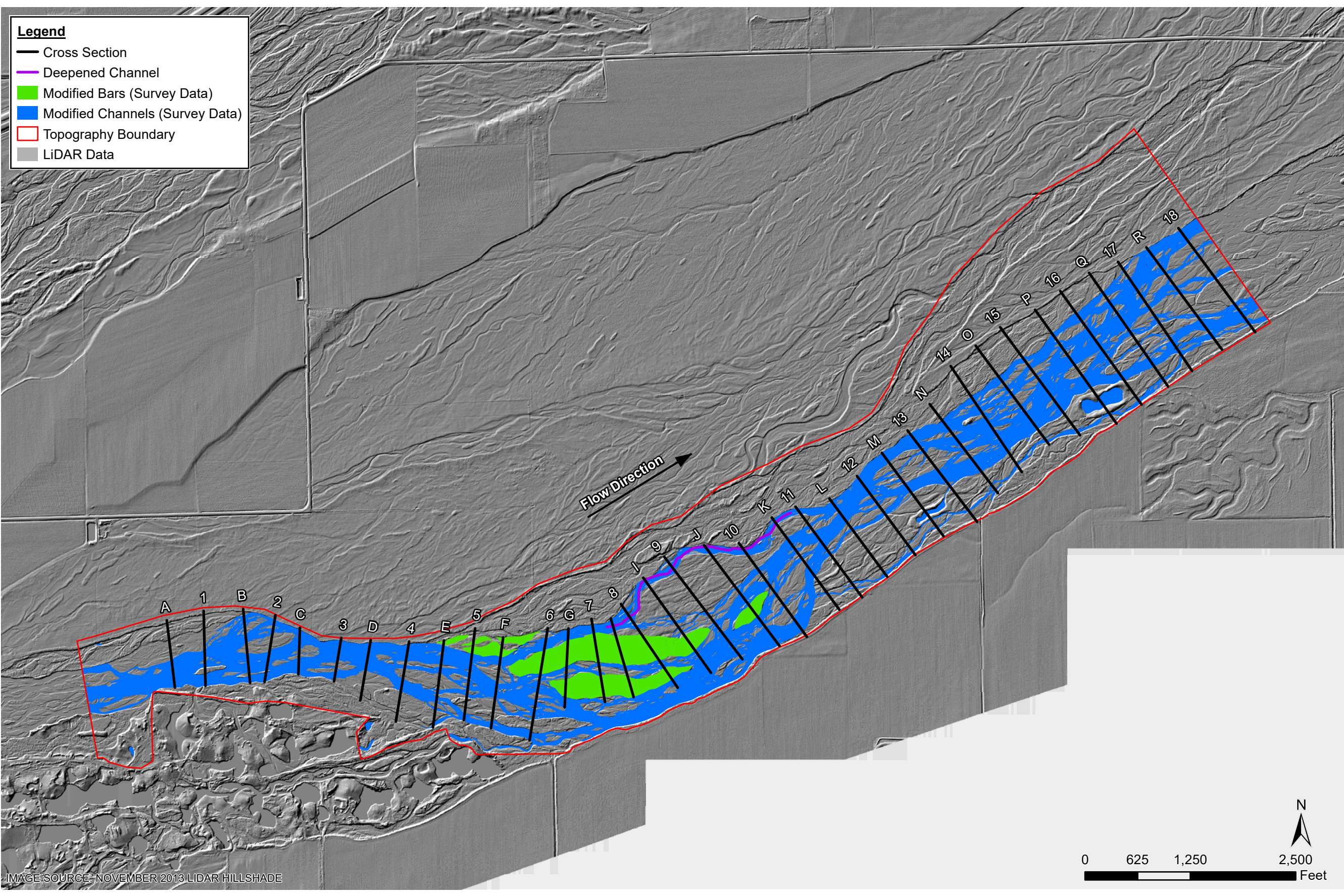


IMAGE SOURCE: NOVEMBER 2013 LIDAR HILLSHADE

Legend

- Cross Section
- Deepened Channel
- Modified Bars (Survey Data)
- Modified Channels (Survey Data)
- Topography Boundary
- LiDAR Data



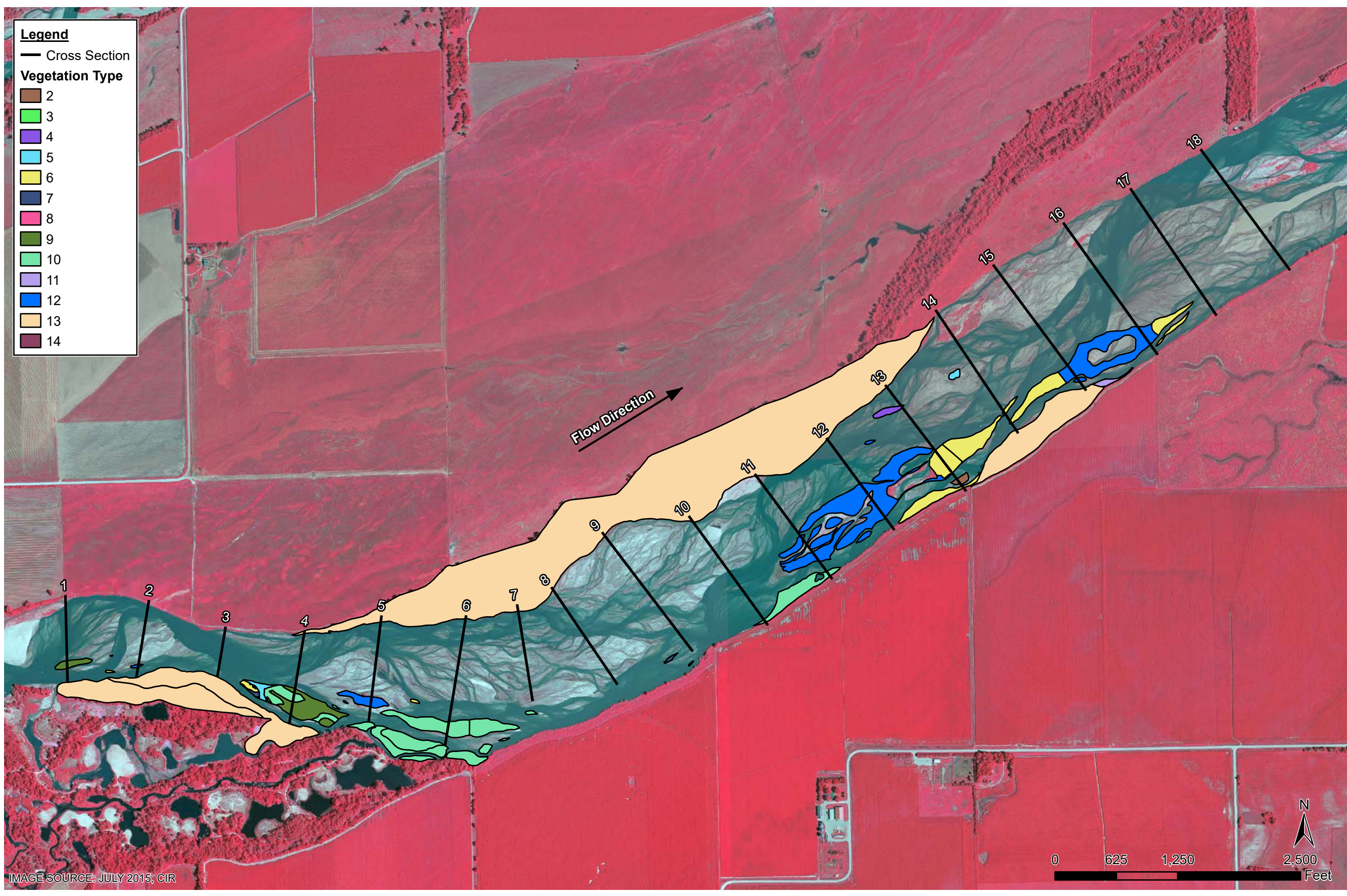
**PLATTE RIVER RECOVERY
IMPLEMENTATION PROGRAM**

**SHOEMAKER ISLAND FSM
PROOF OF CONCEPT**
HALL COUNTY, NEBRASKA

**JUNE 2014 HIGH FLOW
MODEL TOPOGRAPHY**

PROJECT MGR. DLB	DESIGNED BY BP	DRAWN BY BP	CHECKED BY KMD	DATE JAN 2017	SCALE AS SHOWN	PROJECT NO. 1499201	FILE NAME -	DRAWING NO. -	FIGURE 3
---------------------	-------------------	----------------	-------------------	------------------	-------------------	------------------------	----------------	------------------	-------------

2017-01-06 F:\Site & Local\Other\Platte River Recovery Program\Projects\1499201 - Shoemaker FSM Proof of Concept\Figures\MXD\2015\Attachment 1\MXD\Figure 4 - Vegetation Type.mxd EA-Lincoln J.petersen



Legend

— Cross Section

Vegetation Type

- 2
- 3
- 4
- 5
- 6
- 7
- 8
- 9
- 10
- 11
- 12
- 13
- 14

IMAGE SOURCE: JULY 2015, CIR



**PLATTE RIVER RECOVERY
IMPLEMENTATION PROGRAM**

**SHOEMAKER ISLAND FSM
PROOF OF CONCEPT**
HALL COUNTY, NEBRASKA

EFDC MOBILE BED VEGETATION TYPES

PROJECT MGR. DLB	DESIGNED BY BP	DRAWN BY BP	CHECKED BY KMD	DATE JAN 2017	SCALE AS SHOWN	PROJECT NO. 1499201	FILE NAME -	DRAWING NO. -	FIGURE 4
---------------------	-------------------	----------------	-------------------	------------------	-------------------	------------------------	----------------	------------------	-------------



Figure 5. Cumulative grain size distribution of measured data (gray) and grain size distribution used in model (red) for the EFDC SDHF simulations (measured June 2014)

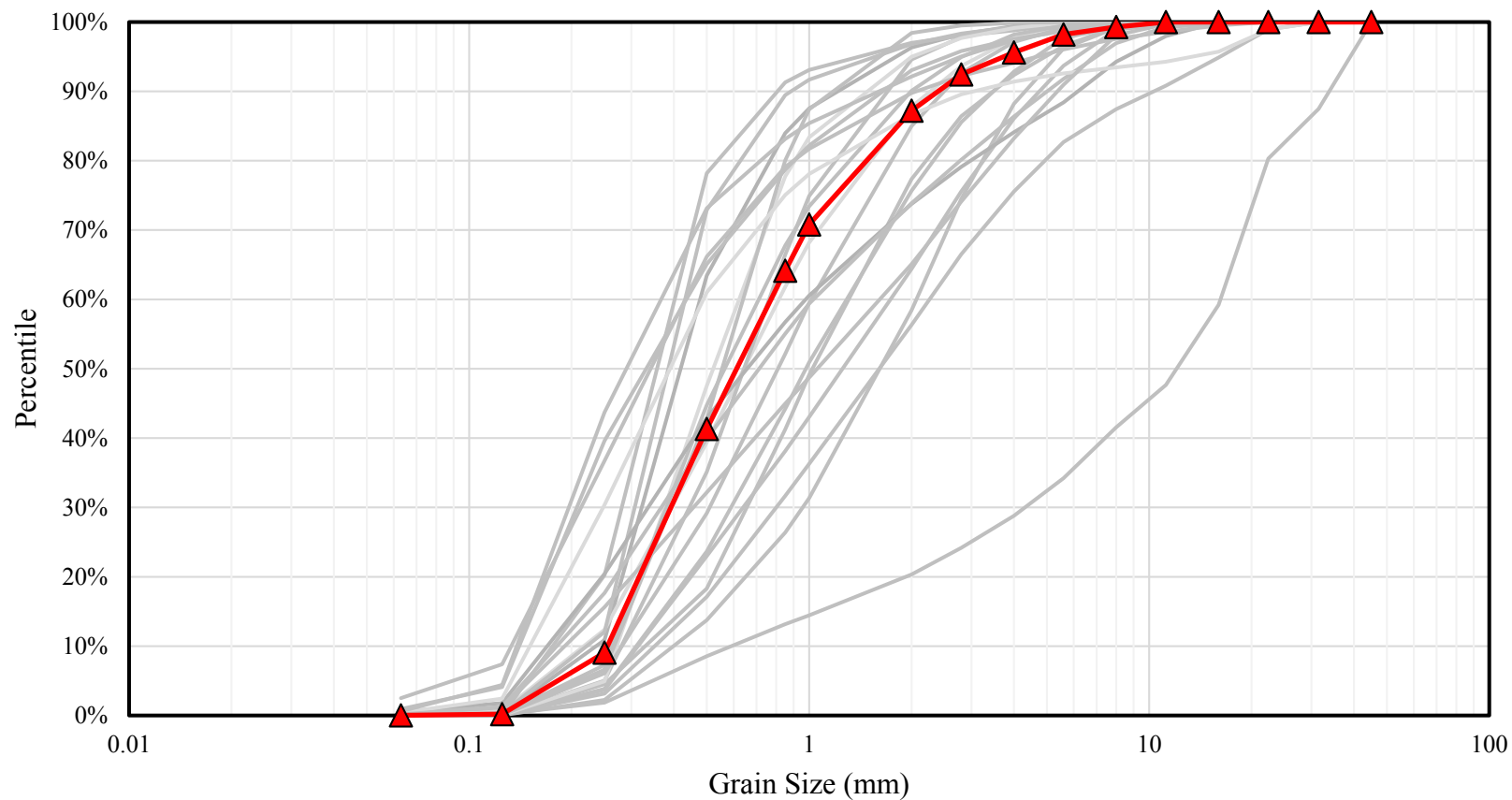




Figure 6. Sediment supply boundary condition applied in EFDC for the SDHF simulations

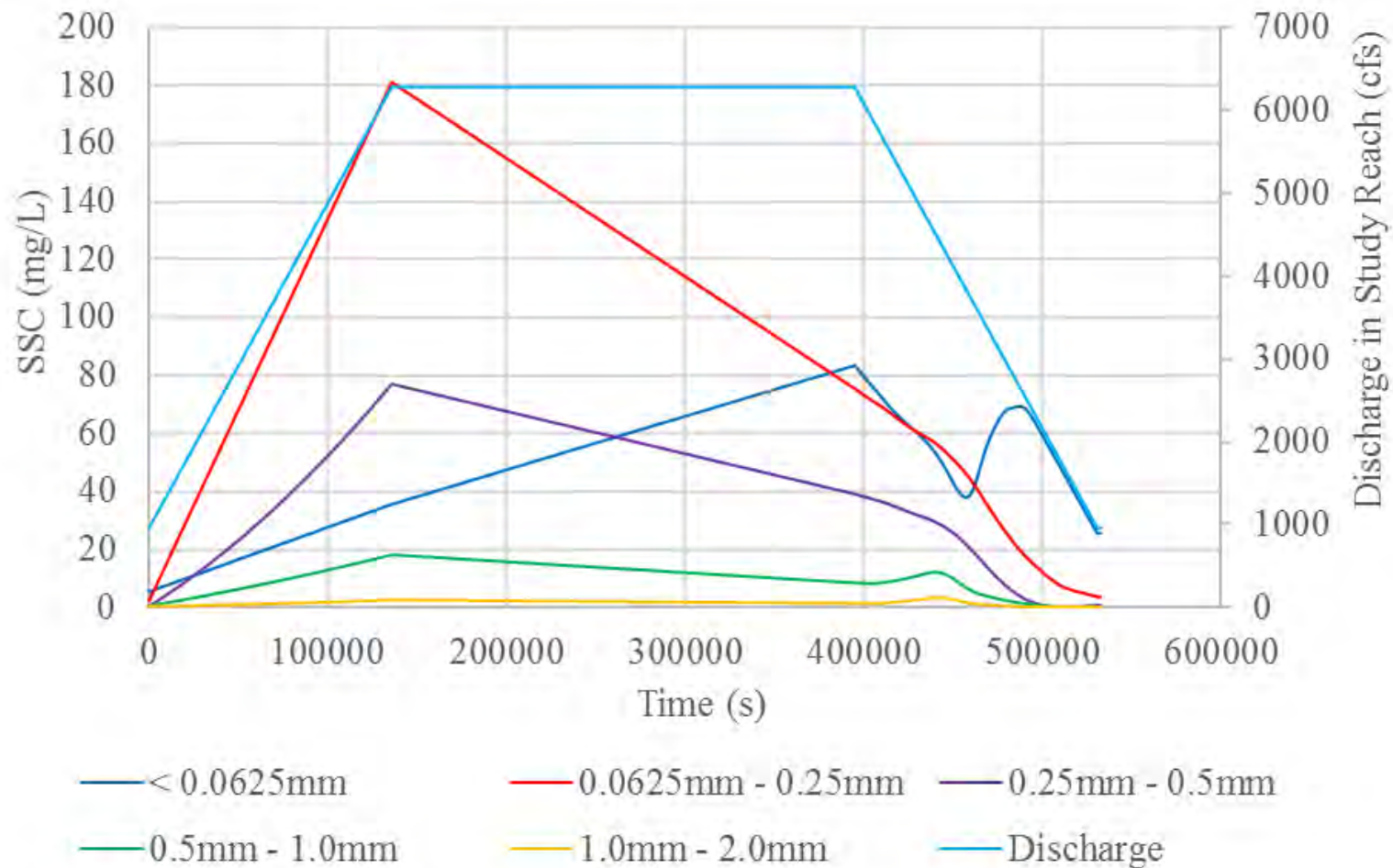




Figure 7. Comparison of measured and predicted water levels for various flows during the fall 2013 (EFDC and FaSTMECH) and June 2014 high flow (FaSTMECH)

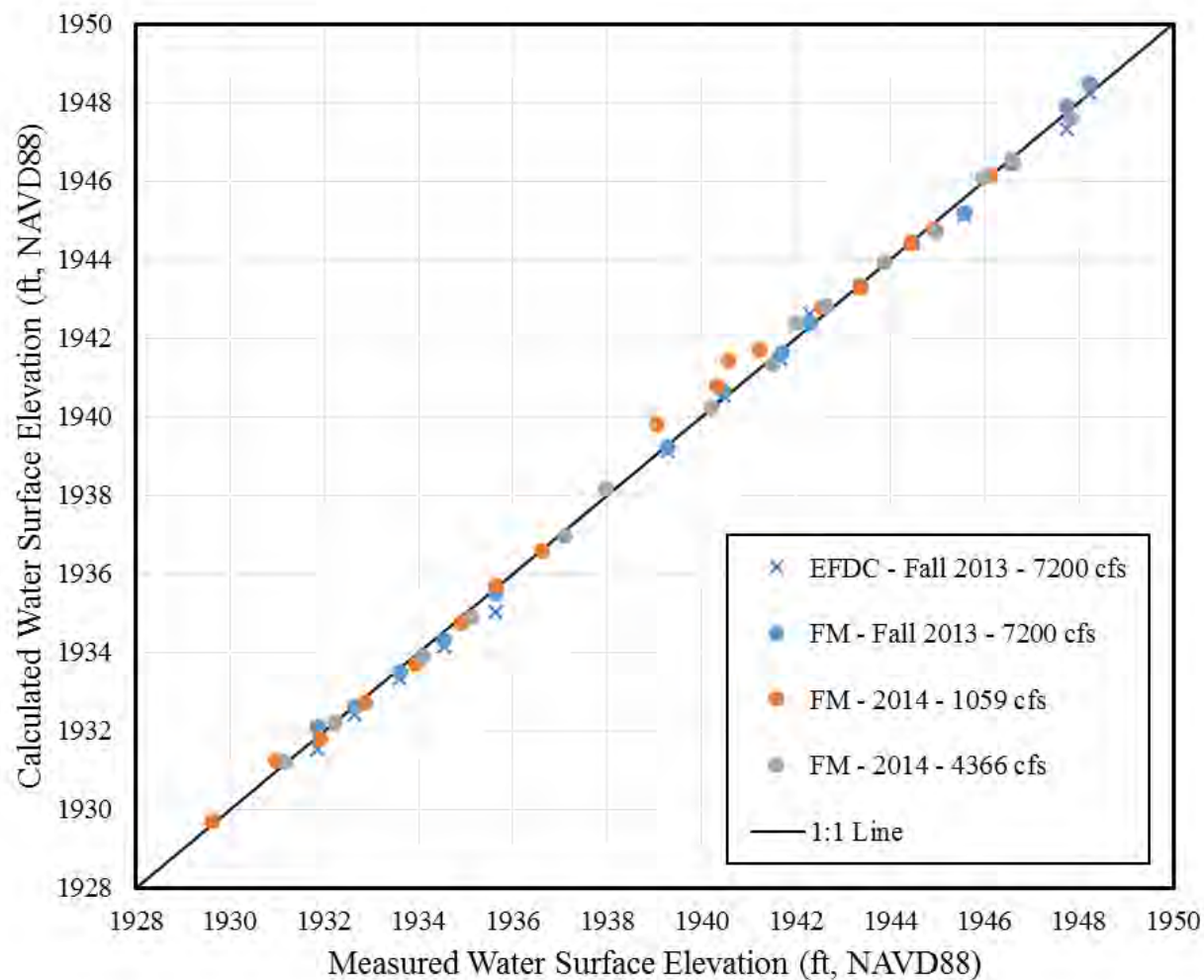




Figure 8. LiDAR data results in a plane bed low flow channel due to lack of data in wetted channels (left). FaSTMECH produces barforms (middle) in the channel that are similar in amplitude and wavelength to those observed in aerial photography (right)

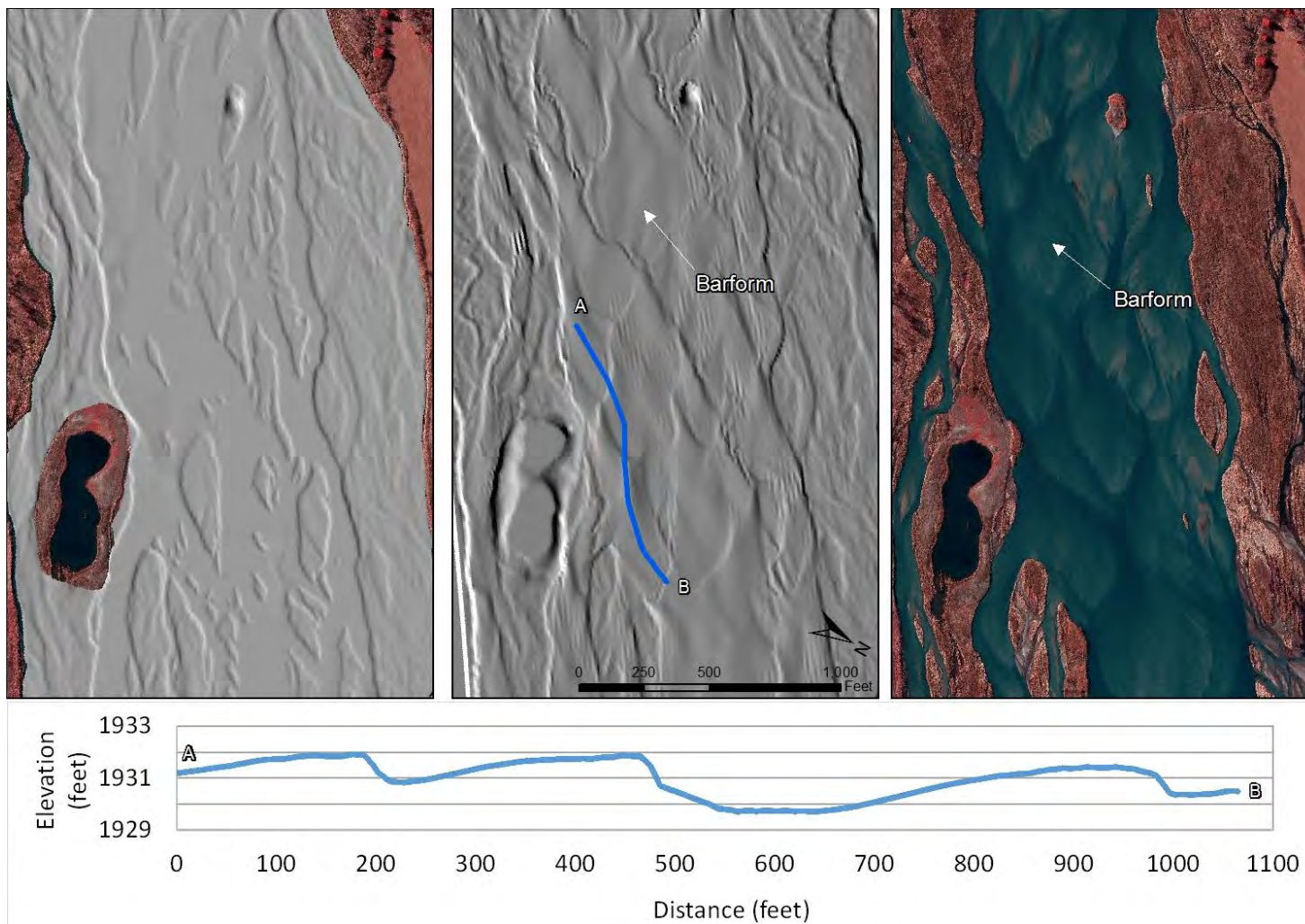




Figure 9. Example of barform changes following a SDHF (8,000 cfs TRF, 3 days)

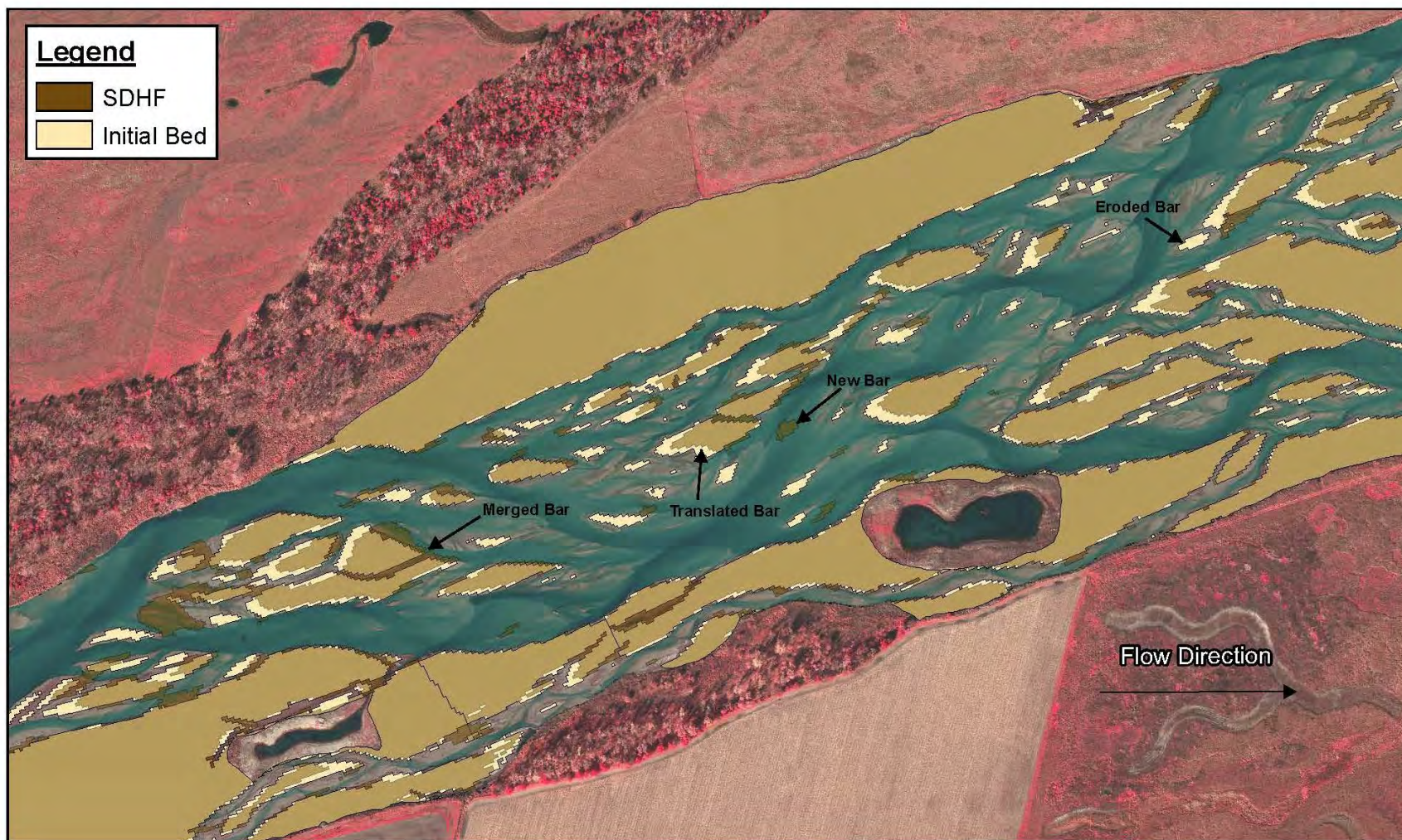




Figure 10. Predicted (FaSTMECH) vegetated bars, established sand bars and new sand bars prior to, and following, a SDHF

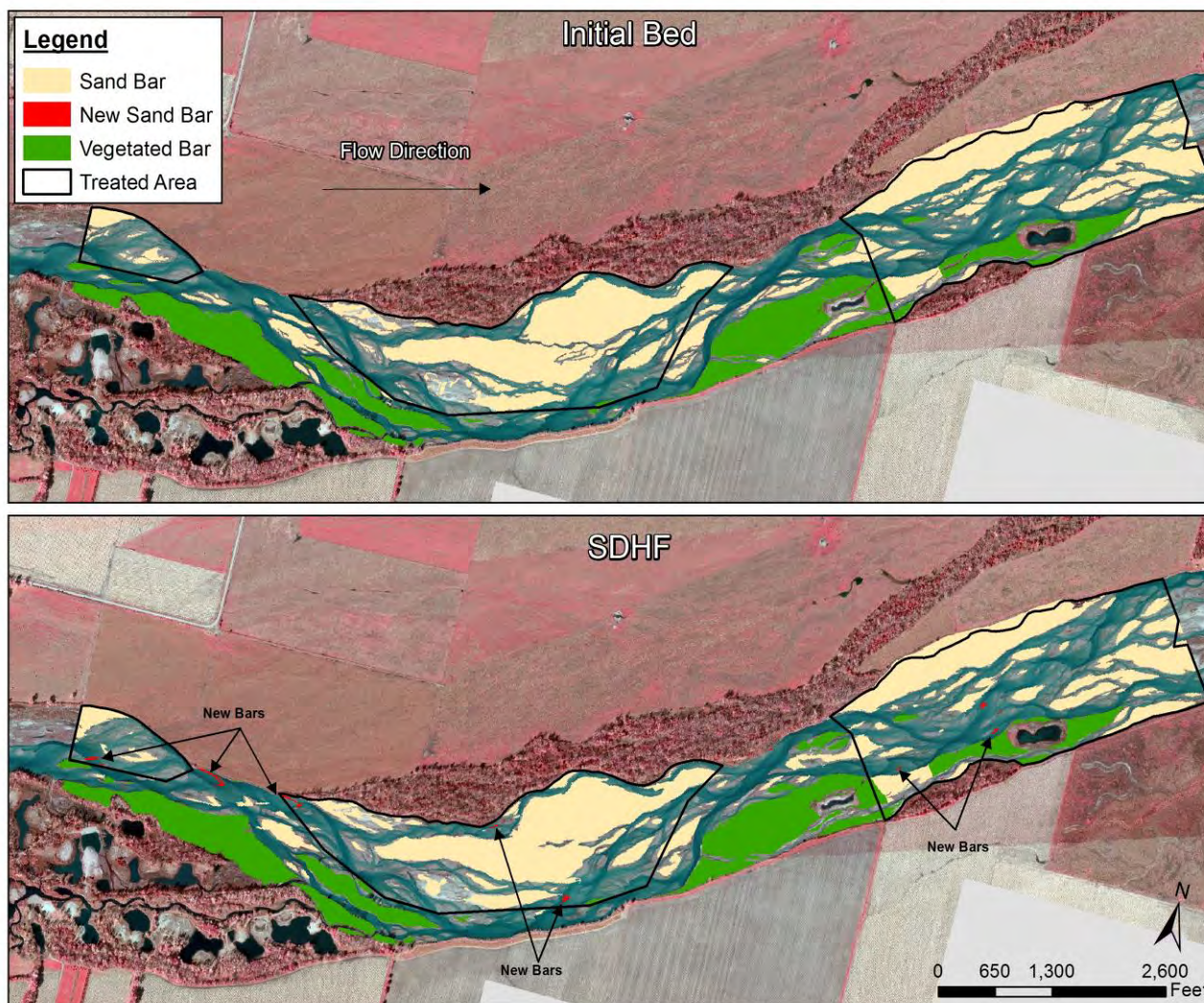




Figure 11. Box plots of mean bar heights and areas of all bars (sand and vegetated) before (IC) and after SDHF with 5,000 cfs and 8,000 cfs peak flow

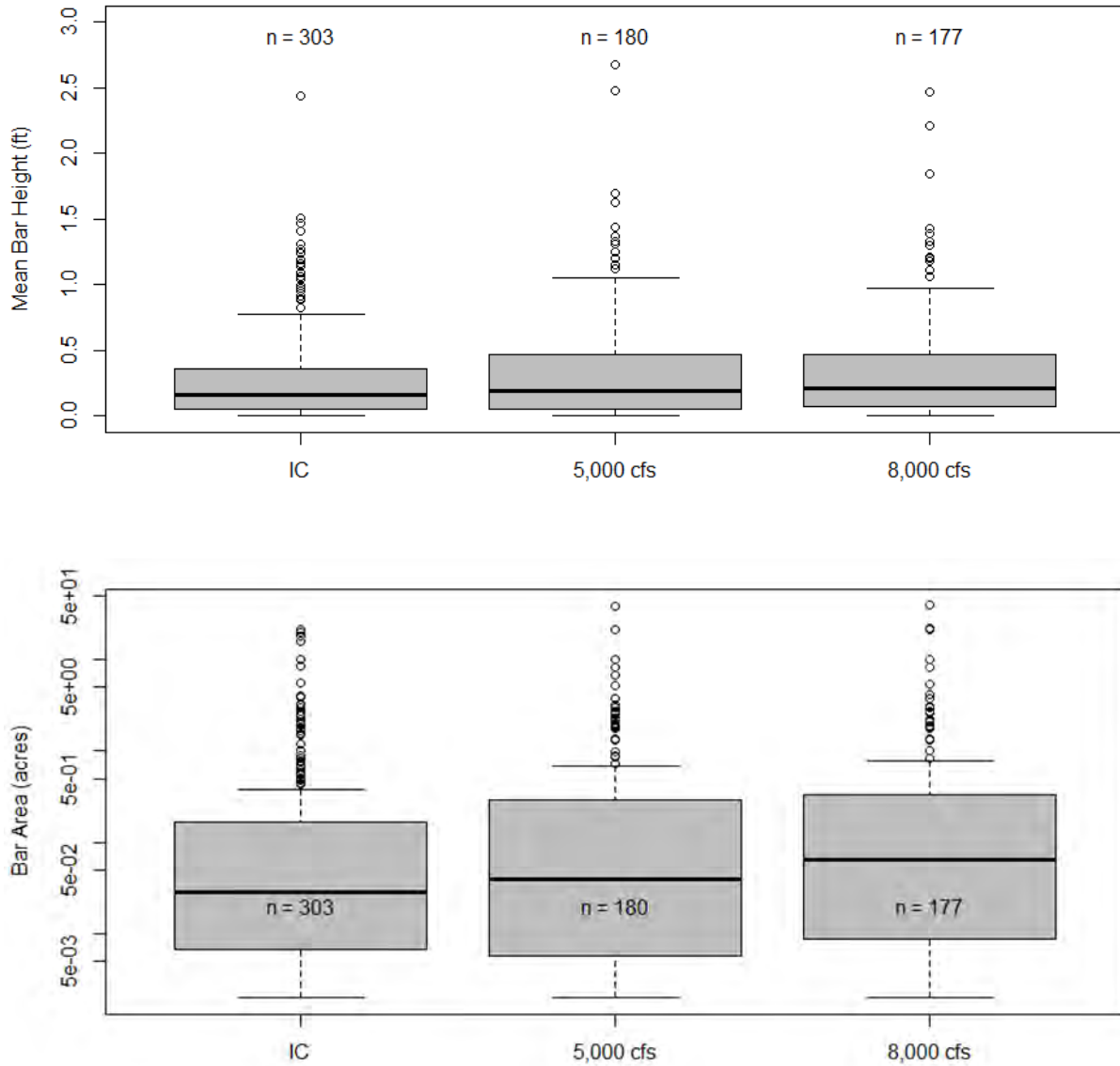




Figure 12. Box plots of mean bar height and area of sand bars following a 5,000 cfs and 8,000 cfs SDHF

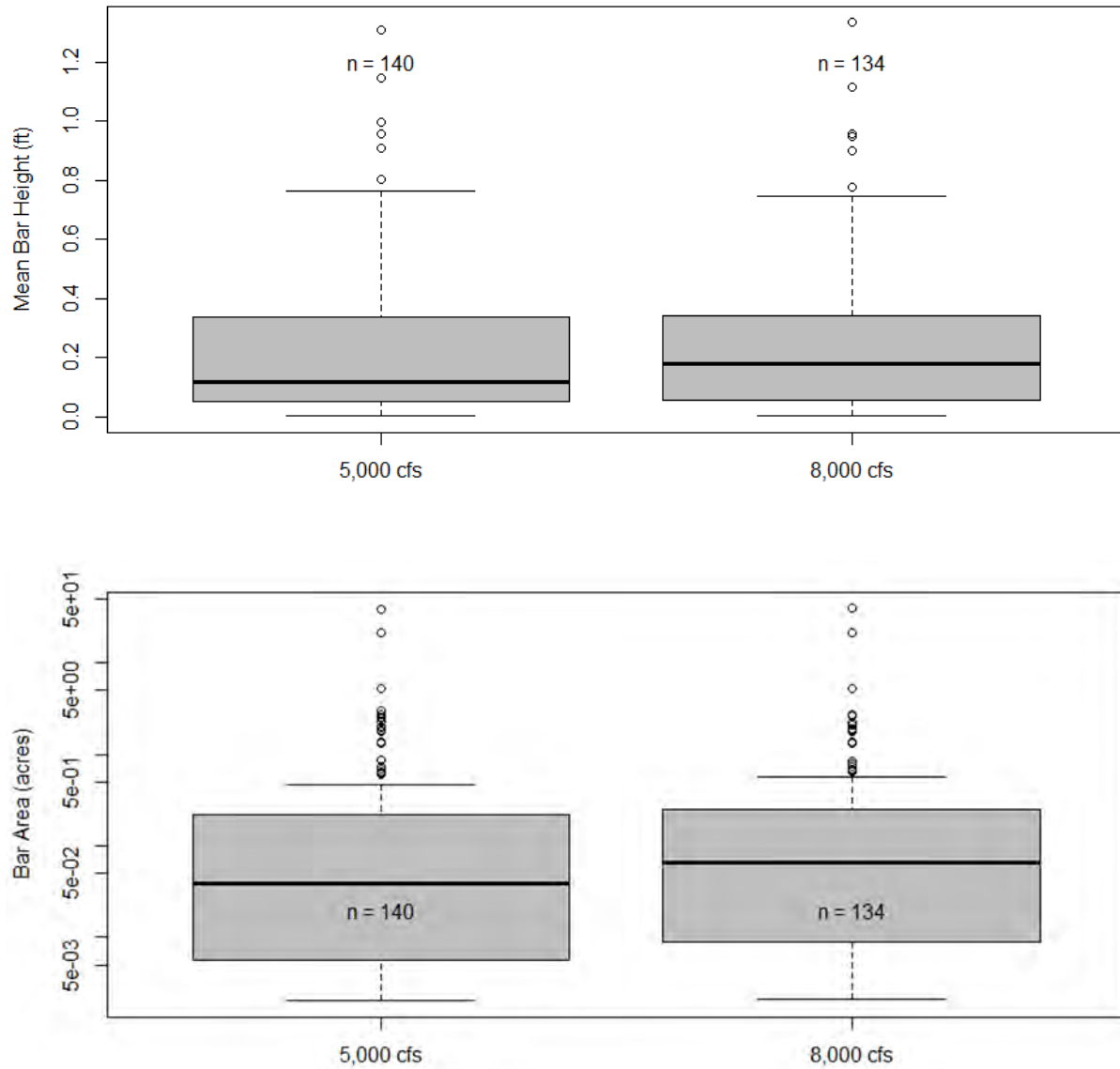




Figure 13. Comparison of mean new sand bar heights above 1,200 cfs formed during a SDHF with a magnitude of 5,000 cfs TRF and 8,000 cfs TRF

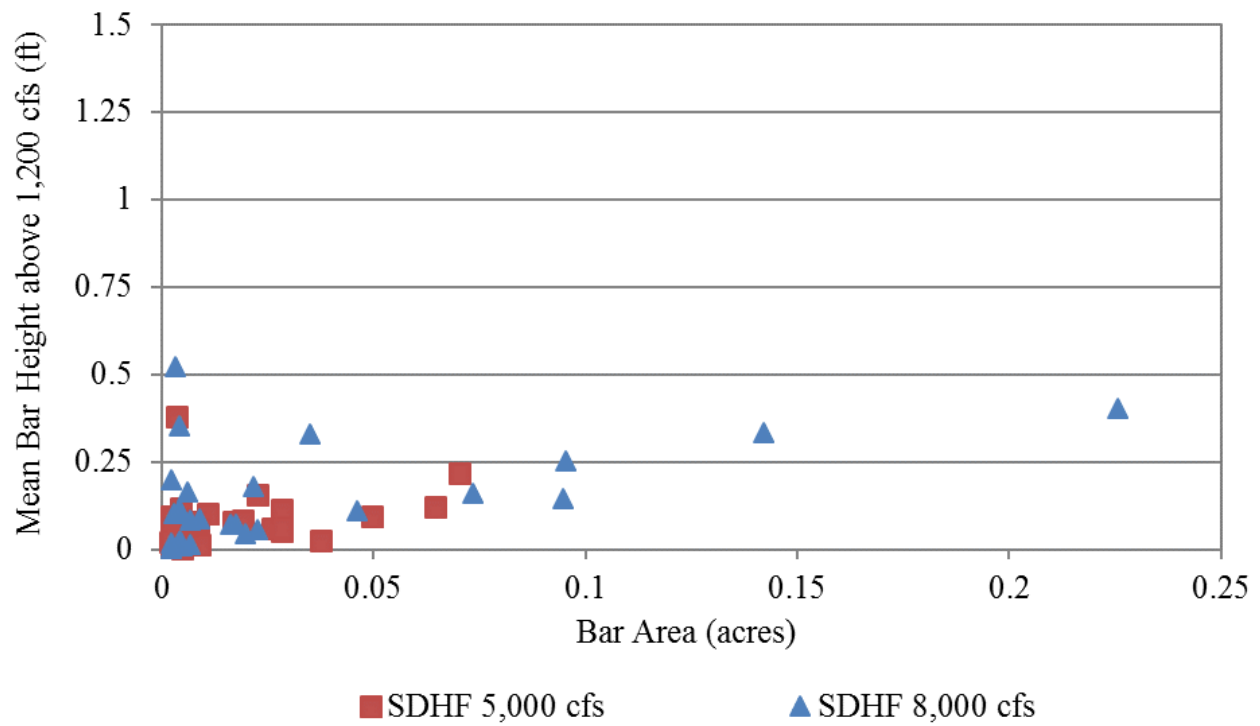




Figure 14. Box plots of mean bar height and area of new bars for 5,000 cfs and 8,000 cfs SDHF

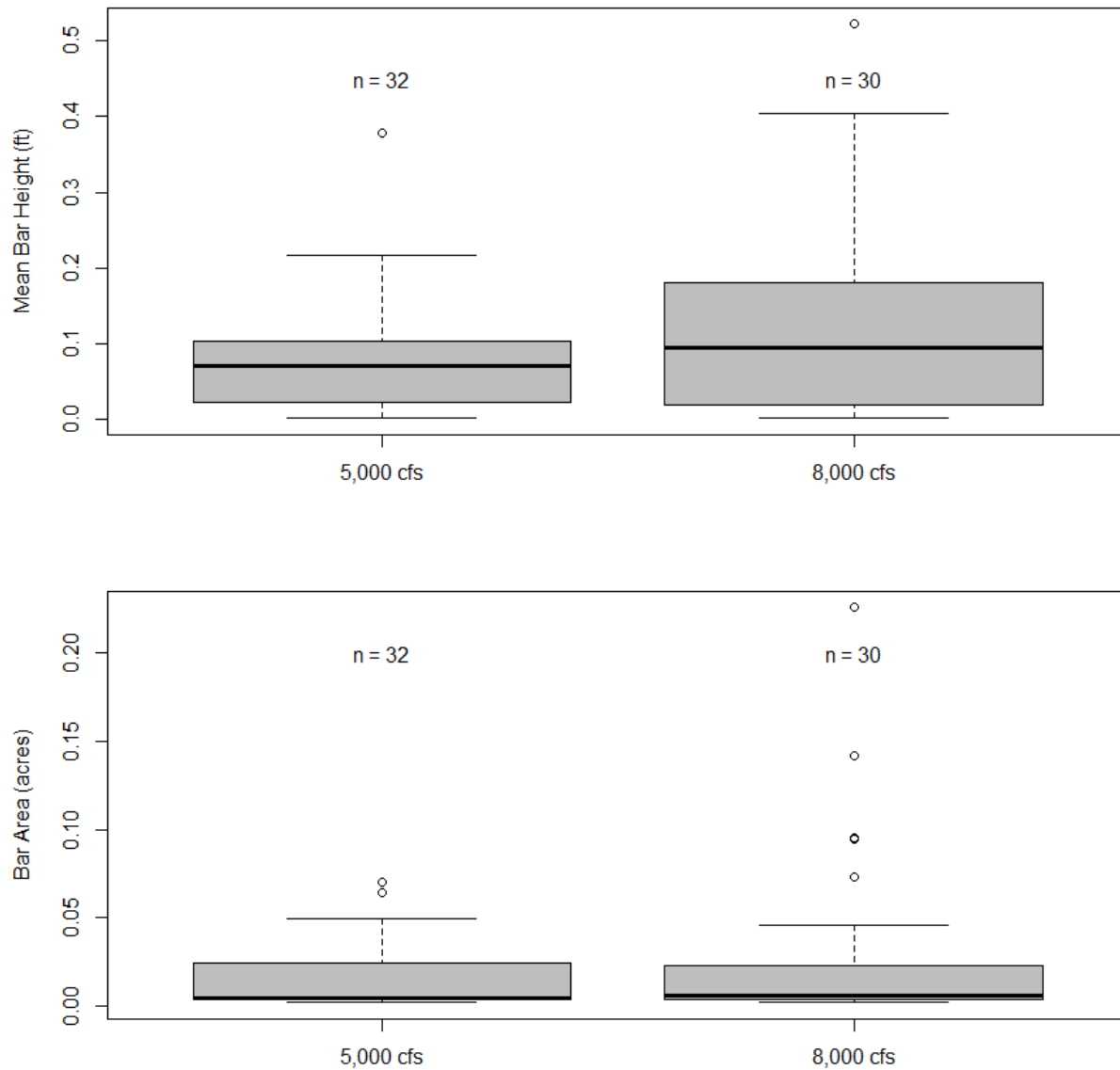




Figure 15. Comparison of depth of new sand bars below peak stage formed during a SDHF of 5,000 cfs and 8,000 cfs TRF. Area reported as individual bar area (top) and cumulative bar area (bottom)

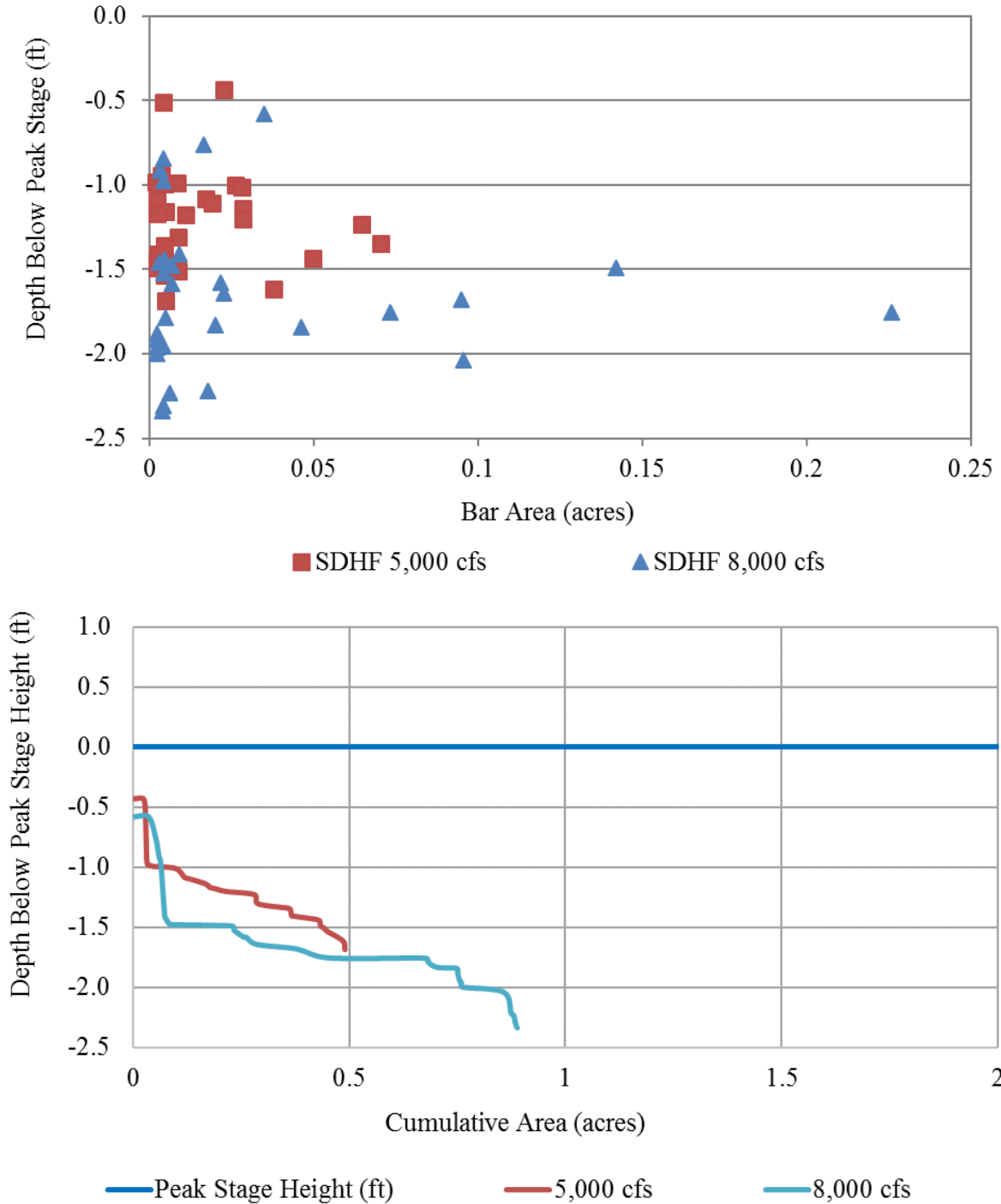




Figure 16. Box plots of mean bar height and bar area of all bars (sand and vegetated) for half (0.5x), equilibrium sediment supply and twice (2x) equilibrium sediment supply

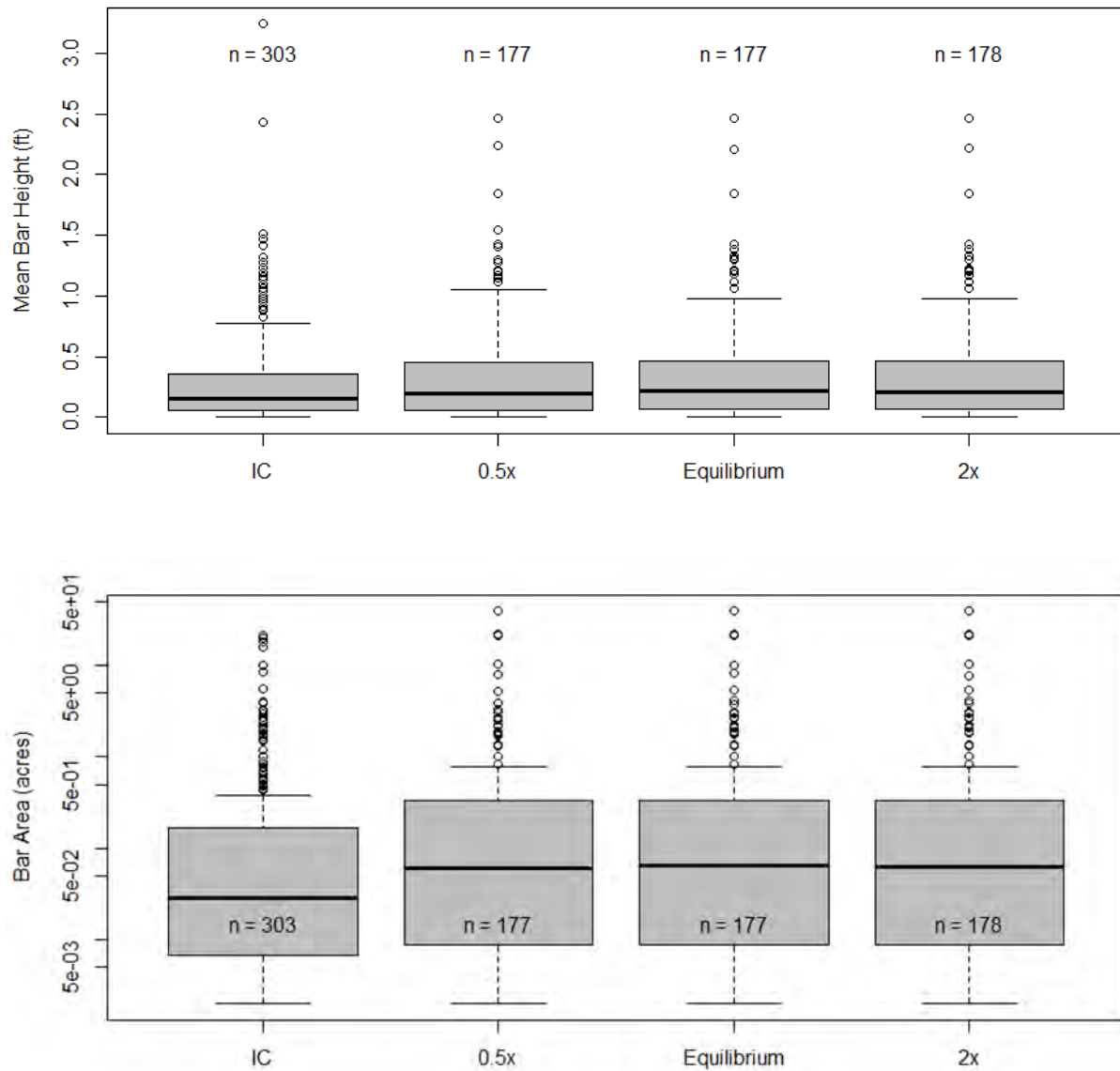




Figure 17. Box plots of mean bar height and bar area of all sand bars for half (0.5x), equilibrium sediment supply and twice (2x) equilibrium sediment supply

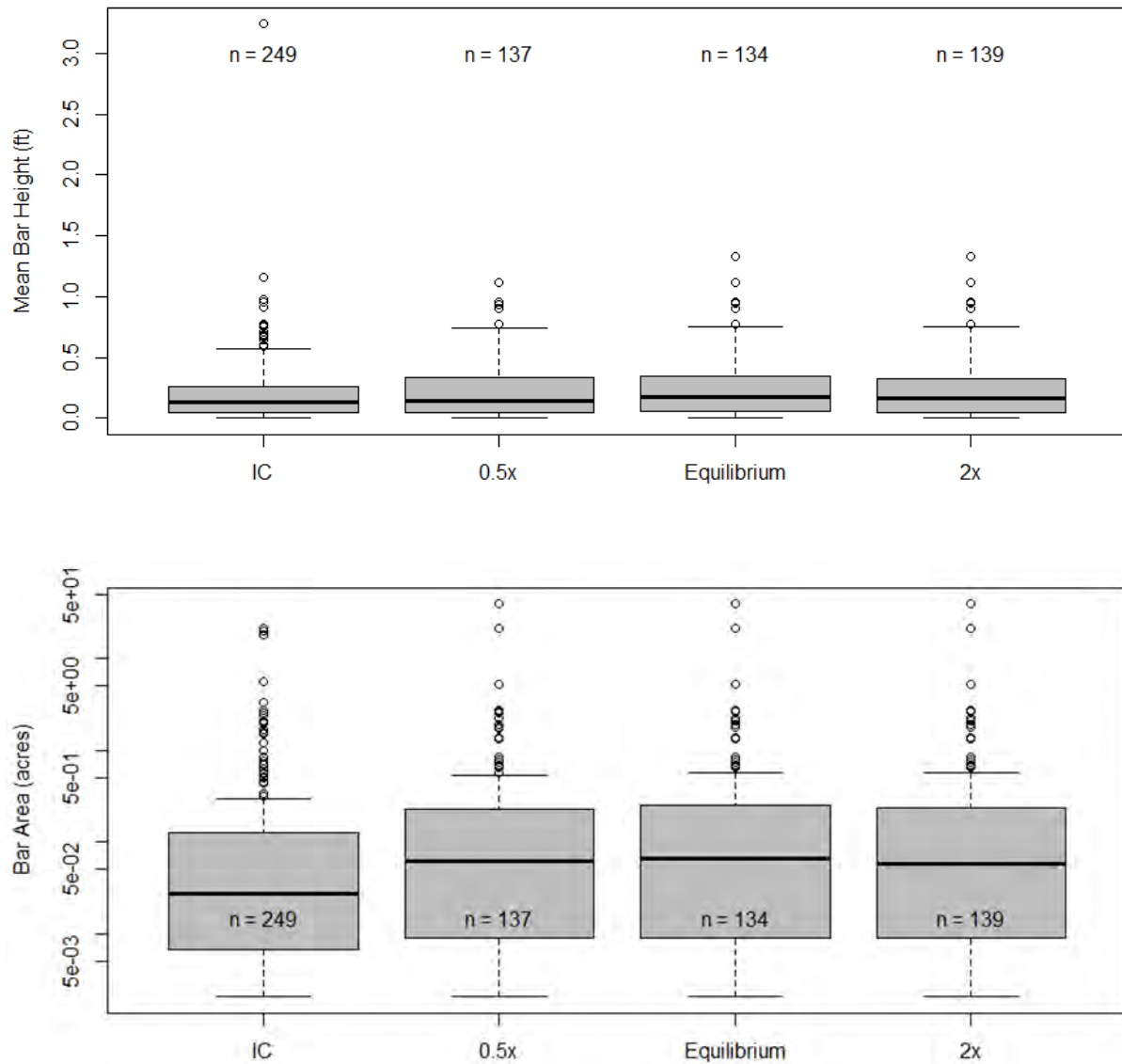




Figure 18. Effect of sediment supply on mean bar height and bar area of new bars predicted by EFDC (top) and FaSTMECH (bottom).

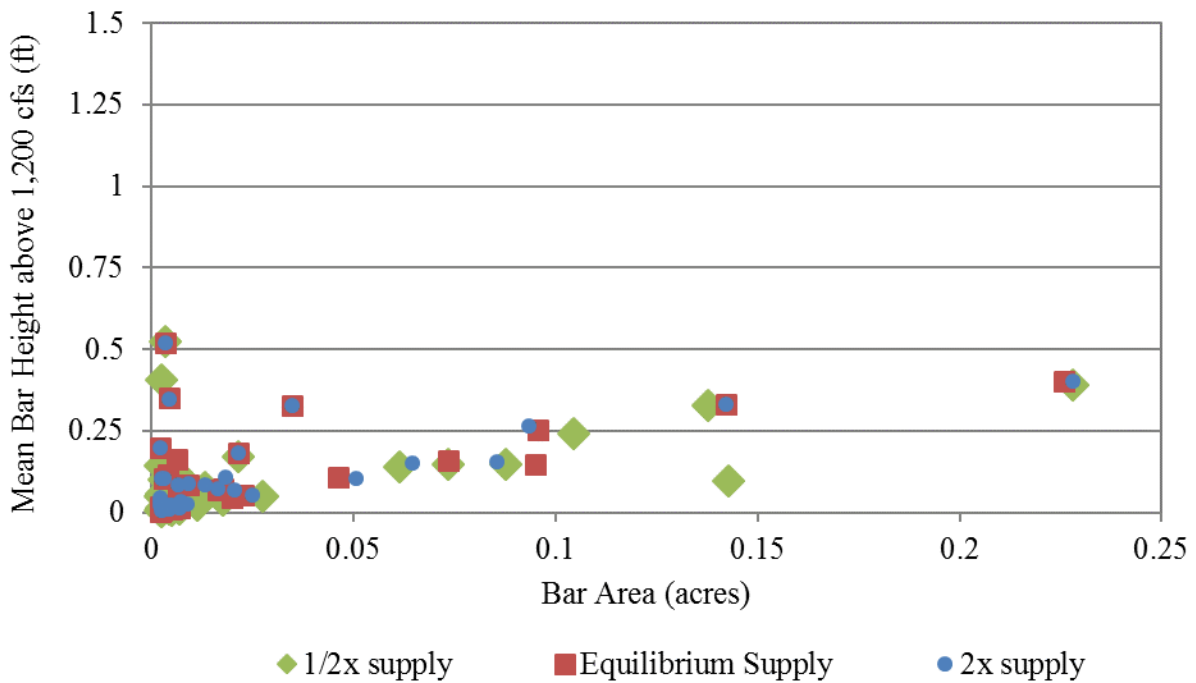
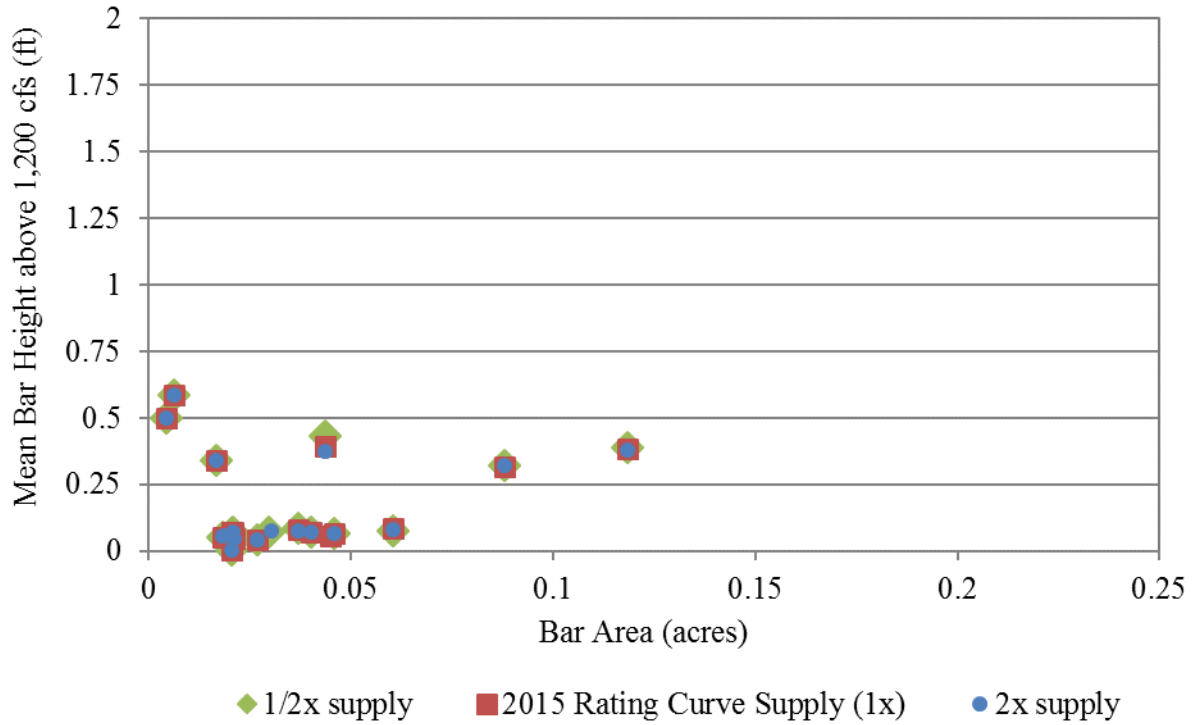




Figure 19. Comparison of depth of new sand bars below peak stage formed during a SDHF with variable sediment supply. Area reported as cumulative bar area

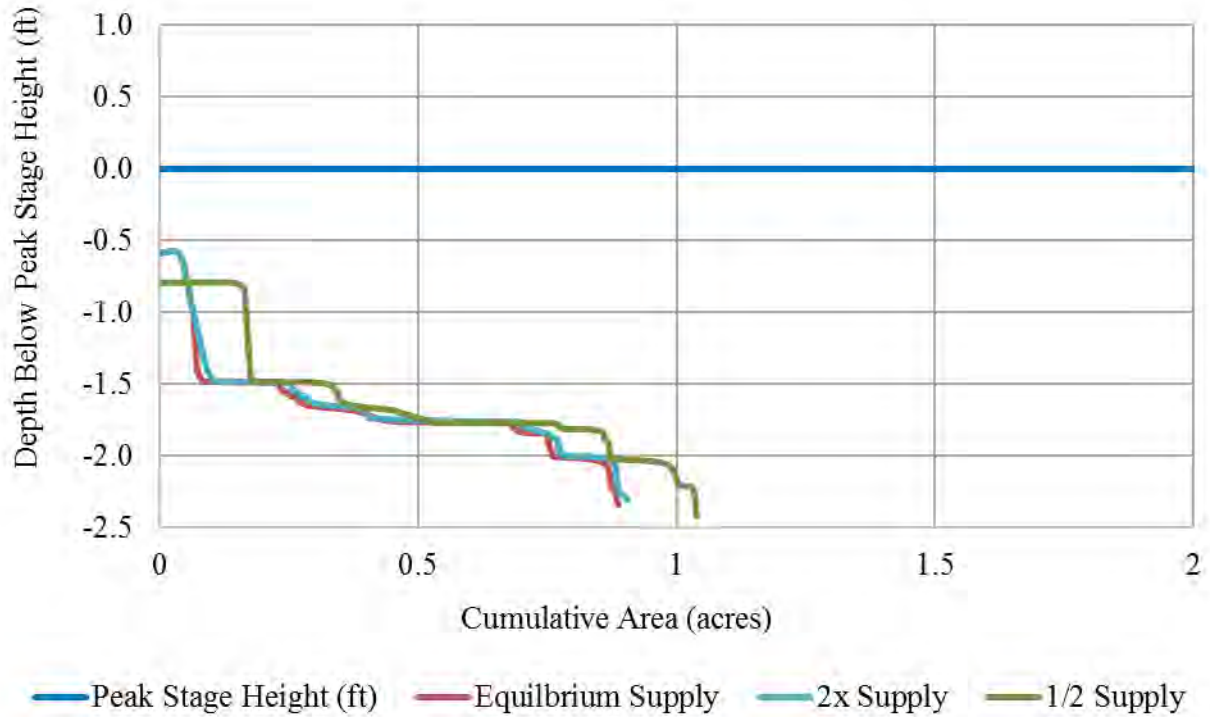




Figure 20. Box plots of mean bar height and bar area of new sand bars for half (0.5x), equilibrium sediment supply and twice (2x) equilibrium sediment supply

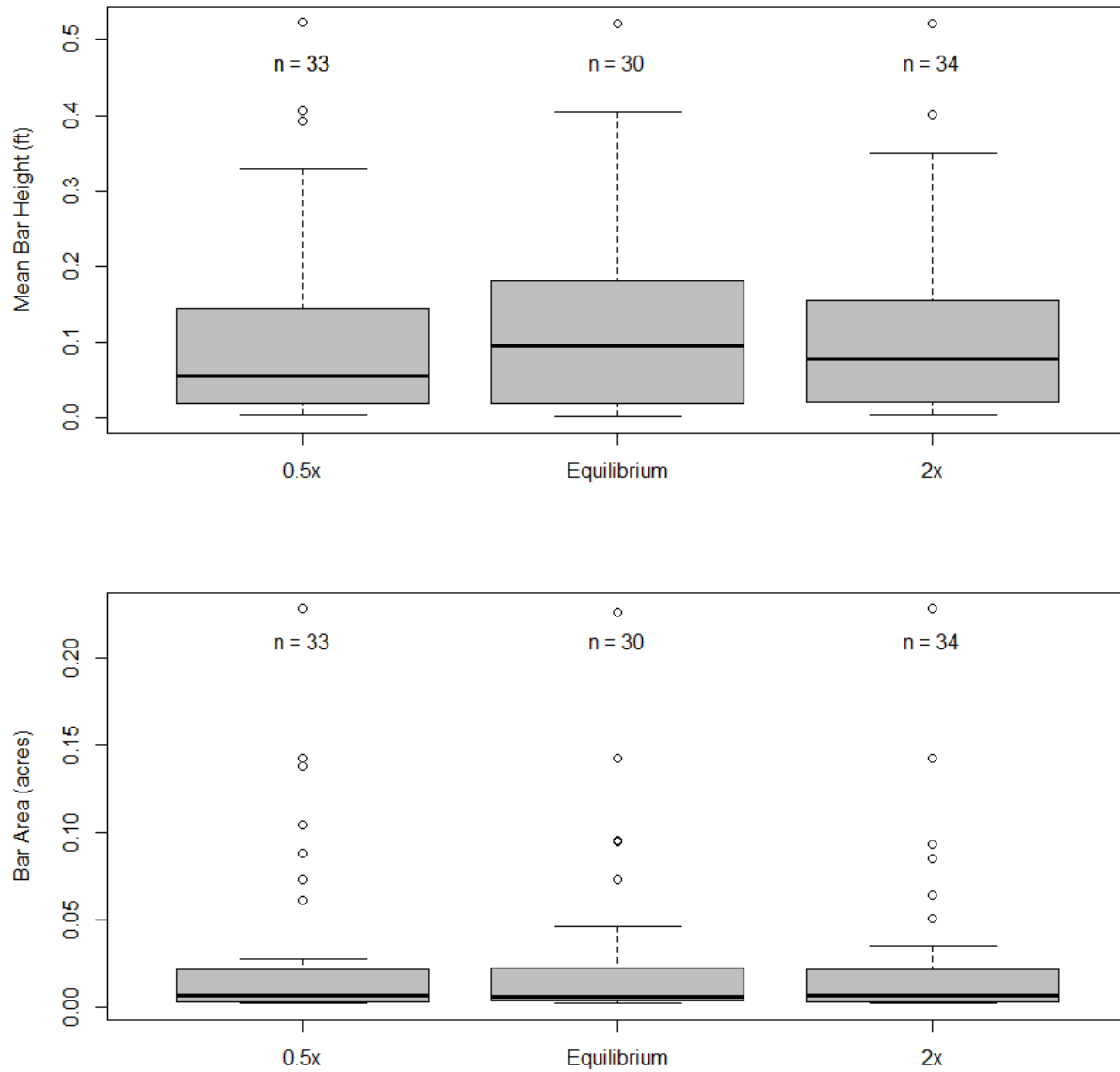




Figure 21. Box plot of bar height and area of all bars (sand and vegetated) before and after a SDHF with bed material grain sizes of 0.75 mm, 1 mm, and 2 mm

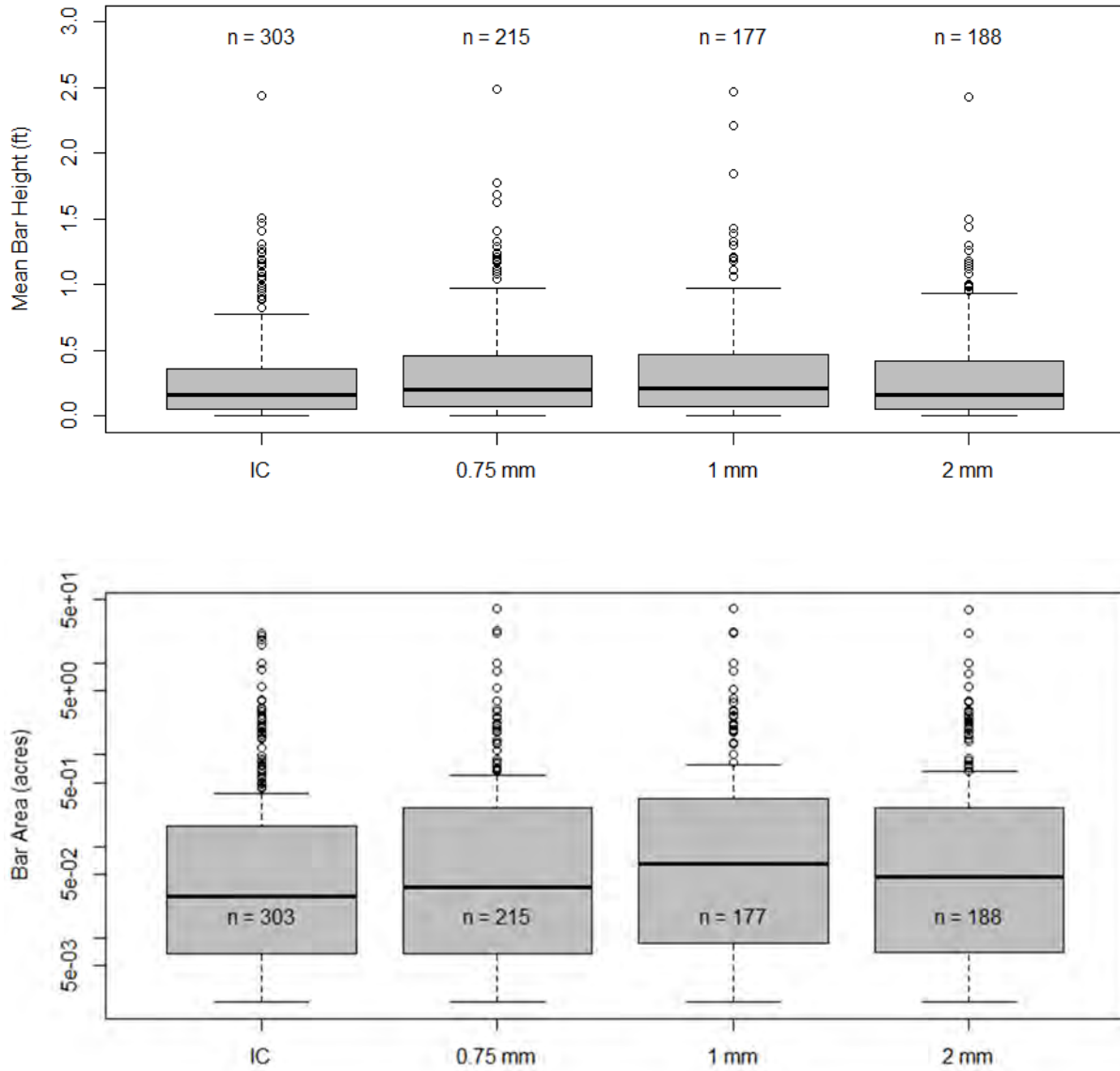




Figure 22. Box plot of bar height and area of sand bars after a SDHF with bed material grain sizes of 0.75 mm, 1 mm and 2 mm

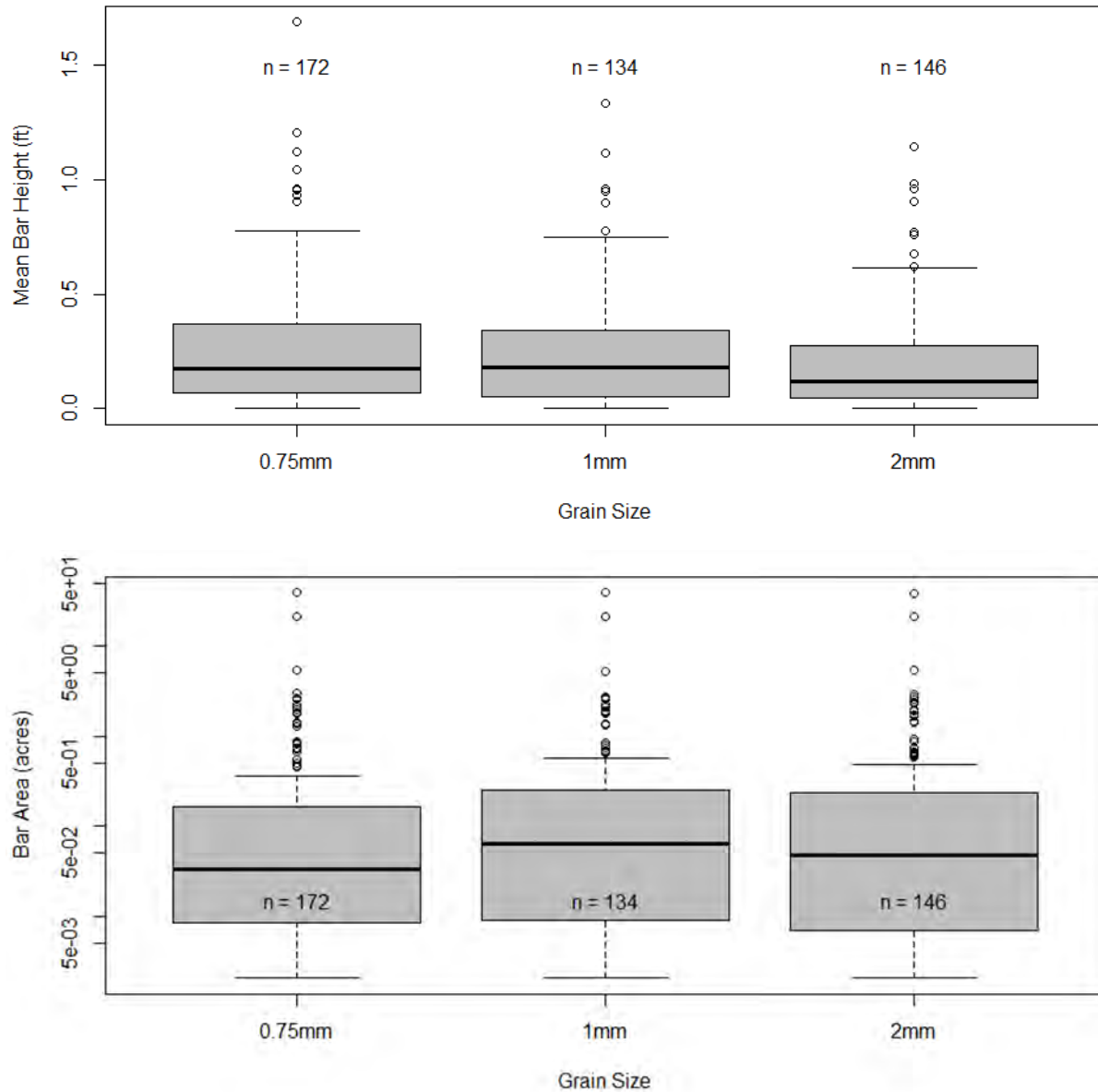




Figure 23. Box plots of mean bar height and area of new sand bars formed during a SDHF with a bed material size of 0.75, 1, and 2mm

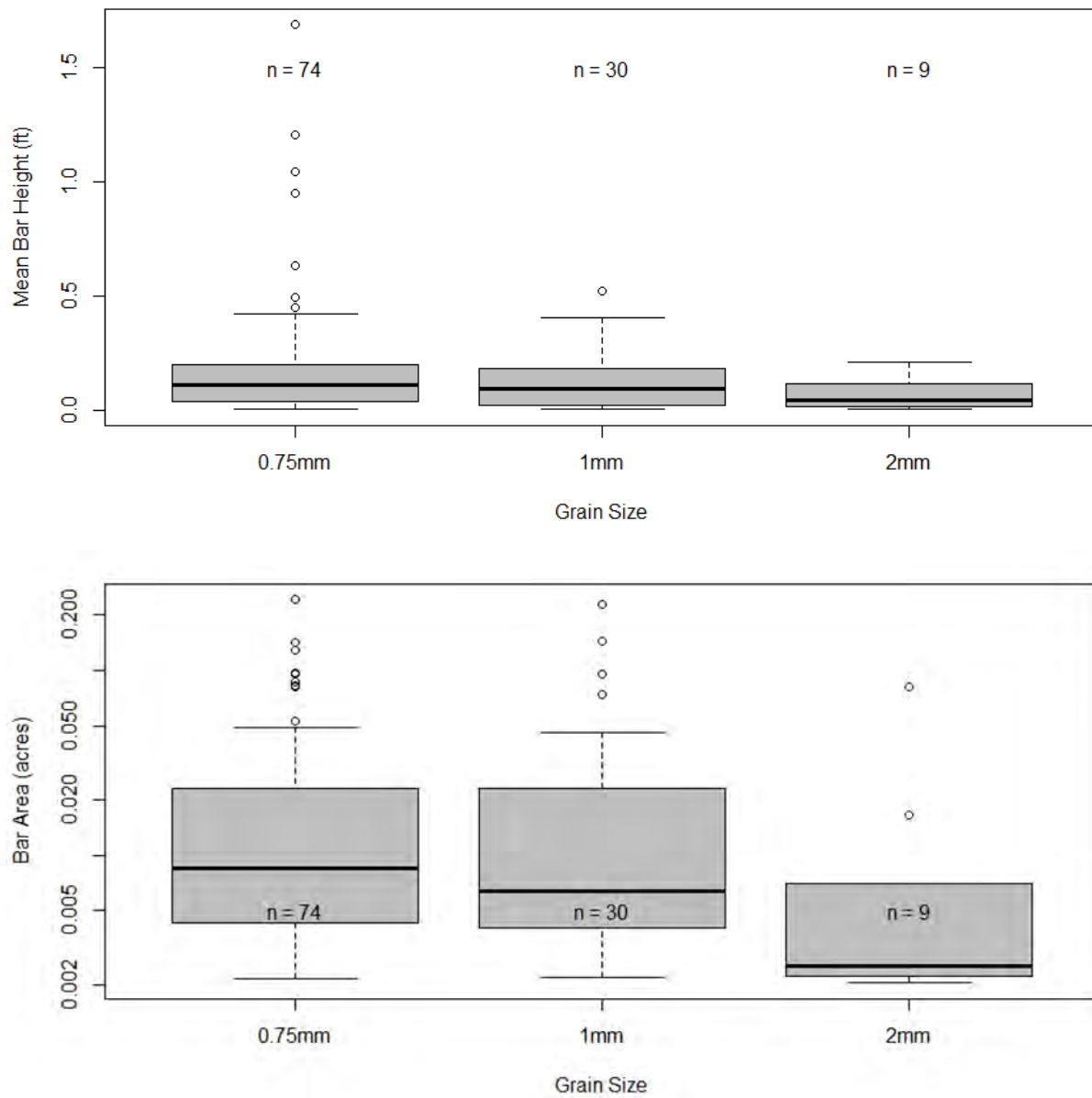




Figure 24. Comparison of mean new sand bar heights above 1,200 cfs and bar area formed with a bed material grain size of 0.75, 1, and 2mm following a SDHF (8,000 cfs TRF)

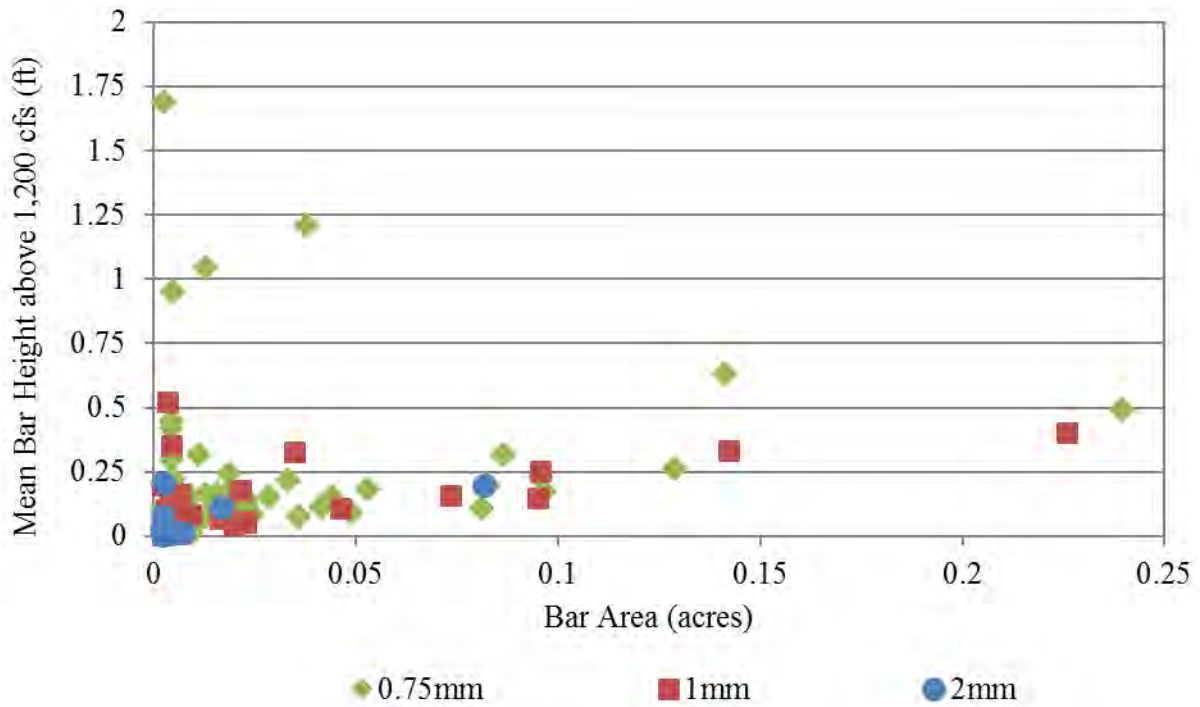




Figure 25. Depth of new sand bars below the peak stage and bar area following a SDHF (peak flow 8,000 cfs TRF) for bed material grain sizes of 1 mm, 2 mm and 0.75 mm. Area is expressed as individual bar area (top) and cumulative bar area (bottom)

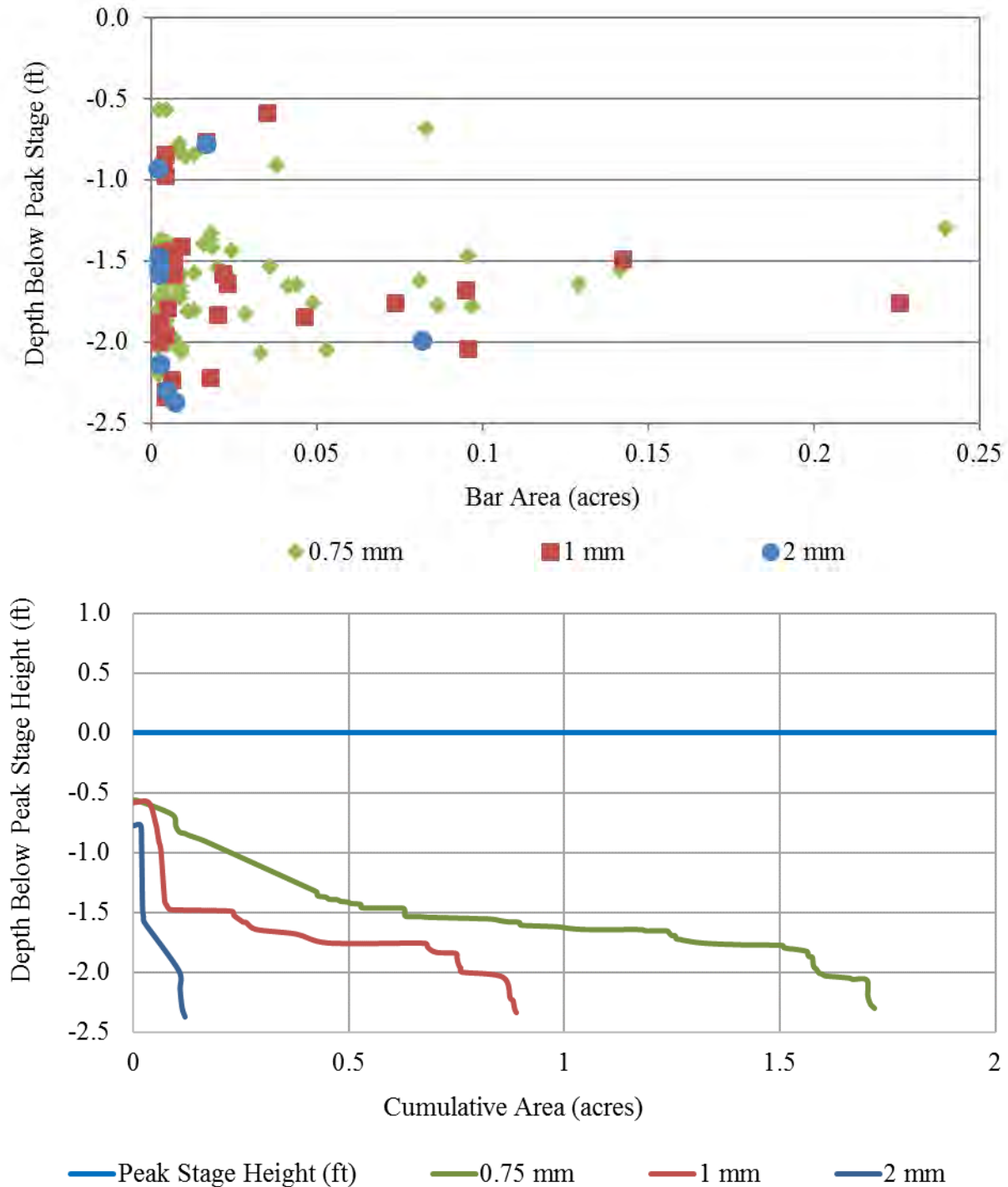
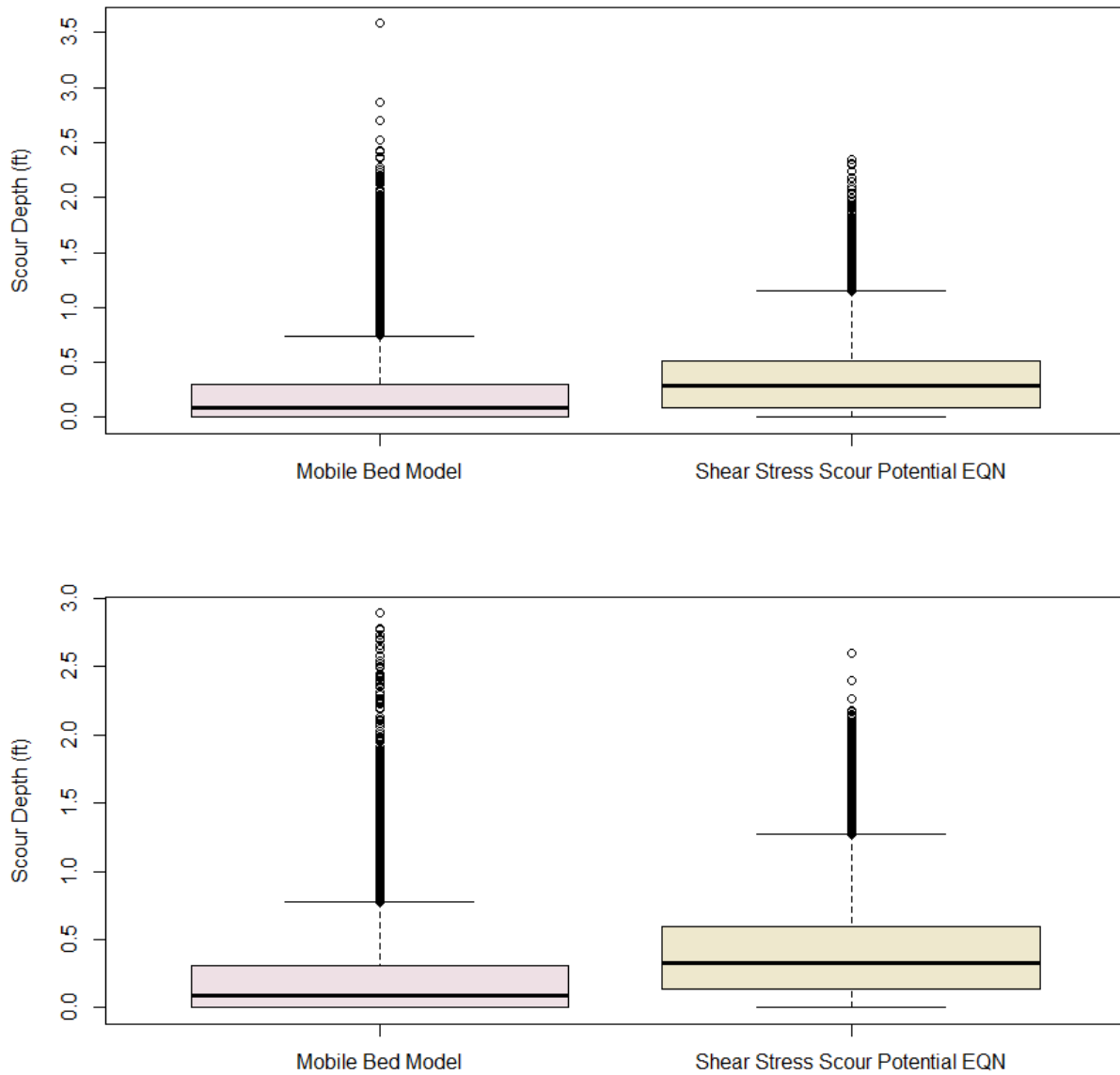




Figure 26. Box plots of scour depth predicted by mobile-bed model (FaSTMECH) and scour potential predicted by an empirical relation between measured scour depth and predicted shear stress. Scour depth on vegetated bars (top) and sand bars (bottom)





PLATTE RIVER RECOVERY IMPLEMENTATION PROGRAM

Shoemaker Island Flow-Sediment-Mechanical “Proof of Concept” Experiment

One-Dimensional Bank Erosion Analysis: Final Summary

Attachment III

FINAL

September 2016

Submitted to:

Platte River Recovery Implementation Program
4111 4th Avenue, Suite 6
Kearney, NE 68845

Submitted by:

Northern Hydrology and Engineering
PO Box 2515
McKinleyville, CA 95519



Table of Contents

I. INTRODUCTION.....	I-1
II. MODEL DESCRIPTION.....	II-1
III. SUMMARY OF YEAR 1	III-1
IV. SUMMARY OF YEAR 2	IV-3
V. SUMMARY OF YEAR 3	V-4
VI. REFERENCES.....	VI-6



I. INTRODUCTION

One-dimensional bank erosion modeling using the USDA-ARS BSTEM model was one component of a multi-faceted analysis conducted for the Shoemaker Reach of the Platte River over the past three years (FY 2013 – FY 2015). The analyses conducted with BSTEM supports previous research suggesting that lateral erosion is a primary fluvial process contributing to riparian plant mortality (Bankhead et al., 2012). A summary of the analyses conducted over the three-year period is synthesized in this report.

II. MODEL DESCRIPTION

The USDA Bank Stability and Toe Erosion Model (BSTEM) is a one-dimensional bank erosion model developed at the USDA Agricultural Research Services (Simon et al. 2011; USDA 2010). BSTEM estimates hydraulic erosion of the bank and bank toe based on hydraulic boundary shear stresses calculated from channel geometry and flow parameters. Hydraulic erosion occurs when the tractive force of the water column [shear stress] exceeds the resisting force of bank materials. Additional lateral erosion through geotechnical bank failure, (gravitational forces exceed cohesive forces), is based on equilibrium factor of safety calculations that include horizontal erosion, vertical tension cracks and cantilever failure (USDA 2010). Input requirements include bank geometry, soil type for bank material, vegetation coverage, channel slope, and water depth at the channel boundary for a given duration of time. Sediment transport is not incorporated into this model and the channel bed elevation is assumed to be fixed. This model does not incorporate incision of the channel bed and the bottom elevation of the bank toe can't erode below the elevation of the channel bed.

III. SUMMARY OF YEAR 1

In FY 2013, BSTEM was used to estimate lateral erosion for five sites that exhibited differing erosion responses to the monitored flow conditions during the time period of March 26 to April 28, 2013. Pre and post-bank profiles were surveyed throughout the reach as part of the standard monitoring protocol. The bank profiles modeled represented profiles that were vegetated (untreated) and unvegetated (treated). They also represented bank profiles where varying amounts of lateral erosion occurred over the monitored flow period ranging from no erosion to fairly significant lateral erosion of nearly 15 feet. BSTEM model inputs were derived from topographical survey data collected before and after the 2013 SDMF (April 13-18, 2013) and from continuous river stage measurements. Details of each profile are provided in PRRIP (2014).

The best method for model calibration was evaluated using four different “calibration” methods. The resulting lateral erosion rates for each calibration method were then compared. The primary calibration parameter used in this analysis is a Manning’s n value which effectively modifies the shear stress acting on the bank profile.

In all simulations, the model was more successful at replicating lateral erosion at the bank toes when Manning’s n was used as a calibration parameter (as opposed to not using the calibration



option). Additionally, in all simulations, the model predictions were better at replicating post-survey profiles when the calibration value for Manning's n was varied at each profile rather than set to a constant value of 0.028, corresponding to the 1D HEC RAS analyses.

Calibrated values of Manning's n ranged from a high of 0.045 at profiles where no erosion occurred to a low of 0.016 at profiles where significant erosion occurred. The model was able to predict no lateral erosion on the vegetated bank profiles with the combined input of vegetation parameters that increased bank resistance to erosion and a Manning's n .

The results of the analysis demonstrated that the preferred approach for using BSTEM for management scenarios was to calibrate the model on a profile by profile basis by adjusting Manning's n to match the shear stress estimated by a 2D model. The shear stresses were matched between BSTEM and the 2D model at the peak of the high flow and the resulting Manning's n was applied over the entire model period. This approach worked very well for unvegetated banks and not as well for vegetated banks. It was difficult to simulate any erosion for vegetated banks

The following conclusions can be drawn from this analysis:

- In four of the five bank profiles modeled, BSTEM was calibrated based on pre and post surveys to within 3% using Manning's n as a calibration parameter. In the fifth bank profile, significant lateral erosion occurred and BSTEM underestimated the erosion by 30%.
- Significant lateral erosion occurred at 2 of the 5 sites. In both cases, only about 12-13% of the predicted erosion occurred during the SDMF. These results can be explained by relatively minor increases in the applied shear stress over a short period of time during the SDMF and the long durations of moderate flow preceding and following the SDMF.
- Lateral erosion of bank profiles was caused by both hydraulic erosion and geotechnical failures. In the 2 sites where significant lateral erosion occurred, the bulk of the geotechnical failures occurred in period after the SDMF. The hydraulic erosion that occurred during the SDMF resulted in steepened bank profiles and bank toe erosion that primed the banks for geotechnical failure.

These results highlight the importance of the timing of pre and post surveys relative to flow release to ensure that the interpretation of channel change is correctly correlated with the flow of interest. These results also have important implications for interpreting the 2D bed mobility modeling results which are conducted over the 6-day SDMF and are compared to cross sections surveyed approximately 28+ days apart.

The results of this analysis indicate the best approach to apply BSTEM for management scenarios are a combination of Approach 3 and 4. Approach 3, calibration of Manning's n to pre and post profiles is required for vegetated banks. Vegetated banks were consistently estimated to be very stable and did not erode under the SDMF event, even when using the lowest



recommended values for additional cohesion strength and increased critical shear stress. The model predicted erosion at the bank toes on both vegetated banks unless the Manning's n value was increased sufficiently to reduce shear stresses below the critical shear stress. This value is only appropriate for flows in the range of the 2013 SDMF and may not translate to higher flows. Additional field data (e.g. water surface slope, stage, discharge) to define an appropriate Manning's n value at higher flows is required. Approach 4, calibrating the applied shear stress at the toe in BSTEM to 2D model shear stresses, is the best approach for predicting erosion of un-vegetated banks. This approach is easily translatable to higher and lower flows. Increases of the magnitude and duration of flow increases bank erosion. However, the magnitude of increase varies depending on the shape of the bank profile. Short duration high flow events will initiate lateral erosion of un-vegetated bars (treated, designed, or natural). However, the amount of lateral erosion that occurs during a short duration high flow event is predicted to be a smaller percentage of the total lateral erosion that occurs over longer duration, more moderate flows that occur in the Platte River.

IV. SUMMARY OF YEAR 2

The analysis conducted in year two addressed a major limitation of the calibration for the 2013 SDMF in that no erosion occurred on the vegetated banks, thus, the calibration to the minimum Manning's n values were required to reproduce zero erosion and may not be translatable to higher flows. Following the 2013 SDMF, two high flows occurred, the fall 2013 high flow and the June 2014 high flow. Both events were natural high flows and have significantly longer durations than the target SDHF duration used in the 2013 analysis. This analysis focuses on lateral erosion of vegetated bars that occurred during the June 2014 high flow.

Seven vegetated banks that exhibited differing erosion responses to the June 2014 high flow during the time period of May 5, 2014 to July 31, 2014 were selected for evaluation. BSTEM model inputs were derived from vegetation, topographic and stage data collected before and after the June 2014 high flow. All banks are vegetated and degree of lateral erosion varies from 0 to 76 feet. Vegetation varies across sites with a mix of herbaceous, woody, emergent forbs and phragmites. No profile had more than 5% bare soil. Sites were surveyed prior to the June 2014 high flow in May, and following the high flow in July. Details of each profile are provided in PRRIP (2015).

The primary finding that differed from PRRIP (2014) was that vegetated bars do not consistently have roots that extend to toe of the bank in the Shoemaker Reach. Undercutting of the bank, just below the root zone was noted on several cross-sections. The rooting depth is critical for prediction of lateral erosion. Banks that have roots that extend to the toe of the bank, tend not to erode, whereas banks that have shallower roots, have undercutting below the root zone that results in bank failures and lateral erosion.

The lateral erosion modeling focused on prediction of erosion of vegetated banks. Measured erosion at the selected profiles ranged from 0 to 76 feet.

The following conclusions can be drawn from this analysis:



- In six of the seven bank profiles modeled, BSTEM was calibrated based on pre and post surveys to within 5% using Manning's n as a calibration parameter. Calibrated values of Manning's n that were based on matching the pre and post surveyed profile ranged from 0.011 to 0.045. In the seventh bank profile, significant lateral erosion occurred and it was not possible to calibrate BSTEM using a Manning's n of a reasonable value.
- For all vegetated banks where no lateral erosion was observed, a calibrated value of Manning's N of 0.045 was found to best match field data, consistent with the findings from PRRIP (2014). The model was able to predict no lateral erosion on the vegetated bank profiles with the combined input of vegetation parameters that increased bank resistance to erosion and a Manning's n .

Based on these results, the recommend approach for prediction of lateral erosion of vegetated banks with shallow root zones (rooting depth is above the toe) is to calibrate the model on a profile by profile basis by adjusting Manning's n to match the shear stress estimated by a 2D model. The shear stresses were matched between BSTEM and the 2D model at the peak of the high flow and the resulting Manning's n was applied over the entire model period. This method produced the best estimates of lateral erosion of vegetated bars where moderate erosion occurred.

This approach over-estimates the amount of toe erosion that occurs at vegetated bars where the root zone extends to, or below, the toe of the bank. In the case of a deep rooting zone below the toe, the Manning's n value is raised to a high enough value such that the critical shear stress is higher than the applied shear stress (0.045).

BSTEM does not provide adequate results when large morphological changes occur in the channel that substantially shift shear stress applied at the toe of the bank.

V. SUMMARY OF YEAR 3

BSTEM is not sufficient at multiple sites over large areas primarily due to two significant limitations. The first limitation is the static nature of the BSTEM model when conducting analysis over a flow hydrograph. The model must be run multiple times as a series of steady flows that represent the hydrograph. The bank profile is updated at the end of each run to reflect the effects of hydraulic erosion. The geotechnical stability of the bank is evaluated at the end of each run as well and if bank failure is indicated the profile is further modified. A dynamic model where a hydrograph could be easily evaluated at a user specified time step would increase the ability to test the sensitivity of lateral erosion to flow depth and duration.

A second limitation of BSTEM is that changes in shear stress that result from erosion and deposition within the channel are not incorporated into the modeling analysis. BSTEM only analyzes the bank profile and interactions that occur between the channel bed and the bank profile are neglected. This limitation would best be overcome by linking BSTEM to a mobile-bed model that can adequately predict the formation of mid-channel/lateral bars. This coupling has been attempted in the past with varying success and is still in the research/development phase (Lai et al., 2012).



In the third year of the project, the potential to address these identified limitations was investigated with the use of a newly integrated Hydrologic Engineering Center's River Analysis System (HEC RAS version 5.0.1 <http://www.hec.usace.army.mil/software/hecras/>) model that combines the USDA-ARS Bank Stability and Toe Erosion Model (BSTEM) with HEC-RAS 5.0. The advantage of using this upgraded model is that the toe scour and bank failure processes modeled in the BSTEM model and the channel deposition and incision processes modeled in the sediment transport module of HEC RAS are coupled allowing for an evaluation that includes the interactions between the erosional processes. The combined model has been successfully validated on Goodwin Creek in northern Mississippi (Gibson et al. 2015).

The integrated HEC RAS BSTEM model requires a calibrated HEC RAS model for unsteady flow and sediment transport. The development of a new sediment transport model would require the largest amount effort, while populating the BSTEM lateral erosion components could be adapted from the existing BSTEM model directly.

The calibration approach used for the BSTEM analysis in Year and 2 that produced the best estimates of later erosion required modification of Mannings N to adjust the shear stress at the bank toe within BSTEM to match the shear stress predicted by the 2D model. This calibration approach would not be appropriate for the coupled HEC RAS BSTEM model because the modification of Mannings N to match shear stresses would also impact the water surface elevations predicted by HEC RAS and result in inconsistent hydraulics. After consultation with the model developers, it was determined that an alternative calibration approach that may work in the integrated model would be to modify the threshold (critical) shear stress, rather than Manning's n. For example, if the 2D shear stress is twice the shear predicted in the 1D HEC RAS model, the critical shear stress at the bank would be reduced by half to achieve the same level of lateral erosion. This approach would be reasonable (and relatively quantitative) given the output available from the 2D model.

After consultation with the project team and model developers, it was concluded that the significant effort required for calibration of the unsteady sediment transport HEC RAS model in addition to testing a new BSTEM calibration approach was not justified.



VI. REFERENCES

- Bankhead, N. R., 2013. "Lateral Erosion Research", presentation to the AMP reporting session, April 22-23, 2013, Omaha, Nebraska.
- Lai, Y.G., R.E. Thomas, Y. Ozeren, A. Simon, B. Greimann, and K. Wu. Coupling a two-dimensional model with a deterministic bank stability model. ASCE World Environment and Water Resources Congress, Albuquerque, New Mexico, May 20-24, 2012.
- Gibson, S., Simon, A., Langendoen, E., Bankhead, N., Shelley, J. (2015) "A Physically-based Channel-modeling Framework Integrating HEC-RAS Sediment Transport Capabilities and the USDA-ARS Bank-Stability and Toe Erosion Model (BSTEM).
- Platte River Recovery Implementation Program (PRRIP), 2014. Shoemaker Island Flow-Sediment-Mechanical "Proof of Concept" Experiment Annual Report 2013. September 2014.
- Platte River Recovery Implementation Program (PRRIP), 2015. Shoemaker Island Flow-Sediment-Mechanical "Proof of Concept" Experiment Annual Report 2014. May 2015.
- Pollen-Bankhead, N, R. Thomas and A. Simon. 2012. Can Short Duration High Flows be Used to Remove Vegetation from Bars in the Central Platte River? Final report to the Platte River Recovery Implementation Program. Directed Vegetation Research Study.
- Simon, A., N. Pollen-Bankhead, and R. Thomas. 2011. *Stream Restoration in Dynamic Fluvial Systems: Scientific Approaches, Analyses, and Tools*, Geophysical Monograph Series 194, American Geophysical Union. 10.1029/2010GM001006.
- USDA. 2010. Bank Stability and Toe Erosion Model: Static Version 5.2, <http://ars.usda.gov/Research/docs.htm?docid=5045>, viewed on October 21, 2013.
- USGS. 2013. National Water Information System: Web Interface, Platte River near Grand Island. http://nwis.waterdata.usgs.gov/nwis/dv?cb_00060=on&format=gif_default&period=&begin_date=2013-04-18&end_date=2013-05-01&site_no=06770500&referred_module=sw, viewed on October 22, 2013.